British Geological Survey

NATURAL ENVIRONMENT RESEARCH COUNCIL

Slope Dynamics Project Report: Norfolk Coast (2000 - 2006)

Slope Dynamics Project Report: Norfolk Coast (2000 - 2006)

P.R.N. Hobbs, C.V.L. Pennington, S.G. Pearson, L.D. Jones, C. Foster, J.R. Lee & A. Gibson

Contributors

K. Freeborough, G.Jenkins, R. Lawley & D. Boon & B. Humphreys

Keyworth, Nottingham   British Geological Survey   2008

BRITISH GEOLOGICAL SURVEY

The full range of Survey publications is available from the BGS Sales Desks at Nottingham, Edinburgh and London; see contact details below or shop online at www.geologyshop.com

The London Information Office also maintains a reference collection of BGS publications including maps for consultation.

The Survey publishes an annual catalogue of its maps and other publications; this catalogue is available from any of the BGS Sales Desks.

The British Geological Survey carries out the geological survey of Great Britain and Northern Ireland (the latter as an agency service for the government of Northern Ireland), and of the surrounding continental shelf, as well as its basic research projects. It also undertakes programmes of British technical aid in geology in developing countries as arranged by the Department for International Development and other agencies.

The British Geological Survey is a component body of the Natural Environment Research Council.

British Geological Survey offices

Keyworth, Nottingham NG12 5GG

☎ 0115-936 3241   Fax 0115-936 3488
e-mail: sales@bgs.ac.uk
www.bgs.ac.uk
Shop online at: www.geologyshop.com

Murchison House, West Mains Road, Edinburgh EH9 3LA

☎ 0131-667 1000   Fax 0131-668 2683
e-mail: scotsales@bgs.ac.uk

London Information Office at the Natural History Museum (Earth Galleries), Exhibition Road, South Kensington, London SW7 2DE

☎ 020-7589 4090   Fax 020-7584 8270
☎ 020-7942 5344/45   email:
bgslondon@bgs.ac.uk

Forde House, Park Five Business Centre, Harrier Way, Sowton, Exeter, Devon EX2 7HU

☎ 01392-445271   Fax 01392-445371

Geological Survey of Northern Ireland, Colby House, Stranmillis Court, Belfast BT9 5BF

☎ 028-9038 8462   Fax 028-9038 8461

Maclean Building, Crowmarsh Gifford, Wallingford, Oxfordshire OX10 8BB

☎ 01491-838800   Fax 01491-692345

Columbus House, Greenmeadow Springs, Tongwynlais, Cardiff, CF15 7NE

☎ 029–2052 1962   Fax 029–2052 1963

Parent Body

Natural Environment Research Council, Polaris House, North Star Avenue, Swindon, Wiltshire SN2 1EU

☎ 01793-411500   Fax 01793-411501
www.nerc.ac.uk

Foreword

This report is the published product of a study by the British Geological Survey (BGS) and details the methodology, results and conclusions of an annual and bi-annual monitoring programme of coastal landslides at three test sites on the North Norfolk coast from 2000 to 2006. The three sites are coastal sections at Happisburgh, Sidestrand and Weybourne.

Acknowledgements

Contents

FIGURES

TABLES

Summary

This work has shown that cliff recession, and the geomorphological processes that result in cliff recession, are capable of being accurately monitored. The methodology developed enables change to be measured quantitatively and facilitates a better understanding of the geomorphological processes associated with cliff recession. These data can then be applied widely to coastal change analyses using models based on algorithms comprising a variety of physical and mechanical properties and derived parameters such as the factor of safety, for example. Whilst the overall approach used here is observational and deterministic, the data provided could be used to guide stochastic models where quantitative input data might be otherwise lacking or where the complex interrelationship between geology, geomorphology and landslide cyclicity might be ignored.

There are three project test sites on the North Norfolk coast. From west to east, these are located at Weybourne, Sidestrand and Happisburgh.

The terrestrial basis (as opposed to aerial) for the monitoring used here has certain advantages and disadvantages. It has allowed multiple repeat surveys to be carried out for little mobilisation cost, when compared with the equivalent aerial survey. At the time of the surveys the amount of detail recorded generally outstripped that available from aerial surveys of the time, particularly where the cliffs are steep (today, more detailed and more cost-effective low-level airborne systems, for example helicopter platforms, are available. However, these are still considered to be more expensive than ground based surveying techniques). The level of detail can also be customised by using multiple scans to reflect complex morphology. The main disadvantage of the terrestrial method, as used here, is its limited coverage, and hence the need to focus on representative test sites. Recently, vehicle-, air- and ship-borne systems have redressed this to some extent. The methods employed here are intended to go beyond simply recording the amount of linear coastal recession. This would be best achieved using aerial methods. Rather, we are attempting to quantify coastal recession in 3D and to elucidate the geomorphological processes taking place. The 3D element is developed in the form of a digital elevation model (DEM), changes in which can be derived from one monitoring epoch to another. Currently, the standard geology map provides no indication of the 3D geology of the UK's cliffed coast. This then produces a key problem in extrapolating any geology-based model of coastal recession from the test site to the cliffed coast as a whole. This problem is highlighted at the Sidestrand site where the complex structure of the glacial geology has resulted in a complex slope stability model which may be difficult to extrapolate along the coast.

Analysis has been made of the coastal recession processes at the three sites. Attention has been paid to the spectacular, albeit artificially accelerated, rate of recession at Happisburgh. Since the destruction of a section of sea defences in the 1990s, this has attracted much publicity and concern for the future of Happisburgh village. A model of embayment development at Happisburgh, and its relation to cliff/platform lithostratigraphy and beach levels at the site has been developed. Landslide activity at Sidestrand over the monitoring period has been considerable; here cycles of landslide activity in relation to embayment development and drainage are proposed. Both these sites differ markedly from the Weybourne test site where the very high shingle beach provides effective protection to the cliff and where little cliff recession has been recorded.

Slope stability modelling tends to be aimed at engineering applications where there is usually a large body of sub-surface data available. The models have, until recently, been solely 2D and of either 'limit equilibrium' or 'finite element' type, or some variation of these. These models are highly site specific and have not as yet been applicable regionally. This report attempts to bridge this gap, and in doing so seeks to parallel other BGS geohazard modelling

based on the quantitative attribution of geological and geomorphological formations. Slope stability modelling has been applied to the Happisburgh and Sidestrand test sites, but not to the Weybourne site. The efficacy of the slope stability analysis method varies between Happisburgh and Sidestrand, due mainly to the different cliff geometry and scale.

During the 6-year monitoring programme, the cliffs at the Happisburgh test site have receded by over 40 m to form a new embayment which exhibits a terminal groyne erosion pattern. The erosion here appears to be influenced largely by direct mechanical abrasion from the sea but also significantly by surface water runoff and groundwater seepage. At the Sidestrand test site two distinct phases of landslide activity have been identified. These have involved deep-seated landslides producing large debris flows which have remained on the platform for several months. At the Weybourne test site there has been little landslide activity and little cliff recession. This has been largely due to the distinctive permanent shingle beach and the protection it affords to the cliff. The relationship between meteorological and oceanographic data and landslide activity has been investigated, and correlations are discussed.

1 Introduction

The report describes the first monitoring dataset and methods, processing, observations, images, and desk study information which were gathered as part of the Slope Dynamics project. It attempts to derive an understanding of the slope processes occurring at three test sites along the active shoreline of North Norfolk. The project has 12 test sites around the English coast (Figure 1-1) most of which have been monitored annually, usually in late summer and early autumn. However, in 2001 and 2002 the sites were monitored bi-annually. The sites were originally selected to represent non-engineered and non-protected soft cliffs incorporating diversity of geology, scale, and landslide type and activity. Some of the 12 sites have been monitored for a short period only and have been discontinued or postponed due both to the inactivity of the sites or funding restrictions.

The three Norfolk coastal sites are at Happisburgh, Sidestrand, and Weybourne (Figure 1-1). These sites were chosen to represent some of the variety and intensity of cliff recession processes found in North Norfolk. The geology is dominated by a complex and diverse assemblage of glacially emplaced materials, almost universally affected by coastal landslides. The cliff recession described includes some of the most rapid found in Europe.

The methodology developed principally involves using terrestrial Light Detection and Ranging (LiDAR) and Global Positioning System (GPS) techniques to create accurate 3D computer models of the cliffs. The raw data produced by LiDAR is in the form of a 'point cloud' of XYZ points with laser reflective intensity and (since 2005) photographic data included. These point clouds are then processed in various software packages to create 'solid' surface models which can be compared from one monitoring epoch to another. This process results in 'change models'. The amount of change is usually referred to a horizontal datum plane, for example sea level, and hence indicates changes in height above sea level. However, the datum may also be vertical, for example to better depict recession of a vertical cliff. Of course, changes in a non-vertical cliff are often not purely unidirectional. For example, as a result of a rotational landslide, parts of a cliff may fall (negative change) while others rise (positive change). That is, there may have been little net loss of material from the cliff, but rather a re-arrangement.

The Norfolk Coast report has benefited greatly from concurrent geological remapping of North Norfolk by BGS field staff, and from their expert knowledge of the glacial deposits exposed at the coast and a fundamental re-appraisal of the lithostratigraphy of the area. The report describes the programme of geotechnical sampling and testing. As part of this, a small number of undisturbed samples were taken for triaxial strength tests, and a larger number of disturbed samples for index testing (particle-size, plasticity etc). A small hand-operated penetrometer was also used to measure cone penetration resistance.

During the first two years of monitoring, the terrestrial LiDAR and GPS surveys and processing were carried out by 3D LaserMapping (Riegl, UK) Ltd staff. Subsequently, the same laser-scanner equipment was purchased by BGS and combined with a newly acquired differential GPS (dGPS), to complete the remaining surveys up to 2006. In 2005 the laser scanner was replaced by a faster and more accurate model which also featured a digital camera. In addition to the monitoring surveys, reconnaissance and geological surveys were carried out, particularly in the earlier part of the period.

Figure 1-1 Locations of Slope Dynamics project test sites on the English coast

2 Background

It is likely that the Norfolk cliffs have been eroding at the present rate for the last 5000 years, when sea level rose to within a metre or two of its present position (Clayton, 1989). Therefore, the future predictions of sea level rise and increased storm frequency due to climate change are likely to have a profound impact on coastal erosion and serious consequences for the effectiveness of coastal protection and sea defence schemes in East Anglia in the near future (Thomalla and Vincent, 2003). Hutchinson (1976) quoted an anonymous description from the 1900's of the Cromer-Overstrand cliffs as being "*the scene of some of the most tremendous denudations in the history of British coast erosion*". Historical maps suggest that the shoreline was not as smooth in form as it is today. Other morphological changes are visible from a map published in the 1600s which identifies a headland or ness feature extending offshore in the vicinity of Cromer. There was also an area of land seaward of Overstrand, which formed a cliffed headland known as Foulness. This was eroded away by the mid 1800s, although the Admiralty Charts show a shallow area offshore off Cromer and Overstrand (Halcrow, 2002). Clayton (1989) analysed historical maps, photographs, and records of landmarks and villages lost to the sea to estimate that the till cliffs of North Norfolk have retreated at an average rate of 1 m per year over the past 5000 years, with the chalk cliffs retreating more slowly. Cambers (1976), using historic OS maps, gave a figure of 0.9 m/yr.

2.1 REGIONAL GEOLOGICAL SUMMARY

A simplified regional geological sequence of the Norfolk study areas comprises the Upper Cretaceous Chalk bedrock overlain by pre-glacial deposits, glacial tills and glaciofluvial outwash deposits. In Northeast Norfolk where the study sites are located, the chalk basement material is overlain by pre-glacial formations. The Chalk is generally masked by these younger deposits, although it is seen in the cliffs as erratics or till rafts. The pre-glacial formations present formed in a basin during the early Quaternary and are known as the Red Crag, Norwich Crag and Wroxham Crag. This collective Crag Group comprises fine to coarse grained micaceous sands, clays and gravels and although Quaternary in age these deposits are considered as bedrock deposits (Moorlock *et al.*, 2002). It is likely that the Wroxham Crag is most prevalent at the study sites although the Red and Norwich Crags have been proved in the Happisburgh borehole and may therefore underlie the Wroxham Crag in the area.

Norfolk has some of the most extensive and thickest glacial deposits in Britain and these are summarised in Table 2-1 showing the latest naming convention as well as the obsolete names. Renaming of the North Sea Drift Formation (Anglian), Lowestoft (Anglian) and Hunstanton Formations (Devensian) has taken place as a result of logging coastal sections, detailed lithological analysis and a reappraisal of stratigraphy (Lee and Booth, 2006).

Table 2-1Stratigraphy of Quaternary deposits present in the area of the study sites (Moorlock *et al.*, 2002).

Banham, 1988	Lunkka, 1994	North Walsham and Mundesley Sheet 132/148 (after Arthurton *et al.*, 1994)	Cromer Sheet 131 Revised Stratigraphy after Moorlock *et al.* (2000); Hamblin (2000) and Hamblin *et al.* (2000)	
Lowestoft Till	Lowestoft Till	Lowestoft Till		
Third Cromer Till	Cromer Diamicton and Mundesley Diamicton	Corton Formation Sand and Gravel Diamicton and galciolacustrine silts	Briton's Lane Sand and Gravel Member	Overstrand Formation
			Trimingham Sand Member Hamworth Till Member Bacton Green Till Member	Beeston Regis Formation
Second Cromer Till	Walcott Diamicton		Unnamed glaciofluvial sands and gravels	Lowestoft Formation
First Cromer Till	Happisburgh Diamicton		Walcott Till Member	
			Corton Sands	Corton Formation
			Happisburgh Till Member	

2.2 REGIONAL ANALYSIS OF COASTAL RECESSION

It is appropriate to consider analysis of coastal recession at the regional scale in order to take into account the connectivity between the various elements that comprise the regional coastal system. On fast-retreating coasts it is therefore important to appreciate more than just the position of the cliff face. Important factors include the onshore environment (including the strength and variability of the geological materials making up the coast), the offshore

environment, the weather and climate, and the influence of engineered structures such as groynes and sea walls.

2.2.1 Onshore

The cliffed coastline acts as a major control defining the coastal system within East Anglia, constraining the position of the lower-lying coastline to the south. The glacial cliffs have offered little resistance to marine erosion and historically there has been a trend of coastal retreat. Erosion of the North Norfolk cliffs produces large volumes of sediment, between Weybourne and Winterton Ness, the cliffs supply approximately 500,000 m^3/yr of sand to the littoral zone (HR Wallingford, 2001). The cliffs along this stretch of coast vary considerably in composition which leads to different volumes of sediment being released at different locations. Fluvial erosion rates per unit area in East Anglia are 1–2 t km^2/yr (t = tonnes) (McCave, 1987); the main input to the sea is from coastal cliff erosion whilst rivers around the southern North Sea contribute very little sand.

Primary controls on long-term rates of cliff retreat on both the soft and hard rock sections are the gradient and elevation (relative to sea level) of the shore platform and beach, as these control the ability of waves to remove landslide debris and then attack and destabilise the cliff toe. The soft cliffs of Norfolk have a low shear strength which means that they are susceptible to landsliding as well as mechanical erosion by marine processes which can lead to undercutting and slope steepening (Lee and Clark, 2002).

2.2.1.1 DEFENCES

Defences have been installed along the Norfolk coast from as early as the 19th Century. DEFRA has overall responsibility for producing policies on both coastal defences and inland flood defences whilst the Coast Protection Act of 1949 gives Local Authorities the powers to erect coastal defences in their constituencies. As well as defences installed by the Council there are also privately owned defences which are sporadically present around the coast (e.g. Fresco, 2004). Shoreline Management Plans (SMP's) introduced in the 1990's collect and hold information relevant for determining the coastal management strategy for a section of coastline. A timeline of sea defence activity along the North Norfolk Coast is outlined in Table 2-2. For the coastline between Weybourne and Cromer, along the Sheringham and Cromer urban frontages, there are seawalls and groynes, with the backing cliffs re-graded to form a grassed slope. Timber palisades and groynes were previously present along much of this section of coastline, but between Sheringham and West Runton these have largely failed and ceased to be effective. The remainder of this section to Cromer is undefended. Between Cromer and Happisburgh, much of this frontage has had some form of hard defence in place since the mid-1900's. There are intermittent stretches of seawall which protect the urban frontages, such as at Overstrand and Mundesley. The cliffs behind these defences have locally been re-graded to form a slope. Timber palisades and groynes front much of the coastline between seawalls. Lower land levels at Walcott have required the presence of a seawall to reduce the risk of inundation.

During recent years, some sections of coastline which were previously defended, such as at Happisburgh, have been subject to defence failure (Figure 2-1). Where the structures have not been repaired/maintained, there has been rapid cliff erosion as the cliff line attempts to realign to a more natural position. It should be borne in mind that even where protected by defences, the cliffs are still subjected to sub-aerial erosion processes and landslide.

The construction of coastal defences along the northeast Norfolk coast has significantly affected the rate of cliff recession. The principal urban settlements of Sheringham, Cromer, Overstrand and Mundesley have been protected by seawalls and groynes since the 19th Century (the earliest seawalls built at Cromer and Mundesley in the 1840s), with the majority of these defences dating from the 1940's and 1950's. During the 1950's and 1960's, much of

the remaining cliff line south to Happisburgh was protected by the installation of timber groynes and palisades. The construction and maintenance of these defences has slowed the cliff recession rates by trapping beach sediment travelling along the coast (typically from north-west to south-east) and reducing the supply of sediment to beaches down-drift of the defences (Ohl *et al.*, 2003). This has, however, caused down-drift starvation and a deficit in the sediment budget at undefended sections thereby increasing the cliff recession rate in these areas (HR Wallingford, 2001).

Figure 2-1 Failing defences at Happisburgh in 2004.
Most of this section of wooden palisade defences has now been removed. A small rock bund now replaces part of this section.

Table 2-2 Sequence of sea defence activity

Date	Event
1820's-30's	First protection schemes at Sheringham, Cromer & Mundesley (limited extent)
1846-1900	Sea wall and promenade built along most of the Cromer frontage
1863	Groynes added along Cromer frontage
1884	Large groyne and sea wall built at Overstrand
1890's	Short sea walls built at Mundesley with groynes between
late 1890's	Groynes built between Cromer and Overstrand
1899	Sea wall built Walcott Gap to Ostend Gap
1900	Timber palisades and groynes built at Sidestrand
1952-1954	Sea wall constructed at Ostend
1953	Timber palisades and groynes built between Mundesley and Horsey
1954	Sea wall at Overstrand rebuilt following 1953 storms
1953-1956	Timber palisade built at Bacton
1965-1967	Bacton palisade extended west to Mundesley
1958/59	Timber palisade built at Happisburgh
1960-61	Bacton to Happisburgh palisades joined

Date	Event
1959-1961	Timber palisades and groynes constructed between Ostend and Cart Gap.
1968	Beach Road, Happisburgh groynes and gabions constructed.
1976	Timber palisades and groynes built at West Runton
1973-1978	Timber palisades and groynes between Overstrand and Mundesley
1982	Partial reconstruction of damaged palisade and groynes at Happisburgh
1986	Concrete sea wall built at Cart Gap
1986	Sea Palling sea wall is extended 600 m west to Happisburgh.
1986/87	Timber palisades and groynes built between Overstrand and Sidestrand.
1991	Following storm damage, section of palisade (300 m long) removed to south of Happisburgh village.
1993	Cart Gap sea wall outflanked - sea wall extended inland to prevent further outflanking.
1994	Landslide remediation and rock bund at Clifton Way, Overstrand
1995	Failure of the timber defences SE of Happisburgh since 1991, led to the development of a 300 m breach.
1996	Storm damage results in the loss of a further 400 m of palisade and the end of Beach Road, Happisburgh
2001	Breach in defences southeast of Happisburgh extended to 500-600 m.
2002	NNDC agree to emergency defence works at Happisburgh. 4000 tonnes of rock placed at the toe of the cliffs.
2007	Further 5000 tonnes of rock armour placed at cliff toe, Happisburgh.

2.2.2 Offshore

The offshore environment has an important influence on coastal erosion and therefore it is essential to understand the oceanographic climate, wave energy and direction, the distribution of sediments moved by wave action and changing sea level.

2.2.2.1 OCEANOGRAPHIC CLIMATE, WAVE ENERGY AND DIRECTION

The northeast Norfolk coastline is exposed to North Sea waves from directions between north-northwest and east-southeast.

- The dominant waves are from the north-northeast to the southeast, with a long fetch due to the coast's orientation to the open North Sea (Halcrow, 2002).

- The 1 in 100 year wave height along this stretch of the coastline has been calculated to be greater than 8 m between Weybourne and Walcott (Anglian Water, 1988).

- The mean spring tidal range is between 2.5 m to 4.5 m. Anglian Water, 1988

- Storm surges are important along this coastline, with their damaging effects being locally severe due to the soft geology (Halcrow, 2002).

- Extreme surges can reach heights of up to 2 m, with surges of approximately 1 m occurring several times a year Anglian Water, 1988.

- The 1 in 50 year storm surge component is predicted to be approximately 1.5 m, with the level of the 1953 storm surge estimated at 3.67 m (Babtie & Birkbeck College, 1996).

This section of coast is relatively linear and faces northeast. As a result, the coastline is exposed to a wide range of wave directions (approximately 300ºN to 90ºN but predominantly 0ºN to 70ºN) and is particularly vulnerable to storms from the north due to the virtually unlimited fetch in this direction (Ohl *et al.*, 2003; Thomalla and Vincent, 2003). Various attempts to numerically model the sediment transport regime along the Norfolk coast have shown that the largest waves arrive from approximately 030ºN, the most frequent wave directions come from the northwest (330ºN) and the largest winds are associated with winds from the northwest and the north; therefore, the most erosive and damaging effects are broadly controlled by the sea conditions in the north (Ohl *et al.*, 2003).

2.2.2.2 CHANGING SEA LEVEL

Sea-level rise and climate change are influential factors associated with increased coastal erosion. There has been a relatively rapid retreat of the coastline during the Holocene in response to sea level rise, which despite the release of beach-building sediment from cliff erosion has been accompanied during the last century by foreshore steepening or beach translation rather than beach accretion (Halcrow, 2002).

Sea level change measurements from tide gauges around the world indicate that global sea level has risen over the twentieth century at rates of 1.5-2 mm yr^{-1} (Miller and Douglas, 2004). Current estimates of the relative sea-level rise in eastern England by the 2080s, taking into account isostatic change and different fuel emission scenarios, range from 22 cm (assuming a 9 cm global rise with low fuel emissions) to 80 cm (assuming a 69 cm global rise with high emissions) (Hulme *et al.*, 2002).

2.2.2.3 DISTRIBUTION OF SEDIMENT

An additional critical factor affecting the rate of erosion is determined by the transport of sediments away from their source – that is, from either the cliffs themselves or from the foreshore, to eventual sediment sinks. It is a particularly difficult task, especially as coarse materials, such as gravels, may remain in local beach systems, whilst finer materials, such as clays and silts, are readily transported offshore and may end-up being deposited on coasts further afield in the North Sea (Shennan *et al.*, 2003).

Net movement of coarse sediment at the shoreline is to the south, with computed net annual transport rates of about 100,000 m^3/yr (Clayton *et al.*, 1983). Sediment in the nearshore zone is generally moved in a northerly direction, with an overall eastward movement of fine sediment. This is because waves and surges dominate the shoreline processes, with tidal currents dominating offshore. The relatively shallow offshore zone deepens to the south, with a key feature being a series of offshore sandbanks (known as the North Norfolk Offshore Banks), and a series of nearshore banks, which lie closer to shore south of Winterton. The origin of the offshore North Norfolk Banks is unknown, but it has been proposed that they formed during the last ice age and may represent reworked glacial deposits. An alternative theory is that they are a function of coastal erosion, and the offshore transfer of sediment due to tidal circulations during the Holocene, with the banks acting as 'stepping stones' for fine sediment to be transported offshore (Halcrow, 2002). Regardless of the mechanism, there is a major transport pathway for fine sediments eastwards across the North Sea.

3 Project Methodology

The coastal sections were surveyed using remote methods, accompanied by geological mapping and geotechnical probing, sampling, and testing. The principal method of surveying the cliffs was long-range terrestrial laser scanning (LiDAR). Whilst trials of terrestrial photogrammetry were carried out, this method was not adopted for the monitoring

programme. Project work began in 2000 with reconnaissance surveys in October and trial laser scans at the three test sites in November by 3-D Laser Mapping Ltd. Between 2001 and 2002 surveys were carried out bi-annually (but not at Weybourne in 2002) and between 2003 and 2006 surveys were carried out annually, though discontinued at Weybourne after 2004. The results were processed to provide data for models of coastal recession. Reprocessing of data collected in the field by combined terrestrial laser scanning and GPS surveys was carried out using RiProfile 1.2.1b13 and then post-processed in various modelling packages, including GoCad 2.1.5, Surfer 8 and QT Modeler 5.1. The resulting computer model enabled volume calculations and observations to be made in order to determine the manner of coastal recession at the test sites.

Due to the fact that terrestrial photogrammetry was not used throughout the monitoring period, and was only used in an experimental capacity, partly in collaboration with Nottingham University's Institute of Engineering Surveying and Space Geodesy (IESSG), the results have not been included in this report. The conclusion drawn from terrestrial photogrammetry trials conducted with both Nottingham University and D. Tragheim (BGS) was that, despite the obvious weight-saving advantages, the method was less universally applicable compared with terrestrial LiDAR, at least for the purposes of this particular project. This was partly due to problems associated with the limitations of aerial photogrammetry software in dealing with slopes and the associated wide depth of field inherent with terrestrial applications. It was also unnecessary to deploy both methods throughout the project. The use of aerial photogrammetry in studies of cliff retreat has been described in Marques (1997) and Mills *et al*. (2005).

3.1 TERRESTRIAL LIDAR (LASER SCANNING)

Mobile laser scanning is in essence a terrestrial version of aerial LiDAR and has been used for a variety of applications such as the monitoring of volcanoes (Hunter *et al.*, 2003; Jones, 2006) earthquake and mining subsidence, quarrying, buildings, forensics (Hiatt, 2002; Paul and Iwan, 2001) and inland- (Rowlands *et al.*, 2003) and coastal- (Hobbs *et al.*, 2002) landslide modelling. As a tool of modern geoscience it allows "unprecedented resolution and accuracy" (Buckley *et al.*, 2008). However, resolution and accuracy are not always easy to quantify, as discussed later in this section.

Laser scanners are instruments which measure the distance and position (relative to the instrument) of a target surface by incremental sweeps which form a grid pattern. The system relies on the fact that the laser beam reflects satisfactorily from natural surfaces within the target area and that the subject is visible from the instrument location. Should not all of the subject be visible, then multiple instrument set-ups are necessary. At this point it becomes essential that these different data sets are accurately referenced to a common co-ordinate system. For this project, this has been achieved using high quality dGPS. In other environments, e.g. urban, different methods may be used, for example by having a common set of targets within the target area visible from all instrument positions. It is possible to use terrestrial LiDAR in a non-mobile scenario where the instrument is mounted and referenced to a permanent monument.

3.1.1 Equipment

Two terrestrial laser scanners have been used during this project: the Riegl LPM2K and the Riegl LPM-i800HA (Figure 3-1). The Riegl LPM2K has a very long-range capability of up to 2500m, is accurate (rangefinding) to ±25mm and has a measurement rate of up to 4 pts/sec. The Riegl LPM-i800HA is medium to long-range and can scan up to 800m with an accuracy of ±15mm. The measurement rate is typically 1000 pts/sec and a high resolution digital camera is mounted on the laser which enables coloured point-clouds, textured triangulated surfaces or orthophotos with depth information to be captured. The relative distance,

elevation angle and asimuthal angle between the laser and the cliff face are measured semi-automatically in each scan and, once processed, a 3-D surface model can be generated.

Analyses of repeated scans over a regular time interval can accurately determine the rate of recession, the nature of landslide processes and any other morphological changes in the cliff face and beach. In addition, laser measurements of targets are carried out at some sites in order to track movements of particular landslide features. The key factor in the successful use of long-range laser scanning is the accurate horizontal and vertical position of the instrument and at least one other point (any positional errors are magnified with distance). In most cases, this is achieved with a high quality GPS, essential for the production of a 3-D model produced and its subsequent orientation to national grid co-ordinates. The laser scanner is not effective where the subject is moving (e.g. water, vegetation), or where the laser is reflected by heavy rain, fog, or smoke. However, low light level does not present a problem to laser scanning, as it does with photography.

Figure 3-1 Riegl LPM2K mobile terrestrial laser scanner (left); Riegl LPM-i800HA mobile terrestrial laser scanner with camera (right).

3.1.2 Method

Despite changes of equipment, the methodology for all epochs was essentially the same. A baseline was designed, with either a pair or a series of tripod locations set-up along its length. The scanner was set up on the first tripod and the GPS on the second; the two forming the ends of a 'baseline' typically parallel with the cliff (Figure 3-2). As a laser scan was carried out from the first tripod the GPS position of the second tripod was measured. A backsight fix was taken with the scanner of the target mounted on the second tripod after the GPS had been removed. These positions were then swapped with the scan taken from the second tripod and the GPS position of the first determined and again fixed with a backsight from the scanner. This alternate scan/GPS cycle was continued along the length of the baseline or on a fresh baseline, depending how many scan positions were used for each epoch either on the foreshore or on the cliff top.

The principal of the terrestrial LiDAR /GPS method used at the test sites is illustrated in Figure 3-2. This method, developed in collaboration with Riegl UK Ltd., is simply repeated

along the beach so that a chain of baselines is created. When the first scan is completed from the first tripod, the laser scanner is swapped with the dGPS unit and scanning carried out from the second tripod. As the primary tie-point reading is repeated in reverse, it acts as a useful check on the tiepoint distance. In the absence of any fixed reference points (e.g. buildings, fences etc.) to act as secondary tiepoints, total reliance is therefore placed on the primary dGPS tiepoint. The primary tiepoint distances are typically between 50 and 200 m depending on the size of the site and weather conditions. The successive scans are wide enough to achieve a reasonable overlap, so that the whole cliff is included. Usually the upper part of the beach or rock platform is included in the scans in order to obtain a clear definition of the cliff-toe and to determine the height of the beach if present. At each tripod location several scans are usually carried out, for example to improve point cloud density and to highlight particular features. If the instrument is not relocated during this procedure the different scans can be merged and viewed on the laptop at the time of the survey without intervention of GPS data. This is because all the point clouds are related to angular datums internal to the scanner.
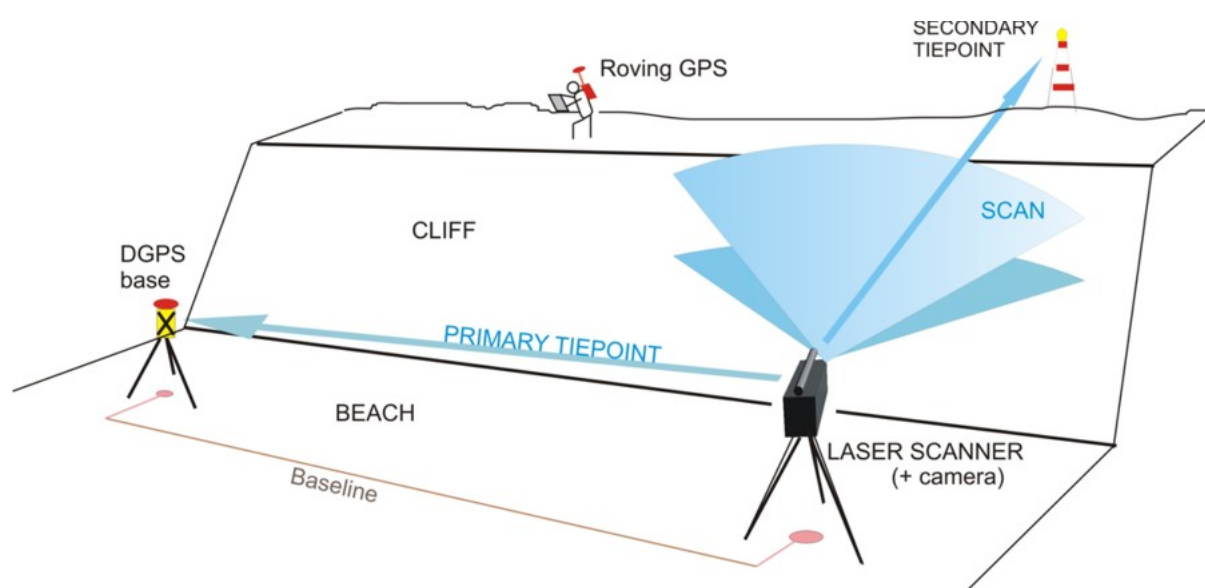
Figure 3-2 Typical layout of a single terrestrial LiDAR/GPS survey baseline

3.1.3 Model integrity and accuracy

A recurrent problem with terrestrial LiDAR, and many other remote sensing methods, is that parts of the subject may be obscured from the laser's view. These are often termed 'shadow areas'. This is particularly the case where the cliff or slope has a shallow angle and where landslide morphologies are complex or where the cliff is wooded. The way to remedy this has been to set up as many scan positions as possible, including if possible some from the cliff-top looking downward. This would have been beneficial at Sidestrand but was not possible due to objections from the landowner. For multiple scans, it is important to have at least three common points in each scan to assist with orientation. The scans also require significant overlap, typically around 10%. This may be difficult to determine on site where the subject's geometry is complex, for example what appears as an adequate overlap on the cliff face may be lacking on the foreshore closer to the scanner. These multiple scans, once oriented with respect to national grid co-ordinates using the GPS data, can then be combined to form a single model. This model can also be augmented by 'roving' GPS data assuming that access to the cliff is possible. This method was used during the early stages of the project to help define the foot and crest of the cliff.

The presence of vegetation is a common problem requiring consideration when using either terrestrial or aerial LiDAR. Normally a grass-covered slope can be scanned with little or no effect on the final 3-D terrain model. However, shrubs and trees have a major impact,

inasmuch as the laser beam does not reach the ground but is reflected from the vegetation. Also, as the vegetation is often in motion, an accurate position for it cannot be determined. Certain software packages, initially developed for aerial LiDAR, are capable of screening out vegetation, provided that a reasonable proportion of the laser 'shots' reach the ground. In the case of the project's three Norfolk test sites, vegetation has been largely absent, and screening for it has not been carried out. However, spurious data points have been identified and removed manually to produce 'cleaned' datasets. These points are usually the result of laser returns from birds, raindrops, or 'overshoot' to objects outside the test area. Standing water tends to produce a 'nil' laser return, whilst moving water will tend to give either a 'nil' or a positive return. If the latter applies, for example from reflections off waves, then these points are also removed from the data.

Table 3-1 Summary of terrestrial LiDAR surveying factors influencing 3-D model accuracy

Method	Source of inaccuracy	Manufacturer's specification: accuracy	Influence on 3-D model accuracy
Laser scanner	Range-finding	25mm (50mm*)	Medium
	Reflectivity of subject		Low
	Atmospheric conditions		Low
	Laser beam divergence	0.8 mrad	Medium
	Platform rotation (V & H)	0.009 degrees	High
GPS	Position (x,y)	5mm + 0.5ppm#	
	Height (z)	10mm + 1.0ppm#	
	Satellite configuration		High
	Post-processing		Low
Platform stability/ levelling	Tripod / tribrach level		High
	Height measurement		High

* = rms for Riegl LPM2K. (otherwise Riegl LPMi800HA)
\# = rms for Leica SR530 system with rapid static & standard antenna

The accuracy of the laser scan models has been assessed as part of the project. However, it is difficult to quantify (Buckley *et al.*, 2008). This is because it relies on several unrelated factors, the principal of these being laser range-finding accuracy and GPS accuracy. In each case the manufacturers supply specifications which include factors such as accuracy, repeatability (precision) and resolution. Additional factors include atmospheric conditions (laser), tripod stability (laser & GPS), and reflectivity of subject matter (laser). The estimated influence of these, and other factors, are summarised in Table 3-1.
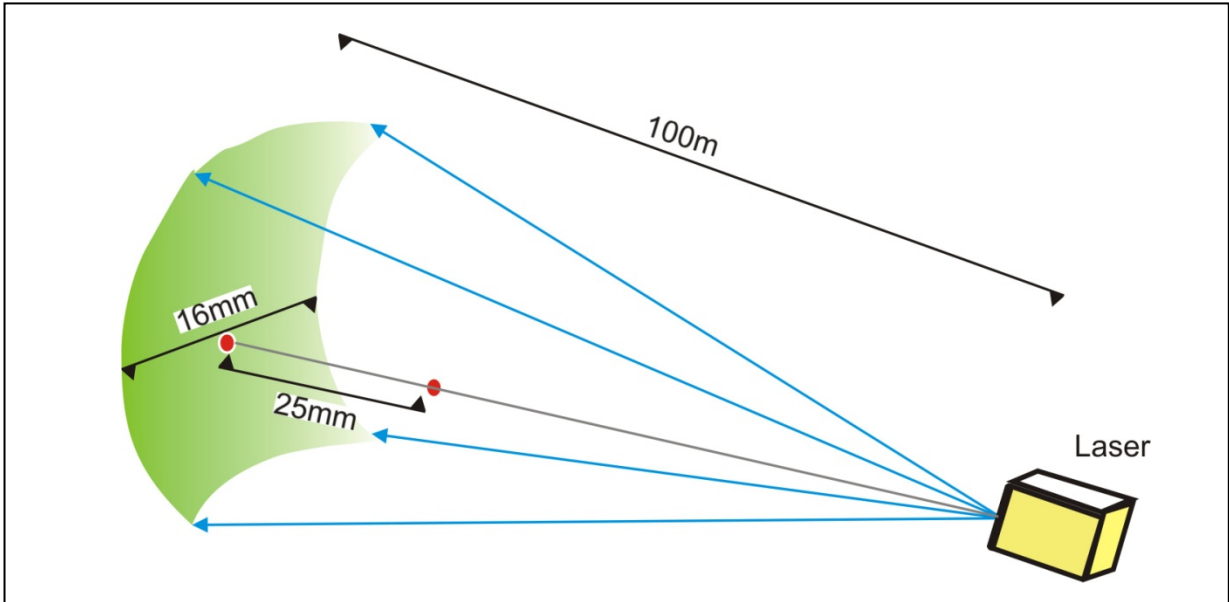
Figure 3-3 Schematic illustrating accuracy of angular (green) and range (red) components of laser scan (xyz) data
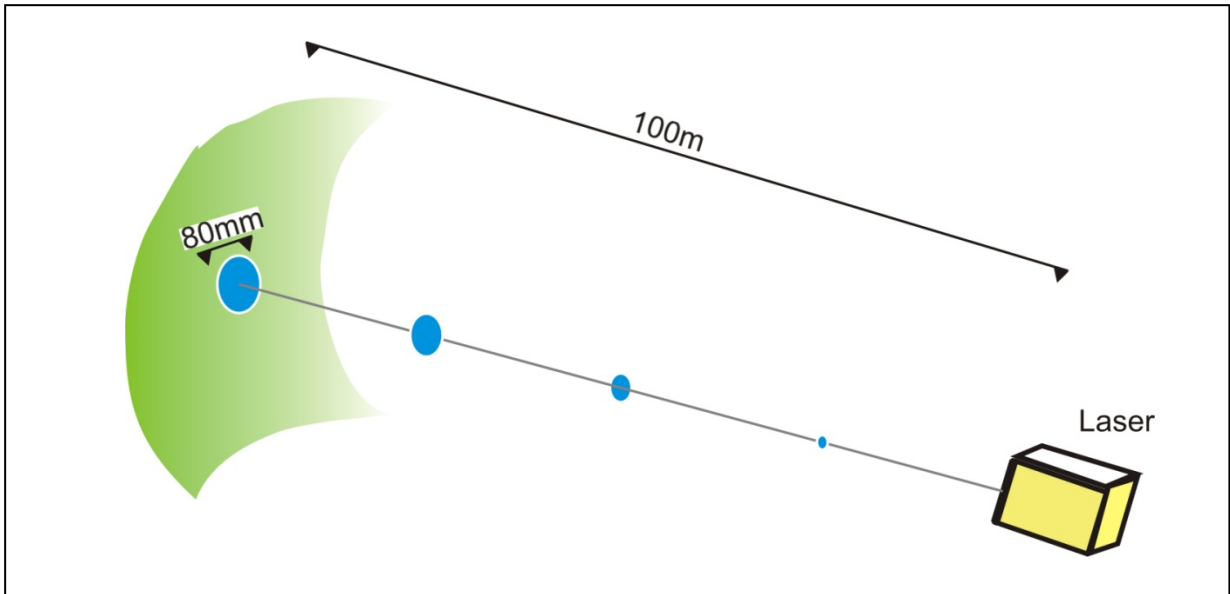
Figure 3-4 Schematic illustrating laser beam footprint expanding linearly with range
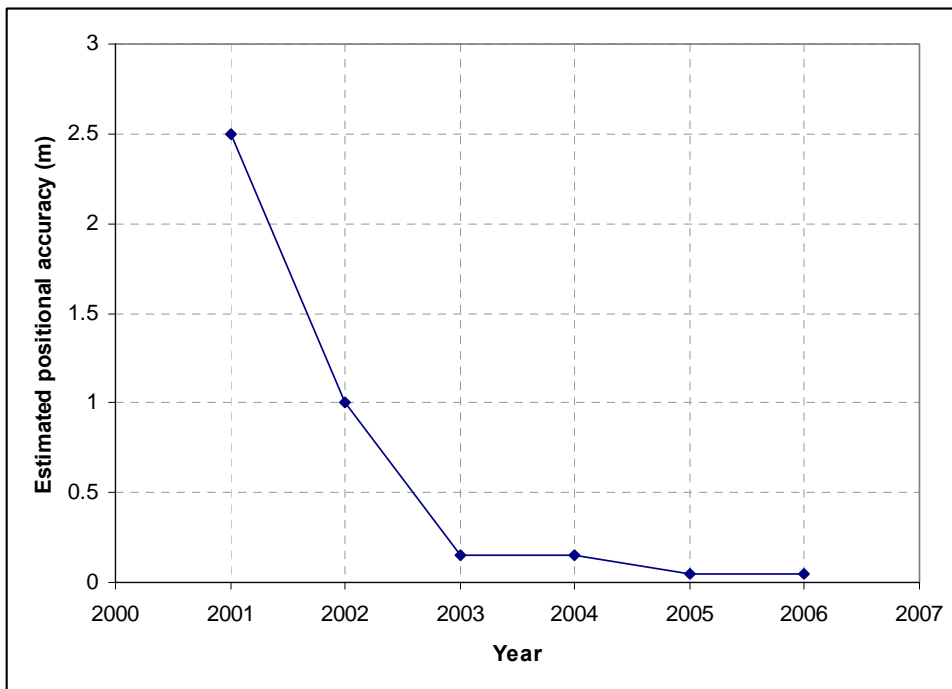
Figure 3-5 Estimated development of model (scanner + GPS) positional accuracy during project

The range-finding accuracy is quoted as 50 mm for the Riegl LPM2K and 25mm for the Riegl LPMi800HA laser scanners, though repeatability is considerably better. It was found that baseline distances of 50 to 100 m were capable of re-measurement to 0.5 mm (1 in 500,000). These values are largely unaffected by range if atmospheric conditions are ignored. With regards to scanning capability the pan/tilt mount is quoted as having a stepper motor accuracy of 0.009°. This represents a movement of 16 mm per 100 m range (Figure 3-3). The quoted laser beam divergence for the LPM2K and LPMi800HA scanners is 0.8 mrad. This is equivalent to an 80 mm increase of beam width per 100 m range (Figure 3-4). Other ranges are linearly proportional in each case. The significance of this is that where a scan involves large distances, those far objects will be less well defined in terms of position and form than close objects. For example, at a range of 500 m, the laser footprint is about 0.4 m in diameter. This factor particularly affects objects inclined at an acute angle to the direction of the laser beam, i.e. not face-on. An estimate of the improvements in the overall positional accuracy of the combined 'scanner + GPS' system during the project is shown in Figure 3-5, showing how accuracy has improved during the project life from around 2.5 m to <20 cm in the later scans. These improvements have been largely due to equipment upgrades.

The possibility of proliferation of errors in terrestrial LiDAR is considered by Buckley *et al.* (2008). They stated that "although LiDAR data provide a much higher level of accuracy and resolution than traditional field work, an awareness of the sources of error and uncertainty in the workflow, from data collection to modelling, is necessary". This conclusion has been borne out by the authors' experience in preparing the data for this report. One of the key problems has been that not all the project data are of equivalent accuracy. Determining where the errors lie in any survey has been a major undertaking, in part due to the fact that, as also stated by Buckley *et al.* (2008), there has been little guidance in these matters in the literature.

3.2   DATA PROCESSING

The terrestrial LiDAR data produced by the oriented laser scan and GPS survey were processed to develop a 3-D terrain model of the cliff. The raw data produced by the RiPROFILE™ program consisted of 'point-clouds' comprising between 6,100 *x, y, z* points for the September 2001 Weybourne survey to 3,432,363 *x, y, z* points for the September 2006

13

Happisburgh survey. These data were oriented using the relative GPS positions of both the scanner and the backsights, and output as an ASCII file, made up of *x*, *y*, *z* and intensity values. The data were imported into GoCAD 2.1.5 (a digital 3-D drawing program) where outlying or extraneous data points and artifacts (e.g. birds caught in the scan, distant 'overshoot' points etc.) were removed and the 'cleaned' data exported. The data were imported into Surfer™ 8 (a surface mapping program) and triangulated using a geostatistical gridding method to produce a solid surface model. From this model cross-sections and volumes could be extracted, and change models calculated. The data were also imported into QT Modeler™ 5.1 (a 3-D model manipulation package), gridded and displayed as a 3-D surface model. The resulting model could then be enhanced by overlaying photographs, maps or intensity colouration onto it.

More recently, the 'IMAlign' package within Polyworks (InnovMetrics ™) has been used to align individual scans, to check for errors in orientation and to produce the final surface 3-D models.
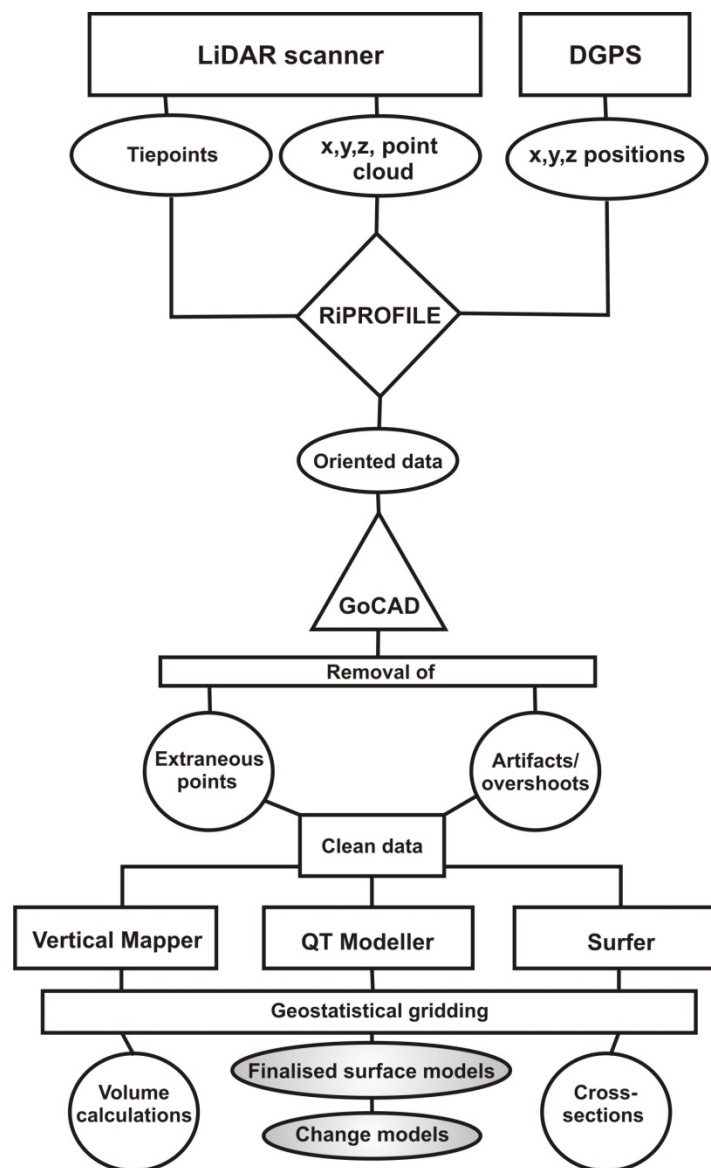
Figure 3-6 Work Flow model for the processing of laser scanned data

3.3 SLOPE STABILITY ANALYSIS

Slope stability analyses were carried out for the Happisburgh and Sidestrand test sites at each of the survey epochs between 2000 and 2006 at three locations within each test site. It was not considered appropriate for the Weybourne test site as the amount and type of slope instability were not suitable for modelling. One outcome of slope stability analysis was to have been the investigation of a concept called *slope stability index* whereby factors of safety against sliding are used to characterise the stability of 3-D cliff zones.

The program used to evaluate the stability of the cliffs was FLACslope™ (produced by the Itasca Corp.) This is a 2-D finite element module of the FLAC suite designed specifically for slopes (Griffiths and Lane, 1999). It is ideally suited to providing a first-time 'look' at a slope where the slip surface location is unknown. Such methods are described as providing a 'natural' analysis (Griffiths and Lane, 1999); that is, the nature of the failure is not forced, but develops naturally as a result of the deformation resolution of a grid of nodes in response to the imposition of a static force regime created by the self-weight of the geological strata.

The FLACslope programme produces a factor of safety based on the principle of strength reduction (Dawson *et al.*, 1999). In common with other finite element programmes, and other modules within the FLAC suite, the calculations are made by iterations of static stresses within a rectangular mesh. The output also features vectors and contours of shear strain. In most analyses these can be interpreted as slip planes or zones.

Each model was defined by inputting the following data:

- Ground surface profile (cross-sections derived from laser scan DEM)
- Geological layers and thicknesses (either measured or estimated)
- Water table profile (estimated)
- Geotechnical parameters (strength and density – either measured or estimated).

The analyses were run using a 'friction/cohesion' model applied to a 'fine' finite element mesh.

The ground surface profile was obtained directly from cross-sections derived from the terrestrial LiDAR digital elevation model (DEM) for each monitoring epoch, by means of a common line reference in space 'cutting' each of the models aligned in the direction of perceived maximum recession.

The geological layers were obtained based on observation of formation thicknesses in cliff and platform exposures, and using photos and measurements taken from the Terrestrial LiDAR models. The same layers and thicknesses were used at each section for all epochs. It should be noted that the program does not allow for layers to cross-cut other layers (all layers must be vertically sequential). This effectively rules out the inclusion in the model of pre-existing landslide deposits. This is not an issue at Happisburgh as landslide debris does not remain on the cliff, due to its steepness, the soft geology and the aggressive action of the sea. However, it is an issue at the Sidestrand test site where landslide debris accumulates on the cliff slope. Thus, any landslide deposits, whilst included in the slope profile, are nevertheless not distinguished from the bedrock formations. For this reason, any planes or zones of weakness unrelated to bedding cannot be represented. This is not the case for 'limit equilibrium' slope stability analysis methods such as described in Hutchinson (1976). However, such methods require the input of shear plane geometry. In most cases for this project, this information is unknown and, importantly, cannot be applied to automated models.

It was not possible to locate the water table by observation as no sub-surface observations were made and no relevant boreholes or water well data were found during the desk study for either Happisburgh or Sidestrand. However, in the case of Happisburgh an estimate was made

using observations of seepage on the cliff face, with the far-field position taken as slightly above the Happisburgh Sand Formation and Ostend Clay Formation boundary. Clearly, transient surface run-off, in response to major rainfall events, is a major factor in the erosion of cliffs at Happisburgh. However, it was not possible to apply this to the slope stability model, and in any event no direct observations were made of water levels (refer to Section 4.7.1). At Sidestrand the ground water regime is likely to be complex, involving as it does a topographic low aligned roughly with the hamlet of Sidestrand and the glaciotectonic syncline straddling the test site.

Geotechnical parameters for strength and density were assigned to each geological layer in the model. These were derived either from field and laboratory tests carried out by BGS or from databases of materials representative of the geological layers present. The main problem when assigning such properties is that laboratory-derived 'intact' values, and to a lesser extent field-based values, frequently differ considerably from conceptual 'mass' values for the formation as a whole. Even field-derived values, such as those from the Panda penetrometer may fail to provide true 'mass' properties. For most materials 'mass' strength is considered to be less than 'intact' strength, due for example to structural features such as joints and faults, or due to stress relief. This would suggest that the use of 'mass' strength in slope stability analysis would result in lower factors of safety than would be the case using 'intact' data. However, the reverse is the case for density, as 'mass' densities are usually less than 'intact' densities and result in higher factors of safety, as the 'driving' forces for landslides increase with increasing density. 'Mass' strength and density data are usually unavailable from conventional investigations, and therefore have to be estimated.

The results of the slope stability analysis exercise are discussed for Happisburgh and Sidestrand in sections 4.10.1 and 5.9.1, respectively.

3.4   GEOTECHNICAL SAMPLING AND TESTING

3.4.1 General

Where sampling could be carried out in safety, a limited number of disturbed and undisturbed samples were taken of representative lithologies at the three Norfolk sites; both from landslipped and unslipped deposits within the cliff. The samples were returned to BGS (Keyworth) for geotechnical testing in the soil mechanics laboratories. In addition, in-situ ultra-lightweight penetrometer tests were carried out at Happisburgh and Sidestrand.

3.4.2 Sampling

Disturbed samples for index testing were collected in medium and large plastic bags. Undisturbed samples were collected by an established BGS method utilising 100 mm diameter x 250 mm long plastic tubes with a metal cutter (Figure 3-7). This requires preparation of a 'plinth' of in-situ material approximately 300 x 300 mm in plan, and at least 250 mm in height, into which the tube and cutter are carefully lowered using a combination of gentle downward pressure and trimming around the cutter with a sharp knife. The filled tube is then recovered by breaking the connection with the plinth at the base, removing the metal cutter and its contents using a cheese wire, and finally trimming the ends of the tube with a knife and straight edge. The ends are sealed with plastic caps, taped to prevent moisture loss, and the sample is then ready for transport. The contents of the cutter are removed and saved in a 'medium' plastic bag so that the cutter is ready for the next sampler. The cylindrical shape of the sample maximises its structural integrity and reduces the likelihood of damage in transit. The method minimises the amount of preparation, and hence disturbance, required in the laboratory when compared with a conventional cuboid-shaped block sample. The method also allows accurate determinations of density to be made, as the dimensions and weight of

the specimen are measured in the laboratory. The tube method is suitable for clays and silts but not for sands or gravels.

NOTE: The tube method is intended to provide specimens for triaxial testing (which uses a cylindrical specimen). When preparing a shear box sample in the field a cuboid–shaped sample prepared in a similar manner but using a metal box with lids, and of a size slightly larger than the final test specimen, is preferable. However, a small (50 mm) shear-box specimen can be prepared from a tube sample.
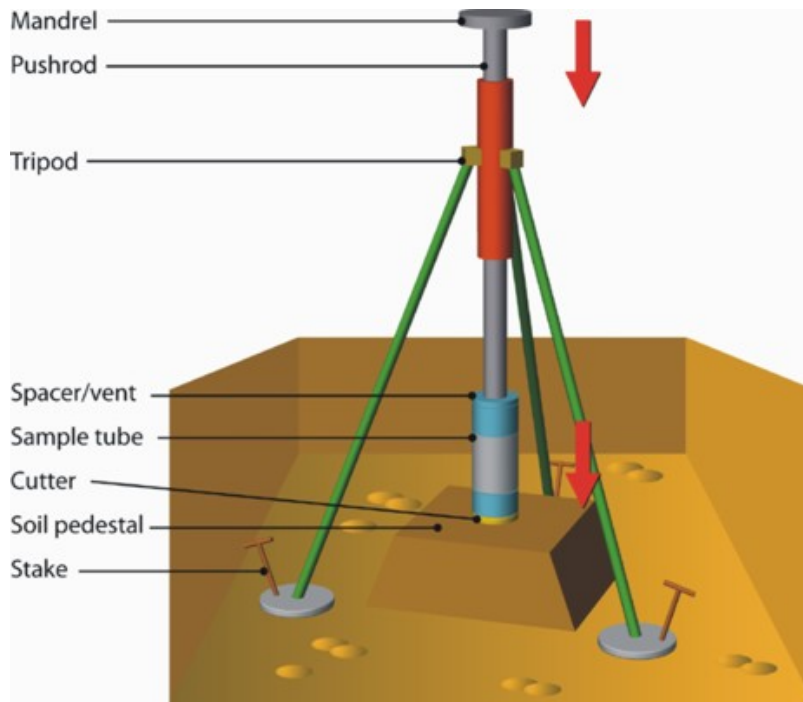
Figure 3-7 BGS tube sampler for obtaining 'undisturbed' cylindrical specimens

3.4.3 Laboratory testing

The laboratory *index* testing programme consisted of determinations of: particle-size, moisture content, density, Atterberg Limits (liquid and plastic limits). These were carried out according to BS1377 (1990) in the BGS (Keyworth) soil mechanics laboratories.

The laboratory *mechanical* testing programme consisted of triaxial testing using a GDS 100 mm stress-path system. The test used was the multi-stage 'consolidated isotropic undrained' (CIU) with pore pressure measurements (Head, 1996), allowing 'peak' effective strength parameters to be measured at effective average stresses of 100, 200 and 400 kPa applied to a single specimen. The specimen size was 102 mm diameter with a target length to diameter ratio of 2:1. Top, bottom, and side drains were used to facilitate consolidation. The specimen was saturated, prior to stage 1 isotropic consolidation, by staged ramping-up to an elevated (back) pressure; the final value being determined by the 'B-test' (i.e. pore pressure response to applied load increment). Axial compression was applied in the undrained state following each consolidation stage, with pore pressures measured at either end of the specimen. Stages 1 & 2 of axial compression were discontinued when the stress ratio reached a peak, whereas the stage 3 axial compression was continued beyond shear failure. A post-failure specimen is shown in Figure 3-8.

Figure 3-8 Post-failure triaxial test specimen (principal shear surface shown by red arrows)

3.4.4 Field testing

Field testing consisted of cone penetrometer tests on the cliffs using the Panda (Types 1 & 2) ultra-lightweight penetrometer apparatus (Figure 3-9 and Figure 3-10). The principal difference between these is that the Type 2 has a solid state accelerometer in the anvil, whereas the Type 1 has a plunger and transducer. The hammers for the two types also differ whilst the cones and rods are identical.

Figure 3-9 Panda™ ultra-lightweight penetrometer (Type 1) Note: alternative cones (right)

18

Figure 3-10 Panda™ ultra-lightweight penetrometer (Type 2)

The Panda is an ultra-lightweight hand-operated cone penetrometer with variable energy input, capable of penetrating soil and other unbound material to 10 m depth and very weak rock to a depth of about 2 m. In the Type 2 PANDA, the anvil at the top of the rod train contains an accelerometer which measures the speed of the hammer impact. A retractable tape measures the penetration produced by each blow. Each of the half-metre length rods weighs 0.58 kg, whilst the small and large cones 0.033 kg and 0.062 kg, respectively. From these data the energy at the cone tip is calculated.

There are two alternative cones: the first is a large (4cm^2 area) disposable cone and the second a small (2cm^2 area) non-disposable cone. The former is suited to weak cohesive soils, whilst the latter is suited to non-cohesive soils and weak rocks. The results are produced in the form of a penetrogram showing variation of penetration resistance (MPa) with depth (m).

Analysis based on the *potential* energy equation:

$$E = m \times g \times h$$

is defined by the manufacturer as follows (adapted from Langton, 1999):

$$q'_d(z) = \frac{E}{x}$$

$$q'_d(z) = \frac{1}{A \times x} \times m \times g \times h \times \frac{m}{m + p}$$

where: q'_d is cone penetration resistance at given depth z
E is hammering energy
x is drive in depth
m is mass of hammer
h is drop height of hammer.
A is cone area
p is rod train weight
g is acceleration due to gravity

Alternatively, analysis of the data may be based on the formula for *kinetic* energy, E:

$$E = \frac{1}{2}mv^2$$

19

as follows (Langton, 1999):

$$q_d = \frac{1}{A} \times \frac{\frac{1}{2} \times m \times v^2}{1 + \frac{p}{m}} \times \frac{1}{x}$$

where: v is velocity

The kinetic energy alternative may be considered preferable due to the variable energy input of each hammer blow by the operator.

The following are some published empirical relationships quoted, from work carried out in France and the UK, in Langton (1999):

$$1q_d = 1 \; CPT \; (MPa)$$

$$1q_d = c_u/15 \text{ to } 20$$

$$\log_{10}CBR = 0.352 + 1.057.\log_{10}q_d \; (MPa)$$

Research by the Transport Research Laboratory (Amor *et al.*, 1999) showed that the Panda gave a good correlation with other types of dynamic cone penetration (DCP) and a good approximation to static cone resistance (q_t), and thereby a correlation via Butcher *et al.* (1997) with the Standard Penetration Test (SPT) as follows:

$$0.1 \text{ to } 0.2 \; SPT(N) = 1 \; q_d \; (MPa)$$

4 Case Study: Happisburgh, Norfolk

4.1   INTRODUCTION

One of the twelve test sites of the Slope Dynamics project includes a section of cliffs adjacent to the village of Happisburgh [NGR TG38003100] on Norfolk's North Sea coast, approximately 25 km northeast of Norwich (Figure 1-1). Agriculture and tourism contribute significantly to the economy of the village and surrounding hinterland although this is threatened by the receding cliff line and has claimed several properties from Beach Road (Figure 4-1) plus significant quantities of agricultural land. A section of coast further north of the study location is a designated Site of Special Scientific Interest (SSSI; Figure 4-1). Over the monitoring period, 2001 to 2006, considerable media coverage of the erosion at Beach Road has been generated with Happisburgh featured in many news and documentary programmes, both in the UK and abroad.
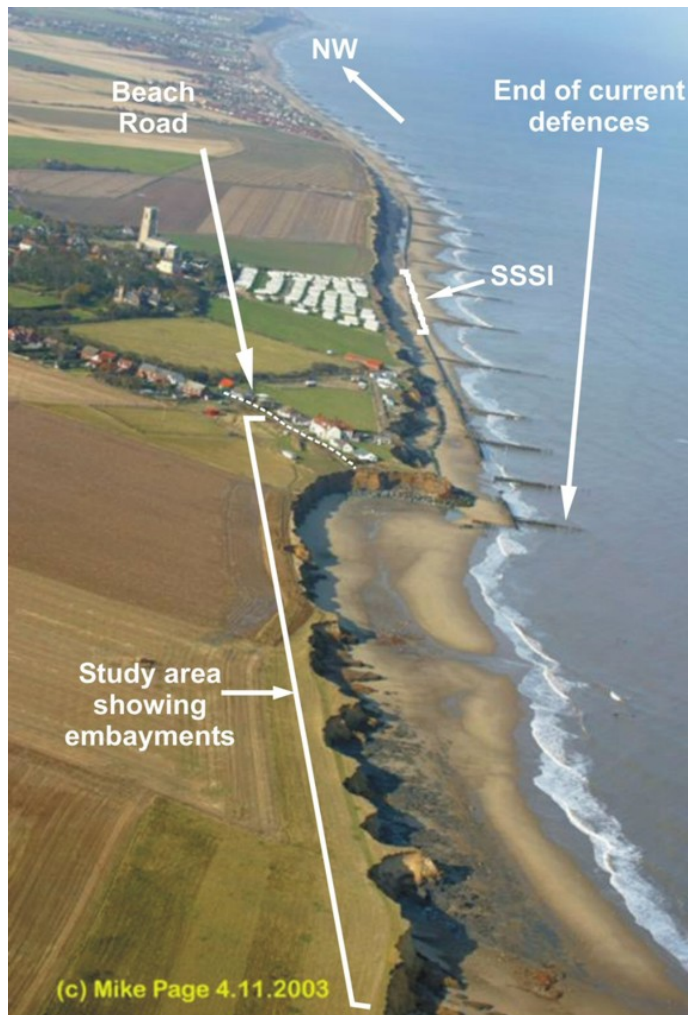
Figure 4-1 Aerial photograph at Happisburgh taken in 2003, facing north, showing the point where the sea defences have failed and been removed.
This sea defence line was once continuous. Also marked is the "Happisburgh Cliffs SSSI" and the study area. Photograph courtesy of Mike Page, Skyview.

4.2   SURVEY ACTIVITIES

Several field visits have been made to the site over the 5 year survey period. These have mainly been monitoring surveys but have also included reconnaissance/geological surveys. Geotechnical testing and sampling was carried out for the early monitoring surveys in 2001-2002.   Over the period, the laser-scanning and GPS equipment has been progressively upgraded and, in the early part, terrestrial photogrammetry trials were carried out by BGS. The monitoring programme to date for the Happisburgh test site is shown in Appendix 1. Details of survey activities are given in Appendix 5.

4.3   LIDAR SURVEYS

The position of scans taken in 2006 at the Happisburgh site is shown in Figure 4-2.

- In 2001, two scans were carried out from two scan positions, both from the foreshore. In total, the survey captured 7,183 points on the cliff surface and the adjacent cliff top and foreshore areas.

- In 2002, four scans (one in April, three in September) were carried out from three scan positions (one site identical in both visits), three from the cliff edge (due to poor tidal conditions) and only one from the foreshore. In total, the survey captured 12,669 points on the cliff surface and the adjacent cliff top and foreshore areas.

21

- In 2003, four scans were carried out from three scan positions, all from the foreshore. In total, the survey captured 11,736 points on the cliff surface and the adjacent cliff top and foreshore areas.

- In 2004, five scans were carried out from three scan positions, all from the foreshore. In total, the survey captured 15,987 points on the cliff surface and the adjacent cliff top and foreshore areas.

- In 2005, eleven scans were carried out from four scan positions, all from the foreshore. In total, the survey captured 1,707,699 points on the cliff surface and the adjacent cliff top and foreshore areas.

- In 2006, seven scans were carried out from three scan positions, all from the foreshore. In total, the survey captured 3,432,363 points on the cliff surface and the adjacent cliff top and foreshore areas.

Figure 4-2 Location of 2006 scan positions relative to the 2006 cliff line at Happisburgh
(NOTE: aerial photo 1999). Scan positions NGR: 638621, 330778. 638659, 330743. 638720, 330692.

4.4   RAINFALL

Monthly and annual rainfall averages for the area around Happisburgh were obtained from the Met Office for weather stations at Coltishall located 14.8 km from Happisburgh and at Barton Hall located 9.2 km from Happisburgh (Figure 4-3 and Figure 4-4). Rainfall data show that over the period of monitoring in Happisburgh annual average rainfall has remained within a range of 20 mm.

- The driest year recorded for the survey period was 2003, with a monthly average of approximately 44 mm.

- The wettest year over the scanning period was 2001 with a high of 67.8 mm of rainfall.

- **2000** – Wet months were recorded in May as well as between September and November

- **2001** - A very wet year with high rainfall in Feb and March as well as between June and September. These wet months were followed by a very dry October and December.

22

- **2002-2003**- Very dry with a more typical wet winter (October-December 2002) and a dry summer in 2003. The highest rainfall in 2003 was in June but this was followed by a very dry August and September.

- **2004**- Annual average rainfall began to increase, a trend that carried on through to 2006.

- **2005**- Peak rainfall this year was in July followed by the second driest month after January, which was August.

- **2006** – A very wet August, September and November were offset against a dry June and July.
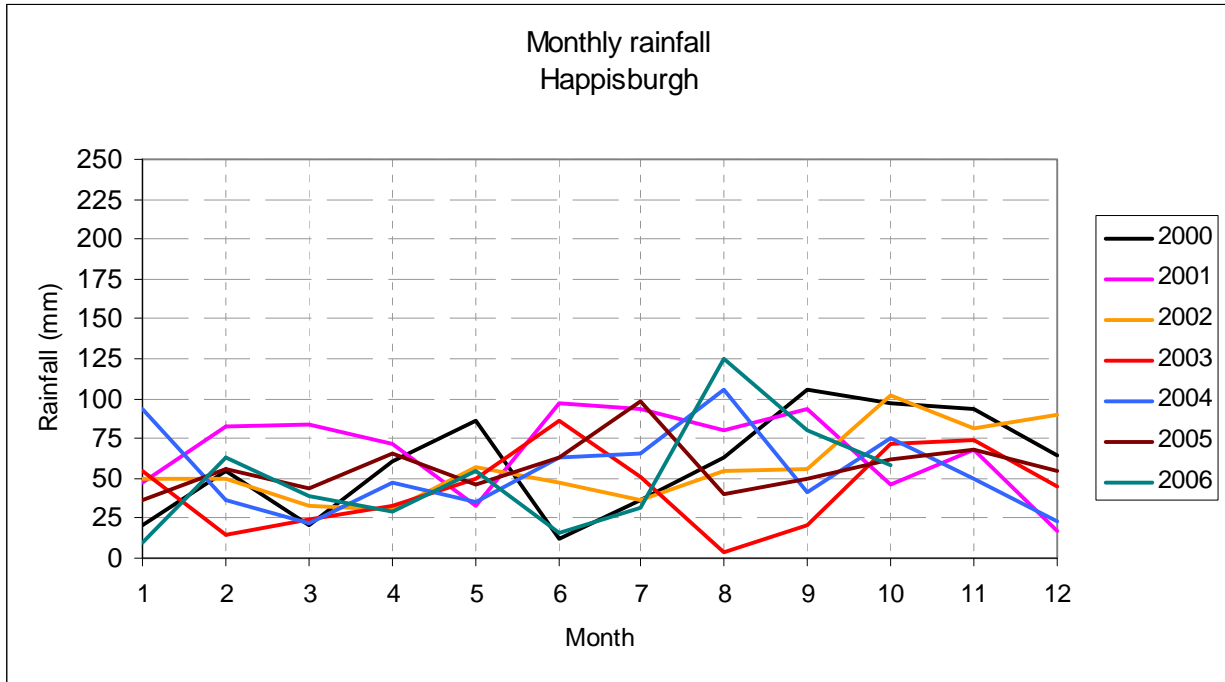
Figure 4-3 Rainfall – monthly averages for Barton Hall (2000 & 2005, 2006) and Coltishall (2001-2004)
(Source: Met Office)
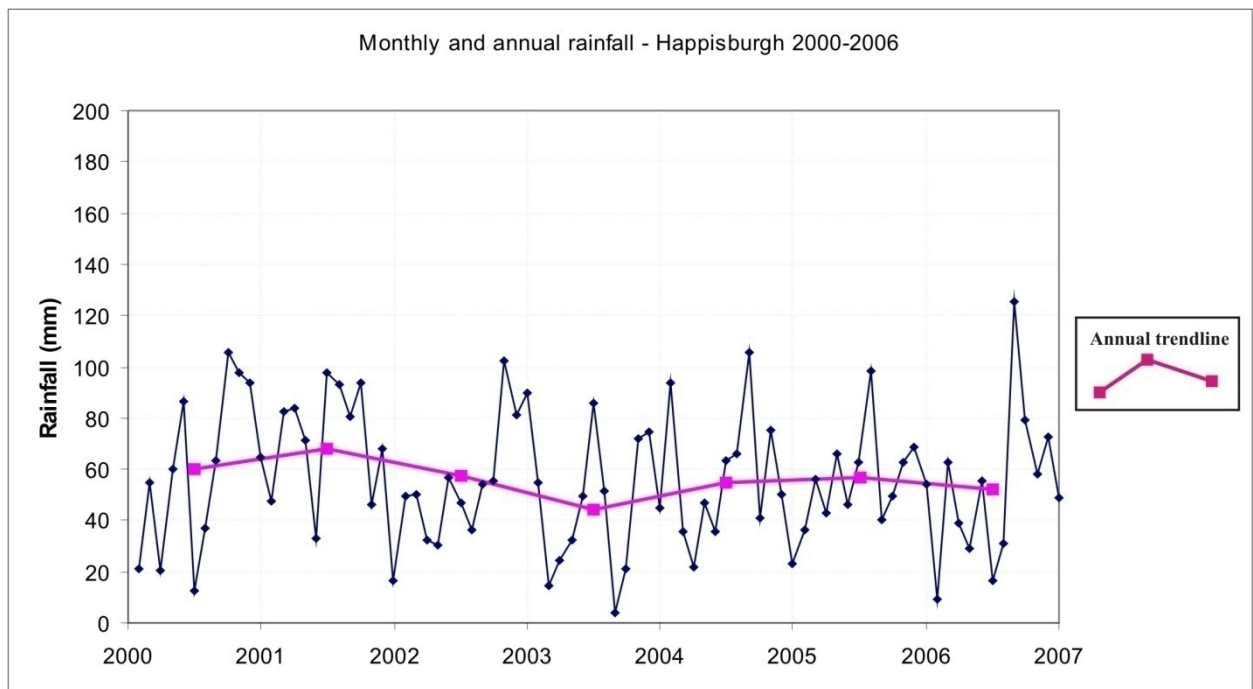
Figure 4-4 Rainfall – monthly and annual averages – Barton Hall (2000, 2005-2006), Coltishall (2002-2004)
(Source: Met Office)

4.5 GEOLOGY

The cliffs at Happisburgh range in height from 6 to 10 m and are composed of a Middle Pleistocene layer-cake sequence of several tills, separated by beds of stratified glaciolacustrine clays and deltaic sands (Hart, 1987, 1999; Lee, 2003; Lunkka, 1988). Previously they have been assigned to the 'North Sea Drift' group of sediments based on their inferred Scandinavian provenance and their Anglian-age, however detailed lithological and sedimentological investigations have since demonstrated that they are of British provenance (Lee *et al.*, 2002), and were deposited during different Middle Pleistocene glaciations (Hamblin, 2000; Lee *et al.*, 2004b). As a consequence of this, a new stratigraphic scheme for northern East Anglia has been proposed, with the coastal locality of Happisburgh representing a critical site since it is the stratotype of the new Happisburgh Formation (Lee *et al.*, 2004a). Five of the six stratigraphic units belong to the Happisburgh Formation, whilst the remaining unit – the Walcott Till Member, forms part of the Lowestoft Formation (Table 4-1).

The basal unit within the stratigraphic succession at Happisburgh is the How Hill Member of the Wroxham Crag Formation. These deposits are typically buried beneath modern beach material but are periodically exposed following storms (Figure 4-28). They consist of stratified brown sands and clays with occasional quartzose-rich gravel seams that are interpreted as inter-tidal/shallow marine in origin.

Unconformably overlying these marine deposits are a series of glacial lithologies deposited during several advances of glacier ice into the region during the Middle Pleistocene (c.780 to 430 ka BP) (Lee *et al.*, 2004b; Lee *et al.*, 2002). The site investigated for the purpose of this study, is located adjacent to Beach Road (Figure 4-1; NGR TG38573084) where a tripartite geological succession can be observed. The Happisburgh Till Member crops-out at the base of the cliffs and its base is frequently obscured by modern beach material. The Happisburgh Till Member is a dark grey, highly consolidated till with a matrix composed of largely massive clayey silty sand with rare pebbles of local and far-travelled material such as sheared inclusions of crushed chalk and Crag material. It reaches a maximum thickness of 3 m at the study locality and texturally, is classified as a diamictic clayey-sand with occasional stones (<1%). It was deposited as subglacial deformation till that accreted by processes of subglacial lodgement and pervasive sub-horizontal shearing (Hart, 1999; Lee, 2001) beneath the British Ice Sheet (Lee *et al.*, 2002). The upper surface of the till undulates and comprises a series of ridges and troughs that formed beneath the ice margin during phases of both active and passive flow behaviour (Lee, 2003; Lunkka, 1994). The overlying Ostend Clay member infills these troughs. This unit is between 2.3 and 3.4 m thick and consists of thinly-laminated light grey silts and dark grey clays. The lowest facies of this unit that occupy the depressions between the ridge crests, are composed of intercalated slumped diamictic material and fine grained water-lain deposits. These pass upwards into thinly laminated silts and clays that were laid down in a shallow (but expanding and deepening) lake basin by turbidites and background suspension settling.

Truncating the upper surface of the Ostend Clay Member is the Happisburgh Sand Member. Approximately 2 to 4 m of this deposit outcrop within the upper parts of the cliffs at the study section, however the unit thickens considerably southwards as the beds are gently inclined in this direction forming the northern limb of a syncline. The Happisburgh Sand Member is composed of massive and horizontal bedded sands with occasional sandy clay layers, representing fluctuating bed-load conditions. These pass upwards into rippled sands (low climb), planar cross-bedding with clay drapes, and shallow channel structures. These sediments are representative of incision and migrating sand bars within a glacial outwash stream. The presence of clay drapes indicates periods of quiet-water sedimentation. They are interpreted as the bottom- and top-set of a prograding delta.

The Corton Till Member does not outcrop within the study section but can be observed several hundred metres to the south where the Happisburgh Till Member (and intervening

units) have dipped beneath the level of the foreshore. The unit rests conformably upon the Happisburgh Sand Member and consists of an olive brown matrix-supported sandy, clast-poor diamicton. The diamicton exhibits a stratified appearance, consisting of beds of massive diamicton (which exhibit grading, variable sorting) with occasional thin sandy stringers, separated by elongate lenses of sand that lie parallel to the plane of bedding. The Corton Till Member is interpreted as a sub-aqueous flow till (Lee, 2003).

Table 4-1 Middle Pleistocene lithostratigraphy and palæoenvironments at Happisburgh.

Lithostratigraphy (Formation / Member)	Palaeoenvironment	Chronostratigraphy
LOWESTOFT FORMATION	Glaciogenic – British Ice source	ANGLIAN
Walcott Till Member	Subglacial till	GLACIATION
HAPPISBURGH FORMATION	Glaciogenic – British Ice source	
Corton Sand Member	Glaciofluvial / deltaic	
Corton Till Member	Subaqueous flow till	HAPPISBURGH
Happisburgh Sand Member	Prograding delta	GLACIATION
Ostend Clay Member	Glaciolacustrine lake basin	
Happisburgh Till Member	Subglacial till	
WROXHAM CRAG FORMATION	Pre-glacial, shallow marine inter-tidal	CROMERIAN COMPLEX
How Hill Member		

The Corton Sand Member outcrops above the Corton Till Member to the south of the study location the northern limb of the syncline. The contact between the two lithofacies is sharp and in places conformable, and often marked by the development of a thin (<1 cm) iron pan. The lowest 7m of the unit consists of beds of yellowish brown massive and horizontal bedded sand with occasional mud flasers, and 0.5 - 1.5 m thick beds of poorly-sorted strong brown clayey sand that exhibit convolute beds and thin laminations of sorted sand. These beds pass upwards into approximately 5 m of horizontal and trough cross-bedded sands with common shallow channel structures.

Massive and horizontally-bedded sands imply that sedimentation of the lower 7 m of the lithofacies was generally rapid but frequented by variability in both the flow regime and the sediment supply. Supporting this interpretation are the mud flasers, representing phases of still-water deposition, and the thick beds of poorly sorted clayey-sand which probably arise from major sediment influx events that overwhelmed the depositional system. Thin sandy stringers within these beds are considered to be a consequence of localised traction current reworking. The overlying trough cross-bedded and channelised sands record the downcurrent migration of lunate sub-aqueous bars and the localised incision of small channels. The association of the lower and upper facies are typical of deltas where the former represent the delta foreset and the latter, the delta topset.

The Walcott Till Member unconformably overlies the Corton Sand Member in the centre of the syncline to the south of the study location. It exhibits a massive olive-yellow appearance, clast-poor and possesses a silt-rich matrix texture, with variable quantities of sand and clay. It is distinctive due to its high chalk content (both clast and matrix). Further to the north towards Ostend, the contact with the underlying deposits was examined in detail and was

sharp and planar in morphology. Underlying sediments were highly tectonised with a direction of shear application from the northwest. The sum of the available sedimentological evidence indicates that the Walcott Till Member was deposited subglacially by grounded ice crossing the region from the northwest.

4.6 GEOTECHNICS

A geotechnical study was carried out at the Happisburgh test site. This consisted of a limited suite of field and laboratory tests on selected horizons. Index and strength properties were determined; the latter using a single triaxial (lab) test and a set of Panda ultra-light penetrometer (field) tests. Engineering field descriptions of the main units are tabulated in Table 4-2. Some additional index properties from the literature are also summarised for comparison in Table 4-7. Where applicable, geotechnical testing was carried out according to BS1377:1990.

A number of in-situ Panda ultra-lightweight penetrometer tests were carried out at Happisburgh at different lithostratigraphic horizons on the cliff and platform (Table 4-3). The resulting profiles were combined to form a partial synthetic profile of undrained strength of the cliff and platform, as shown in Figure 4-5. The profile is notable in that there is a marked decrease in strength within the Happisburgh Sand Member from the cliff-top to a depth of 2.5 m. The member varies from 'very loose' to 'dense' in consistency with two distinctive weaker/looser horizons at 0.9 and 2.0m. The remainder of this member was not tested. The high values near the cliff-top are due to a stony layer beneath the topsoil. However, the Ostend Clay Formation, though thin, constitutes a distinct weak zone with 'very soft' to 'soft' consistencies. The variation in stiffness may distinguish the silt, clay and sand rich laminations and beds. Within the underlying Happisburgh Till Member there is a rapid strength increase with depth. The weakening of material may be due to the effect of surface weathering and stress release, and changes in water content with depth.

Table 4-2 Summary engineering descriptions

	Happisburgh Till Member (deformation till)	Ostend Clay Member (glaciolacustrine)	Happisburgh Sand Member (glacio-deltaic)
Thickness (m)	3.0	2.3 – 2.4	2.0 – 4.0
Lithological descriptions made to BS5930 (1999)	Stiff to very stiff fissured grey clayey sandy silt with occasional gravel and rare cobbles. The matrix is chalky in parts. Sand and gravel includes weak white chalk, flint, belemnites, quartzite, schist, gneiss and igneous rocks (probably Scottish and Scandinavian origin).	At base, variable thickness of multicoloured laminated silty clay, silt and sand with cross-bedding and contorted thick laminations of orange fine sand and blue clay. Passes up into stiff, fissured grey blue laminated clay and silt with occasional stratified sand laminations.	Very loose to dense orange and yellow thickly bedded massive and cross-bedded quartzitic fine sand and clayey sand with occasional clay laminae.
Discontinuities	Sub horizontal shear zones picked out by chalk smears. Folding and faulting. Deformation till. Some very strong cobbles.	Small scale folding and faulting. Persistent undulating shear zones with white chalky smear at basal boundary.	Prone to seepage and sapping erosion at its basal boundary and along clay drapes.

Table 4-3 Panda ultra-lightweight penetrometer tests in Happisburgh Till Formation

PANDA			
Date	Member	Penetration Depth (m)	Test Number (Location)
19/04/01	Happisburgh Till Member	0.66	HAP1 (1.5m above beach, 6m below cliff-top)
19/04/01	Happisburgh Till Member	0.69	HAP2 (as for *HAP1*)
19/04/01	Ostend Clay Member	0.65	HAP3 (30m NW of *HAP1*, 4m above beach, 3.5m above U100 sample)
10/09/03	Happisburgh Sand Member	2.53	HAP4 (Taken from cliff-top)
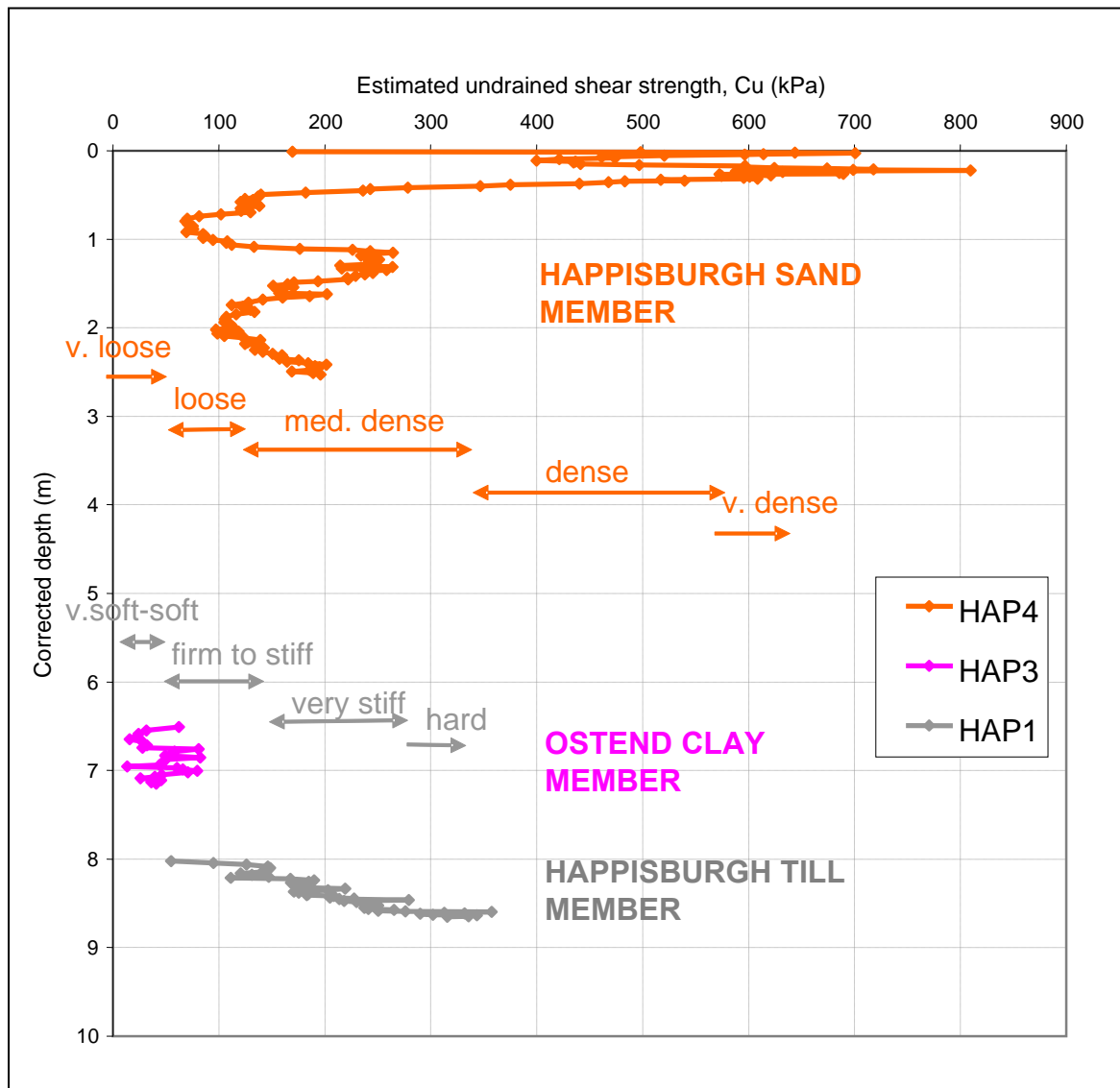
Figure 4-5 Composite shear strength (partial) profile (from depth-corrected Panda profiles, refer to Table 4-3 for explanation of geology names)

Geotechnical samples including Bulk and Undisturbed samples were collected for index and strength testing. Samples are listed in Table 4-4.

Table 4-4 Geotechnical samples taken at Happisburgh

SAMPLE				
Date	**Formation / Member**	**Depth**	**Type**	**Location / Lithology**
19/04/01	Ostend Clay Member	0m	m. bag	HB1 (Upper Till)
19/04/01	Happisburgh Till Member	0m	m. bag	HB2 (Lower Till)
19/04/01	Happisburgh Till Member	0m	m. bag	HB3 (cutting from sample *HB4*)
19/04/01	Happisburgh Till Member	0.25m	U100	HB4 (Lower Till)
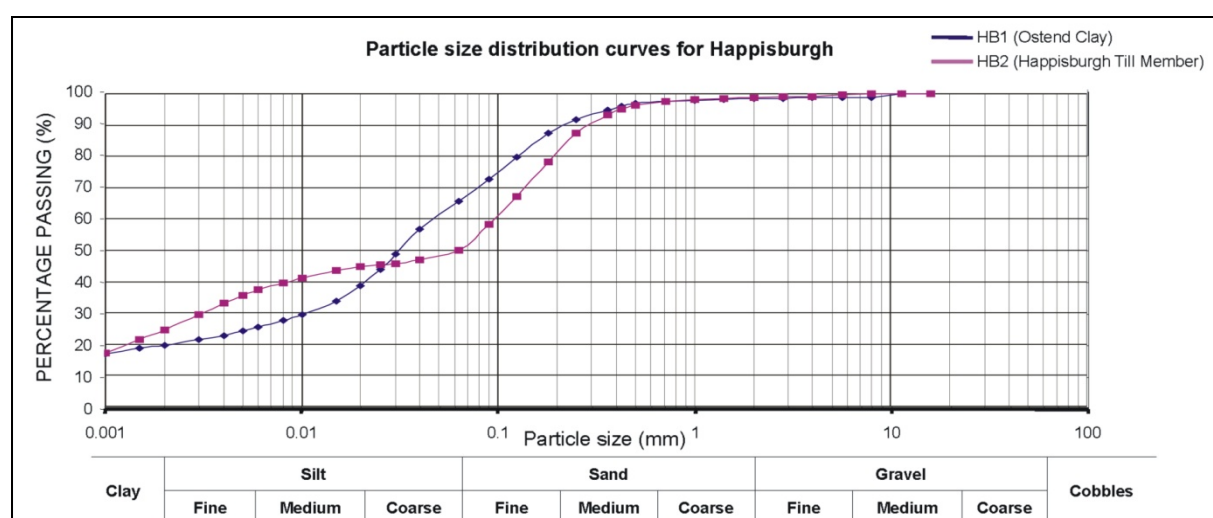
Figure 4-6 Particle size distribution curves for Happisburgh Till and Ostend Clay Members

The particle-size data (Table 4-5) indicate that the Ostend Clay Member (sample HB1) is a well-graded sandy clayey silt, whilst the Happisburgh Till Member (sample HB2) is a gap-graded clayey silty sand with little or no clast content. It is likely that the results for sample HB2 are unrepresentative in terms of the coarse gravel content. Kazi & Knill (1969) report clay contents between 20 and 25 % in the Happisburgh Till, which matches our particle size determination shown in Table 4-5. Bell (2002), records 18-30% Clay, 18-32% Silt, and 28-64% Sand in the Happisburgh till (previously referred to as the Lower Cromer Till). Pawley *et al*. (2004) gave agreeable mean averages of 22% Clay, 27% Silt, and 51% Sand.

Table 4-5 Summary of particle-size data

Sample	Member	Clay (%)	Silt (%)	Sand (%)	Gravel (%)
HB1	Ostend Clay	19.7	45.8	32.8	1.7
HB2	Happisburgh Till	24.5	25.6	48.7	1.2

Plasticity data and linear shrinkage data are shown in Table 4-6. Norfolk tills generally contain 'inactive' to normally active clays with low sensitivity and consolidation

characteristics typical if stiff clays (Bell, 2002). The BGS data in Table 4-6 suggest the clay matrix of the Happisburgh Till is of low to intermediate plasticity and the Ostend Clay Member also low to intermediate plasticity. However, Table 4-5 shows that sample HB1 has a high silt content and may be from a silt rich lamination. Kazi & Knill (1969) reported a low to high plasticity range after testing specifically clay (50%) and silt laminations at Happisburgh. A low to high range may be more representative of the mass. They also show that liquid limit decreases with depth ranging from high to low. Liquid limit also decreases laterally eastward near Happisburgh. These variations may be due a decrease in silt/sand input during sedimentation, and not necessarily clay mineralogy. The behaviour low plasticity clays can be sensitive to even small changes in moisture content Bell and Forster, 1991. This means that even a small increase in water content of a few percent by weathering can change the clays phase from a brittle solid material to a plastic solid.

Table 4-6 Plasticity and linear shrinkage data where w_L = Liquid limit, w_p = Plastic limit, I_P = Plasticity index, LS = Linear shrinkage, w = Natural water content.
Samples refer to Table 4-4.

Sample	w_L (%)	w_P (%)	I_p (%)	LS (%)	LS @ w (%)
HB1	27.5	18.5	9.0	5.2	27.8
HB2	31.4	14.6	16.8	10.5	32.4
HB3	31.0	15.0	16.0	9.8	33.5

As the Happisburgh Till is generally fissured clay, the unconfined compressive strength test results published by Kazi & Knill 1969 are not representative or appropriate Craig, 2004. Direct shear tests were carried out by Kazi & Knill 1969 recording minimum shear strength values of 172 kPa at Happisburgh. Geotechnical data are reported by Hutchinson 1976 for a landslide investigation at the cliff near Cromer golf course. No data were obtained for un-slipped material. Residual strengths from triaxial and shear-box tests gave values as shown in Table 4-7. In-situ shear-vein tests were performed in the Happisburgh Till which, after correction, gave undrained peak shear strength values (c_u) of 149 to 143 kPa, classifying the clay as 'Stiff'. This is in agreement with the Panda data. The ratio of undisturbed to remoulded strength is high indicating that the tills are 'low sensitivity'. Its stiffness is due to pre consolidation by glacial loading Bell, 2002. The glacial deformation has created shear-zones, may of which have soft clay infill and lower the strength of the soil mass. Effective shear strength values predict a higher cohesive strength than our estimate based on multi-stage CIU stress-path triaxial tests on sample HB4 (Table 4-7). Friction coefficient values are similar to our triaxial test results for both the Happisburgh Till and Ostend Clay. Due to the presence of sand, silt and clay laminations horizontal permeability will be significantly greater than vertical and pore pressures within the cliff may become locally elevated shortly after rainfall.

Table 4-7: New and published index and effective strength data for the Happisburgh Till Formation where w= Natural water content, w_L= Liquid limit, w_P= Plastic limit, Ip= Plasticity index (w_L-w_P), G_s= Specific gravity, c'= Effective cohesion, ϕ'= Angle of friction (Peak), ϕ'$_r$ =Angle of residual friction.

	w (%)	w_L (%)	w_P (%)	I_p (%)	G_s	c' (KPa)	ϕ' (°)	ϕ'$_r$ (°)
Ostend Clay[1] Silty	9 - 21	20 - 40		3 - 20		34	28	27° (30% Clay)
Clayey	20 - 26	40 - 47		20 - 40		55	16	15° (50% Clay)
Ostend Clay[4]		35 - 43	20 - 23					19 - 24
Happisburgh Till [1]	11.5 - 13	28 - 36		14 - 21		34 - 55	25 - 30	
Happisburgh Till [2,3] Range	11.9 - 15.8	27 - 40	14 - 20	13 - 24		12 - 19	26 - 32	18 - 29
Happisburgh Till [5]	**14**	36	16	20	2.7	**28.8**	**24.5**	

[1]**Kazi & Knill (1969) (Happisburgh),** [2]**Bell (2002),** [3]**Bell and Forster (1991),** [4]**Hutchinson (1976) (Cromer),** [5]**BGS (sample HB4, Happisburgh)**

4.7   GEOMORPHOLOGY

4.7.1 Cliff

The cliffs at Happisburgh typically range from 6 to 10 m within the study area, consisting largely of sands of the Happisburgh Sand Member, underlain by a distinctive bench of Happisburgh Till Member (Figure 4-28). The intervening Ostend Clay Member outcrops intermittently where it produces a spring line between the Happisburgh Sand Member. A notable feature of cliffs in these materials is the erosion of the sand lithologies, apparently by ground water. This extends several metres landward of the cliff in the form of narrow gullies, presumably produced by field run-off during heavy rain. This non-uniform erosion process is reflected in the cliff surface profile (Figure 4-7), with the formation of embayments in the upper cliff. The landsliding process involves rock/block falls and topples (Figure 4-8), mudflows and running sand.

Figure 4-7 Cliff face at Happisburgh showing the Happisburgh Till Member (grey)

Figure 4-8 Landslide (fall) at the Happisburgh test site

31

4.7.2 Platform and beach

The platform is formed in the Wroxham Crag Formation (Figure 4-9a), an intertidal or shallow marine deposit. Platform exposure typically varies from summer to winter, dependent on beach level. The sand beach is usually present in the summer (Figure 4-9a), with variable amounts of coarser material, but can vary significantly in beach height - by up to 2 m - in a single storm event (Figure 4-9b). There is very little permanent backshore along this section of coastline. Beach thicknesses were recorded at Happisburgh during November 2002 and April 2003 as approximately 0.9 m and 0.75 m respectively, reflecting the thin beach cover at this time. A study carried out by Halcrow in 1991 identified that this high beach mobility was due to the oblique incidence of the waves at the coast (Thomalla and Vincent, 2003). Leggett (1993) estimated that over 140,000 m^3 of sediment was lost from the beach and more than 400,000 m^3 were lost from the near-shore area to 500 m offshore between Happisburgh and Winterton from July 1992 to March 1993 (Thomalla and Vincent, 2003). Between Mundesley and Happisburgh the sediment transport rate is reasonably constant to the southeast along the coastline (HR Wallingford, 2002).
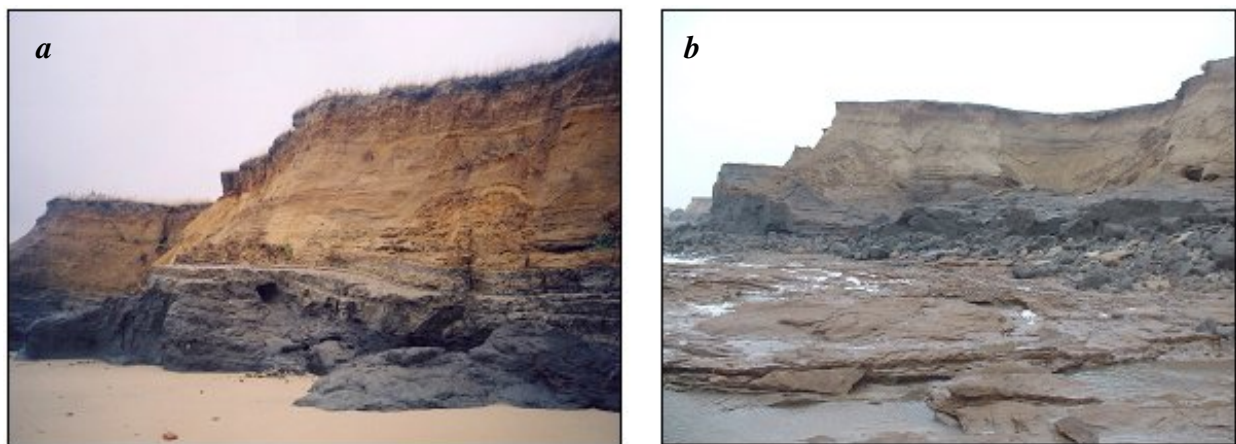
Figure 4-9 (a) Exposure of till (b) sand beach stripped by winter storms exposing Wroxham Crag Formation which underlies the till (taken from Poulton _et al._, 2006).

4.8   COASTAL EROSION AND SEDIMENT TRANSPORT

The rate at which the Norfolk cliffs are eroding has attracted considerable research. Estimates vary from 0.30 to 0.75 m/yr in North Norfolk with an average of 0.9 m/yr for the entire Norfolk coast from 1880 to 1967 (Cambers, 1976; HR Wallingford, 2001, 2002; Thomalla and Vincent, 2003). The Norfolk coast has retreated landward approximately, 1 to 2 km over the past 900 years records, and records such as the Domesday Book (1086) and other historical accounts, demonstrate the presence of villages that have since been lost to the sea (Clayton, 1989).

At Happisburgh, coastal erosion has been an issue for many years. In 1845, rapid coastal retreat was recognised as a threat to St Mary's Church "_having an under stratum of sand and gravel, is so continuously wasted by the agitation of the tides and storms, that it is calculated the church will be engulphed in the ocean before the close of the ensuing century, the sea having encroached upwards of 170 yards during the last sixty years_" (White, 1845). Despite this prediction St Marys Church still stands at the present time, although it is less than 150 m from the cliff edge.

Sediment derived from the erosion of the cliffs between Weybourne and Happisburgh is transported to the northwest and southeast along the beaches by longshore drift, with the dominant transport to the east (Cameron _et al._, 1992). A coarsening of sand grain-size on the beaches in the direction of transport is due the removal of finer-grained sand from the beaches by wave action, followed by the transport into the nearshore zone where the sand is removed by tidal currents (McCave, 1978).

Between Weybourne and Winterton Ness, the North Norfolk cliffs supply about 505,000 m³/yr of sand into the littoral zone (HR Wallingford, 2001). The cliff erosion also supplies fines and gravel, the fines being transported offshore in suspension, while the sands and gravel are transported along the shore and also in the offshore area (HR Wallingford, 2002). Between Mundesley and Happisburgh the transport rate is reasonably constant to the southeast along the coastline (HR Wallingford, 2002).

The laser scan 3-D models have been analysed for each monitoring epoch in Vertical Mapper™ by using a surface to surface calculation, with the lowermost surface at the 1.5m AOD contour line (to avoid the beach) and the upper surface at the change in slope represented by the highest point of the cliff. The landward surface has been defined by the rearmost part of the backscarp. Results for Happisburgh show an average of 16,800 m³ of sediment a year is lost from a section of 200 m of cliff, this equates to approximately 35,000 t of sediment annually. The figures for each year are shown in Table 4-8, and it is clear that 2005-2006 shows a significant decrease in the level of erosion at the site. The negative figure for 2005-2006 reflects the increase in beach level featured in 2006 and does not imply that the cliff has moved forward (refer to Figure 4-13).

Table 4-8 Volume changes for a 200 m section of cliff at Happisburgh

Happisburgh	
Epoch	Volume change (m³) per 200m cliff
2002-2003	21,000
2003-2004	12,600
2004-2005	36,785
2005-2006	-3193

Figure 4-11 shows the point where the sea defences no longer exist at Happisburgh. It is clear from this image that the coastline has eroded significantly where it is no longer defended. To obtain a long term erosion rate, the data for the top of the cliff for each scanned epoch was digitised onto an aerial photograph from 1999 (Figure 4-11). Data was also obtained from historical maps which allowed the drawing of the 1885, 1907 and 1950 coastlines and North Norfolk District Council on cliff top position between 1994-2000. In this 121-year period the coast has retreated by approximately 145 m along a 400 m section. After the loss of some defences in the early 1990s the coastline has receded by approximately 110 m between 1992 and 2006, an average annual loss of approximately 8 m/yr. Ohl *et al.* (2003) quote rates of 50 m of cliff retreat in the three years subsequent to the loss of defences, between 1996-1999.

The overall 3-D model for the monitored cliff recession at Happisburgh is shown in Figure 4-10. During the scanned period (2001-2006) the loss of land was approximately 45 m, an average of 6-8 m/yr. The notable hiatus in recession between 2005 and 2006 is in contrast to the large recession exhibited between other epochs (the 2005-2006 hiatus has resulted in the 'speckled' effect in Figure 4-10 where small errors in the scans have alternately brought each to the foreground). The recession between the other epochs are relatively consistent.
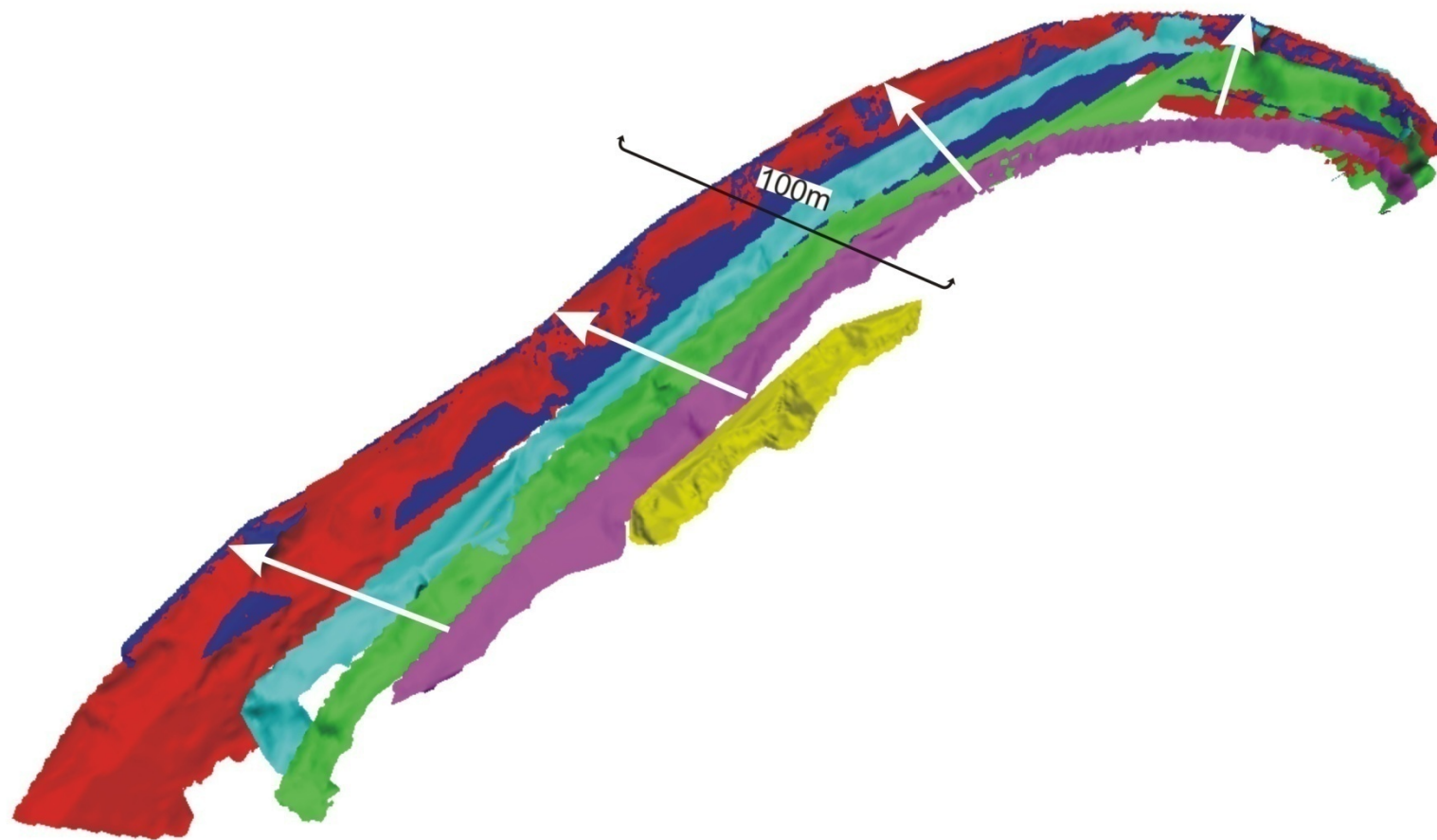
Figure 4-10 3-D laser scan solid models for 2001 to 2006 at Happisburgh
yellow=2001, magenta=2002, green=2003, cyan=2004, red=2005, blue=2006; white arrow=direction of recession

Legend

— 2006 BGS top of cliff LiDAR
— 2005 BGS top of cliff LiDAR
— 2004 BGS top of cliff LiDAR
— 2003 BGS top of cliff LiDAR
— 2002 BGS top of cliff LiDAR
— 2001 BGS top of cliff LiDAR test site
— 2000 Ostend to Cart Gap Study
— 1999 Ostend to Cart Gap Study
— 1998 Ostend to Cart Gap Study
— 1997 Ostend to Cart Gap Study
— 1996 Ostend to Cart Gap Study
— 1994 Ostend to Cart Gap Study
— 1950 Historic OS map
— 1907 Historic OS map
— 1885 Historic OS map

1:1,500 scale

0   25   50   100 Meters

Figure 4-11 A 1999 aerial photograph with lines showing the position of the top of the cliff measured by BGS between 2001-2006 plus historical data extracted from data collected by HR Wallingford on cliff top position between 1994-2000 (HR Wallingford, 2001) and Ordnance Survey maps.
Note that the cliff was re-landscaped in the north west area of the photograph several times in the 1990s.

Earlier publications on this work using data from 2001-2004 (Poulton *et al.*, 2006), show that where the defences have failed and been removed, and where the cliffs are exposed (Figure 4-1), average recession rates of the cliff top range between 8-10 m/yr at Happisburgh. The subsequent surveys update this figure to 6-8 m/yr for 2001 – 2006.

Cliff profiles from 2004 and 2005 show how significant the recession of the coastline is, between these two epochs 36,785 m^3 of material was lost along 200 m of this cliff line with a total recession of 12 m. From the cliff profile cross sections of 2005 and 2006 (Figure 4-12 and Figure 4-13) it can be seen that only a small amount of material compared to previous years was lost at the top of the cliff, approximately 2 m, whilst towards the base the beach appears to be up to 1 m higher, this could account for the perceived increase in stability.
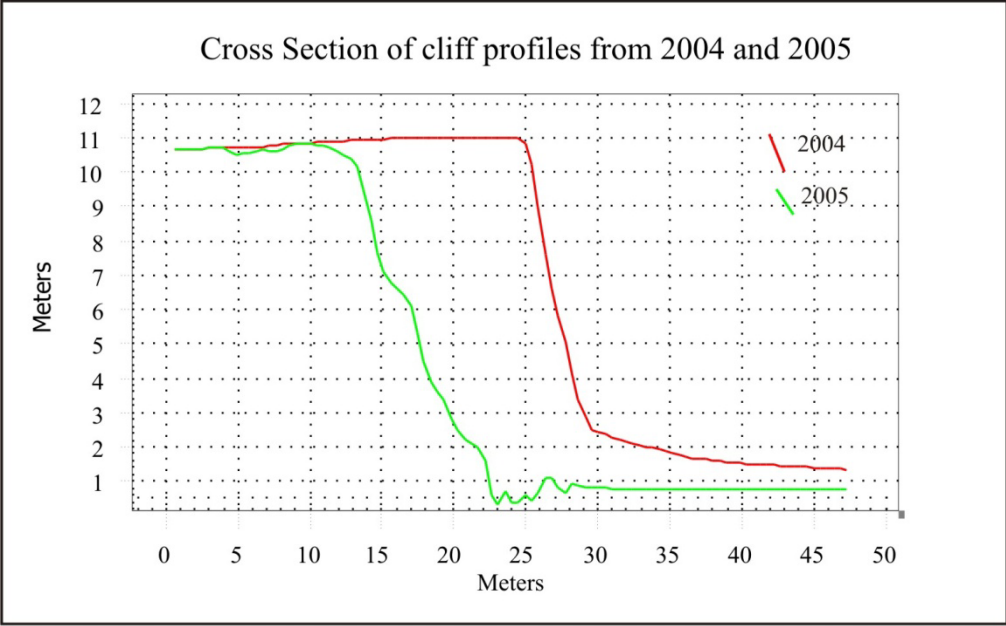
Figure 4-12: Cross sections of cliff profiles from Happisburgh extracted from scanned data for the 2004 and 2005 epochs
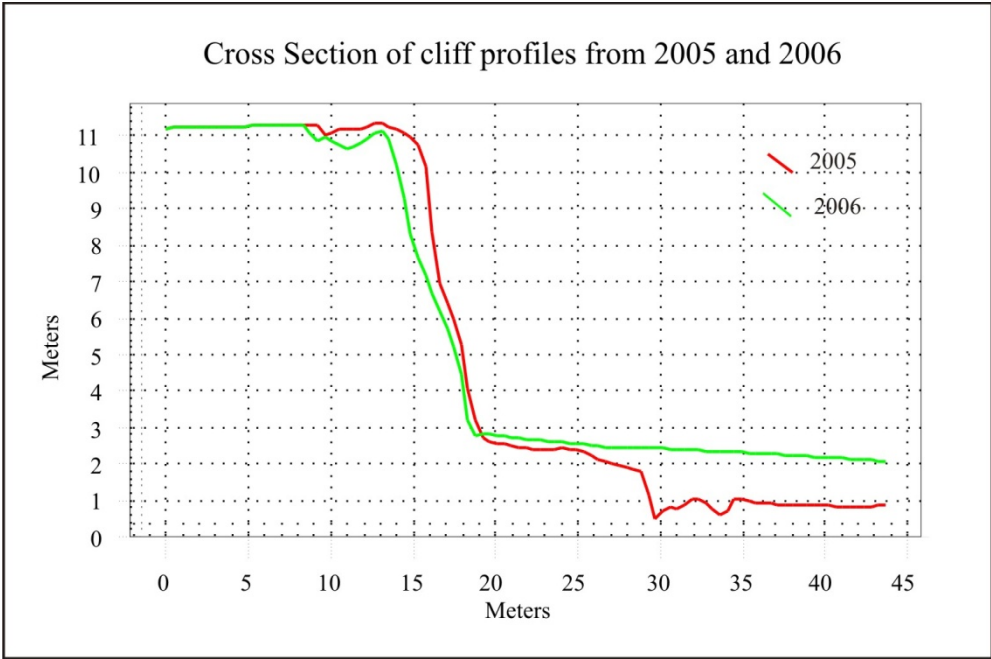
Figure 4-13 Cross sections of cliff profiles from Happisburgh extracted from scanned data for the 2005 and 2006 epochs

4.8.1 Embayment formation

An observation derived from comparing historic maps, aerial photographs and top-of-cliff GPS data collected as part of this survey, is the development of a pronounced embayment within the undefended section of cliff line to the south of the village; with its updrift limit at the village's southern limit, and downdrift limit at the seawall at Cart Gap. The cliff line shows a linear plan-form in the years 1885-1997, by which time embayment formation has begun following damage to the revetment defences post-1991. This process appears to accelerate in the subsequent years from 1999 by which time there was a significant breach in the defences (see Table 2-2).

The term *headland-bay beach* defines a sandy shoreline bounded by rock outcrop or headlands where its shoreline assumes some form of curvature (Short and Masselink, 1999; Klein and Menezes, 2001). Headland-bay beaches are commonly found in the lee of natural barriers, such as rocky headlands, or off artificial obstacles, such as groynes (LeBlond, 1979). They are characterised by a shadow zone with strong curvature adjacent to the updrift headland, a gently curved transition zone, and a straight end that is normal to the angle of incidence of the more energetic waves Klein *et al.*, 2002). This may be understood in terms of a balance between the effects of the headland and the nearshore bathymetry on wave refraction and diffraction and a relation between beach slope, wave energy and grain size (LeBlond, 1979; Lavalle and Lakhan, 1997). *Headland-bay beach* may not strictly apply to the embayment at Happisburgh, however, as the northern limit of the embayment is not defined by a headland *per se*, rather a 'fixed' point held in place by coastal defences. This 'fixed' point has in fact been migrating onshore due to the breakdown of defences which were previously holding its position. At the time of the first survey in 2001, it was armoured with a makeshift protection comprising scaffolding poles and other material down to beach level to offer protection. Despite this and the addition of a rock bund defence in 2002, extended in 2007 (Table 2), subsequent erosion has resulted in the landward movement of this point by 5-10 m.

The southern 'fixed' point is the northern end of the concrete sea wall at Cart Gap and is subject to flanking (or terminal scour), a process whereby accelerated erosion occurs at the end of the sea wall where it meets erodible sediment. Flanking has been occurring at this location for a number of years; the seawall was extended inland in 1993 to try to arrest the process. Although not measured as part of the LiDAR survey, air photo evidence indicates flanking erosion at this location of approximately 15 m.

Another explanation of the plan-form shape observed at Happisburgh is that it is the result of downdrift erosion and the *terminal groyne effect* (Brown *et al.*, 2007). At the time of writing, there are still shore-normal defence structures present to the north of the study area, in varying states of deterioration, which trap sediment moving south thereby depleting the beach on the downdrift side. The juxtaposition of shoreline protection and an adjacent unprotected shore will display a set-back in the line of the unprotected shore (Brown and Barton, 2007).

4.9   COASTAL INSTABILITY AND LANDSLIDES

The landsliding processes typically observed in the section at Happisburgh are small scale (<1 to 10 m^3) and on a rapid timescale. Landslide types include topples (Figure 4-8,

Figure **4-14**), falls (Figure 4-15) and rotational slumps (Figure 4-16). The landslide deposit at the toe of the cliff remains until removed by the next high tide. It is, therefore, impossible to detect all such small and rapid landslides on an annual monitoring cycle. Observations during fieldwork in stormy weather conditions and at high tide have shown that considerable volumes of sediment are released from the cliffs by direct mechanical erosion by wave action (Figure 4-15).

Figure 4-14 Example of a 'topple' at Happisburgh in 2003

Figure 4-15 Example of a 'fall' landslide in action during high tide at Happisburgh in September 2002.

Figure 4-16 Rotational 'slump' landslides, Sep 2007.

The active cliff erosive processes in the Happisburgh area (for the upper part of the cliff only) could be depicted using the repeated cycle of the following three stages (based on Ohl *et al.*, 2003; Figure 4-17):

1. basal undercutting of the intact toe by wave action, leading to steepening of the cliff profile and a reduction in slope stability;
2. cliff failure, involving failures of blocks of material;
3. deposition of debris at the base of the cliff, protecting the cliff toe;
4. removal of debris from the foreshore by wave action, leading to the onset of basal undercutting (stage 1 above).
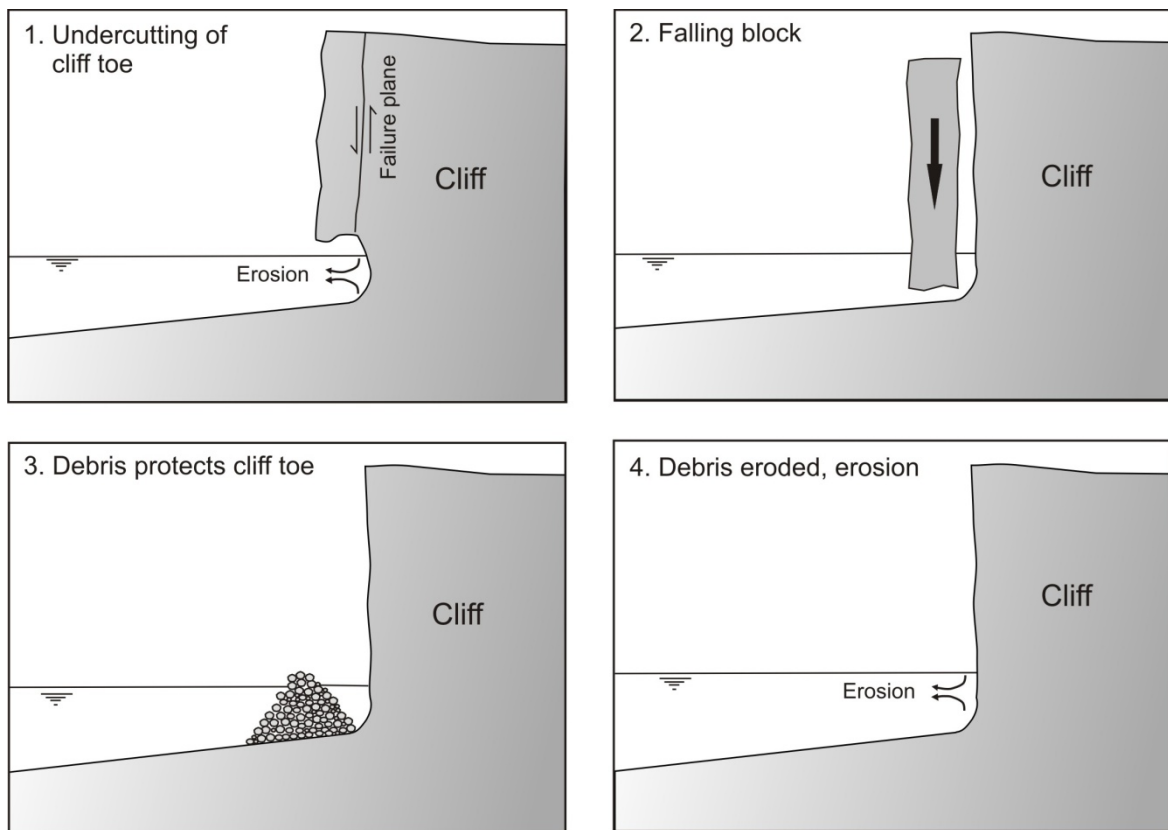
Figure 4-17 A conceptual toe erosion model based on Ohl *et al.* (2003).

4.10 CLIFF MODELLING

4.10.1 Slope stability analysis

Slope stability analysis was carried out using three cross-sections at Happisburgh, labelled 'south', 'central', and 'north'. Their locations in relation to the cliff are shown in Figure 4-18 along with terrestrial LiDAR derived contour maps for the first and most recent epochs. For each epoch a cross-section was derived from the intersection of each of the red lines shown in Figure 4-18 and the corresponding 3D models gridded in Surfer. The sampling interval was taken at 0.5 m throughout (whilst the 3D model is capable of being sampled more densely, the slope stability analysis program would not accept a finer resolution). The geological model for the three cross-sections at Happisburgh is shown in Figure 4-19.
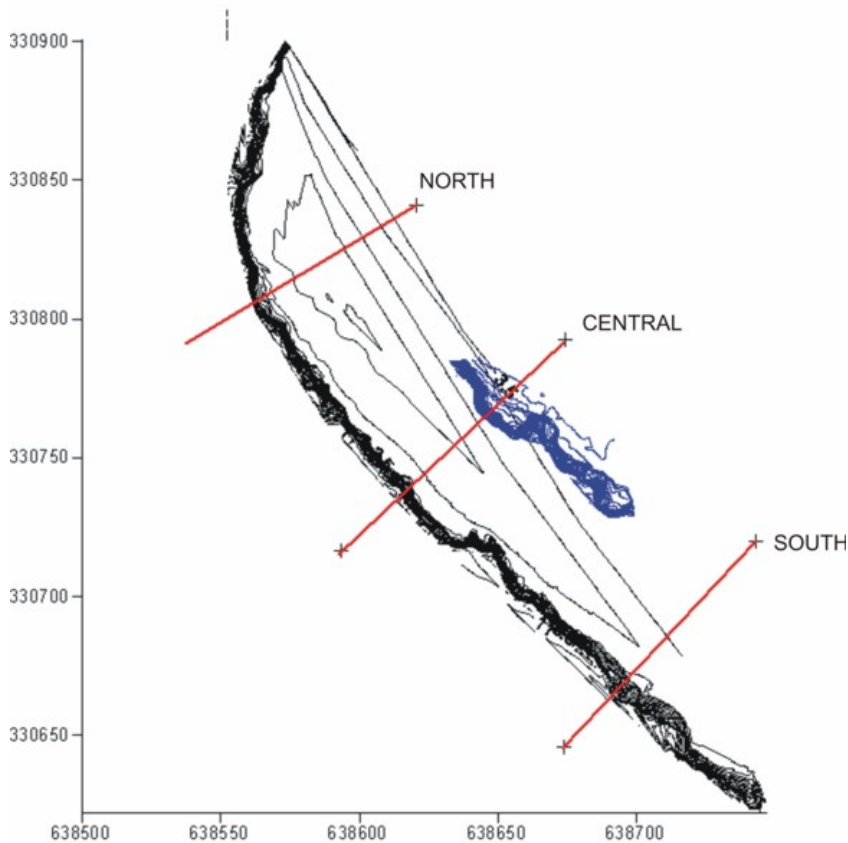
Figure 4-18 Terrestrial LiDAR derived map showing the three cross-sections used for slope stability analysis at Happisburgh
Note: blue contours = Sep 2001, black contours = Sep 2006

The slope stability graphic results are not produced here in full, but rather an assessment with examples is given (full results are shown in Appendix 4). The results for the three locations at Happisburgh (central, south & north), in the form of displacement contour/vector diagrams, show that the displacements tend to have either a slightly or a strongly rotational trend from top to bottom. The concentration of displacements tends to lie within a zone which can be equated with one or more broad slip planes that has a semi-rotational form. Usually, there is a single major zone of displacement, occasionally with a secondary zone at shallower depth. It is notable that the presence of a till bench at the base of the cliff profile tends to result in a shallow movement confined to the upper cliff, whereas the absence of a bench produces a deep-seated movement. However, the latter type of movement has not been observed in the field. Usually, the major zone of displacement becomes linear at the rear and is inclined either parallel or sub-parallel to the cliff profile (Figure 4-21). This tends to give a larger cliff-top recession than observed. This has thrown into doubt the suitability of the method.

40
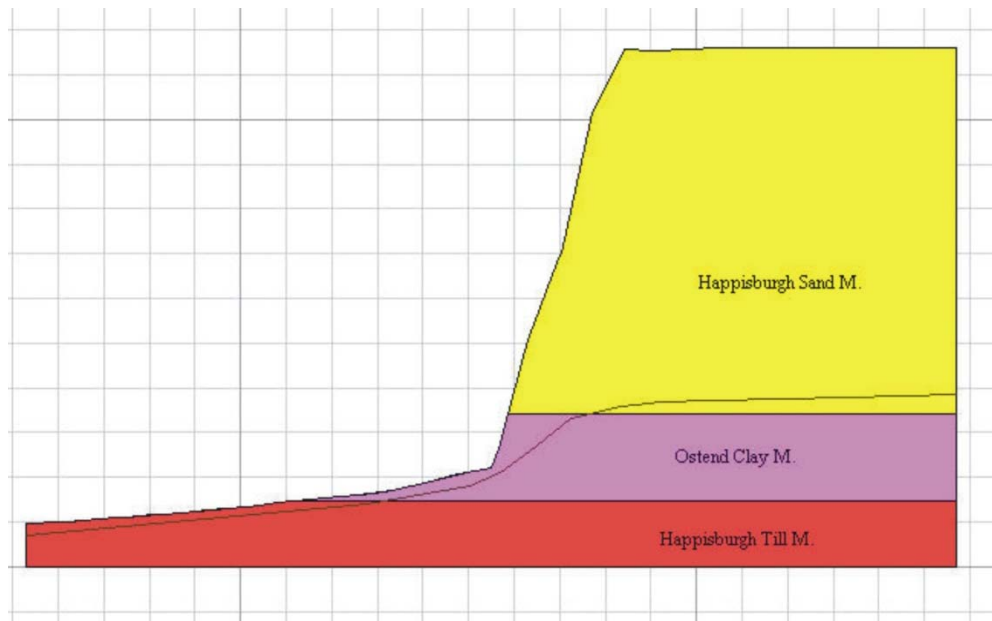
Figure 4-19 Generalised section showing geological layers and water table applied to slope stability analysis at Happisburgh (Scale grid = 1m)

Table 4-9 Summary of geotechnical parameters applied to the slope stability model at Happisburgh.

Member	Density (Mg/m³)	Porosity n	Strength, c' (kPa)	Strength, Φ' (degr.)	Tension (kPa)
Happisburgh Sand Member	1,800		7	35	20
Ostend Clay Member	1,850		12	14	30
Happisburgh Till Member	2,210		28.8	24.5	2

There are two primary reasons why this might be the case at Happisburgh. These are:

1. Incorrect geotechnical parameters (in particular, mass strength)

2. Incorrect ground water profile

With regard to the first, the influence of soil suction may be a key factor at the Happisburgh site. The role of soil suction in effective stress analysis, and hence mass strength properties and slope stability analysis, has been highlighted for London Clay cliffs in Kent (Dixon, 1987). Briefly, rapid recession of a 'soft' clay cliff will exceed the rate at which pore pressure equilibration, due to the vertical and horizontal unloading, can take place. This results in high pore suctions which, as negative pore pressures, increase the effective strength of the clay mass within the cliff, and hence augment the short-term stability. This process proposed for rapidly receding cliffs is analogous to the observed delayed failure of cuttings and banks, excavated on an undrained time scale, in clay formations; a classic example being that of railway cuttings in London Clay constructed in the late 19th century ultimately failing in the mid 20th century following several decades of pore pressure equilibration. This suction effect cannot readily be modelled in the FLACslope programme, and no attempt has been made to do so.

With regard to the second factor, the ground water table is unknown at Happisburgh. However, observations over the period of surveys suggests that the height of the ground water table is highly variable within the Happisburgh Sand Member in response to rainfall intensity and to surface runoff from a large expanse of cultivation extending virtually to the cliff edge.

It is also likely that the ground water table's lower bound is at or above the top of the Ostend Clay Member for most of the year. A shallow angled ground water profile close to this boundary was therefore chosen for the slope stability analyses (Figure 4-19).

It is clear from the results for Happisburgh that the FLACslope displacement models are effective in indicating broad types and scales of landslide, but are ineffective as temporal predictive tools for the reasons given above. The program does not respond to subtle changes in profile. However, gross changes, for example the presence or otherwise of a till bench at the cliff toe, do produce significant changes in the scale and, in some cases, the type of landslide indicated.

The 'factor of safety' results of the slope stability analyses for Happisburgh are shown in Table 4-10 and Figure 4-22.
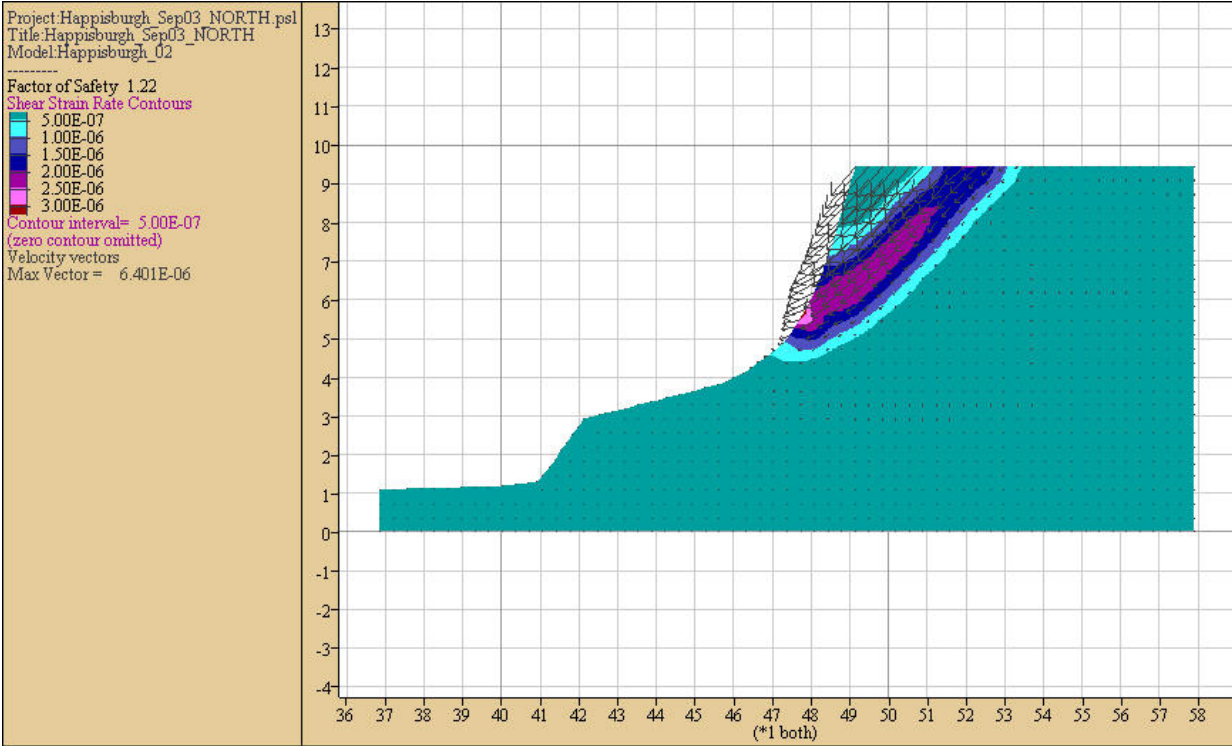
Figure 4-20 Example of displacement strain contour/vector diagram: Happisburgh, North, Sep 2003
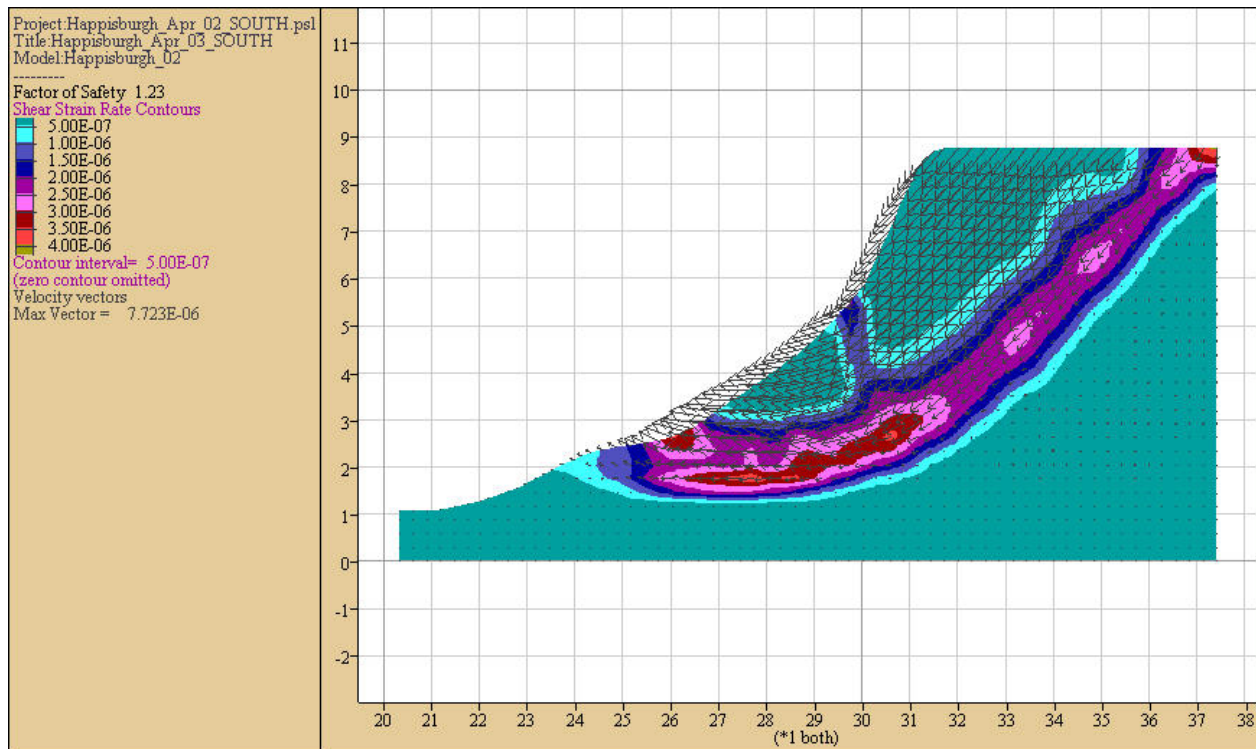
Figure 4-21 Example of displacement strain contour/vector diagram: Happisburgh, South, April 2002

Table 4-10 Factors of safety, Happisburgh – FLACslope v.4

Epoch	North	Central	South
Sep 2000			
April 2001			
Sept. 2001		1.05	
April 2002			1.23
Sept. 2002	0.73	0.77	1.07
Sep 2003	1.22	0.66	1.21
Sep 2004	0.69	0.92	0.96
Sep 2005	1.03	0.83	1.28
Sep 2006	1.1	0.91	1.43

Note: friction / cohesion (fc) option used in FLACslopev4

43
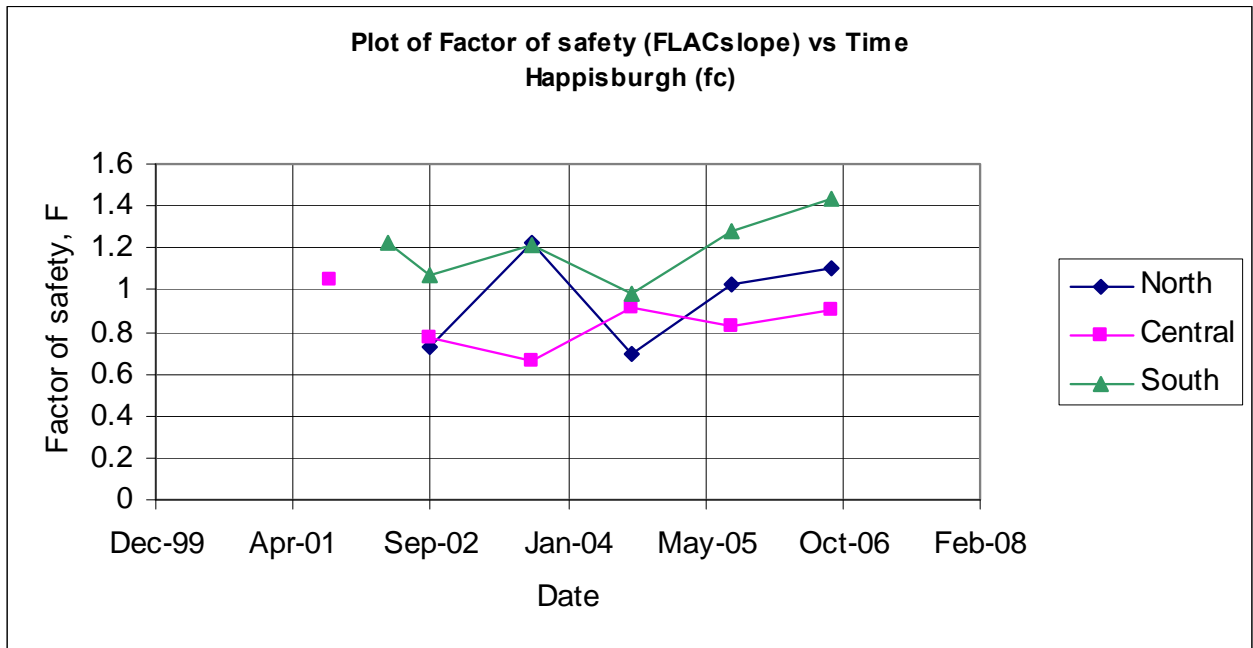
Figure 4-22 plot of factor of safety vs. time (monitoring epoch) for Happisburgh test site cross-sections

In addition, the 'shear strain rate' contour/vector diagrams from the slope stability analysis are shown in Appendix 4.

4.11   DISCUSSION

Average annual recession of 6-8 m/yr remained relatively constant in the years 2002, 2003 and 2004; however this rate increased significantly in 2005 followed by a year of below average recession in 2006. Possible reasons for the acceleration and following decrease in erosion have been assessed. One possible reason for yearly changes in recession rate is the amount of rainfall, which appears to show a correlation when plotted as annual average rainfall against annual average movements. Figure 4-23 shows how the pattern of annual average rainfall is matched by annual average movement in 2002, 2003 and 2004. Increases in rainfall in 2005 are accompanied by increases in the recession rate in 2005. However the subsequent decrease in rainfall is not matched in scale by the significant drop in recession rate in 2006. The rise in beach height in 2006 is probably a key factor here.
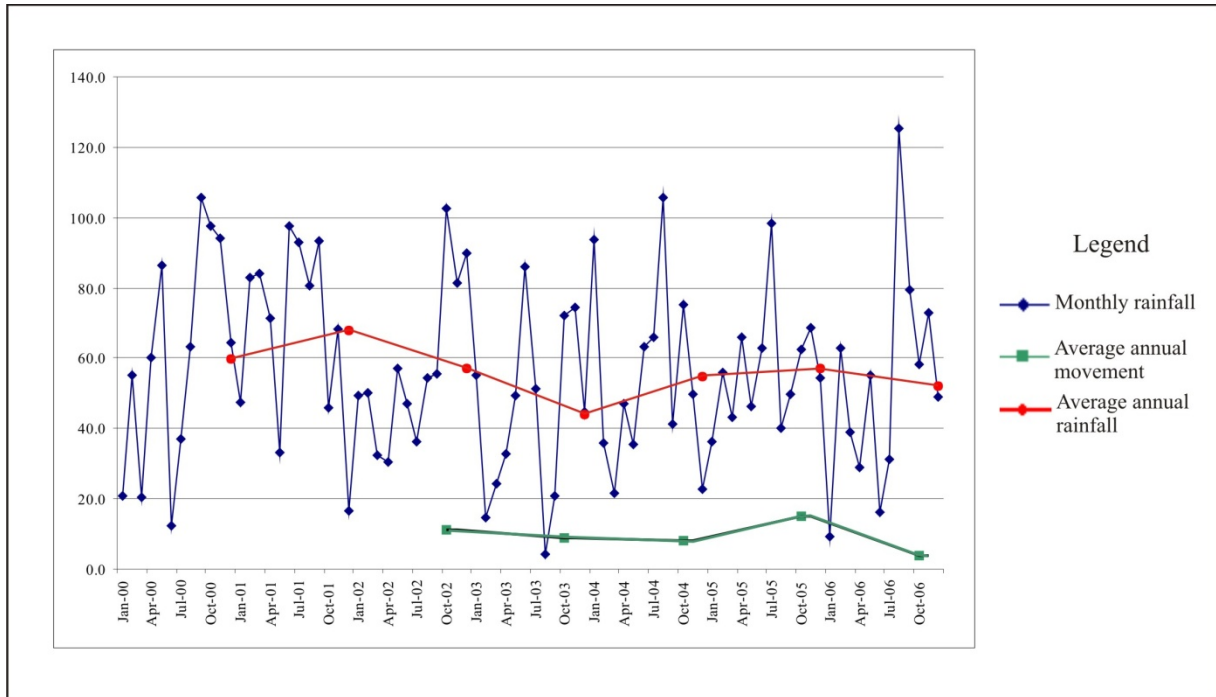
Figure 4-23 Annual average rainfall (2000 – 2006) compared to annual average movement in 2002-2006

Another possible reason for changes in the recession rates relate to the state of defences along this stretch of coast. Between 1994 and 1996 recession rates appear to be slower than present, loss of sea defences SE of Beach Road had taken place in 1991 but at this point the breach was 300 m. Subsequently erosion appears to increase, matched by an increasing breach of sea defences, reaching 600 m in 2001. From 2002 a rock bund was built SE of beach road, which was extended in 2003 and 2007. However the rate of recession does not entirely match the rate of deterioration and subsequent rebuilding of sea defences. After the rock bund was extended in 2003 the rate of cliff erosion accelerated between the 2004 and 2005 scans. Whilst this was matched by an increase in rainfall, this appears to have occurred independent of the new sea defences. However between 2005 and 2006 the rate of recession had slowed and was on average only 4 m. This pattern of accelerated and decreasing recession may relate to height of the beach, storm surges, weather events or the effects of the sea defences.

Beach height and exposure of the base of the cliff was observed to change annually (Figure 4-24 to Figure 4-27). The base of the cliff is more extensively exposed in years of high recession when the beach was correspondingly low. In 2005 the beach level was lower than in previous years. In 2006 the base of the cliff was much less exposed with corresponding higher beach level. This increase in beach thickness correlates to the reduction in recession observed between 2005 and 2006. However, these observations were made at the point of scanning and do not necessarily represent the conditions experienced for the year as a whole.

Figure 4-24 Exposure of the lower cliff in 2003 at Happisburgh

Figure 4-25 Exposure of the lower cliff in 2004 at Happisburgh

Figure 4-26 Exposure of the lower cliff in 2005 at Happisburgh

Figure 4-27 Exposure of the lower cliff in 2006 at Happisburgh

4.11.1 Conceptual Model

The cliff recession conceptual model put forward by Ohl *et al.* (2003) is largely correct. However, the seasonal and yearly beach-level changes at Happisburgh have a considerable effect on the erosion and landsliding process. The following conceptual model is proposed (Figure 4-28):

- Winter: Erosion caused by surface runoff and groundwater seepage as seen in the gullying of the cliff face, coupled with increased seasonal storminess, causes small-scale, frequent, shallow landsliding in the Happisburgh Sand Member (Figure 4-8). The Happisburgh Sand Member is easily eroded and undercutting of the cliff toe reduces slope stability and cliff failure occurs. The beach surface is low and scouring of the upper surface of the till extends the till platform.

- Summer: The beach surface is higher and covers the 'winter platform'. Wave attack is the dominant form of erosion accompanied by landsliding in the Happisburgh Sands.

The cliff surface profiles show that the erosion process is non-uniform, involving the cyclic formation of a series of embayments that continually enlarge (Figure 4-1, Figure 4-29). This could infer landsliding processes involving block falls, mudflows and running sand.
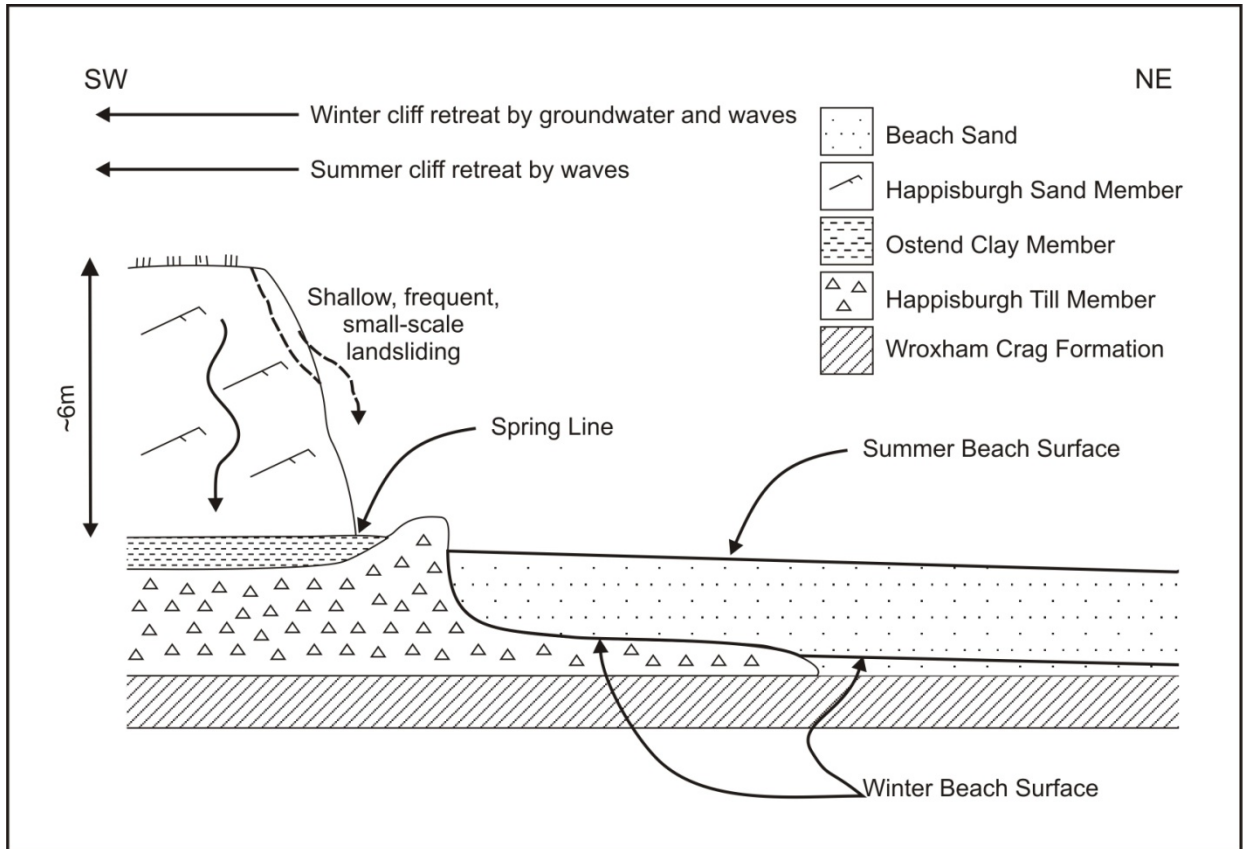
Figure 4-28 Cross-section at Happisburgh, showing cliff and platform stratigraphy (Poulton *et al.*, 2006)
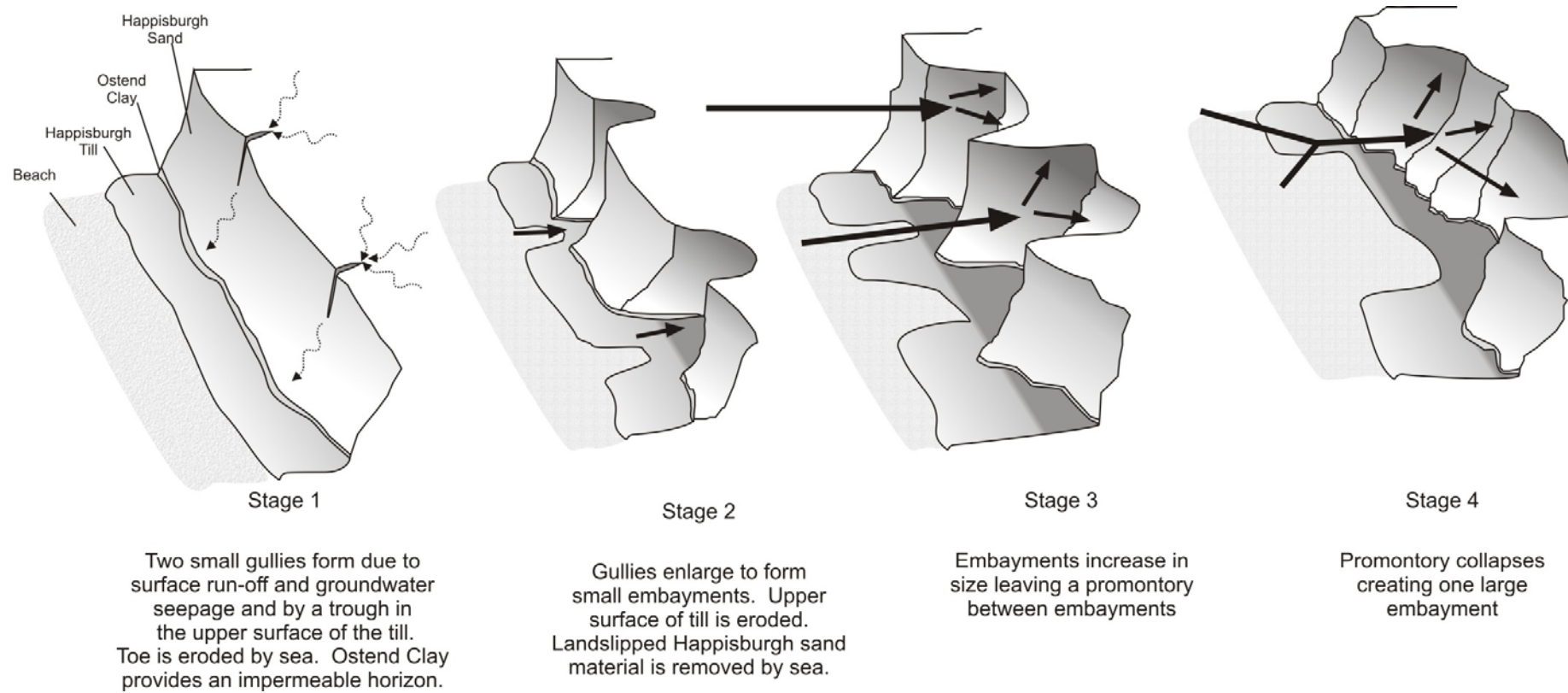
Figure 4-29 Diagram to represent embayment formation process in the cliffs at Happisburgh within the Happisburgh Sand Member (based on Poulton *et al.*, 2006)

5 Case Study: Sidestrand, Norfolk

5.1 INTRODUCTION

The test site at Sidestrand on the North Norfolk coast (Figure 1-1) is approximately 400 m in length, and occupies a section of high cliff (60 m) featuring distinct landslide embayments and highly active complex mechanisms. It is situated north of the hamlet of Sidestrand, and approximately 1.3 km southeast of the village of Overstrand. Active deep-seated rotational landslides and mudslides predominate. The cliff faces northeast and consists of a complex assemblage of glacial deposits including tills, sands and gravels, rafted chalk and chalk talus, much of which is micro-tectonised. The beach is very wide and sandy; the underlying chalk daylighting at low tide beyond the test site. A considerable amount of work has been carried out on the geology Banham, 1988; Hamblin, 2000; Hart and Boulton, 1991; Lee *et al.*, 2004a; Lunkka, 1994, and to a much lesser extent the geotechnical properties Hutchinson, 1976; Kazi and Knill, 1969, of the tills of North Norfolk.

A particular hazard at Sidestrand is access, which may be difficult in poor weather and tide conditions. Mudslides and mudflows also represent a hazard during, or following, wet weather. Accessibility is poor for heavy equipment due to the combination of a rock bund and groynes at Overstrand, and the cliff path at Trimingham; both access points are equidistant and 1.5 km from the test site.
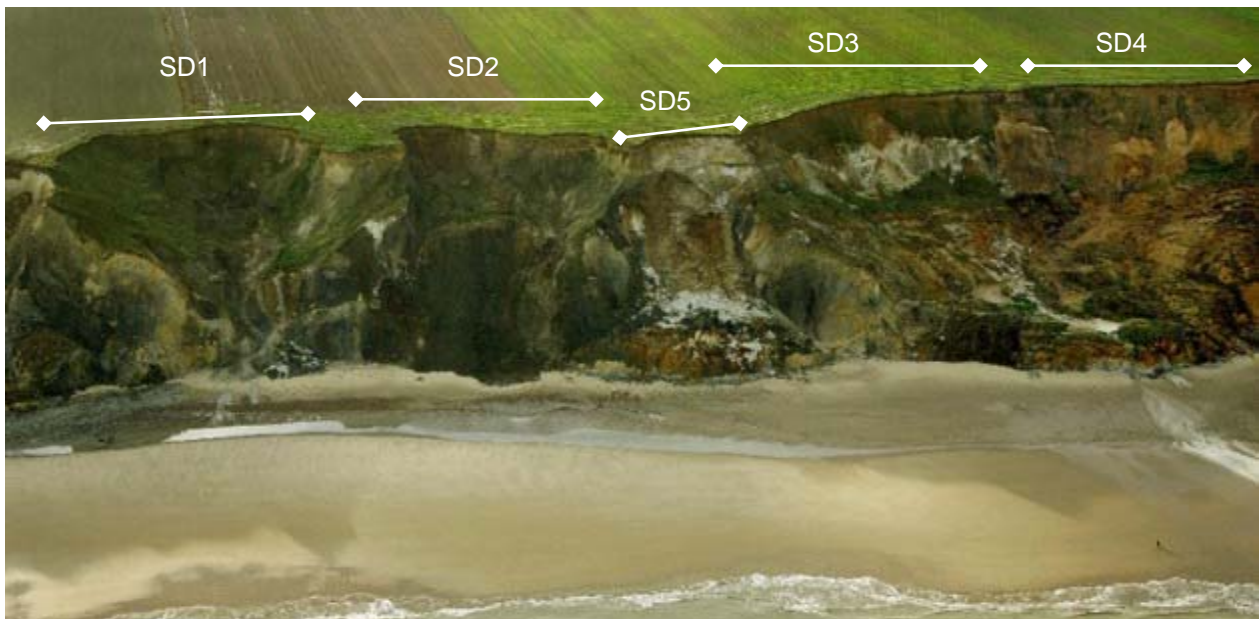
Figure 5-1 View of Sidestrand test site, Nov 2006 (Mike Page, Skyview). Length of view approximately 300m.

5.2 SURVEY ACTIVITIES

The monitoring, sampling, and testing programme at Sidestrand began in November 2000 and finished in September 2006; a total of 9 surveys having been completed (Appendix 1). Details of survey activities are given in Appendix 5.

The rate of erosion at the Sidestrand test site has so far been monitored every year from 2000, to 2006 using laser scan systems combined with GPS. Figure 5-2 shows the position of the scan locations and target points, from the 2006 survey.

The equipment used varied between epochs, as the quality and precision of the instruments improved:

2000 – 2001 A Riegl LPM2K terrestrial laser scanner, with a published accuracy of 50 mm was used in conjunction with a Garmin GPS12 hand-held GPS. The GPS data were post-processed using a pseudo-differential calculation programme ('Gringo'), giving a reported positional accuracy of >1 m. The combined accuracy of the LiDAR and GPS was estimated as **2.5 m**.

2002 A Riegl LPM2K terrestrial laser scanner, with a published accuracy of 50 mm was used in conjunction with the Leica GS50 GPS/GIS system, giving a real-time positional accuracy of <0.5 m. The combined accuracy of the LiDAR and GPS was estimated as **1 m**.

2003 – 2004 A Riegl LPM2K terrestrial laser scanner, with a published accuracy of 50 mm was used in conjunction with the Leica SR530 differential GPS system. The GPS data were post-processed in SkiPro 3.0, giving a positional accuracy of <25 mm. The combined accuracy of the LiDAR and GPS was estimated as **0.15 m**.

2005 – 2006 A Riegl LPMi800HA terrestrial laser scanner, with a published accuracy of 15 mm was used in conjunction with the Leica SR530 differential GPS system. The GPS data were post-processed in SkiPro 3.0, giving a positional accuracy of <25 mm. The combined accuracy of the LiDAR and GPS was estimated as **0.05 m**.

The above reflects the concerted effort to improve survey quality throughout the monitoring period. It should be noted that the quoted accuracy figures are the best achievable by the scanner and are not necessarily achieved throughout a scan. The actual accuracy of a survey is difficult to determine and depends on a variety of factors including range, temperature, humidity, and target material.

- In 2000, two scans were carried out from two scan positions, from the foreshore. In total, the survey captured **5,056** points on the cliff surface and the adjacent cliff top and foreshore areas.

- In 2001, four scans (two in April, 2 in September) were carried out from two scan positions (sites identical on both visits), from the foreshore. In total, the survey captured **16,597** points on the cliff surface and the adjacent cliff top and foreshore areas.

- In 2002, six scans were carried out from four scan positions, from the foreshore (two sites identical on both visits). In total, the survey captured **27,689** points on the cliff surface and the adjacent cliff top and foreshore areas.

- In 2003, five scans were carried out from three scan positions, from the foreshore. In total, the survey captured **17,264** points on the cliff surface and the adjacent cliff top and foreshore areas.

- In 2004, three scans were carried out from three scan positions, from the foreshore. In total, the survey captured **14379** points on the cliff surface and the adjacent cliff top and foreshore areas.

- In 2005, six scans were carried out from three scan positions, from the foreshore. In total, the survey captured **723,573** points on the cliff surface and the adjacent cliff top and foreshore areas.

- In 2006, six scans were carried out from three scan positions, from the foreshore. In total, the survey captured **2,881,697** points on the cliff surface and the adjacent cliff top and foreshore areas.
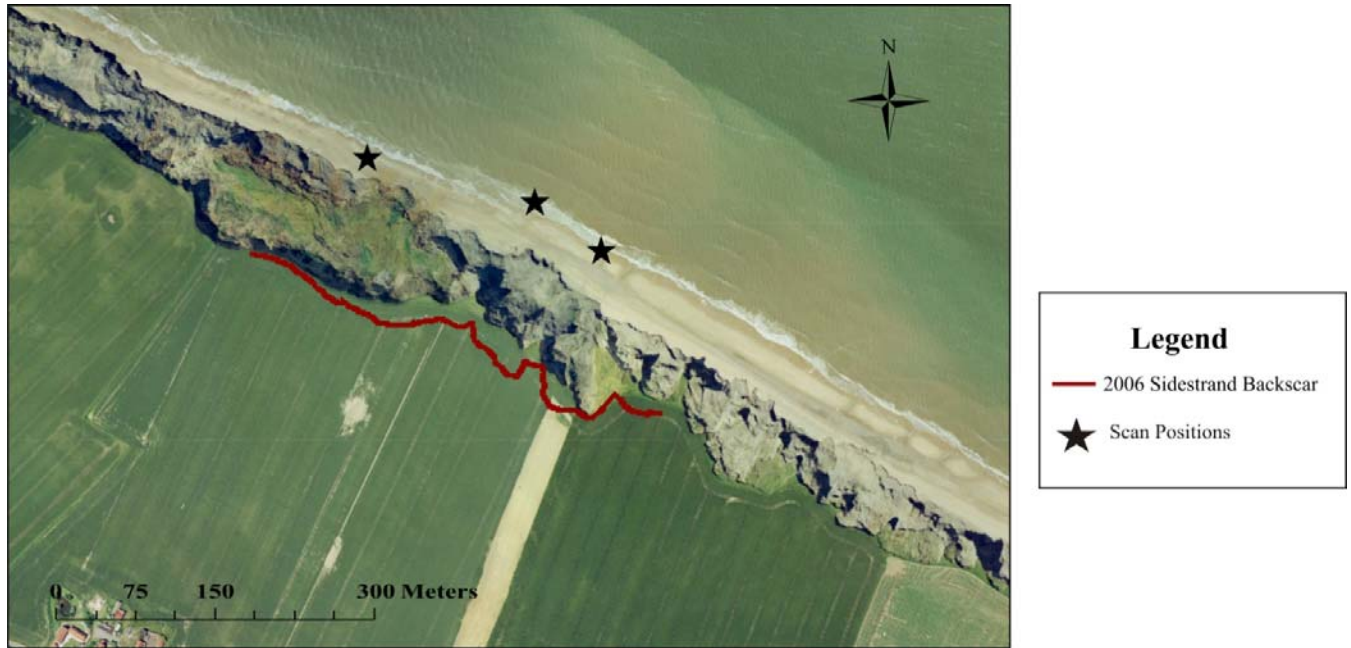
Figure 5-2 Scan layout (2006) for Sidestrand test site
NOTE: aerial photo 1999. Scan positions NGR: 626992, 339628. 626917, 339681. 626777, 339720.

5.3   RAINFALL

The total annual rainfall figures for the Southrepps and Cromer weather stations are shown in Figure 5-3 and Figure 5-4.

- Highest average annual rainfall was in 2000 and 2001.

- The peak rainfall event was in August 2006 with another above average peak in November 2000.

- Lowest annual average rainfall was in 2003.

- The lowest monthly rainfall figure recorded was in August 2003.

- **2000**-Second highest annual average and the second highest monthly rainfall amount recorded this year. January and March were low rainfall months. Across the country 2000 was the wettest Autumn on record.

- **2001**- Wettest year between 2000-2006 with the highest annual average. High rainfall months between June and September.

- **2002**-Compared to previous years the annual average rainfall has decreased significantly. Peak rainfall was over the winter months with a small scatter in averages for the remaining months of 2002.

- **2003**- Driest year between 2000-2006 with the lowest annual average. A high rainfall month in June was distinguished from much lower rainfall averages across the rest of the year. Record temperatures were recorded by the Met Office in 2003.

- **2004**-Annual average rainfall begins to increase again after two drier years. January, July, August and October had the highest monthly average rainfall for the year.

- **2005**-Annual average rainfall continues to increase. Peak rainfall months were June, July and November.

- **2006**-Whilst annual average rainfall decreases slightly from 2005 the highest rainfall in any month between 2000-2006 was recorded in August. This was preceded by a very dry June and July.
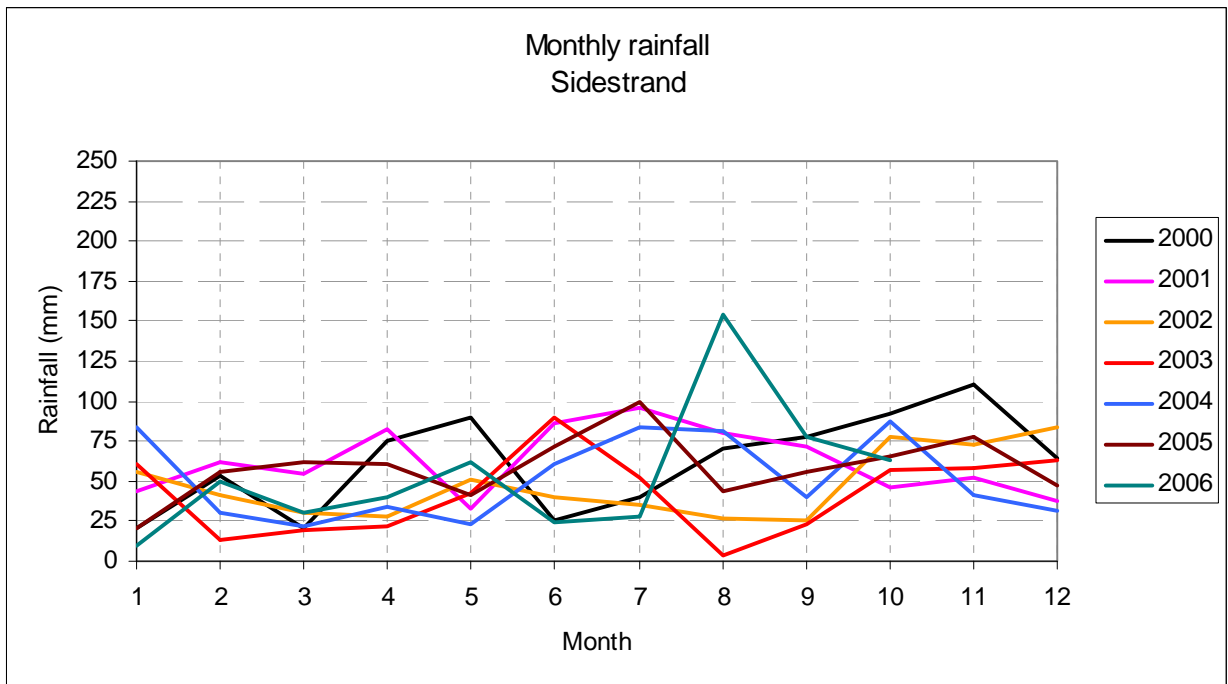
Figure 5-3 Rainfall – monthly averages – Southrepps (2000), Cromer (2001-2006)
(Met Office)
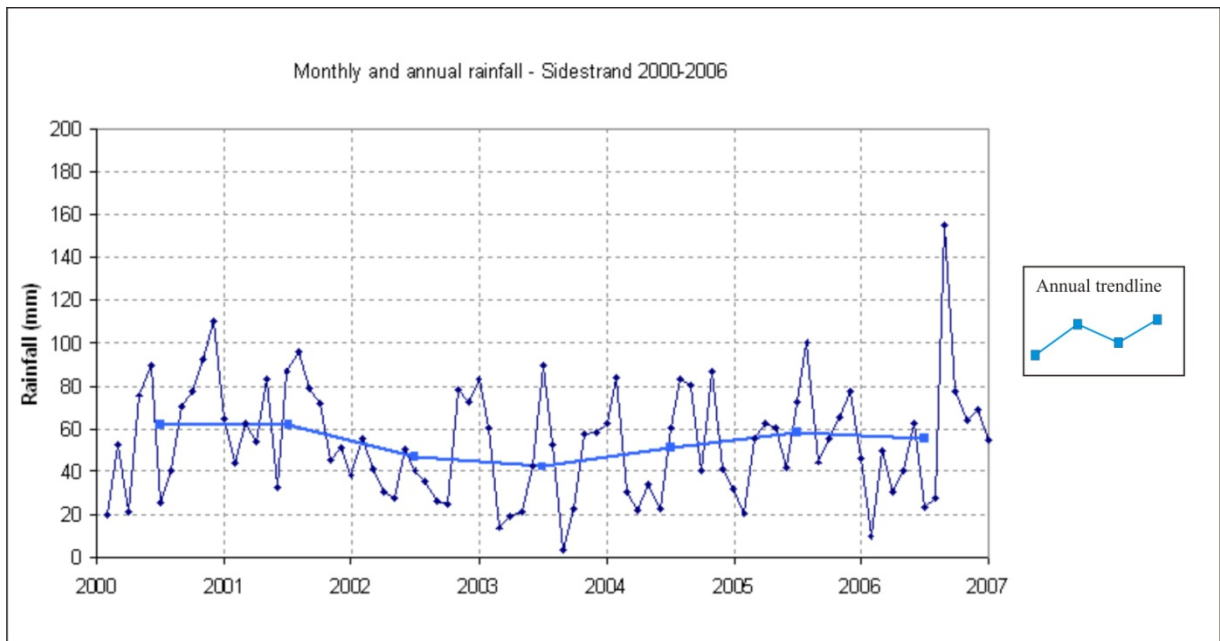
Figure 5-4 Rainfall – monthly and annual averages – Southrepps (2000), Cromer (2001-2006)
(Met Office)

Tidal information has been obtained for the Sidestrand test site monitoring period from the Southampton Oceanographic Centre (British Oceanographic Data Centre, 2008) for the Cromer tidal observation point (Figure 5-5). This appears to show a slight but steady increase in mean monthly tidal level over the monitoring period. However, there is also a hiatus between July and September 2001. It is suspected that this hiatus is an error in the data collection.
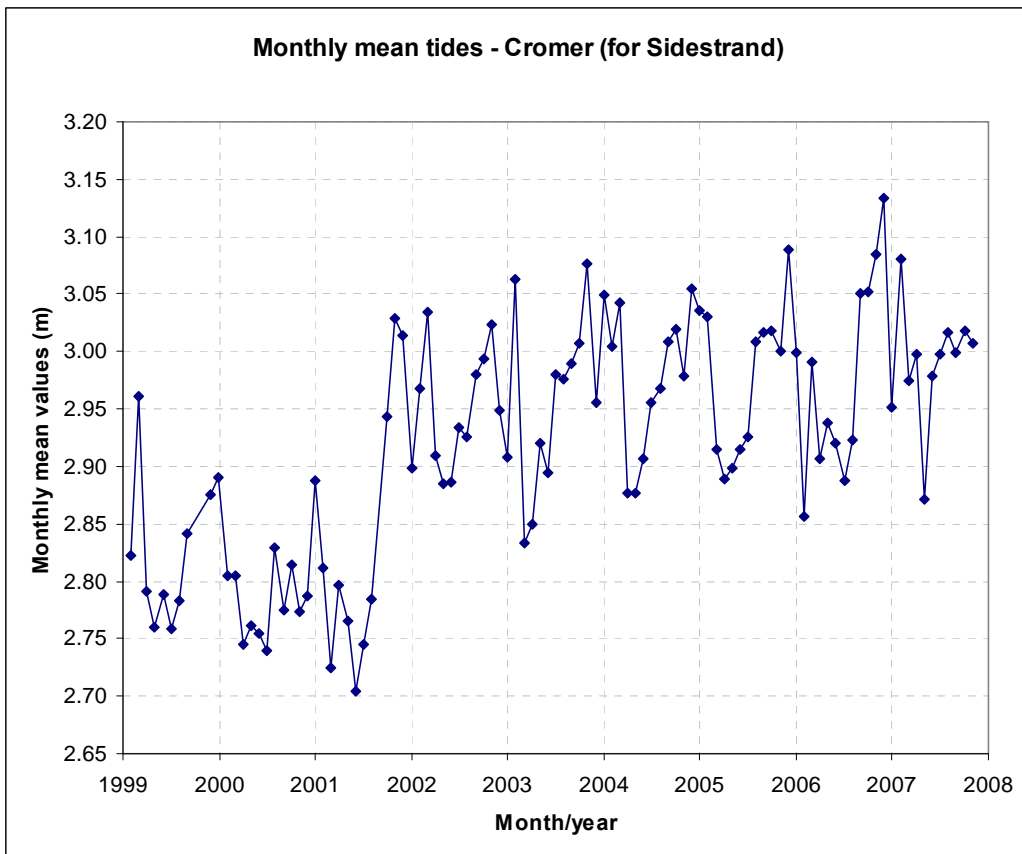
Figure 5-5 Monthly tidal means for period 1999 to 2008 at Cromer (for Sidestrand)
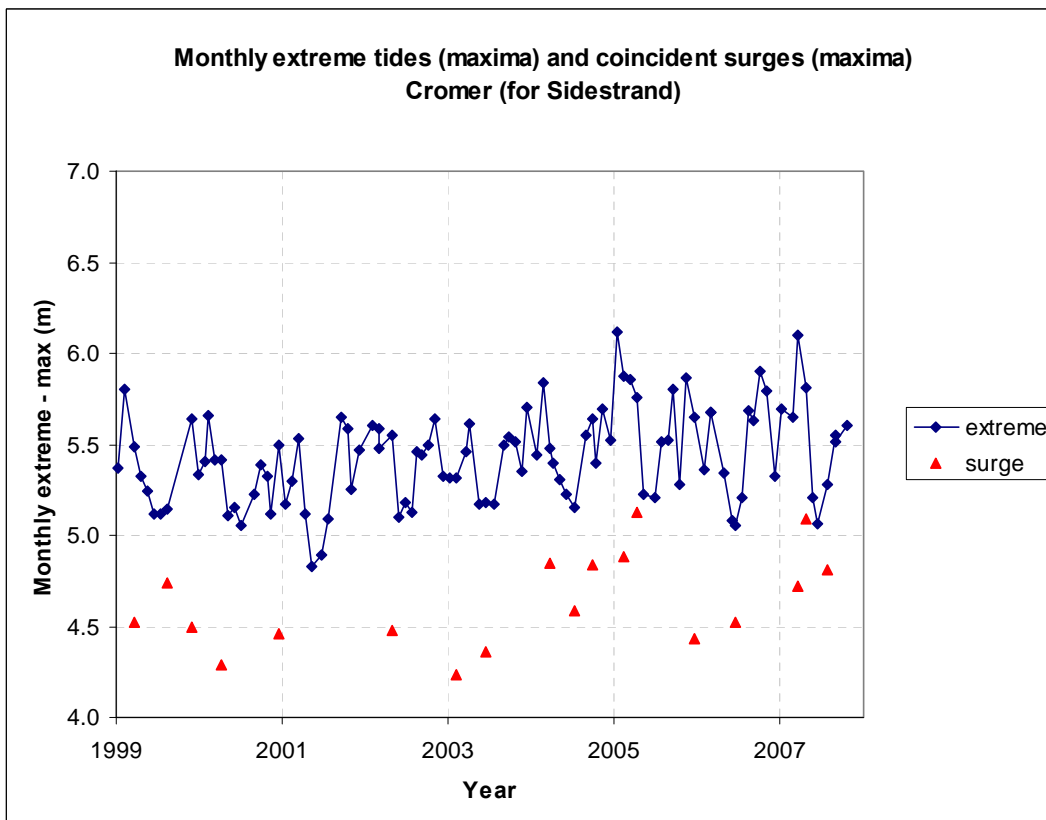
Figure 5-6 Monthly extreme tides (maxima) and coincident residuals for surge maxima, Cromer (for Sidestrand)

Monthly extreme tides and tidal surge maxima are shown in Figure 5-6. The surges are calculated as the difference between measured and predicted tide levels.

5.4 GEOLOGY

The current interpretation is that of Lee *et al.,* (2004a), shown in Figure 5-7. This scheme equates the Lowestoft Till with the Second Cromer Till. However, it should be noted that the stratigraphy and the thickness of the formations differs considerably across the test site at Sidestrand. These differences are reflected in the stratigraphic models used for the slope stability analyses applied to each embayment.

Important features of the test site and neighbouring cliffs are the tectonically-controlled syncline and large-scale shears (Lee *et al.*, 2004a). The deposits within the platform and lower part of the cliff consist of the matrix-dominant dark grey Happisburgh Till Member of the Happisburgh Formation (Figure 5-8 and Figure 5-9). This till has been subjected to small-scale folding (Figure 5-9), glaciotectonic in origin and, as with most tills of this type, is regularly jointed. The folding is observed in freshly eroded or landslide-exposed sections in the cliff, and also in the platform. The pattern of folding has enhanced the process of rock-fall and 'notch' formation close to the foot of the cliff (Figure 5-9). It is not clear whether some or any of the folding observed on the platform has been caused by previous deep-seated landslides.

The deposits in the mid part of the cliff are largely obscured by landslides. They consist of the Ostend Clay Member (Happisburgh Formation), the Walcot Till Member (Lowestoft Formation), and the lower and central components of the Sheringham Cliffs Formation, viz. the Mundesley Sand Member, Ivy Farm Laminated Silt Member, and the Bacton Green Till Member.

In the upper part of the cliff the exposure is good. Here the uppermost part of the Sheringham Cliff Formation (Trimingham Clay and Weybourne Town Till Members) is seen (Figure 5-8 and Figure 5-9). This is overlain by the Stow Hill Sand and Gravel Member of the Briton's Lane Formation (Figure 5-9).

Whilst a typical stratigraphic section is shown in (Figure 5-7) for the section between Overstrand and Trimingham, detailed cliff sections are shown for the three embayments at Sidestrand in Table 5-1.
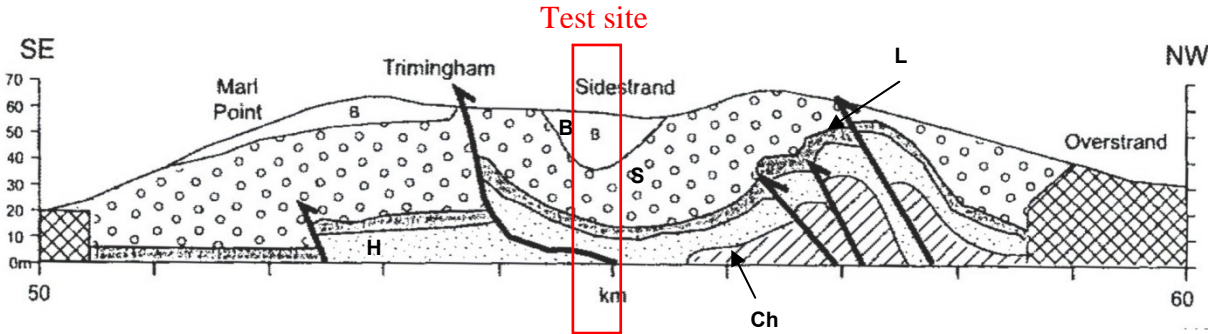
Figure 5-7 Coastal section (Lee *et al.*, 2004b) [B = Briton's Lane F., S = Sheringham Cliffs F., L = Lowestoft F., H = Happisburgh F., Ch = Chalk/pre-glacial, hachuring = obscured by defences; black arrow = thrust]

55

Figure 5-8 Happisburgh Till Member fabric (toe of cliff, unslipped) (08/08/01). Trowel for scale.

Figure 5-9 Happisburgh Till Member 'chevron' folding (base of cliff, SD3, unslipped) (Sep 2003)
Note: rock-fall from folds at base of cliff and consequent 'notch' formation (1m staff)

Table 5-1 Stratigraphic sequences at Sidestrand test site (from Banham, 1988; Hamblin, 2000; Lee *et al.*, 2004a) (# = Lunkka, 1994).

(Hamblin, 2000)		(Banham, 1988)	(Lee *et al.*, 2004a)	
Overstrand Formation		Gimingham Sands	Briton's Lane Formation	Stow Hill Sand & Gravel Member
Beeston Regis Formation	Hanworth Till Member	3rd Cromer Till	Sheringham Cliffs Formation	Weybourne Town Till Member
				Trimingham Sand Member
				Trimingham Clay Member
				Bacton Green Till Member
		2nd Cromer Till		Ivy Farm Laminated Silt Member
				Mundesley Sand Member
Lowestoft Formation	Walcott Till Member		Lowestoft Formation	Walcott Till Member
	Walcot Diamicton #			
Corton Formation	Happisburgh Clays #	1st Cromer Till	Happisburgh Formation	Ostend Clay Member
	Happisburgh Till Member			Happisburgh Till Member

Table 5-2 Geological sequence between Overstrand and Trimingham (Total thickness 40m)

Stratigraphy (Lee *et al.*, 2004a)		Lithology	Provenance (Lee *et al.*, 2004a)	Thickness (m)*
Formation	**Member**			
Briton's Lane	Stow Hill Sand & Gravel	Massive GRAVELS/sands	Glaciofluvial outwash	4.0
Sheringham Cliffs	Weybourne Town Till	Grey chalky, silty, clayey TILL, clast-dominant	Lodgement till (British – North Sea)	2.5
	Trimingham Sand	Massive SAND	Glaciolacustrine (deltaic)	1.0
	Trimingham Clay	Grey CLAYS / silts	Glaciolacustrine (ice-distal), low energy	2.5
	Bacton Green Till	Brown/grey sandy TILL & yellow sand	Sub-glacial flow till (British)	6.0
	Ivy Farm Laminated Silt #	Pale yellow MARLS over grey SILTS	Glaciolacustrine (ice-distal)	13.0
	Mundesley Sand	Yellow/orange/brown SANDS	Glaciodeltaic (British)	2.0
Lowestoft	Walcott Till	Grey silty, clayey TILL	Sub-glacial till (British-North Sea)	1.5
Happisburgh	Ostend Clay	Grey CLAY / silt	Glaciolacustrine, low energy	2.0
	Happisburgh Till	Grey sandy till, matrix-dominant	Sub-glacial till	5.5

= Stratotype area is Sidestrand; Green fill = strata affected by thrusting; *=estimated

Figure 5-10 Contorted, laminated, variegated clay/silt/sand (Trimingham Clay Member) beneath chalk till (Weybourne Town Till Member) (mid-cliff, unslipped) (08/08/01). Trowel for scale.
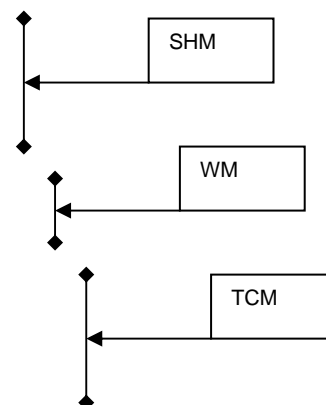
Figure 5-11 Trimingham Clay Member (TCM), Weybourne Town Till Member (WM), and Stow Hill Sand & Gravel Member, SHM (SD3, top of cliff, unslipped) (08/08/01)

Virtually the entire thickness of the Briton's Lane and Sheringham Cliffs Formations has been subject to glaciogenic thrusting (Lee *et al.*, 2004a). Distinguishing syn-depositional and post-depositional thrust/shear features from modern landslide features is difficult in some cases. Some shear features visible in marine-eroded cliff sections are clearly the basal and side-shears of modern mudslides (see Section 5.8). The Happisburgh Till Member is a 3 to 6 m thick, massive yellow-brown sandy till (see Happisburgh section below), while the Walcott Till Member is a stiff blue-grey chalky, flinty till.

The key differences in the stratigraphy between embayments SD1, SD2, and SD3 is (a) the thickening of the Happisburgh Till and thinning of the Bacton Green Till from SD1 to SD2, (b) the absence of the Trimingham Sand, Trimingham Clay, Bacton Green Till, and Happisburgh Till from SD3, and (c) the appearance of the Walcott Till in SD3 only.

5.5   GEOTECHNICS

The geological sequence at Sidestrand is structurally complex with a range of materials that have been disturbed by glaciotectonic deformation and recent landsliding. The basal units exposed along the coast at Sidestrand are the Happisburgh Till and Ostend Clay Members of the Happisburgh Till Formation. The geotechnical properties of those members are described in Section 4.6. The permeability of the sediments is extremely variable and the hydraulic connectivity between units is difficult to predict. The hydrogeological regime within the glacial succession is complex including a regional water table (phreatic surface) and possibly several perched water tables.

The Walcot Till Member, previously known as the Upper Cromer Till (Bell, 2002; Bell and Forster, 1991; Kazi and Knill, 1969) or the Second Cromer Till (Pawley *et al.*, 2004) is a stiff fissured grey silty gravelly clay with some cobbles. The gravel is fine to coarse consisting of mostly chalk which can form up to 40% of the matrix. The matrix comprises low to intermediate plasticity clays. Where the Happisburgh Till is absent the Walcot Till may rest on the Cromer Forest Bed (a firm fibrous brown lignite) or the Leda Myalis Bed. Bell (2002) tested the strength of the Happisburgh Till Member but no specific strength data for the Walcot Till (Upper Cromer Till) was quoted. The strength of the Walcot Till is probably similar to that of the Happisburgh Till given in Table 4-7. The Walcot Till may, however be more susceptible to strength loss upon weathering due to removal of calcite cements. These sub-glacial tills generally have a low to medium compressibility and rapid rates of consolidation (Bell and Forster, 1991).

The Mundesley Sand Member is a loose to dense slightly clayey silty sand. It has a moderate to high primary permeability and where underlain by less permeable deposits probably forms an aquifer unit within the cliff and has a large influence on the hydrogeology of the cliff.

The Bacton Green Till Member is generally a firm to stiff or loose to dense, thinly laminated to thickly-bedded, green grey or orange brown clay, silt and sand with mostly sub-angular to rounded fine to medium gravel chalk and flint. Few geotechnical data are available for laminated glacial clays and standard test results can be misleading due to the small-scale lithological variability of the material. Where the deposit is horizontally bedded the permeability is likely to be higher in the horizontal direction than the vertical. Shear strength is likely to be lower along clay rich laminations.
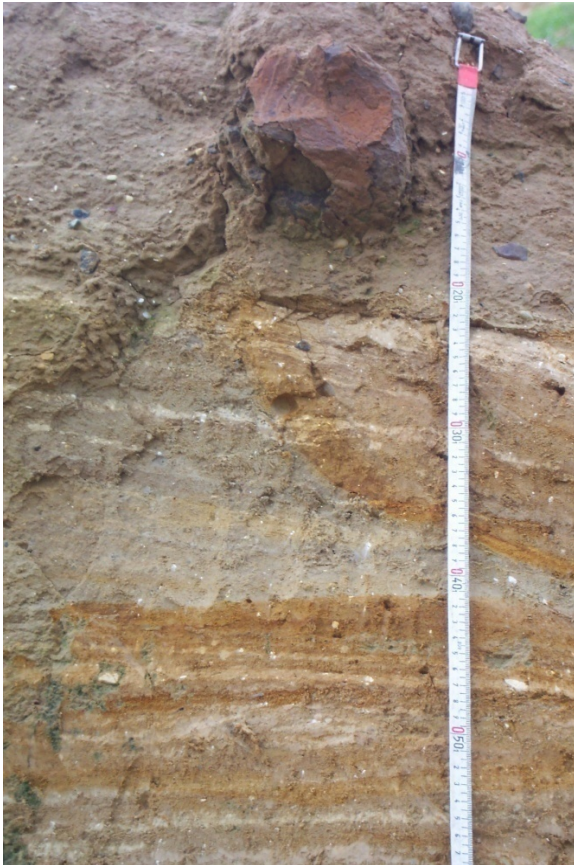
Figure 5-12 Bacton Green Till Member (exposed at West Runton, Norfolk). Section approximately 0.6 m

The Ivy Farm Laminated Silt Member is prone to sapping erosion where the water table intersects the cliff forming spring lines. Localised erosion of the silt by sapping leads to undermining of sections of the cliff. Sudden loading of the saturated silt debris by falls is likely to cause liquefaction and fluidisation of silt which mobilises earth flows that run out down slope.

The Chalk is a 'weak' to 'moderately weak' white rock, forming the lowest and the strongest geotechnical unit of the succession. It contains sporadic beds of gravel-sized up to small boulder-sized, sub-rounded to highly irregular shaped flints. It is likely that the basal shear surface of the deep seated landslides terminate at the upper boundary of the in-situ chalk. Rafts of chalk within the cliff may cause very abrupt local variation in strength and permeability of the cliff and serve to protect some areas of cliff focussing wave energy to unprotected parts.

Limited in-situ strength testing was carried out where access permitted. A total of nine Panda ultra-lightweight penetrometer tests were carried out at Sidestrand within the large debris flow of winter 2000/01 (Table 5-3). Tests 'SDP1' to 'SDP7' were within landslipped Happisburgh Till Member material. Tests 'SDP8' to 'SDP9' were within landslipped Walcott Till Member material.   Resulting profiles are shown in Figure 5-13.   Samples were collected at the Sidestrand test site as shown in Table 5-4.
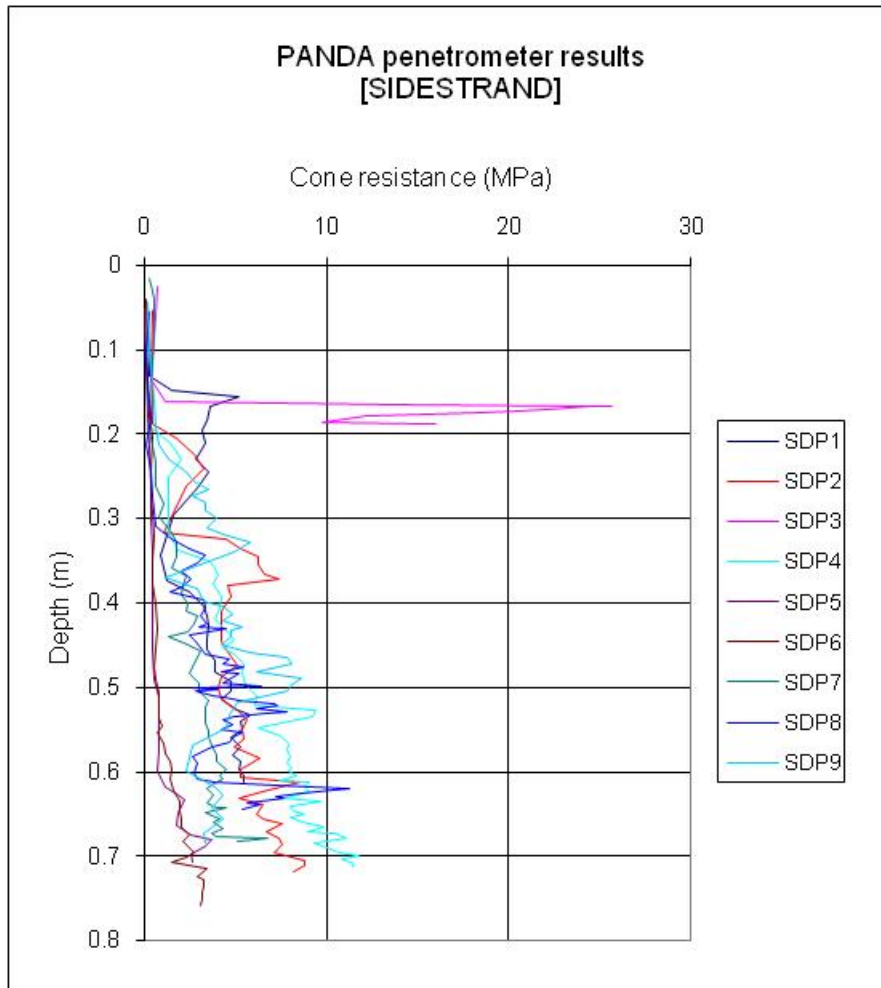
Figure 5-13 PANDA penetrometer results for <u>landslipped material at Sidestrand.</u>

Table 5-3 PANDA ultra-lightweight penetrometer tests for landslipped material at Sidestrand.

PANDA			
Date	**Formation / member**	**Depth (m)**	**Location**
20/04/01	Grey/green plastic till	0.61	SDP1 (0.3m above beach level)
20/04/01	Grey/green plastic till	0.72	SDP2 (0.3m above beach level)
20/04/01	Grey/green plastic till	0.19	SDP3 (0.5m NW of SDP1)
20/04/01	Grey/green plastic till	0.71	SDP4 (0.5m NW of SD2)
20/04/01	Grey silty clay till	0.71	SDP5 (30m NW of SDP1, 0.3m above beach)
20/04/01	Grey silty clay till	0.76	SDP6 (30m NW of SDP1)
20/04/01	Grey silty clay till	0.68	SDP7 (30m NW of SDP1)
20/04/01	Lt. grey lamin silty clay till	0.64	SDP8 (parallel to laminations, adjacent to sample tube ST5)
20/04/01	Lt. grey lamin silty clay till	0.68	SDP9 (parallel to laminations, adjacent to sample tube ST5)

Particle size analyses were carried out on the samples highlighted in Table 5-4. The particle size distribution curves in Figure 5-14 show two distinct sediment types. ST6 is a gap-graded clayey silty sand and little fine gravel similar to the Happisburgh Till Member seen in

Happisburgh in Figure 4-6. Samples ST1, ST2, ST4, and ST9 are characteristic of very silty clays, consistent with mudslide deposits gradings.

Table 5-4 Geotechnical samples

SAMPLE				
Date	**Formation / Lithology**	**Type**	**Ref.No.**	**Location**
20/04/01	Light grey till	m bag	**ST1**	
20/04/01	Dark grey till	m bag	**ST2**	
20/04/01	Tube cutter	m bag	ST3	
20/04/01	Medium grey silty clay till	TUBE	**ST4**	Mudslide, adjacent to PANDA 'SD5'
20/04/01	Light grey till	TUBE	**ST5**	Debris flow, adjacent to PANDA 'SD8'
08/08/01	Trimingham Clay Member	m bag	**STA**	4m below blue-grey clay. NGR TG 26851 39610
08/08/01	Trimingham Clay Member (top)	m bag	STB	NGR TG 26851 39610
08/08/01	Trimingham Sand	m bag	STC	Erosive scour in top of TCM. NGR TG 26852 39610
08/08/01	Clay	m bag	STD	Above sand (sample *STC*). NGR TG 26851 39610
08/08/01	Trimingham Clay Member	m bag	STE	NGR TG 26868 39616
08/08/01	Happisburgh Till Member	m bag	**ST6**	Base of cliff. NGR TG 27161 39473
08/08/01	Chalky clay till	m bag	ST7	NGR TG 26780 39577
07/08/01	Walcot Till Member	s bag	ST8	
07/08/01	Clay	m bag	**ST9**	Undisturbed, base of main b/scarp/ NGR TG 26870 39564
07/08/01	Chalky till	s bag	ST10	NGR TG 26899 39633

Note: s=small, m=medium. Bold samples have index property or strength data.
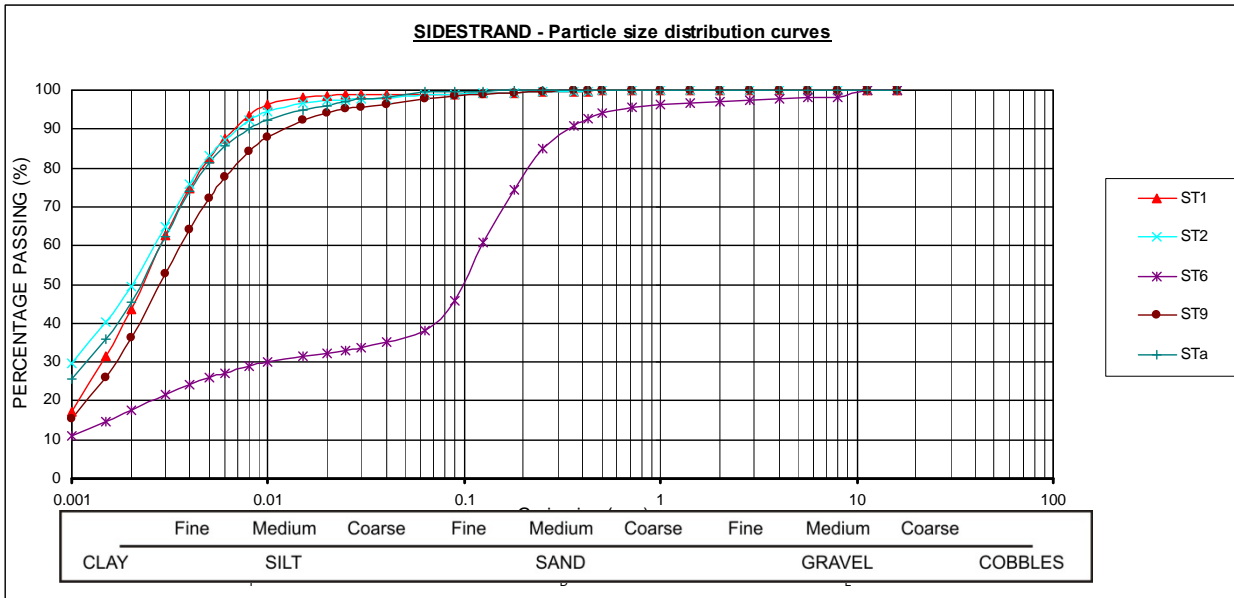
Figure 5-14 Particle-size distribution curves (refer to Table 5-4)

Table 5-5 Summary of particle-size results (refer to Table 5-4)

	Clay (%)	Silt (%)	Sand (%)	Gravel (%)
ST1	43.7	55.2	1	0
ST2	49.4	49.4	1.2	0
ST6	17.5	20.5	59.1	2.9
ST9	36.3	61.6	2.1	0
STa	45.3	54.3	0.4	0

Table 5-6 Summary of index test results

	w_L (%)	w_p (%)	I_p (%)	LS (%)	w @ LS (%)
ST1	38.5	21.0	17.5	4.0	38.6
ST2	61.0			15.8	62.1
ST6	22.0	NP		5.1	
ST7	26.0			6.9	25.8
ST9	50.5	21.7	28.8	11.3	51.9
STD	55.0			13.9	54.6

The Panda is only able to test the top 0.75 meters of the deposits, which restricts the results. The data produced (Figure 5-13) relates to the strength of failed materials and assesses the

63

undrained strength of remoulded or partially remoulded mudflow and debris flow deposits. At ST4, which tests a mudflow, the Panda results indicate a fairly uniform increase in undrained shear strength with depth. Profile ST5 tests the top of a debris flow and shows much weaker near-surface strength possibly due to grading during deposition and variations in moisture content.

Direct strength testing was carried out on two undisturbed samples involving consolidated undrained triaxial testing with pore pressure measurements. The effective strength parameters are tabulated in Table 5-7. The low cohesion value of ST4 is probably due to the fact that the material has lost most of its inter-granular strength bonding during transport.

Table 5-7 Effective strength parameters - triaxial test (refer to Table 5-4)

Sample	Deposit Type	w_0 (%)	c' (kPa)	Φ' (degr.)
ST4	**Mudslide (silty CLAY)**	22.0	0.4	26.7
ST5	**Debris slide (light grey till)**	21.7	7.4	17.6

Residual strength data (Table 5-8) from a landslide at Cromer (Hutchinson, 1976) indicated little loss in strength between remoulded samples and undisturbed material. This indicates the tills are 'low sensitivity' in strength terms. Peak undrained strength data (Table 5-9) from a landslide investigation at Overstrand gives typical properties of some of the units. The 'sand and gravel' unit tested is likely to be from the Britons Lane Formation. The friction angle reported is typical of a moderately dense, angular, uniform coarse soil (Terzaghi, 1955).

Kazi and Knill (1969) observed that the undrained shear strength of the Happisburgh Till Formation was slightly greater (max 220 kPa) at Sidestrand than at Happisburgh (max 172 kPa). They attributed this increased strength to greater overburden pressure along the Cromer Ridge due to variations in ice thickness.

Table 5-8 Residual strength & index parameters – shear-box, landslide, Cromer golf course.   [TG236415] (Hutchinson, 1976)

Ref. stratum	Stratigraphy	Material	State	w_L (%)	w_P (%)	c_R' (kPa)	ϕ_R' (°)
Bed 4, clay, silt, sand	Ivy Farm Laminated Silt Member (?)	Slip plane	Remoulded	41.0	18.0	0	24.0
Bed BS1, silt, clay	Ostend Clay Member	Slip plane	Intact	35.0	20.0	0	24.0
Bed BS2, silt, clay	Ostend Clay Member	Slip plane	Intact	43.0	23.0	0	19.0

Table 5-9 Undrained strength parameters - quick undrained, Ostend landslide investigation (Frew and Guest, 2001)

Material	Bulk Density Mg/cm^3	(Φ) degrees
Slip Debris	1.8	25
Brown Clay	2	29
Laminated Clay	2	20
Sand / Sand gravel	2	35

5.6   GEOMORPHOLOGY

5.6.1 Cliff

The cliff at the Sidestrand test site is a highly complex feature. Whilst the cliff is sub-divided into landslide embayments, the complexity of the landslide processes and geometry within those embayments contrast greatly with the other test sites in Norfolk and elsewhere. This is largely a result of the complex geology at the site. The test site cliff is representative of the entire coastal section between Overstrand and Trimingham. However, the Sidestrand location appears to feature greater than average landslide activity, and greater penetration of embayments.

5.6.2 Platform and beach

Part of the solid platform exposed beneath the beach at low tide is shown in Figure 5-15. This represents the base level to which the beach can reach during the seasonal cycle of beach lowering. As at Happisburgh, platform exposure typically varies from summer to winter, dependent on beach level, although a significant cover of beach material was observed at the Sidestrand site during all fieldwork epochs, with the platform only intermittently exposed at around the low water level during spring tides. Small-scale or micro-folding is shown (foreground), and some jointing is also shown (mid-ground). The former indicates a north-south thrust direction, whilst the latter trend is approximately east-west. The folding matches that seen at the cliff toe (Figure 5-9).

Figure 5-15 Platform at Sidestrand test site (Happisburgh Till Member) at SD2
Note: micro-folding and jointing

The beach is predominantly sand (Figure 5-16) with variable amounts of coarser material. Beach composition can vary considerably over relatively short distances, depending on the relative supply of material from the local updrift sources. Beach thicknesses were recorded at Sidestrand during November 2002 and April 2003 at around the mid-beach level as 0.55 m and 1.15 m respectively.

Figure 5-16 Contrasting beach sediment type over a short distance of coast either side of the main landslide at Sidestrand.
View looking north-west (top) and south-east (bottom). Photographs taken in April 2002.

5.7   COASTAL EROSION AND SEDIMENT TRANSPORT

Accounts of cliff recession provide a useful guide to the rate of erosion. For example, cliff recession reached the (former, Foulness) lighthouse, east of Cromer, and destroyed it in 1866; the new (current, Cromer) lighthouse built in 1833 having been positioned 250 yards inland of the old. This gave an average recession rate of 1.1 m/yr at that location for the late 19th and early 20th century (Hutchinson, 1976). Prior to the destruction of the Foulness lighthouse a

large landslide was recorded by Trinity House staff (Hutchinson, 1976) seaward of the lighthouse which cut the cliff back by 30 m and produced a large debris apron.

The laser scan 3-D models have been analysed for each monitoring epoch in Vertical Mapper™ by using a surface to surface calculation, with the lowermost surface at the 1.5mAOD contour line (to avoid the beach) and the upper surface at the change in slope represented by the highest point of the cliff. The landward surface has been defined by the rearmost part of the backscarp. Results for Sidestrand show an average of 24,260 m³ of sediment a year is lost from a section of 200 m of cliff, this equates to approximately 45,000 t of sediment annually. The figures for each year are shown in Table 5-10, and it is clear that 2002-2004 shows a significant decrease in the amount of erosion at the site. This pattern differs significantly from that at Happisburgh where the significant decrease occurs in 2005-2006 (section 4.8). The highest volume changes are for 2000 to 2001 and 2001 to 2002. The very low and negative values for volume changes for 2002 to 2003 are due to the virtual coincidence of the two scans and to errors associated with the volume change method. It should be noted that at Sidestrand the total amount of material lost does not necessarily equate to the amount of material involved in landslide events during the specified period. This is due to the fact that the volume change figures include debris remaining from earlier landslide events. This tends not to be the case at Happisburgh where removal of debris is relatively instantaneous.

Table 5-10 Volume changes for 200m and 100m sections of cliff at Sidestrand

Sidestrand		
Epoch	Volume change (m³) per 200m cliff *	Volume change (m³) per 100m cliff #
2000-2001		45,670
2001-2002	64,790	43,367
2002-2003	1,414	-11,124
2003-2004	4,132	2,357
2004-2005	12,084	1,896
2005-2006	38,880	9,600

  # embayments SD1 & SD2
   * embayments SD1, SD2 & SD3

There appears to be no clear correlation between annual rainfall and annual volume changes. Such a correlation might be anticipated for cliff stability where rainfall is known to be the dominant factor; this being considered more likely at Sidestrand than Happisburgh. However, the volume change concept here is complicated by the fact that the net value includes debris from previous events. As such the figure will be influenced by factors such as storminess, as well as rainfall. Conversely, at Happisburgh, whilst the erosion volume change scenario is simple, the dominant factor here is probably not rainfall. Additionally, the impact of rainfall on slope instability is not instantaneous. The possible effects of delayed infiltration have not been investigated.

5.7.1 Embayment formation

Embayment formation at Sidestrand might be expected to be controlled largely by landslides. Evidence gathered during the monitoring period supports this. However, there is likely to be a more fundamental controlling factor; that is, the underlying geological structure itself which is determining the shape and size of the embayments. This in turn affects the nature of the landslide activity. This is illustrated by the images in Figure 5-17 which shows the thrust-affected marls of the Ivy Farm Laminated Silt Member, and Figure 5-18 which shows folding within the underlying Ostend Clay Member. These are folded in such a way that the upturned limbs act as resistant zones and tend to form promontories, whereas the lower and flat-lying parts form a trough within which landslides can develop and travel. Also the low-lying zones feature thicker deposits of overlying weak sands which are more prone to instability. Embayment SD3 is a much broader feature due to the generally flat-lying form of the Ivy Farm Laminated Silt Member in this section. As a result the landslide processes are different here. The structural features illustrated are more often than not obscured by landslides deposits and slopewash.

Figure 5-17 Promontory between embayments SD1 and SD2 showing thrust-affected folding (red line) of Ivy Farm Laminated Silt Member (Sep 2004).
Note: debris flow in foreground. Approximate height of promontory = 20m.

Figure 5-18 Folding in Ostend Clay Member between embayments SD2 and SD3 (Sep 2004).
Approximate height of foreground mass = 2m

5.8   COASTAL INSTABILITY AND LANDSLIDES

The landslides at the Sidestrand test site are complex, consisting partly of large-scale, deep-seated movements and partly of mudslides and debris flows. The deep-seated movements tend to have a dominant rotational component, but are in part translational. In some cases these extend to depths several metres below platform level, but are more usually entirely within the cliff. The landslides form deeply incised embayments which are arcuate in plan, but also form elongate embayments with a large part of the backscarp parallel with the coastline, though the latter can be sub-divided using minor geomorphological features within them. The head- or back-scarps at the cliff-top tend to be sharply defined vertical features which persist after the landslide event. Deep-seated landslides tend to rotate to angles of 10 to 20 degrees and break up during failure transport, producing large debris aprons which spread across beach and platform. These are short-lived as the debris is readily removed by the sea. Such large events spawn many mudslides and mudflows.

The test site initially covers three embayments (SD1, SD2, SD3), each of different width and each with significant differences in their stratigraphy. Two further embayments are identified after increased landslide activity (Figure 5-1). The level of activity during the survey period has been high, particularly during the winter of 2000/01, and has included various types of movement at beach level (e.g. Figure 5-26), and a large-scale debris flow, which ran-out across the beach and persisted for two years (Figure 5-30). Active beach thrusting and deep-seated rotation have been observed periodically. Knight (2005) describes similar shallow thrusting of beach material at West Runton.

The first engineering geological assessment of landslides on this part of the Norfolk coast was made by Hutchinson (1976). He catalogued in considerable detail the history of coastal

69

landslides between Cromer and Overstrand and related them to the geology, largely based on Banham (1968), and included data from a number of boreholes and geotechnical tests obtained from a landslide in 1962. Hutchinson (1976) described a large landslide at Cromer golf course in a cliff 65 m high, the cross-section of which is shown in Figure 5-19. This section, based on field observation and four boreholes, shows a deep-seated (maximum proved slip surface depth = 17 m, post-slide), largely rotational, landslide which produced an 80 m long debris run-out and a cliff-top recession of 15-20 m. The volume was estimated to have been 250,000 m^3. In plan, the landslide produced an arcuate cliff-top embayment. Hutchinson (1976) also demonstrated the effectiveness of the groynes in halting south-eastward beach drift and hence promoting landsliding immediately down-drift of the final groyne. The use of an innovative resistivity sounding technique below beach level to detect a salt/fresh water discontinuity, and hence infer the location of a landslide slip surface, was also described.

The level of activity, and the nature of the landslides at the test site, has been heavily influenced by the local glacio-tectonic features, notably the synclinal structures and the associated drainage regime. Additionally, it is believed that the local topography and drainage landward of the cliff-top has also had an influence. Direct erosion from precipitation and seepage is very active, largely due to the juxtaposition of inter-bedded sands, clays, and chalks. Chalk (erratic) rafts within the Happisburgh Formation have resulted in more resistant zones and the development of characteristic buttresses separating the embayments (Figure 5-20).

The complexity of the landsliding regime at Sidestrand is compounded by the more or less continuous reworking and erosion of pre-existing landslide features (Figure 5-21). This brings unrelated stratigraphies together, allows earlier slip planes to be utilised by later landslides, and makes discrete landslides difficult to distinguish. Unusually in October 2000, a deep-seated rotational landslide mass was observed rising from beneath the beach at an estimated rate of 10 cm per tide (Figure 5-22). The morphology of landslides can often be examined from unusual angles at the Sidestrand test site. For example, Figure 5-23 shows an underside view of a mudslide. This was probably possible because of renewed movement following erosion of the snout rather than because of removal of the underlying material.

The feature shown in Figure 5-22 is an exposure on the beach of the underside of a rotational landslide seated beneath beach level. A simplified mechanism is shown schematically in cross-section in Figure 5-24. As the slip mass rotates it raises material above beach level beyond the cliff toe, thus exposing the underneath of the slip surface. Wave erosion removes this prominence, the 'resisting' forces are thus reduced, and the rotation is re-activated. Debris from above the landslide also moves onto the top of the slide, thus adding to the 'driving' forces and promoting further rotation. Seasonal accretion and depletion of the beach may also play a part in, respectively, resisting and activating the rotation. In reality it is unlikely that the slip plane is perfectly circular. The base of it is more likely to be flat, or at least to have some planar components, often associated with bedding or pre-existing slip planes. This mechanism has only been observed at the test site on one occasion (embayment SD3). It is probably more common for such rotational failures to daylight above beach level.
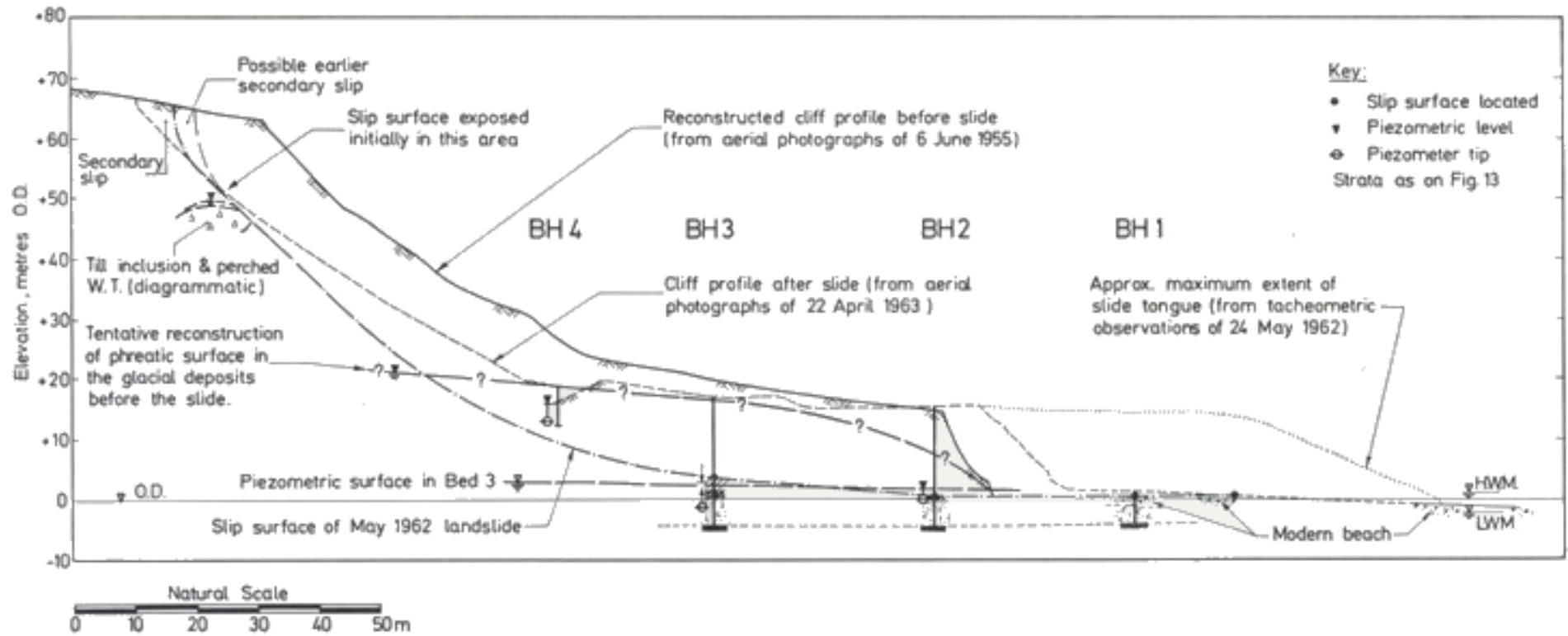
Figure 5-19 Cross-section of May 1962 landslide at Cromer golf course [TG236415 approx.] (Hutchinson, 1976)

Figure 5-20 Chalk till buttress separating SD1 and SD2.
Note: very active till-rich mudflows, debris flow covering beach deposit (26/10/00).

Remnant
slip mass

Figure 5-21 Exposed undulose slip surface (white arrows) at base of former debris flow/mudslide on grey till at cliff toe, SD3.
Note: Horizontal slickensides & striations – slip direction: green arrow. (Sep 2004).

Figure 5-22 Actively rotating slip mass rising from beneath beach level at SD3.
Note: base of slip plane exposed, direction shown by green arrows (26/10/00). Note trowel for scale.

Figure 5-23 Exposed base of desiccated mudslide mass showing inclined slickensided slip plane, SD2
Note: Direction of movement shown by green arrow (Oct 2000). Approximate length of arrow = 10cm
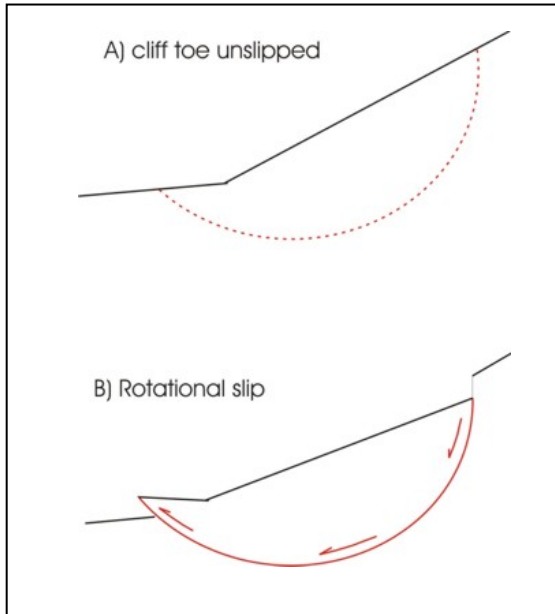
Figure 5-24 Mechanism of rotational landslide at cliff toe (from Figure 5-22)

The feature shown in Figure 5-23 is the underneath of a mudslide slip plane approximately 2m above beach level within embayment SD2. The slip plane shows slickensiding and hence the direction of movement of the overlying slip mass. The mechanism that is believed to have resulted in this exposure is shown schematically in cross-section in Figure 5-25. The toe of the cliff and the original slip (A) has been eroded by wave action (B). This has unloaded the zone of accumulation of the mudslide and allowed the slide to re-activate, thus moving the slip mass beyond the new cliff toe and exposing the underneath of the slip surface (C). This process is essentially the inverse of that shown in Figure 5-21 which both appear to be common within the test site.
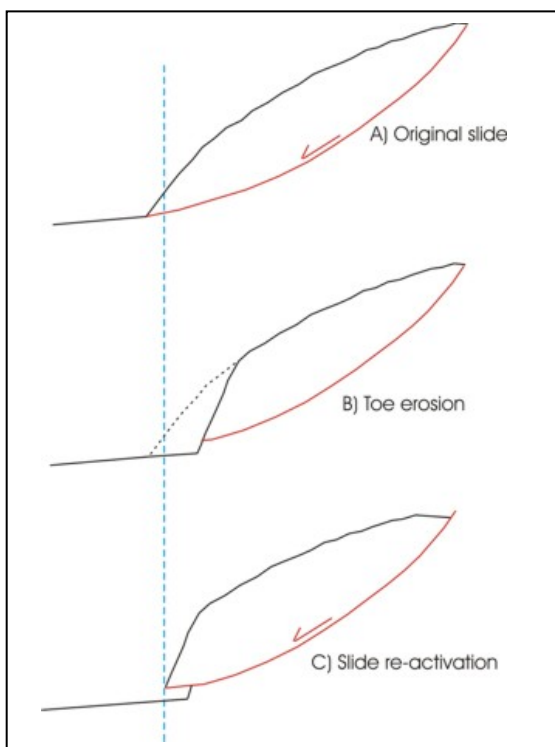
Figure 5-25 Schematic of mudslide development at cliff toe, SD2.

5.8.1.1 Landslide activity at Sidestrand in 2000

During the first year of monitoring at Sidestrand considerable landslide activity was observed at the test site (Figure 5-22 and Figure 5-26). These took the form of widespread mudflows in embayments SD1 and SD2, and an unusual active rotational movement at beach level in SD3. The latter proved that deep-seated rotational movements occurred and were founded at depths below beach level, though precisely at what depth it was not possible to ascertain. This kind of movement differed from that shown at SD2 (Figure 5-22) in that the latter, though also distinctly rotational, appears to have occurred largely above beach level, and resulted in a thrusting forward of the beach material. A movement rate of 1.0 cm /hour was estimated based on time available since last high tide and destruction of features. Of course, it is unlikely that the movement was perfectly circular (as shown in Figure 5-24), and was more likely to have been 'flattened' in the lower part with an upturn at the toe (Figure 5-27). Such geometries are seen elsewhere in deep-seated landslides in capped mudrocks; for example Folkestone Warren, Kent and Bindon, Dorset. However, it is unclear whether the feature described at SD3 represents the toe of a 'full-height' landslide or merely the re-activation of landslide debris stacked against the lower part of the cliff. In either case the platform itself may have been involved in the movement. The mudflows tended to involve largely clay-rich and silt-rich deposits from the central cliff (Bacton Green Till Member and Ivey Farm Laminated Silt Member).

Figure 5-26 Active thrusting of beach deposits as a result of deep-seated landslide movement in SD3.
Note: uptilted tills (mid-ground) (26/10/00)

75
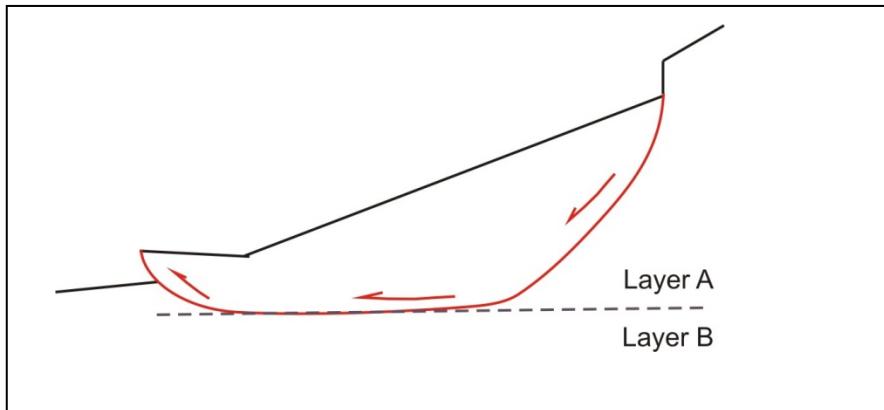
Figure 5-27 Schematic of 'non-circular' (compound) rotational landslide constrained by geological boundary (from Figure 5-22).
Note: typically the interface between layers A & B is a plane of weakness

5.8.1.2 LANDSLIDE ACTIVITY AT SIDESTRAND IN 2001/2002

A combination of field notes, photographic evidence and change models produced from scan data allows us to assess the levels and distribution of activity of landslides within the three embayments. From the change model in Figure 5-29 it is evident that during the period 2001-2002 a large debris flow (**A**) occurred at the eastern end of embayment SD3 (Figure 5-30). The eastern edge of embayment SD3 in Figure 5-29 shows a clear loss of material whilst there is an increase in height at the base of the slope as a consequence of the toe being built up (**B**). The morphology of the landslide toe is clearly shown in Figure 5-28 and Figure 5-29. The debris flow emanated from the easternmost corner of the embayment's backscarp and spread down the slope and about 30 m across the beach to a thickness of about 7 m. It took over 18 months for the debris to be eroded away by the sea back to its pre-flow position.

Figure 5-28 Lower section of large landslide in SD3
Note: active condition, ponding, compression ridges, desiccation cracks (05/09/01)
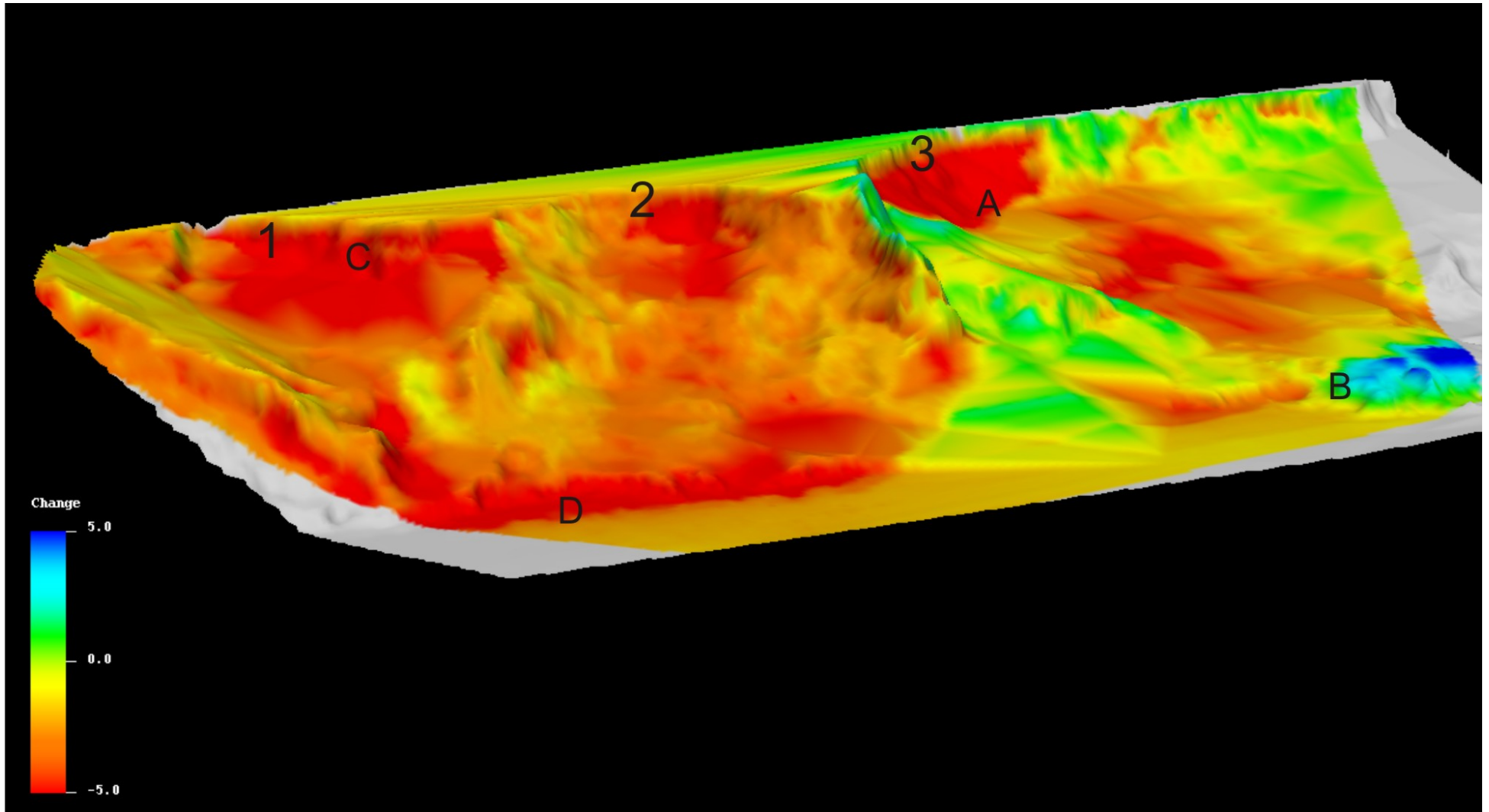
Figure 5-29 **Height change model for the 01/02 scanning season**
Red indicates an overall loss of material whilst blue indicates an overall gain in material. The embayments are numbered and the letters referred to in the text. Length of section approx. 370 m.

Figure 5-30 Large debris flow of winter 2001/02 at SD3 (11/04/02)

In embayments SD1 and SD2 fairly active removal of material from the back scar is taking place, which is visible from the change model produced from the 2001/2002 laser scanned data. Removal of material from the back scar is accompanied by mudflows and debris removal from the mid slope which was probably emplaced by a previous rotational failure (**C**). Removal of material is taking place through marine erosion, which is evident from the steep cliffs in the toe of the landslide (**D**).

5.8.1.3 LANDSLIDE ACTIVITY AT SIDESTRAND BETWEEN 2002 AND 2003

Evidence from the change models (Figure 5-31) suggests that the toe of the large debris flow of 2001/2002 is still apparent but is smaller in size (**A**). In contrast to the previous years SD1 and SD2 show little evidence of activity on the same scale. There is some loss of the buttress between SD2 and SD3 (**B**). SD2 does show some evidence of mudflows (**C**) and there is a general loss of material form the toe area of both SD1 and SD2 (**D**). In general SD3 appears to have been more active during this period of monitoring.

5.8.1.4 LANDSLIDE ACTIVITY AT SIDESTRAND BETWEEN 2003 AND 2004

In the period between 2003 and 2004 it appears from the change model (Figure 5-32) that SD3 has become much less active, whilst the debris toe from 2001/2002 appears to have been almost fully eroded (**A**). Some activity in SD3 is evident on the steep back scar area, which may be minor falls of material of removal of material by wash (**B**). It appears from Figure that SD1 is more active than previous years with material lost from the back scar (**C**) and some evidence of a flow (**D**). There has also been loss of material between SD2 and SD3 at the base of the buttress (**E**).
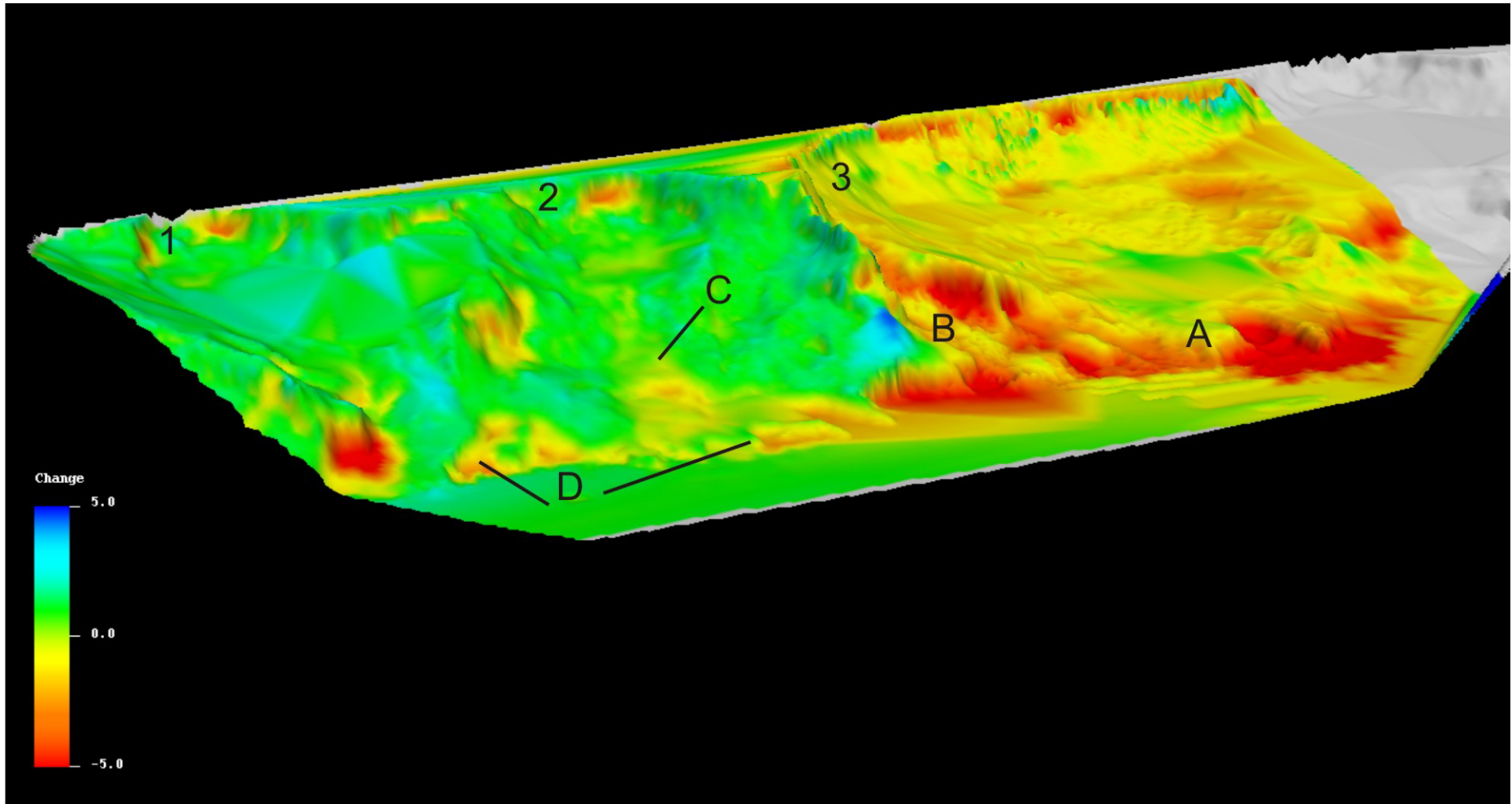
Figure 5-31 Height change model for Sidestrand for the period 2002-2003. Length of section approximately 370 m.
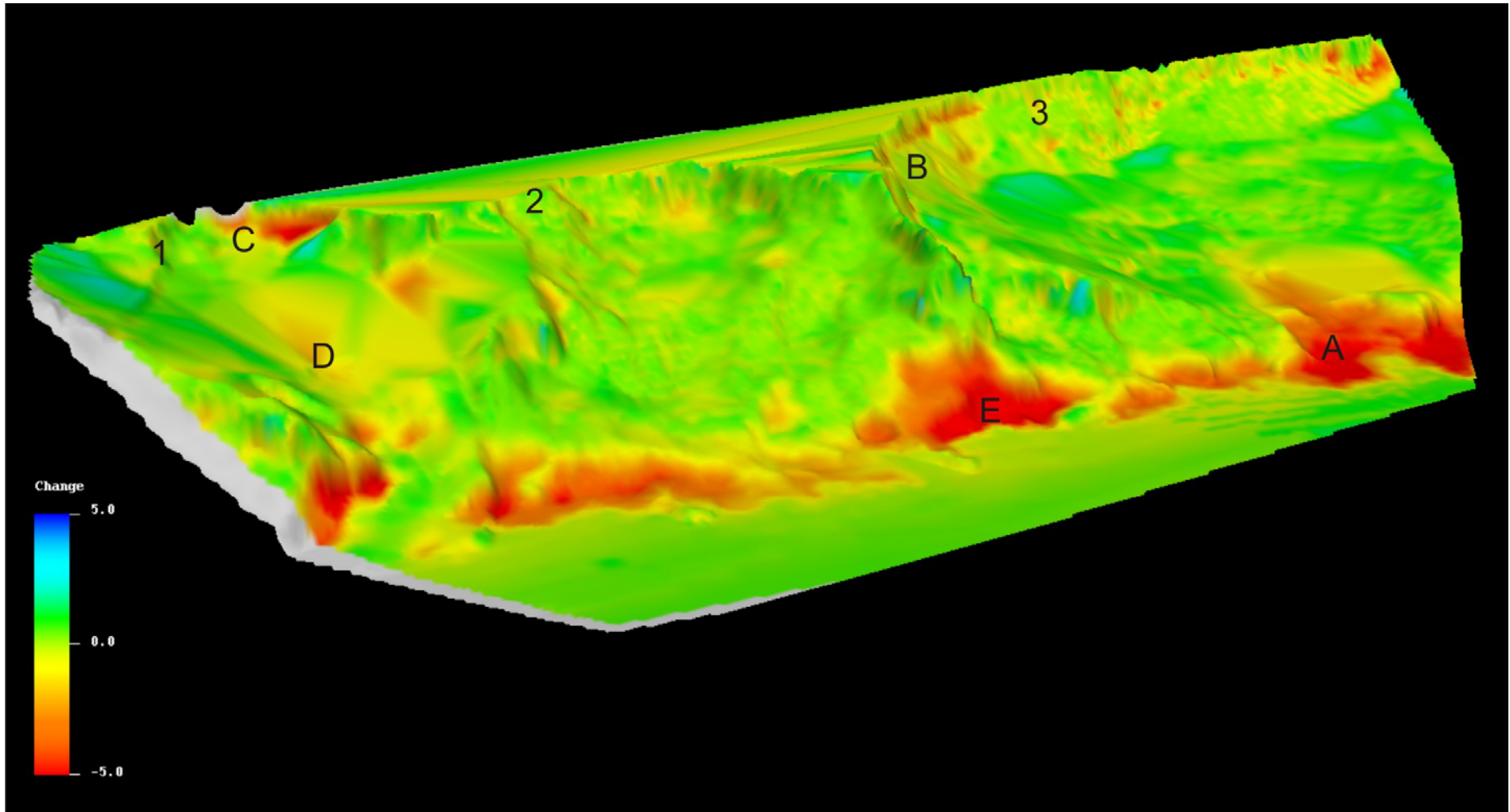
Figure 5-32 Height change models of Sidestrand for the period 2003-2004. Length of section approximately 370 m.
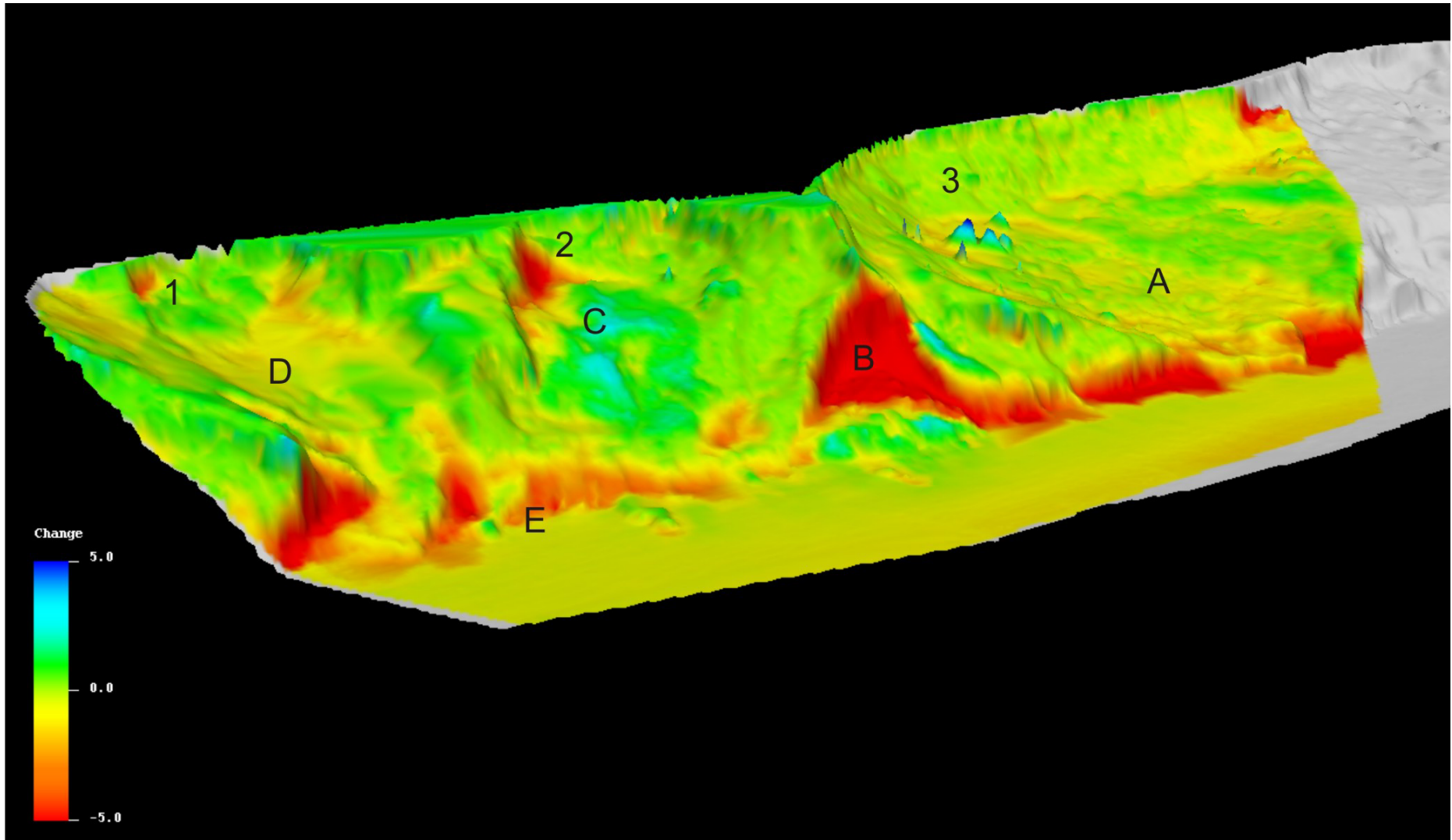
Figure 5-33 Height change models of Sidestrand for the period 2004-2005. Length of section approximately 370 m.

5.8.1.5 LANDSLIDE ACTIVITY AT SIDESTRAND BETWEEN 2004 AND 2005

The presence of a failure and subsequent mudflow in SD3 are still visible in the 2004/2005 change model (Figure 5-33). It appears that SD3 may have been more active than the previous period between 2003-2004, evidenced by the loss of material in the mid slope (**A**). The front of SD3 has been scoured back to form a steep cliff either side of the toe of the flow track. The buttress area shows a high rate of loss on the seaward side (**B**). SD2 shows little evidence of activity apart from in the back scar area from where material has been lost. The toe area of both SD1 and SD2 is also being eroded forming steep cliff areas at the base of the embayments. SD1 shows evidence of flow-like activity with the loss of material in the track area (**D**), the source area being higher up on the back scar. It appears that the flow from SD1 spills over the steep base of the slope onto the beach where marine action is able to erode it back.

5.8.1.6 LANDSLIDE ACTIVITY AT SIDESTRAND BETWEEN 2005 AND 2006

Changes in the Sidestrand test site between 2005 and 2006 were considerable. Large-scale landslide activity both within, and adjacent to, the test site were observed at 09.30 hrs on Thursday 28th September, 2006. These included a large toppling failure, possibly in embayment SD1, which pitched a single block (probably Ivy Farm Laminated Silt Member) forming the lower cliff into the sea at high tide (4.41 m at 10.05 hrs. at Cromer). This appeared to be driven forward by a large-scale rotational (slump) movement generated from behind and above, which resulted in a small wave which radiated seaward. Widespread mudslides and debris flows were also observed. A particular feature noted was clouds of 'dust' above the landslide, presumably caused by disturbance of the sand (Stow Hill Sand & Gravel Member) from the upper cliff. The observed sequence of movements took place over approximately 15 minutes. At the time it was not possible to gain access to the test site because of the state of the tide. Hence no record of the observations was possible, with the equipment to hand, from the vantage point at Overstrand (1.5 km distant). The aftermath of these movements were recorded as part of the scheduled survey a week later, during which minor movements of debris were observed. The landslides apparently followed heavy rainfall in North Norfolk on 25th September 2006, and prior to that the highest monthly rainfall average (155mm, August 2006) recorded during the whole project monitoring period. A conceptual model of the events observed on 28th September 2006 is shown in Figure 5-35.

It was noted that during the survey, large volumes of ground water were entering the beach, particularly at the foot of embayment SD3. This had created tripod stability problems, even at low tide, at scan location S3 during the 2006 survey. During the 2006 survey no beach thrusts or other disturbance of the beach related to rotational landsliding, of the kind observed in 2000 (Figure 5-22), were noted. However, a debris flow of the same type, and in the same location at SD3, as that which occurred in 2001/02 (see Section 5.8.1.2), was noted extending about 10 m across the beach (**A**).

The embayment between SD2 and SD3 had enlarged between scanning epochs and displayed what appeared, from the change model, to be a debris cone at the base (**B**). The change model shows that SD1 was being eroded at the base of the cliff and was subject to high losses of material (**C**). In SD2 there appears to have been renewed activity with loss of material at the back scar and possible gain of material through the centre of the embayment and at the toe (**D**). This is also visible from the panoramas in Figure 60 which document the changes between 2005 and 2006.

a) Rotational landslide occurs
 in mixed glacial deposits

Mixed
glacial
deposits

Tills
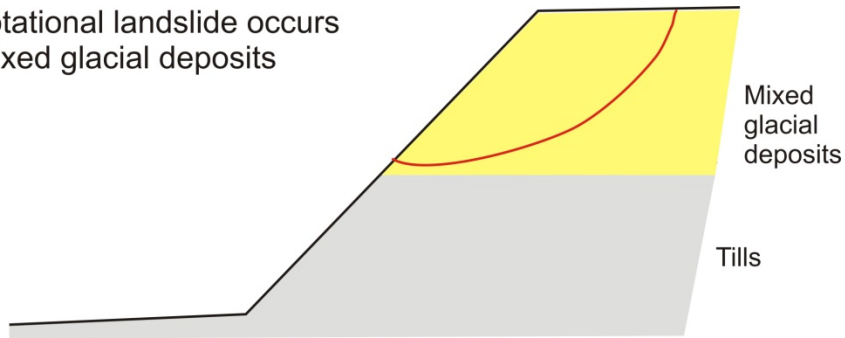
b) Debris flows, mudslides
 and mudflows scour embayment.
Sea steepens till cliff.
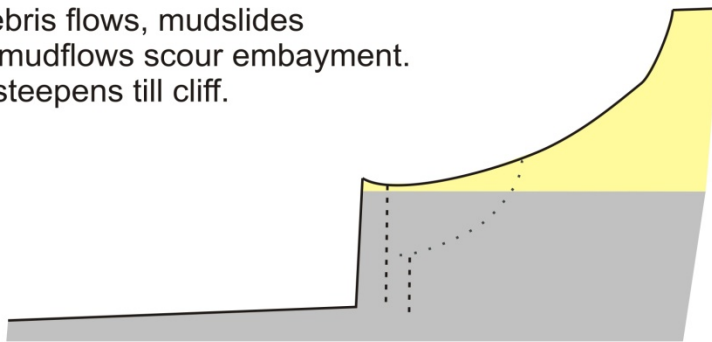
c) Stress-relief, weathering and ponding cause
 detachment & toppling failure of till, possibly
 with thrust from secondary rotational slide
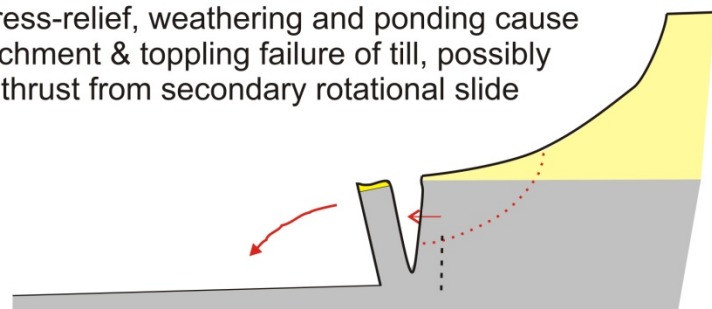
Figure 5-34 Conceptual model for landslide events observed on 28th September 2006.
For discussion of this event see Section 5.8.1.6.
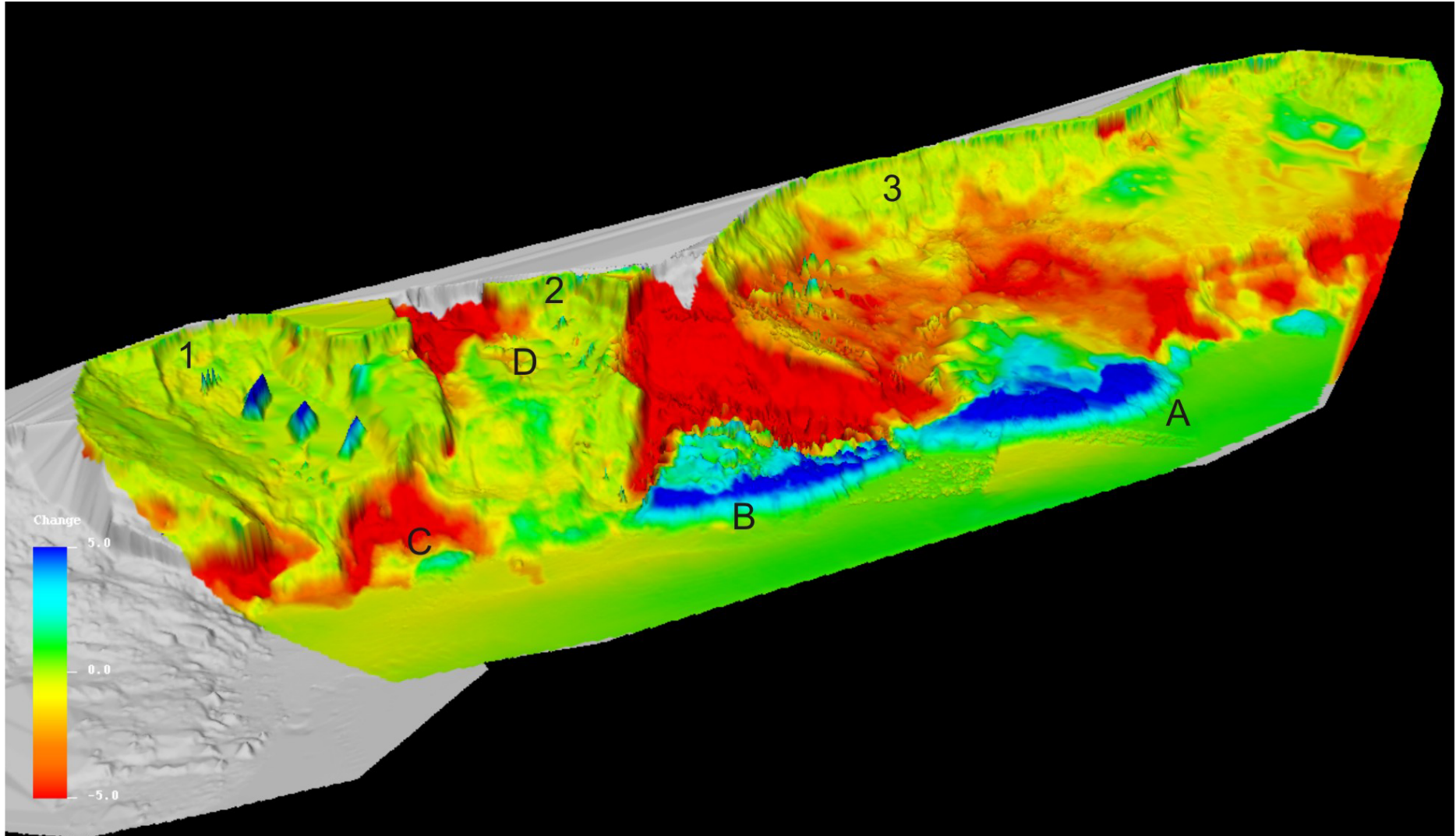
Figure 5-35 Height change model for Sidestrand between 2005 and 2006. Length of section approximately 370 m.
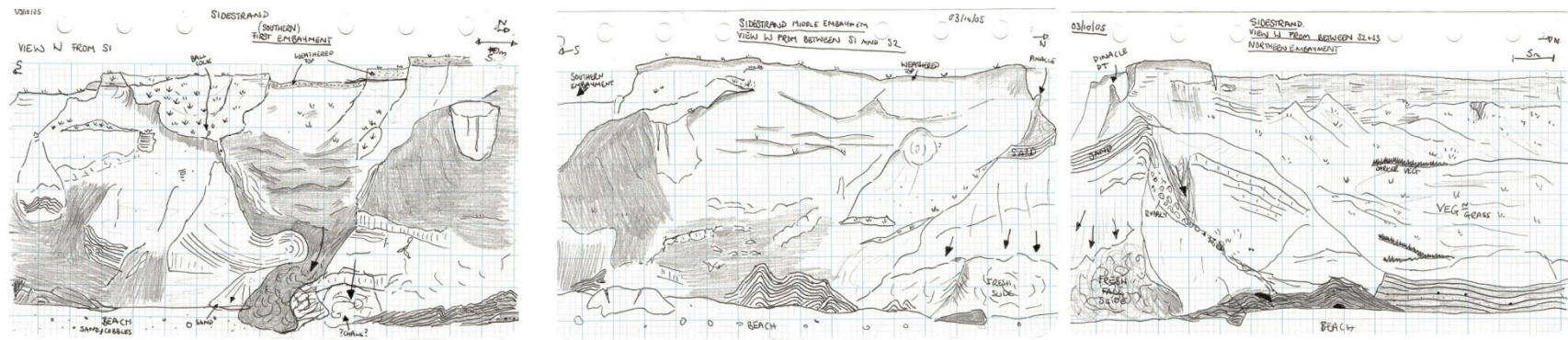
Figure 5-36 : Field sketch and associated panorama photograph for Sidestrand, October 2005.
Length of section approximately 250m.
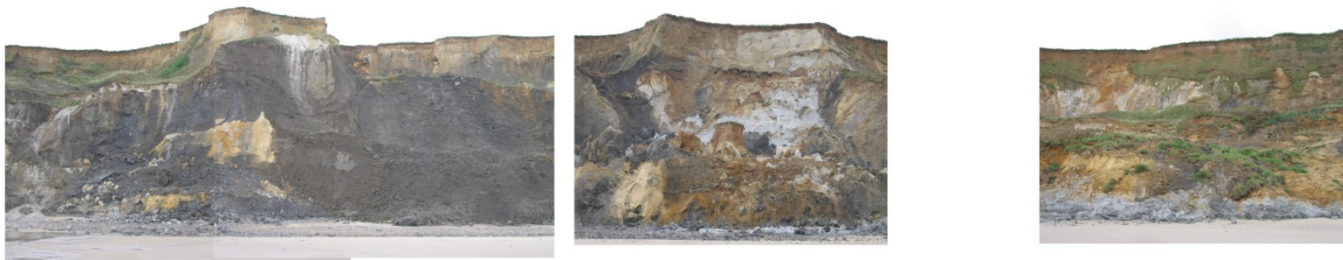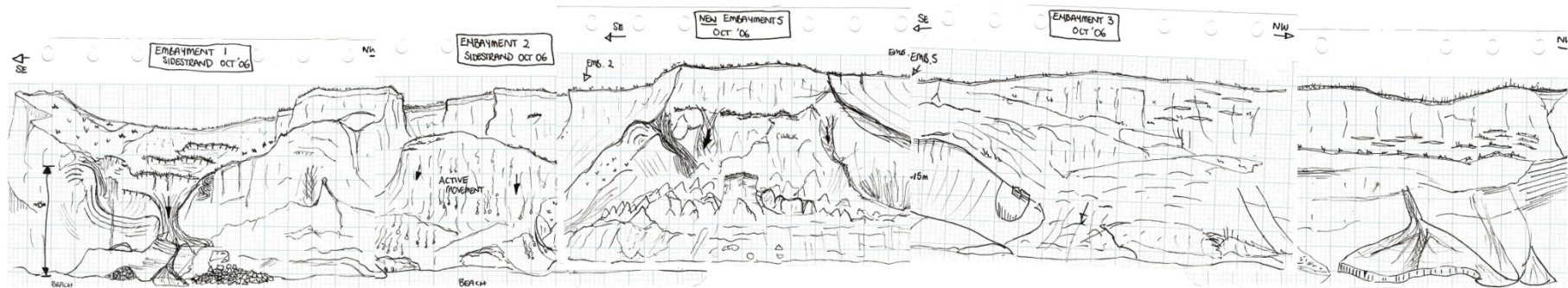
Figure 5-37: Field sketch and associated panorama photograph for Sidestrand, October 2006.
Length of section approximately 350m.

The panoramic photos taken as part of the survey (Figure 5-38 and Figure 5-39) show the major changes and landslide movements which are indicated in the change models. The first of these was a major rotational movement involving almost the entire cliff height producing a large debris apron on the beach, and its own embayment (referred to as SD5 and marked by a red arrow). This movement had already initiated in the lower cliff prior to the 2005 panorama, either in the form of slumping or toppling (or both), thus destabilising the upper cliff and preparing it for the September 2006 movement. The movement has revealed the shapes and extents of chalk till deposits within the cliff. The movement appears to occupy a 'syncline' defined by the pale-grey/white marls of the Ivy Farm Laminated Silt Member, the 'limbs' of which have remained un-slipped, and the precise geometry of which had been obscured prior to the movement. The western limb of the syncline has remained largely intact since the first survey in 2000. The movement has also brought down chalk till material from the upper part of the cliff, along with sand. This new feature was scanned and lies within the 2006 laser-scan model. In addition, further movements in the upper and eastern part are noted as having caused significant regression of the cliff top at this point, with debris cascading over the lower cliff, and a narrowing of the promontory between SD1 and SD2.

The second was a major landslide, possibly of progressive type which mobilised a previously unslipped, near-vertical section of the lower cliff but also regressed in the upper cliff. Though largely unaffected by the 2006 movements, embayment SD1 illustrates clearly the importance of the more resistant marls in the mid and upper cliff in determining the precise geometry of the landslides and resulting embayments. The freshly-exposed, apparently synclinal (and micro-folded) Ivy Farm Laminated Silt Member feature at SD1 has resulted in funnelling action for landslide debris and flows from the upper cliff and a buttressing action to the promontories at either flank. *This new feature was scanned as part of the 2006 model but only from the west side, and cannot be compared in full with scans from previous years as it is beyond the test site.*

Figure 5-38 Comparative panoramas of the central part of the Sidestrand test site taken in 2005 and 2006
(red arrow = westward). Length of section approx 200m.

Figure 5-39 Comparative panoramas of the eastern part of the Sidestrand test site taken in 2005 and 2006.
(red arrow = westward). Length of section approx 200m
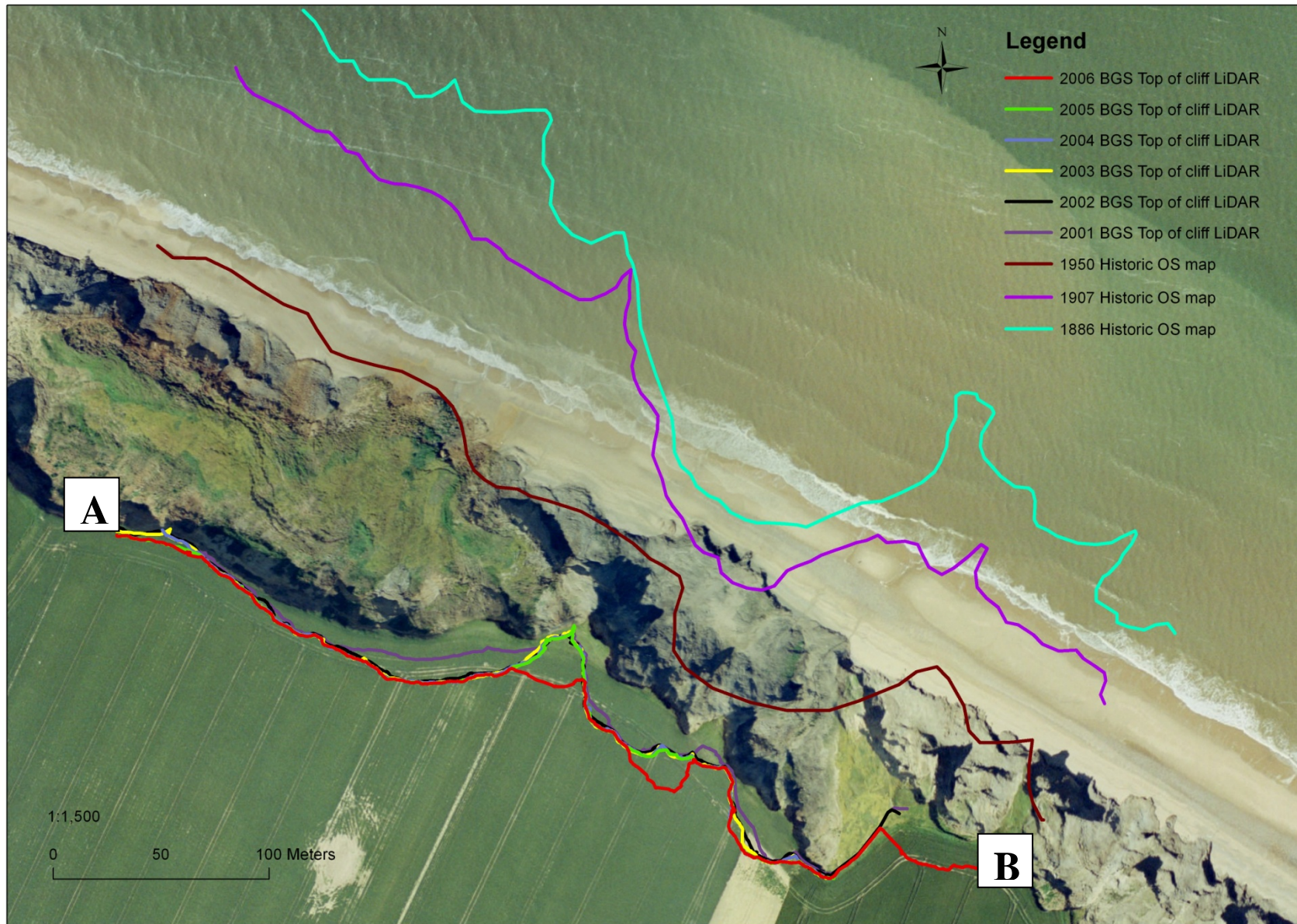
Figure 5.36: Recession of the Sidestrand cliff line between 1886-2006 on 1999 aerial photograph.
1886-1950 historic OS maps. 2001-2006. BGS LiDAR survey. Grid Reference of A (626650, 339623) and B (627049, 339465).

Data taken from the laser scanned images shows the recession of the cliff line between 1886 and 2006 (Figure 5-39). Compared to a similar plot of recession at Happisburgh the rate of recession at Sidestrand is not as significant annually. The most significant loss of material occurred between 2005 and 2006 with the loss of a pinnacle of material creating another embayment (SD5). Annual rates of recession over the period 2001-2006 range from 5 m/yr to 1.6 m/yr, an average annual rate of recession was calculated at about 3 m/yr. Over a longer time period (1885-2006) the rate of erosion appears to be lower at between 1-1.85 m/yr, indicating that conditions may have changed at the site.

Volume losses between each scanning epoch were calculated from cross sections taken from the scanned data. Results from the surveys show an average of 24,260 m^3 of sediment a year is lost from a 200 m section of cliff, this equates to approximately 48,000 tonnes of sediment annually. The figures for each year are shown in Table 5-11, and it is clear that between 2002-2003 the least amount of sediment was lost, compared to the peak year of 2005-2006.

Table 5-11 Volume changes for a 200 m section of cliff at Sidestrand

Epoch	Volume change (m^3)
2001-2002	64790
2002-2003	1414
2003-2004	4132
2004-2005	12084
2005-2006	38880

5.9   CLIFF MODELLING

5.9.1 Slope stability analysis

The geological part of the model was input as layers of horizontal strata of constant thickness. These were as close to the true perceived stratigraphy at the location of the section as was possible (Table 5-12). Clearly, the strata at Sidestrand tend not to be horizontal or of constant thickness. However, as the slope stability model is essentially 2-D and the landward disposition of strata is unknown, the simplification is considered reasonable. It will be noted that the geological models at the three embayments, SD1, SD2, and SD3, are different (unlike that at Happisburgh), and that the slope stability analysis applies only to the particular section chosen in each case. The three embayments and the position of lines used in the slope stability analysis are shown in Figure 5-40. The geological layer models applied at Sidestrand for each of the three embayments are shown in Appendix 4.

The geotechnical properties of the strata modelled were largely unknown. However, some formations e.g. the Happisburgh and the Ostend Clay have been subjected to laboratory tests. For these materials the laboratory data were used (see Section 5.5). For the remainder, typical values were used from the literature and from databases. Knowledge of the consistency of the materials from hand-specimen examination and hand-augering was also used. The analyses were based on the Mohr-Coulomb failure criteria using strength parameters, c' and ϕ'. The geotechnical data used in the model are summarised in Table 5-12.
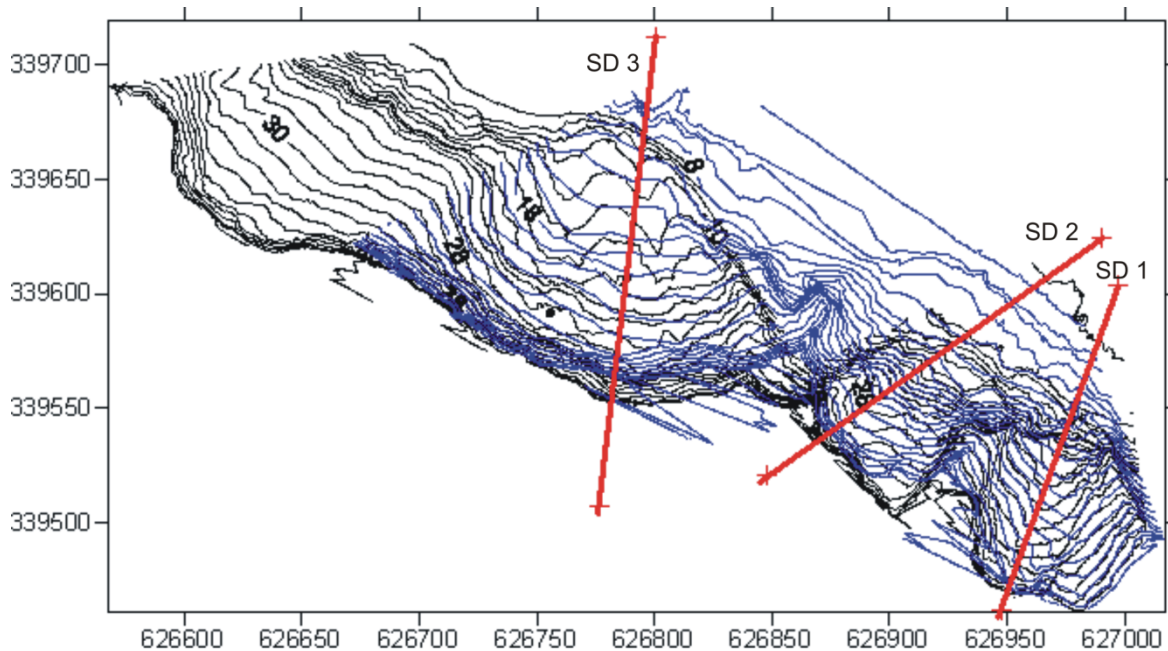
Figure 5-40 Terrestrial LiDAR derived map showing the three cross-sections used for slope stability analysis at Sidestrand

Note: blue contours = Sep 2001, black contours = Sep 2006

Table 5-12 Thicknesses of geological layers applied to the slope stability model at Sidestrand.

Embayment:	SD1		SD2		SD3	
Member	Lower boundary (mASL.)	Thickness (m)	Lower boundary (mASL.)	Thickness (m)	Lower boundary (mASL.)	Thickness (m)
Stow Hill Sand & Gravel	37.7	4.0	38.1	4.9	36.4	7.8
Weybourne Town Till	35.6	2.1	35.5	2.6	26.8	9.6
Trimingham Sand	33.4	2.2	33.0	2.5	absent	
Trimingham Clay	30.9	2.5	30.5	2.5	absent	
Bacton Green	17.1	13.8	25.1	5.4	absent	
Ivy Farm	3.3	13.8	13.9	11.2	10.4	16.4
Mundesley Sand	absent		11.1	2.8	8.3	2.1
Walcott Till	0.8	2.5	9.3	1.8	5.1	3.2
Ostend Clay	-0.7	1.5	7.1	2.2	1.3	3.8
Happisburgh Till (except #)	-4.0	3.3	-4.1	11.2	-3.7#	5.0
Chalk	-	-	-	-	-	-

= **Wroxham Crag F.**

92

Table 5-13 Summary of geotechnical parameters applied to the slope stability model at Sidestrand.

Member	Density (Mg/m^3)	Porosity n	Strength, c' (kPa)	Strength φ' (degr.)	Tension (kPa)
Stow Hill Sand & Gravel	2	0.5	3	38	0
Weybourne Town Till	1.9	0.4	30	35	15
Trimingham Sand	1.6	0.5	0	32	0
Trimingham Clay	1.8	0.5	8	20	8
Bacton Green	1.8	0.45	10	15	10
Ivy Farm	1.75	0.5	8	25	5
Mundesley Sand	1.6	0.5	0	34	0
Walcott Till	2.0	0.5	10	25	8
Ostend Clay	1.85	0.5	12	14	10
Happisburgh Till	2.21	0.28	15	25	10
Chalk	2.7	0.01	2000	42	750

Table 5-14 Factors of safety, Sidestrand – FLACslope v.4

Epoch	SD1	SD2	SD3
2000	1.21	1.03	
April 2001	1.22	1.03	
Sept. 2001	1.28	0.94	1.42
April 2002	0.94	0.94	1.41
Sept. 2002	1.10	1.05	1.19
2003	0.97	1.00	1.22
2004	1.13	1.02	1.06
2005	0.92	1.16	1.39
2006	1.17	1.03	1.05

Note: All analyses include friction, cohesion, & plastic flow rule
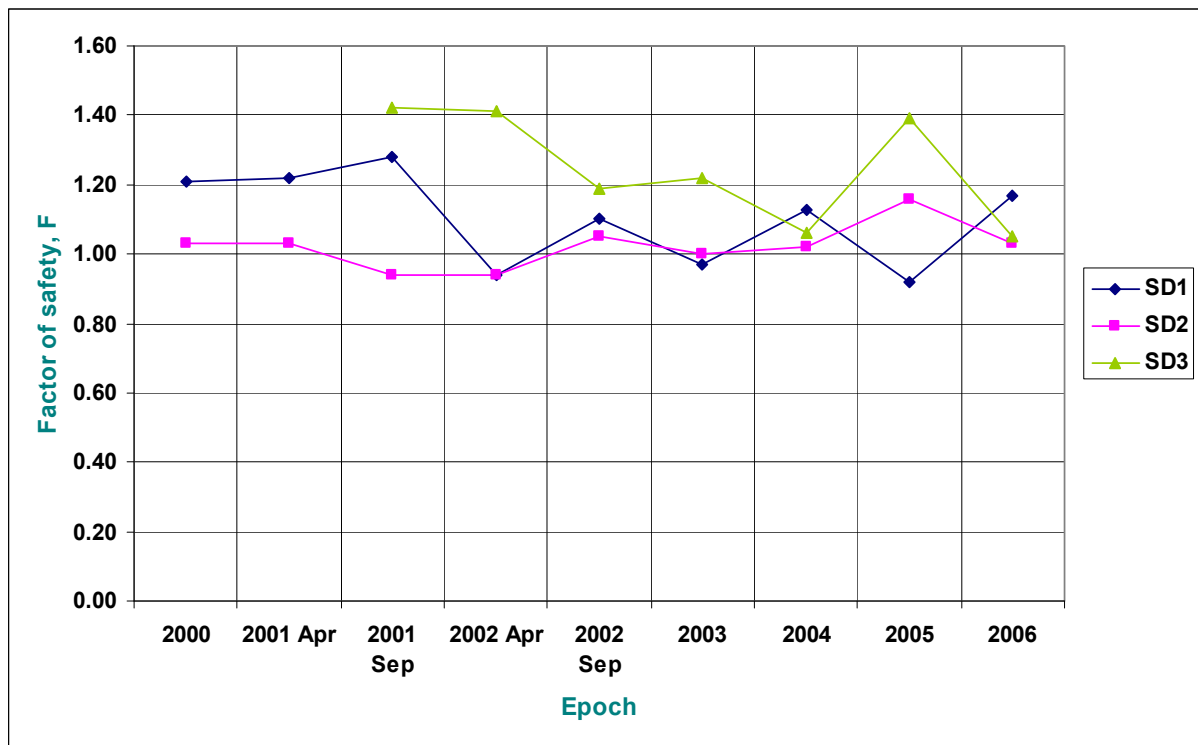
Figure 5-41 Plot of factors of safety (FLACslope, v.4) for Sidestrand embayments SD1, SD2, & SD3
Refer to Appendix 4

The slope stability graphic results are not produced here in full, but rather an assessment with examples is given. The results for the three locations at Sidestrand (SD1, SD2 & SD3) (Figure 5-40) show that the displacement vectors tend to have either a single rotational, multiple rotational, or compound geometry. As was the case at Happisburgh (section 4.10.1), these tend to produce cliff-top recessions exceeding those observed. However, unlike Happisburgh, the three locations have produced different types of deformation which may be interpreted as different landslide types. The sections for embayment SD1, with one exception (Sep 2000), indicate moderately deep-seated single rotational (Figure 5-42) or successive rotational landslides
(Figure 5-43). Embayment SD2 results may be interpreted as having a wide variety of sizes of landslide, the larger ones having a slightly compound shape. Embayment SD3, in contrast to SD1 and SD2, is characterised by very large, deep-seated compound landslides (Figure 5-44). The inclination of the rear part of the displacement zone tends to be steeper than the cliff profile, but nevertheless, as at Happisburgh, tends to produce a larger cliff-top recession than observed, in some cases up to 40 m. Despite the fact that a nearby failure at Overstrand resulted in 70m recession in one landslide event, landsliding on such a scale has not been observed at Sidestrand. There are three primary reasons why this might be the case at Sidestrand. These are:

1. Incorrect geotechnical parameters (in particular, mass strength)

2. Incorrect geological sequence (i.e. existing landslide deposits not modelled)

3. Incorrect ground water profile

With regard to the first, few geotechnical data specific to the 10 geological strata were available for the Sidestrand site. Hence reliance was placed on characteristic parameters gathered from experience elsewhere in similar materials.

With regard to the second factor, it should be noted that the FLACslope program does not permit geological layers that cross-cut other layers. This precluded the representation of pre-existing landslide deposits. Therefore, each slope stability model assumed a first-time slide

94

scenario. Whilst at Happisburgh this matched the observed situation, it did not necessarily apply at Sidestrand where considerable thicknesses of pre-existing landslide deposit remained on the cliff, particularly the lower part, and were available for re-activation. However, as many of the landslides at Sidestrand are deep-seated this factor becomes less-significant, although there remains the issue of pre-existing slip planes which are not capable of being satisfactorily modelled in the FLACslope program.

With regard to the third factor, the ground water table within the cliff is unknown at Sidestrand. However, observations over the period of surveys suggest that ground water plays a key role in the instability at Sidestrand. In the absence of a measured ground water table profile, a relatively steeply-angled profile was modelled (Figures 71 to 73), taking into account the relative permeabilities of the top-most strata and those of the landslide deposits themselves, and the observations of seepage in the cliff. Seepage at the cliff face was frequently obscured by landslide deposits, though it was observed that the landslide masses as a whole varied in saturation from one year to the next and from one season to the next. This was reflected in the ability or inability to traverse the landslides on foot. The test site lies within a shallow north-south trending valley centred on the village of Sidestrand, with slightly higher cliffs to the west and east. This tends to funnel ground and surface water into the test site cliffs. The possible effect of the landslide masses in blocking seepage from the cliff has similarly not been taken into account due to a lack of observable features. As a result of the above, a common water table has been applied to all three embayment models which, it is hoped, reflects the nature of the deposits and the overall topography. The FLACslope model is not capable of dealing, in a straightforward manner, with multiple (e.g. perched) water 'tables'. Such water 'tables' may be anticipated in complex glaciogenic sequences of alternating coarse and fine-grained sediments.
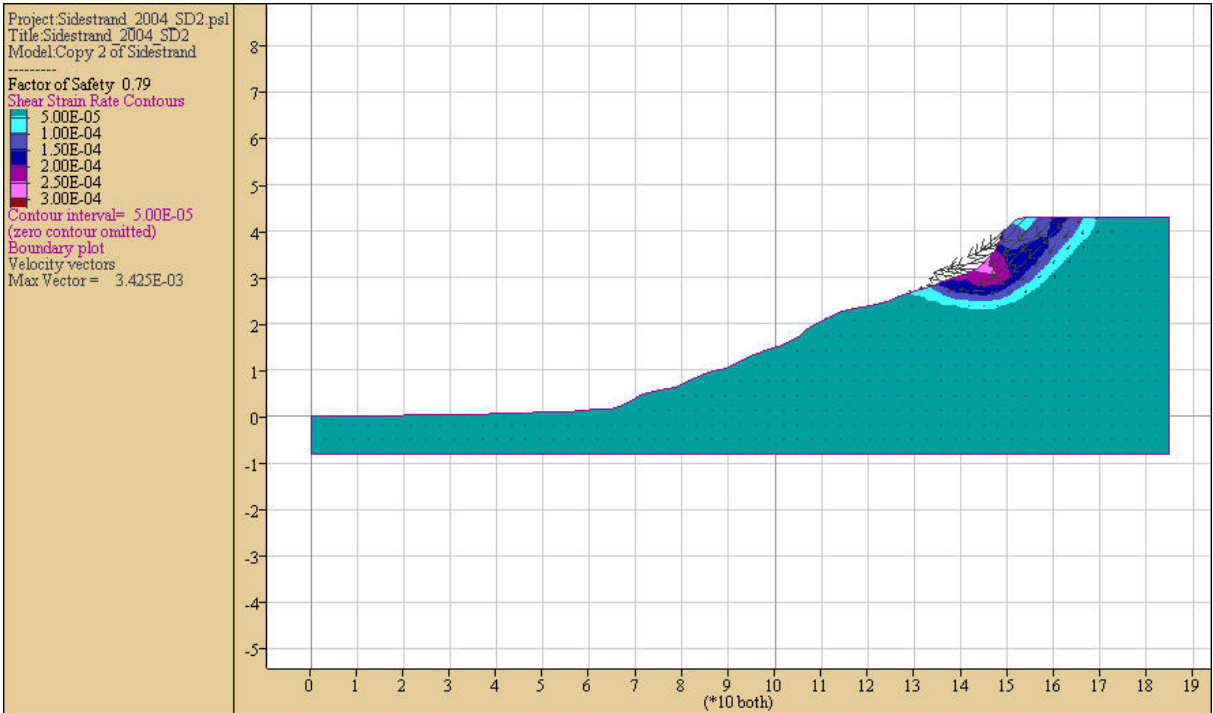
Figure 5-42 Example of displacement strain contour/vector diagram: Sidestrand, SD2, Sep 2004
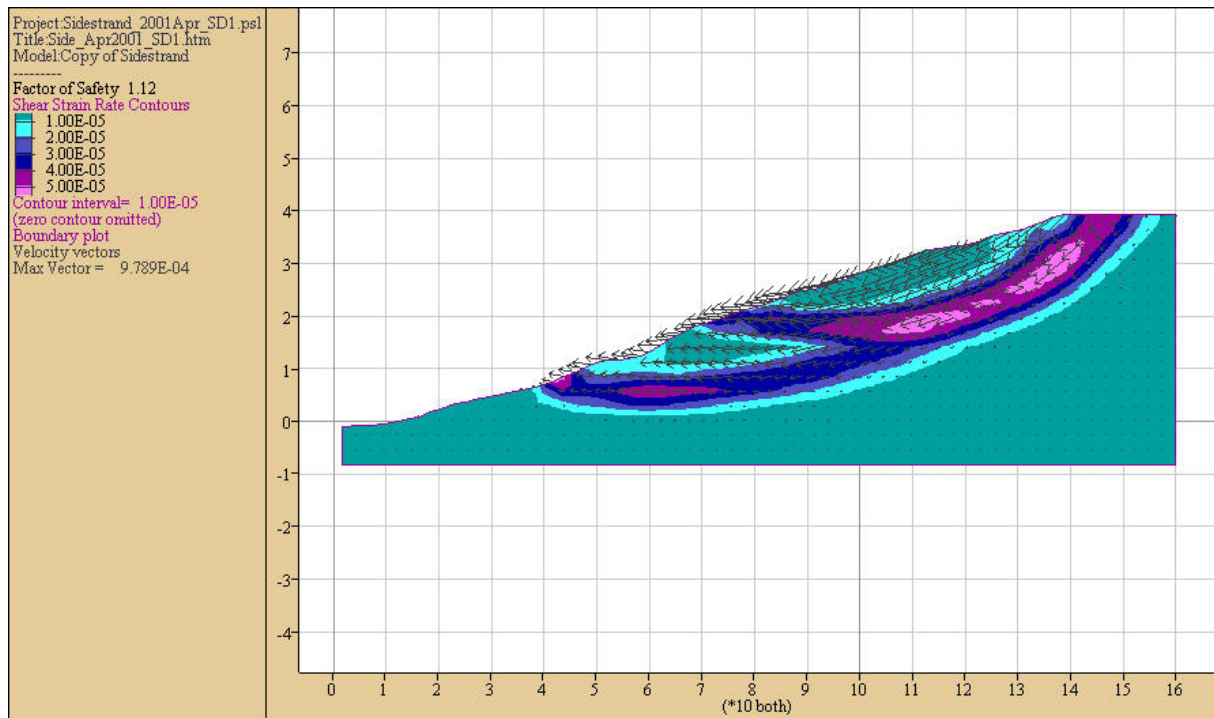
Figure 5-43 Example of displacement strain contour/vector diagram: Sidestrand, SD1, Apr 2001
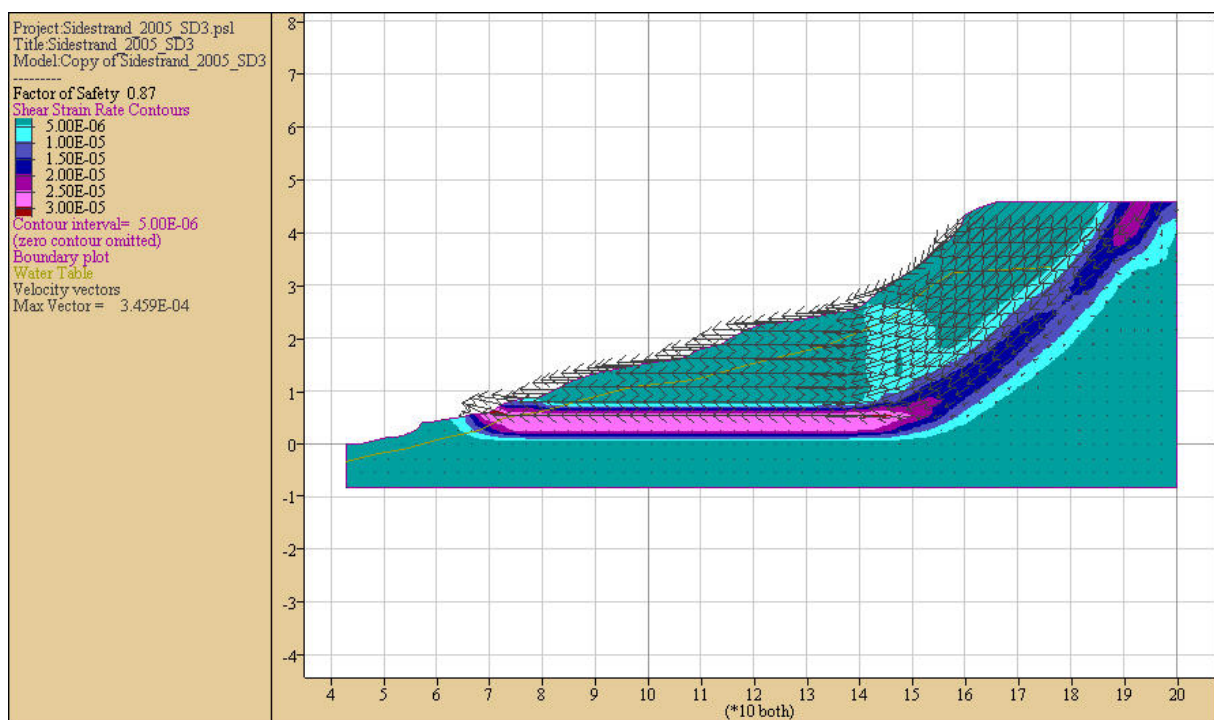
Figure 5-44 Example of displacement strain contour/vector diagram: Sidestrand, SD3, Sep 2005

5.10   DISCUSSION

The structural geology and landslide geomorphology at the Sidestrand test site are complex. There is evidence that embayment development has followed the thrusts and thrust-related folding within the Sheringham Cliffs Formation and to a lesser extent the gross structural folding within the Happisburgh Formation. The data suggest that embayments SD1 and SD2 behave similarly, but differently from embayment SD3. Embayments SD1 and SD2 appear to

96

follow the shape dictated by a pair of localised 'synclines' caused by the glacial over-thrusting described previously. This has resulted in listric (spoon-shaped) features occupying the mid and upper cliff which have acted as channels for ground and surface water, and produced characteristic mudslides and mudflows (Figure 5-20), emanating from the largely coarse-grained deposits in the mid and upper cliff, and observed during the period of monitoring. These features are sufficiently frequent to become layered one upon the other; these layers being sectioned by sea erosion, and occasionally revealing their multiple slip surfaces (Figure 5-21, Figure 5-23). Embayment SD3 on the other hand has produced a laterally-persistent, deep-seated rotational landslide involving almost the entire cliff height. During the period of observation this has produced a notably large debris flow (Figure 5-30) and subsequent smaller ones at the same location. The neighbouring cliff, approximately 200 m to the west of SD3, has failed in a similar manner (during winter 2004/2005) to that which probably produced SD3 (date unknown). The strata visible in SD3 appear to be much less folded than in SD1 and SD2, and also lack the exaggerated thicknesses of marl/chalky till produced by the glacio-tectonic folding and thrusting.
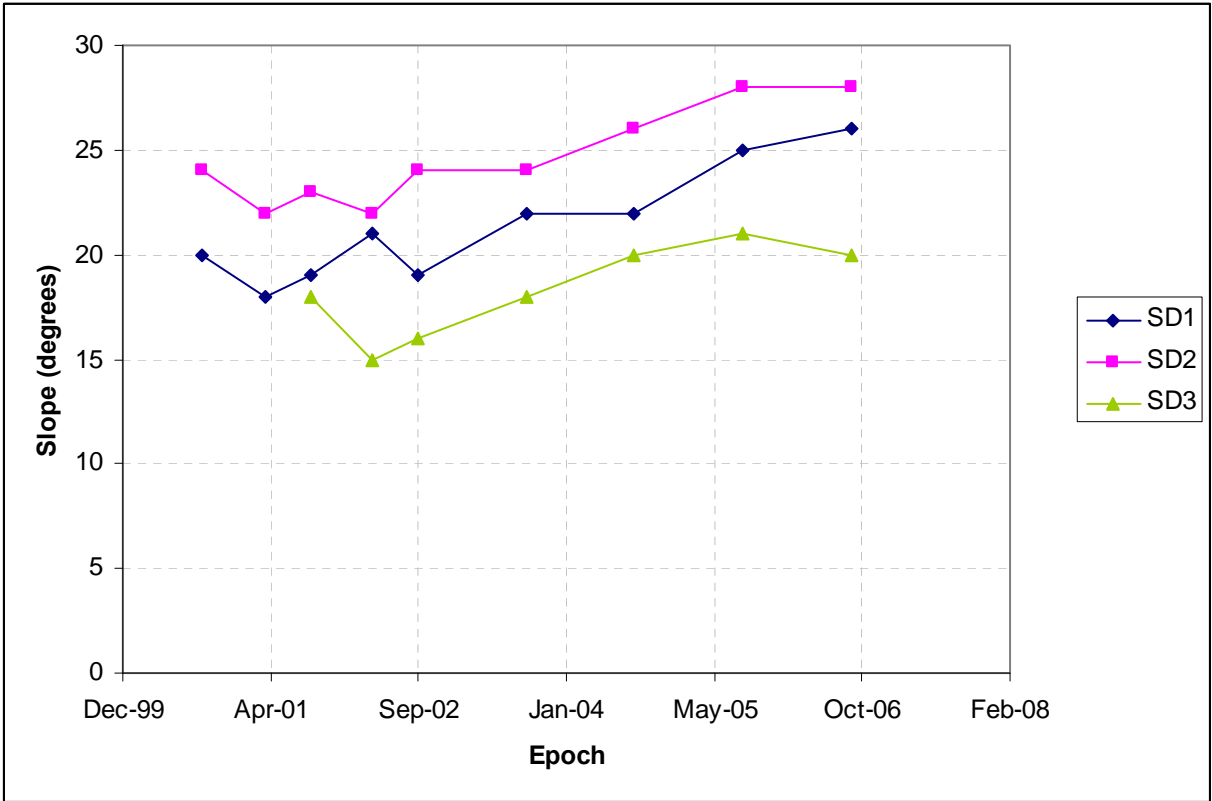
Figure 5-45 Overall slope angle against epoch for Sidestrand

The plot (Figure 5-45) shows the change in overall slope angle, measured from cross-section profiles (cliff toe to cliff-crest), for SD1, SD2, and SD3. This shows an overall increase in slope angle over the monitoring period, though in the case of SD3 it is modest. Embayment SD1 shows the greatest overall increase from 20 to 26º.

The slope stability displacement contour/vector diagrams for SD3 (Appendix 4) show similar types and scales of landslide. This probably accounts for the relatively constant factor of safety for SD3. The plots (Appendix 4) indicate an essentially deep-seated compound landslide with a principal shear plane at, or slightly below, platform level which is unchanging with time. Such a 'non-circular rotational' failure mechanism, shown in schematic in Figure 5-27, matches that described in Hutchinson (1976) for a cliff section at Cromer (Figure 5-19) and in other large coastal landslides formed in Jurassic and Cretaceous mudrocks, and in particular in the Gault Formation, for example at Folkestone Warren, Kent

(Trenter and Warren, 1996). At Sidestrand the basal shear is horizontal and lies within the Ostend Clay Member. A basal shear below beach level with an uptilted toe area was also observed at SD3 during the early stage of the monitoring programme (Figure 5-26 and Figure 5-22). This contrasts with the plots for SD1 and SD2 which show wide variations in landslide form and depth, but typically much shallower than for SD3 (Appendix 4). The variability is reflected in the factors of safety. The only plot which shows any similarity to SD3 is that for September 2000 at SD1 which is also deep-seated and based several metres below beach level. Several plots in SD1 demonstrate bifurcation of the shear plane, giving upper and lower shear zones. This type of failure is not indicated in SD2 or SD3. Several of the SD2 plots feature small failures at the crest of the slope, presumably associated with over-steepening of the backscarp. These distinct behaviours are probably also associated with the plan geometry and size of each embayment; SD2 being the smallest of the three and SD3 the largest. In the case of a narrow embayment, such as SD2, the buttressing (or arching) influence of the flanks becomes significant. This factor cannot, however, be modelled by a 2D slope stability analysis. The shear planes indicated from the plots for SD1 suggest a variety of host geological layers. Those for SD2 appear to alternate between a deeper type within the Walcott Till and a much shallower type within the upper four layers (Stow Hill Sand and Gravel, Weybourne Town Till, Trimingham Sand and Trimingham Clay Members).

Comparison of the slope stability analysis results, discussed above, with field observations of landslide activity, suggests that there are some positive correlations. There have been three periods of heightened landslide activity indicated by field observation, in 2000, 2001/02 and 2006 (Sections 5.8.1.1 and 5.8.1.6). The first was dominated by mudslides and mudflows at SD1 and SD2, and as such will not have been reflected in the slope stability analysis. There was also, however, an active deep-seated movement recorded at beach level at SD3. The second was a single large debris flow, and the third a complex of landslides probably confined to SD1 and the eastern end of SD3. The most notable recession of the cliff's crest was at SD1 and SD2 between September 2000 and April 2001 where about 15 m was lost in each case. Of course, field observations and monitoring surveys in such weak materials are not able to record every landslide movement, as their evidence is rapidly removed by further instability and by the eroding action of the sea. It is conceivable, therefore, that occasionally small and moderate-sized landslides would be completely missed by the monitoring programme; the sole remaining evidence being possibly debris on the slope and recession of the source backscarp.

The types and scales of the landslides indicated by the slope stability analysis are in agreement with field observations. Embayment SD3 features deep-seated landslides affecting the entire cliff height and founded at a level below the beach and possibly below the platform. Embayments SD1 and SD2 feature, for the most part, shallower and more variable landslides founded in the mid or upper parts of the cliff with a relatively stable lower cliff over which these landslides slide and flow in frequent succession. The abundant mudslide events, and for that matter mudslide deposits, observed at SD1 and SD2, and the large-scale debris flows at SD3 are not capable of being modelled satisfactorily by FLACslope.

Table 5-15 Comparison of factors affecting cliff recession

Monitoring epoch	Volume change (200 m)	Rainfall (total 12-month) (mm)	Mean monthly tide means (m)	Mean monthly extreme tide (m)	No. Tidal surges#
2000-2001		805.5	2.8	4.79	1
2001-2002	64790	468	2.95	5.39	1
2002-2003	1414	560	2.95	5.39	2
2003-2004	4132	636.9	2.97	5.45	2
2004-2005	12084	672.2	2.98	5.6	3
2005-2006	38880	666.5	2.97	5.51	2

Number of tidal surges coinciding within 24 hours of monthly extreme tidal maxima

Tidal data from http://www.bodc.ac.uk

5.10.1 Conceptual model

The proposed models for landslide and cliff recession at the Sidestrand test site are shown in Figure 5-46 (Model A) and Figure 5-47 (Model B). The site comprises three major embayments, SD1, SD2 and SD3. Of these, SD1 and SD2 are comparable in size, whereas SD3 is much wider. This is probably due to the geological structure which features thrust-derived 'synclines' at SD1 and SD2 in the middle and lower parts of the cliff. This has provided both elevated hard points at the promontories flanking the embayments and has allowed for a greater thickness of less-competent material above. In addition, this structure has tended to 'funnel' ground water through the permeable upper strata. As a direct result of these factors the hard points have provided greater resistance to erosion while the enhanced thicknesses of incompetent and saturated materials within the embayments have been more susceptible to landslide. In SD1 and SD2 the landslide mechanism has been driven from the upper part of the cliff containing the less competent materials. These landslides have been debris flows, mudflows and mudslides which have tended to move over the more competent strata forming the lower cliff, and thence onto the beach (Model A:1). In the upper part of the cliff these initiate as rotational slumps or as (rock) falls which develop retrogressively (Model A: 2). The debris deposits on the lower cliff accumulate one above the other, their structure being exposed by erosion (Model A: 2). In embayment SD3 the landslides form a complex and have two distinct types: firstly, debris flows, mudflows and mudslides, similar to those in SD1 and SD2, and secondly deep-seated rotational compound landslides emerging at or below beach level (Model B:1). This deep-seated movement has resulted in backtilt and extension features on the cliff slope, which have led to the formation of ponds which appear to be seasonally persistent. Some of the debris flows are large and the deposits have survived on the beach for several months, and in one case over a year. As the 3-D geology of the cliff is not fully known, the precise mechanism of each landslide cannot be determined. The deep-seated landslide at SD3 has been observed in action and appeared to have its basal shear plane several metres below beach level with a vertical upthrusting component of movement at the toe (Model B:2). It is assumed that this landslide extends from cliff-top to below the toe, as one movement. This has been confirmed by slope stability analysis. The frequency of movement on this landslide cannot be ascertained where annual monitoring is concerned. However, it is likely to be less frequent than the shallow landslides overlying it in SD3 and the landslides in SD1 and SD2. Saturated conditions on the cliff,

Sidestrand - Model A (SD1/SD2)
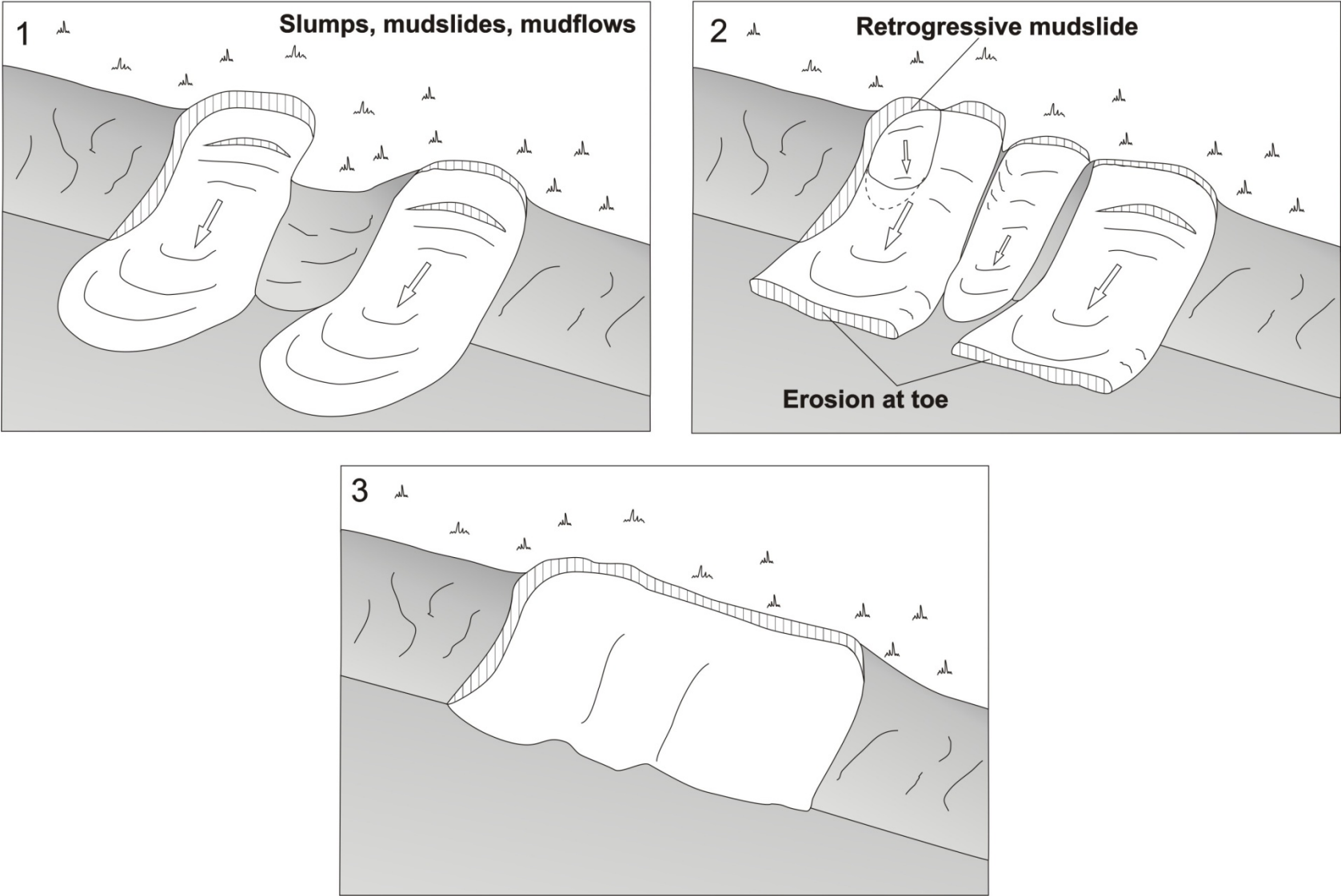
Figure 5-46 Conceptual Model A for embayments SD1 and SD2 at Sidestrand.

Sidestrand - Model B (SD3)
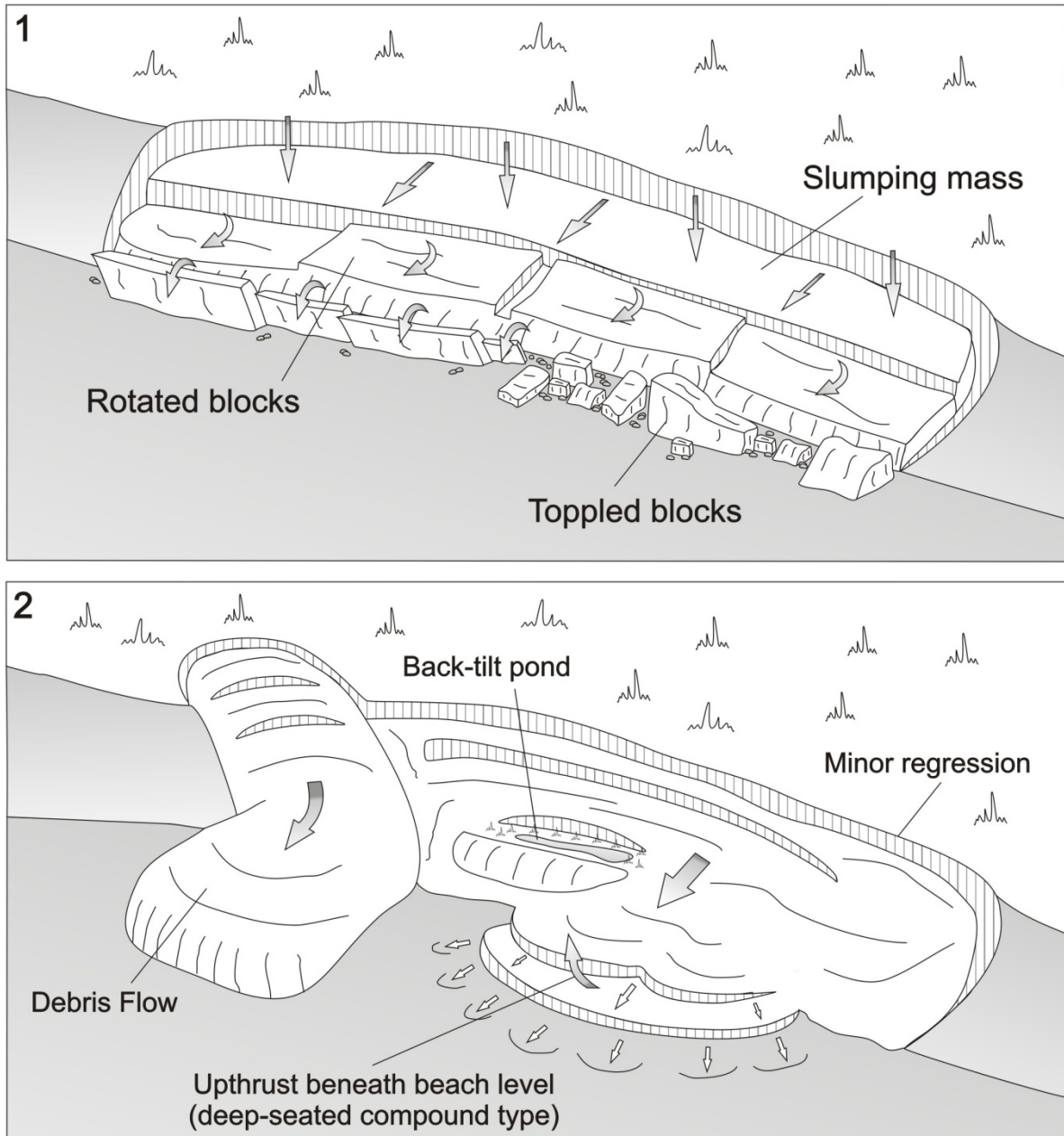
Figure 5-47 Conceptual Model B for the embayment SD3 at Sidestrand.

making access difficult or impossible, have predominated for most of the surveys with the exception of years 2000 and 2001. At the Sidestrand test site, unlike the Happisburgh test site, landslide debris remain on the cliff slope and are gradually removed by erosion from the sea. This has meant that volume change calculations at Sidestrand are complicated because there is a depletion and an accumulation element to each. These elements are not easily distinguished numerically, though can be appreciated visually (e.g. Figure 5-35). The main landslide and erosion activity at the Sidestrand test site is summarised in Table 5-16 using data obtained from 3-D models and from direct observation.

Table 5-16 Landslide and erosion activity during monitoring period

Epoch	Landslide activity			Erosion
	Major	**Minor**	**Notes**	
2000 - 2001	Depletion SD3	Depletion SD1, SD2	Deep-seated slide	
2001 - 2002	Depletion SD3 (E end) Accumulation (lower cliff & beach)	Depletion SD1, SD2	Large debris flow	Toe (all)
2002 - 2003	Depletion SD3 (lower cliff).	Depletion SD3 (upper cliff).		Toe SD3
2003 - 2004			Little movement overall.	Toe (all)
2004 - 2005	Depletion SD5	Depletion SD2	Initiation of embayment SD5	Toe SD1, SD2, SD3 (all)
2005 - 2006	Depletion SD5. Accumulation SD5 (beach). Depletion SD3 (E end). Accumulation SD3 (E end) (beach)	Depletion at toe SD1 Depletion at head SD2 Depletion SD3 (W-end)		Minor toe erosion SD1

6 Case Study: Weybourne

6.1 INTRODUCTION

The test site at Weybourne on the North Norfolk coast is approximately 100 m in length, situated 200 m to the east of the beach car park along a stretch of coast known as Weybourne Hope. The cliff faces north, is low (20 m) and reducing in height to zero at the car park. It consists of Anglian deposits: sandy tills of the Weybourne Town Till Member (Sheringham Cliffs Formation) overlying glacio-fluvial outwash sands and gravels of the Mundesley Member (Wroxham Crag Formation) overlying Norwich Crag (Lower Pleistocene), overlying Lower Cretaceous chalk (Lee *et al.*, 2004a; Pawley *et al.*, 2004). The substantial shingle beach is narrow and steep, typically stepped in profile, and subject to storm erosion. A view of the cliff and beach is shown in Figure 6-1. Subglacial shear processes in relation to till deposition have been investigated at three sites in Weybourne (Hart, 2007). One of these locations is close to the test site. A particular hazard at Weybourne is the steep foreshore in rough weather. Access is good from the car park on Beach Lane.

Figure 6-1 View westward of part of test site showing chalk (White Chalk Subgroup, WhCk), sands (Wroxham Crag Formation, WRCG) and Weybourne Town Till Member (WTTM).

6.2 SURVEY ACTIVITIES

The monitoring, sampling, and field-testing programme for the Weybourne test site is summarised in Appendix 1.

The rate of erosion at the test site at Weybourne has to date been monitored in 2001, 2002, 2003, and 2004 (Appendix 2) using the laser scan (terrestrial LiDAR) system combined with GPS. Figure 6-13 shows the position of the scan locations and target points from the 2004 survey.

The equipment used varied between epochs, as the quality and precision of the instruments was improved:

2001   A Riegl LPM2K terrestrial laser scanner, with a published accuracy of 50mm was used in conjunction with a Garmin GPS12 hand-held GPS. The GPS data were post-processed using a pseudo-differential calculation programme (Gringo), giving a positional accuracy of >1 m. The combined accuracy of the LiDAR and GPS was estimated as **2.5 m**.

2002   A Riegl LPM2K terrestrial laser scanner, with a published accuracy of 50mm was used in conjunction with the Leica GS50 GPS/GIS system, giving a real-

time positional accuracy of <0.5 m. The combined accuracy of the LiDAR and GPS was estimated as **1 m**.

2003 – 2004   A Riegl LPM2K terrestrial laser scanner, with a published accuracy of 50mm was used in conjunction with the Leica SR530 differential GPS system. The GPS data were post-processed in SkiPro 3.0, giving a positional accuracy of <25 mm. The combined accuracy of the LiDAR and GPS was estimated as **0.15 m**.

The Weybourne site has not been monitored since 2004 for funding reasons.

6.3   RAINFALL

Rainfall data for the period 2000-2004 was obtained from the Met Office for the Weybourne weather station.

- The highest average rainfall occurred in 2001, followed by a decline in average rainfall.

- 2003 had the lowest average annual rainfall, after which average rainfall began to increase.

- The highest monthly rainfall figure was in August 2006, and then July 2001.

- **2000**- A dry summer followed a wet spring and was preceded by a wet winter. Peak rainfall was in October.

- **2001**- There was an increase in overall average rainfall from 2000. Apart from the peak rainfall month of July, the average monthly rainfall was fairly constant.

- **2002**- A further reduction in overall average rainfall for the year. The highest monthly rainfall for the year was between October and December.

- **2003**-Annual rainfall averages were the lowest for the whole scanning period. The driest months were July-September which followed the peak rainfall month of June.

- **2004**- Average rainfall increased slightly with peak rainfall in June, July and October.
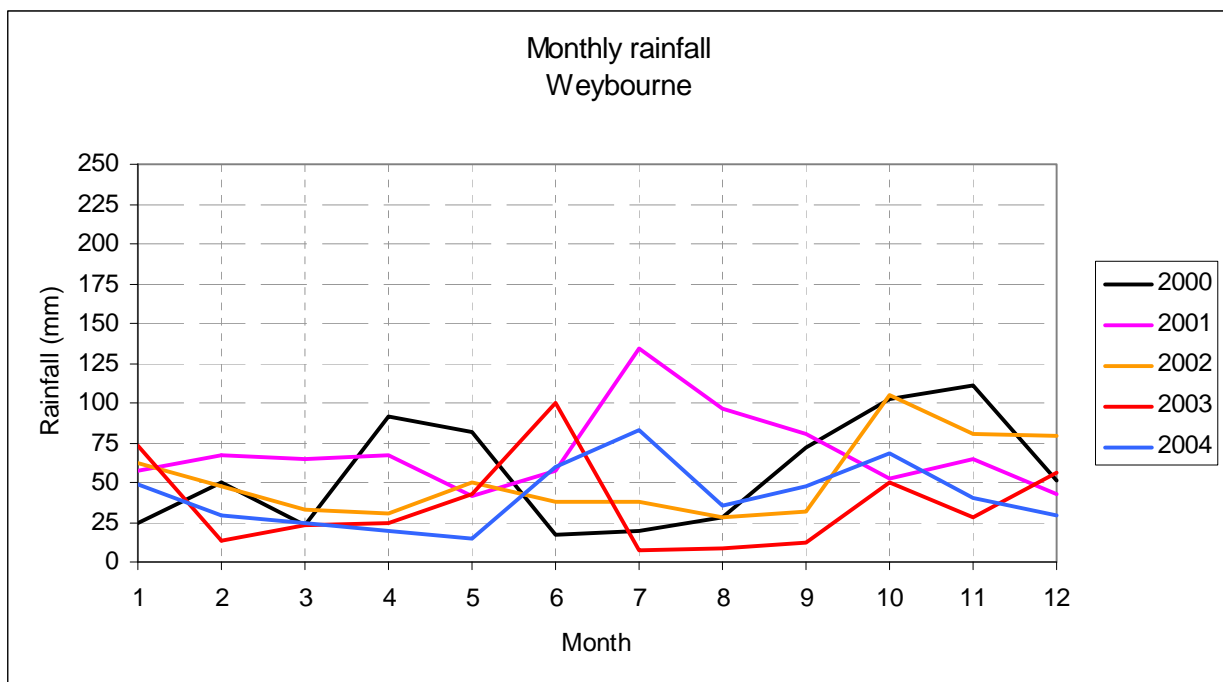
Figure 6-2 Rainfall – monthly averages – Weybourne
(Met Office)
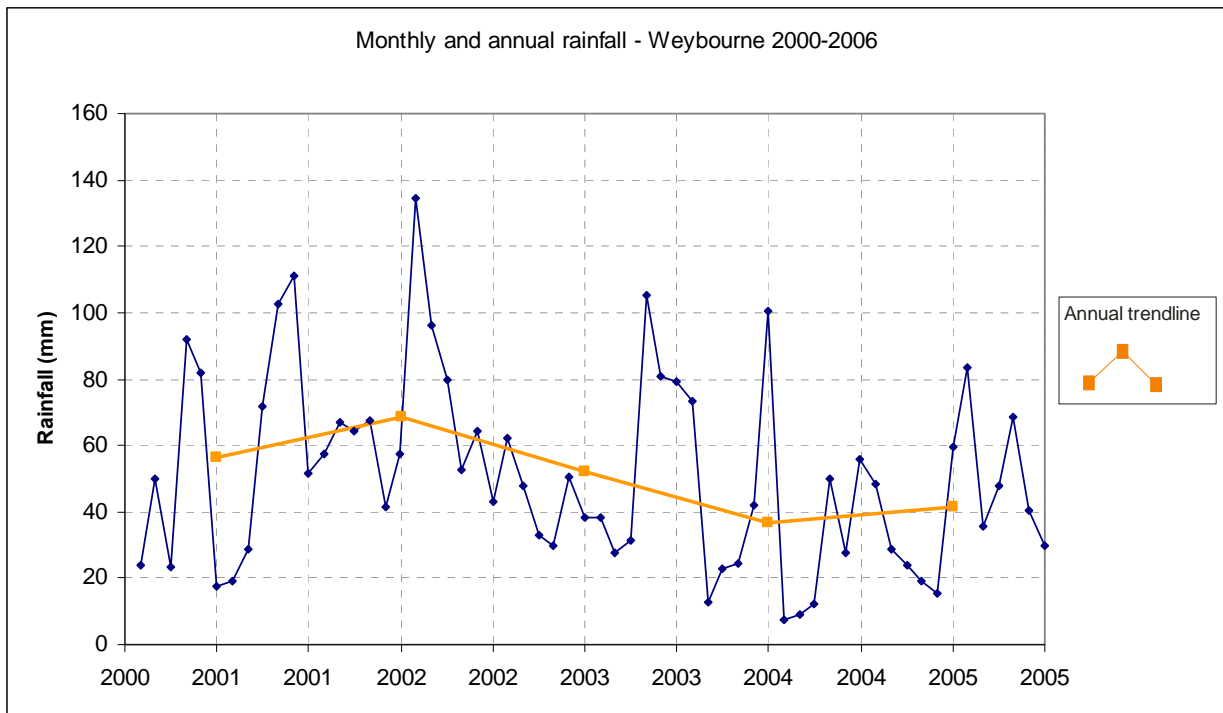
Figure 6-3 Average monthly and annual rainfall for Weybourne
(Met Office)

6.4   GEOLOGY

The complex Pleistocene sediments of North Norfolk, on the 35 km stretch of coastline between Weybourne and Happisburgh, have attracted geologists since the late 19th Century. There have been a variety of stratigraphic schemes, for example those described by Banham & Ranson (1965) (Table 6-1), Lunnka (1994) and Bowen (1999). Many of these have been based on regional assessments rather than on detailed local study. Recently, a stratigraphy consisting of four formations has been proposed (Lee *et al.*, 2004a). This comprises assemblages of till formations and associated outwash lithofacies. The geological succession of superficial deposits at the test site contains highly contorted glacigenic sediments that have been deformed by glaciotectonic deformation and gravitational loading (Hart, 2007). In his original mapping work for the Geological Survey in the 1880's, Reid considered that stratigraphy was impossible to determine in the Weybourne area due to the severe deformation, and termed it 'Contorted Drift' (Reid, 1882).

The bedrock in the area comprises the 'Weybourne Chalk'(Figure 6-4), part of the White Chalk Sub-Group (WhCk), which covers the former 'Upper' and Middle' Chalks of the Upper Cretaceous, is soft, closely bedded, and significantly fractured and brecciated near its upper boundary. The chalk contains closely spaced interbeds of tabular and nodular flint cobbles, and has an undulating upper boundary. In places, a thin chalky diamicton rests upon the upper surface of the chalk, and this reflects an episode of solifluction (Neogene) prior to the deposition of the overlying sands and gravels.

The lowest of the Pleistocene deposits is the Wroxham Crag Formation (WRCG), part of the Crag Group, consists of shallow marine and inter-tidal lithofacies that rest on the upper surface of the chalk. The outcrop tends to be discontinuous due to glacial erosion and consists of soft coarse sand with laminations and lenses of clay, shell debris, and pebbles of quartzite and flint (Figure 6-5). Cryoturbation and pipe features penetrate the underlying chalk. Dome and basin load structures were produced by rapid deposition of overlying Briton's Lane Sand & Gravel Member (Banham, 1988).

105

Table 6-1 Stratigraphy at Weybourne (Banham and Ranson, 1965; Lee *et al.*, 2004a; Pawley *et al.*, 2004)

Epoch	Thickness (m)	(Banham and Ranson, 1965)	(Lee *et al.,* 2004a)	
			Formation	**Member**
Recent	0 - 3	Blown Sand		
	0 - 4	Beach Sand Gravel		
	0 - 1.5	Peat		
Pleistocene			Briton's Lane Formation	Briton's Lane Sand & Gravel Member
	1.5 - 13	'Contorted Drift'	Sheringham Cliffs Formation	Weybourne Town Till Member*
	0 - 5	Weybourne Crag	Wroxham Crag Formation	Mundesley Member
Cretaceous	0 - 7	Chalk with flints	White Chalk Supergroup	'Weybourne Chalk' plus soliflucted chalk residue

 (* contains glaciotectonic inclusions of an earlier till, the Bacton Green Till Member)

The Weybourne Town Till Member (Figure 6-6) of the Sheringham Cliffs Formation overlies the Wroxham Crag Formation, and is a chalky till deposited by grounded ice flowing over chalk bedrock, that has locally overridden and incorporated pre-existing brown sandy till called the Bacton Green Till Member (once part of the Beeston Regis Formation and formerly called the Cromer Diamicton or 3rd Cromer Till). The regional dip is at a very low angle eastward. High-angle joints and shears are oriented ENE and SSE, probably associated with a principal stress from the NNE (Banham and Ranson, 1965). Locally the mélange of till contains thin boudins and tectonic laminations of pale brown/grey, fine and medium, uncemented sand which reflect the pervasive shearing and attenuation of sand bodies under conditions of moderate strain associated with subglacial glaciotectonic deformation. These sand bodies are subject to erosion by both precipitation and wind. Wind erosion produces small 'caves' in the cliff at a height several metres above the influence of waves. Elsewhere along the coast wind erosion has stripped individual beds of folded sand to produce smooth sculptured surfaces at mid-cliff height (e.g. at West Runton). The sand laminations have been subject to folding, the local disposition of which affects the nature and extent of erosion. In one location within the test site the beds are upturned to a near-vertical position (Figure 6-12).

The Briton's Lane Sand and Gravel Member (BRLSG), of the Briton's Lane Formation (formerly of the Overstrand Formation), consists of coarse-grained outwash sands and gravels that occupy small load-induced basins within the upper units of the Weybourne Town Till Member. They were deposited from an ice-sheet containing a Scandinavian clast component (Clark *et al.*, 2003).

Figure 6-4 Chalk exposed at base of cliff (Weybourne Chalk)
Height of exposure (foreground) approx 1m.

Figure 6-5 Thinly bedded, laminated, and folded sand and gravel layers (Wroxham Crag Formation)
Height of section approx 1m

Figure 6-6 Highly contorted melange of brown sandy till and chalky till that from the Weybourne Town Till Member of the Sheringham Cliffs Formation
Height of section approx 7m.

6.5   GEOTECHNICS

The particle size distribution result (Figure 6-8) shows the sample of Briton's Lane Sand Gravel Member is a clayey silty sand. Sand and gravels typically have a frictional angle of $\phi = 35 - 40^o$. The Briton's Lane Member is highly permeable compared with the other deposits and will behave as an aquifer unit.

The Weybourne Town Till (previously Marley Drift) is a sheared, lightly fissured, stratified firm light grey to pale yellow gravelly calcareous SILT with inclusions of laminated sand, silt and clay of the Bacton Green Till Member. Gravel is mostly weak chalk with subordinate flint. Index properties are summarised in Table 6-5. The Weybourne Town Till is a highly plastic soil, which according to range of liquid limit, has low to intermediate plasticity. The clay activity is classified as 'inactive'. Bell and Forster (1991) report some index property data for the Marley Drift, but it is later referred to as Chalky Boulder Clay (Bell, 2002). It is important to note that inconsistent use of lithostratigraphic terminology in the literature has led to confusion amongst authors publishing geotechnical data. Therefore caution must be used when matching physical properties with lithostratigraphic units.

The Mundesley Member is a medium dense yellow-orange to dull yellowish brown stratified silty sand with much chalk gravel near the base, and opaque heavy minerals. Like the Briton's Farm Member, the high permeability of this material will dictate its behaviour to act as a minor aquifer and possibly create perched water tables.

The Weybourne Chalk is a medium density chalk (Lord *et al.*, 2002) with a UCS of 4–5 MPa. It is generally a very weak to weak rock yet is the strongest material in the succession. In

Norfolk it has a dry density of 1.5-1.6 mg/m^3. Strength tests show up to four times reduction in strength between dry (stronger) and saturated (weaker) samples.

Two samples were collected at Weybourne including one small block of Chalk and one disturbed bag sample of Briton's Lane sand and gravel (Table 6-3).

A small number of Panda ultra-lightweight penetrometer tests were carried out at Weybourne (Table 6-2; Figure 6-7).

Table 6-2 Panda ultra-lightweight penetrometer tests

Date	Formation	Depth (m)	Number / Location
19/04/01	Wroxham Crag	0.51	WEY1 (Crag/chalk junction at 0.3m?)
19/04/01	Wroxham Crag	0.64	WEY2 (Platform cut in cliff, failed during test)
19/04/01	Wroxham Crag	0.14	WEY3 (Platform cut in cliff, failed during test)
19/04/01	Wroxham Crag	0.52	WEY4 (0.5m NW of WEY3)
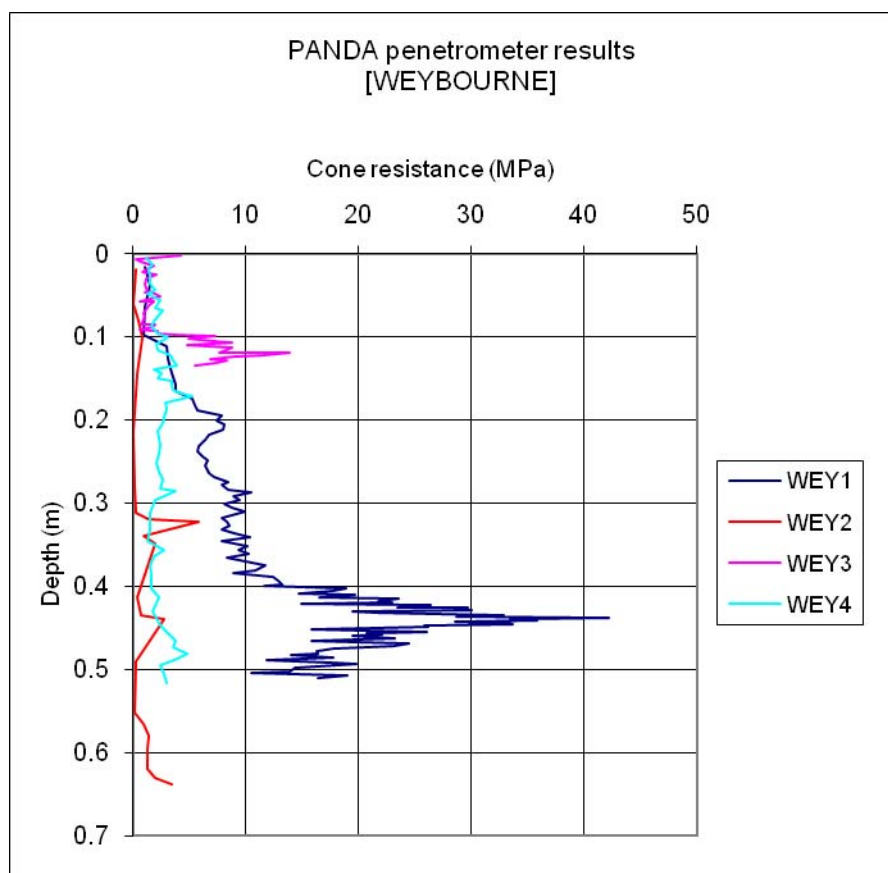
Figure 6-7 PANDA penetrometer profiles for Weybourne (refer to Table 6-2)

Table 6-3 Geotechnical samples taken at Weybourne

Date	Formation / Lithology	Type	Location
19/04/01	Glacial sand (BRLSG)	m bag	WB1
19/04/01	White Chalk Sg. (WhCk)	Block	WB2

Figure 6-8 Particle-size distribution curve for sample WB1, Briton's Lane Sand & Gravel Member (Briton's Lane Formation)

Table 6-4 Summary of particle size results

	Clay (%)	Silt (%)	Sand (%)	Gravel (%)
WB1	22.2	31.1	46.3	0.4

Table 6-5 Some reported geotechnical index properties for the Weybourne Town Till

	w %	w_L %	w_P %	Ip %	Gs	c' KPa	ϕ' (°)	$\phi'r$ (°)
Weybourne Town Till[1]								
Range	16.8 - 18.6	32 - 45	18 - 21	14 - 26	2.68 - 2.72	7 - 16	21 - 28	16 - 25
Mean Av.	23.6	7	20	18				

[1]Bell, 1991 (Marly Drift)

w= Natural water content, w_L= Liquid limit, w_P= Plastic limit, Ip= Plasticity index (LL-PL), Gs= Specific gravity, c'= Effective cohesion, ϕ'= Angle of friction (Peak), $\phi'r$ = Angle of residual friction.

6.6   GEOMORPHOLOGY

6.6.1 Cliff

The majority of the cliff is cut into unconsolidated glacial sands and gravels, which in places include large chalk erratics (Figure 6-9). Chalk is exposed as a resistant platform at the base of the cliff, compared with the glacial sands above it (Figure 6-10). The form of the cliff profile is influenced by the relative thicknesses and erosion resistance of the formations, the most resistant being the Chalk, followed by the Crag sand/gravel. The sands above and below the Crag are much less resistant to erosion. The Chalk outcrops at Weybourne provide a potential source of flint to the beach, but this is only likely in small quantities. The chalk platform dips eastwards and to the east of Weybourne it is only present within the intertidal zone.

Figure 6-9 Wroxham Crag Formation gravels (arrowed) separating White Chalk and Sheringham Cliffs Formations.
Height of section approx. 2.5m

Figure 6-10 View of cliff looking eastward

6.6.2 Platform and beach

The chalk platform underlies a substantial and persistent beach and has not been visible during the survey. The steeply-sloping beach consists of graded pebbles, predominantly of flint (Figure 6-11), which become increasingly coarse-grained towards the top of the beach. Much of the beach gravel is relict, with small amounts being added to the beach at present. The fine-grained sediment derived from the cliffs is largely washed offshore and represents an important source of sediment for subtidal areas (Halcrow 2002). The profile of the beach varies seasonally, but typically exhibits two distinct foreshore berms. These represent the limits of high tide swash action during spring and neap tidal cycles. The beaches are highly mobile due to the high onshore-offshore wave energy. The steepness of the beach profile serves to dissipate the high wave energy, but this energy is sufficient along this shoreline to both attack the cliffs and remove eroded material, meaning that the beach volumes do not continually increase, with rapid movement of beach material alongshore. There is a net drift of beach sediment eastwards, but this can vary in both direction and rate (Halcrow, 2002). The volume of gravel diminishes eastwards towards Sheringham, where the lower beach becomes progressively sandier.

6.6.3 Landslides

Whilst the landslides at Weybourne are not particularly prominent, at least in comparison with the other two Norfolk test sites, the cliff is distinctly embayed (Figure 6-10). Removal of landslide debris is relatively rapid. The principal mechanism appears to be sand runs from the

Figure 6-11 View of shingle beach looking eastward

Sheringham Cliffs Formation (Figure 6-12). Some of this activity is probably promoted by ground water seepage. Occasionally, a narrow slump is observed in the upper part of the cliff, but this is probably not the main landslide process. The chalk forming the bench tends to be brecciated and erodes by mechanical erosion, accompanied by dissolution from seawater rainwater and groundwater. Small block falls, controlled by bedding thickness and joint/fracture spacing, also occur. The flint beds provide some 'reinforcement' to the chalk against the direct mechanical erosion by the sea.

Figure 6-12 Sand run from the Sheringham Cliffs Formation within embayment (Note: upturned bedding)

6.7 LIDAR SURVEYS

The position of scans taken in 2006 at the Happisburgh site is shown in Figure 6-13.

- In 2001, two scans were carried out from two scan positions, from the foreshore. In total, the survey captured 4701 points on the cliff surface and the adjacent cliff top and foreshore areas.

- In 2002, four scans were carried out from four scan positions, from the foreshore. In total, the survey captured 6118 points on the cliff surface and the adjacent cliff top and foreshore areas.

- In 2003, four scans were carried out from three scan positions, from the foreshore. In total, the survey captured 12408 points on the cliff surface and the adjacent cliff top and foreshore areas.

- In 2004, three scans were carried out from three scan positions, from the foreshore. In total, the survey captured 12376 points on the cliff surface and the adjacent cliff top and foreshore areas.

It should be noted that the length of the study area in 2001 and 2002 was smaller than that in 2003 and 2004.

Figure 6-13 Plan of scan locations at Weybourne test site
(NOTE: aerial photo 1999). Scan positions NGR: 611381, 343678. 611349, 343683. 611320, 343684.

6.8 CLIFF MODELLING

Slope stability analysis was not carried out for Weybourne due to the limited amount of recession and the lack of landslide types suitable for the finite element method. The principal slope processes observed at Weybourne were sand runs, sand flows, and small 'earth' falls in the upper cliff.
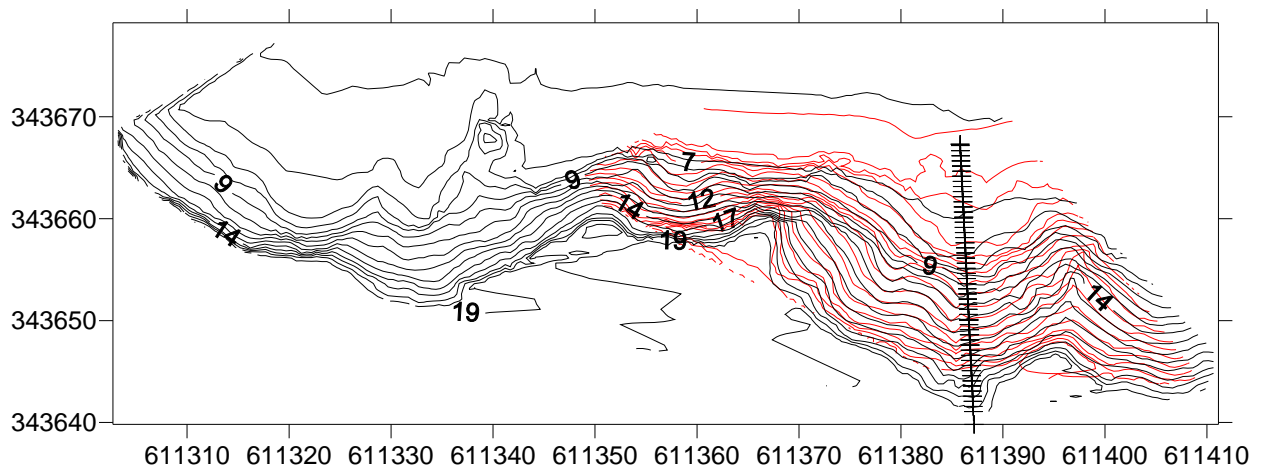
Figure 6-14 Terrestrial LiDAR derived map showing the cross-section at Weybourne
Note: red contours = Sep 2001, black contours = Sep 2004
Note: section line (black cross-ticks) (Refer to Figure 6-15)
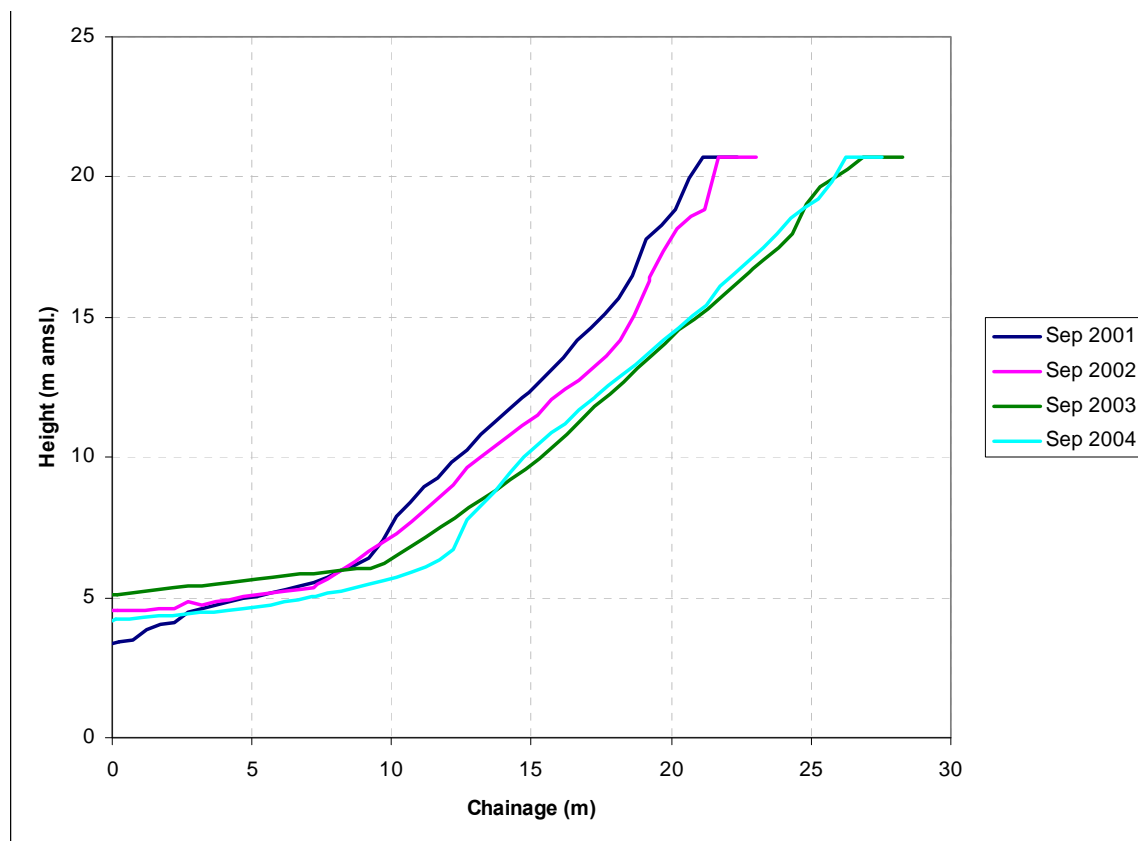
Figure 6-15 Cross-sections, Weybourne, 2001-2004
Note: recession from left to right (Refer to Figure 6-14 for section location)

As shown in Figure 6-15 the only recession event of any significance took place between September 2002 and September 2003 at one embayment location (Figure 6-12, Figure 6-14) within the test site. This location appeared to be affected by the structural conditions of the dominantly sand-rich formation locally in the mid and upper-cliff. The chalk forming the lower cliff was unaffected by slope instability but has undergone erosion over the monitoring period.

6.8.1 Slope stability analysis

Due to the fact that negligible cliff recession has taken place at the Weybourne test site during the monitoring period 2000 to 2004, no slope stability analyses have been carried out.

Due to the changes in the length of the study area, and to a small positional error in the 2002 survey (GPS positioning) change models can only be made between the 2001 and 2002 surveys (Figure 6-16), and between the 2003 and 2004 surveys (Figure 6-17).
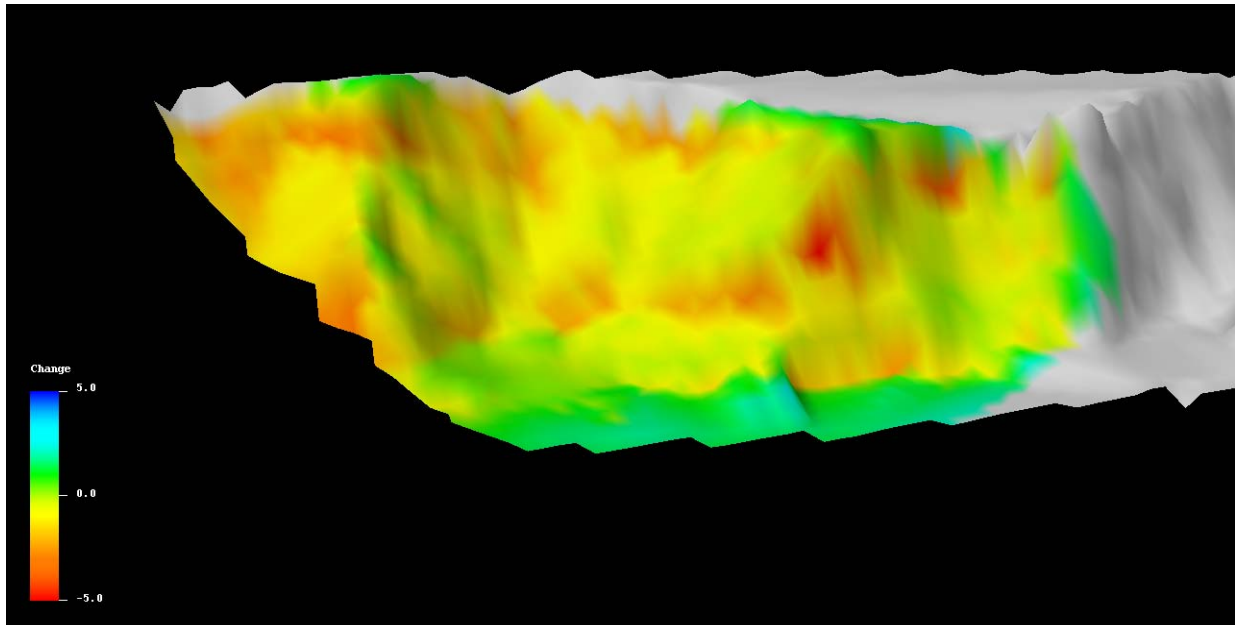
Figure 6-16 Height change model for Weybourne between 2001 and 2002 (+5m = blue, -5m = red).
Length of section approximately 75m.
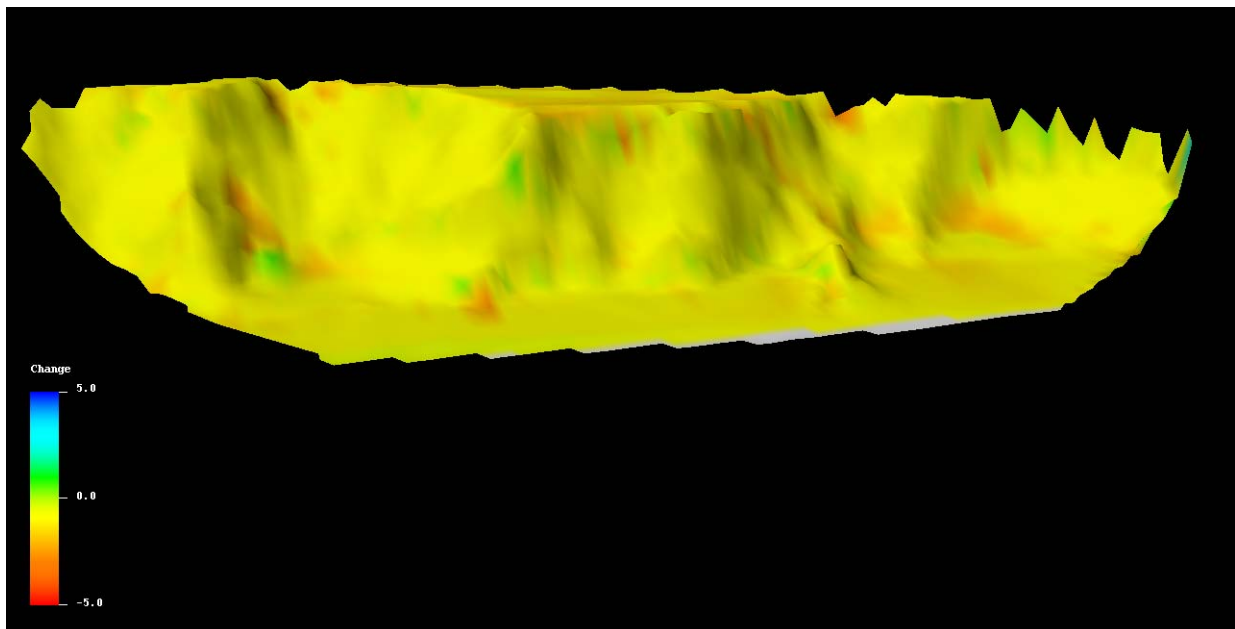
Figure 6-17 Height change model for Weybourne between 2003 and 2004
(note that a larger extent was scanned in 2003 and 2004 compared to previous years) (+5m = blue, -5m = red).
Length of section approximately 120m.

6.9   DISCUSSION

The data show that the cliffs at Weybourne are not subject to large-scale landsliding. This is due to a combination of the scale, lithology (presence of chalk at the base of the cliff) and protection afforded from wave action by the steep gravel beach. The process is more likely to be related to sand runs or flows (Figure 6-18) initiated by wind erosion and precipitation (sub-aerial landslide processes). There is also evidence of gullying due to surface runoff from the top of the cliff. Minor 'earth' falls from the upper cliff have also been observed.

Figure 6-18 Examples of sand runs at Weybourne in 2003 (left) and 2004 (right)
Section heights approx. 20m

Calculations based on the 2003 to 2004 change models show volume changes relating to a loss of material along 100m length of the test site of approximately 235 m^3 and a gain of material (i.e. accumulation of landslide sediment at the base of the cliff) of 135 m^3. This is most likely due to sand runs and small 'earth' falls.

7 Discussion

7.1   METHODOLOGY

The terrestrial LiDAR methodology used at the Happisburgh, Sidestrand and Weybourne test sites has successfully produced 3-D models of the cliff slope and the immediately adjacent sections of platform or beach. The 12-monthly, and in a few cases 6-monthly, surveys between 2001 and 2006 have enabled changes in the cliff/platform profile to be observed and measured. Clearly, this survey frequency has not captured all landslide or erosion events resulting from individual events such as storm surges for example.

In the case of Happisburgh, the gross recession picture has been captured effectively. The site is notable for the fact that almost none of the epoch models coincide. This is in contrast to Sidestrand where the time scale of cycles of instability is much greater and the debris from multiple landslide events remains on the slope, in some cases for several years.

At Sidestrand the removal of large debris flows by the sea has been observed and partially 'captured' in the models over two or three year periods. An important observation at

Sidestrand in the first year of the project was the active rotational landslides rising upward through the beach. This has been successfully independently modelled by the finite element analysis.

One factor noted for these models, however, was the fact that they invariably produce much greater cliff-top recession than observed. This applied to both Sidestrand and Happisburgh. The factors most likely to affect this were considered to be the lack of knowledge of the water table position, inaccurate mass geotechnical properties (due to a lack of sub-surface data), and the inability of the model (at Sidestrand) to include the landslide deposits on the slope.

The use of the 3-D models in geomorphological assessment of slopes has proved highly effective. The selection of time intervals for monitoring semi-continuous or sporadic events has proved more problematic, in common with other types of geohazard monitoring. The development of a form of numerical 'stability index', based on the 'factors of safety' from the slope stability analyses, applicable to adjacent coastal slopes, has not proved workable, within the constraints of the current project, technology and funding, and the complexity of the geology, particularly at the Sidestrand site.

Practical field factors have come to light. The early surveys (particularly up to 2002) suffered from poor GPS positioning of laser stations and targets. Considerable post-processing using a proliferation of software packages has been necessary to rectify this, using programmes such as ER Mapper™, GoCAD™, Surfer™ and, more recently, Polyworks™. A further problem has been the stability of conventional survey tripods on beaches, particularly in wet sand. A remedial measure has recently been instituted. This consists of extra-large tripod feet. The possibility of employing some form of digital pitch/roll/yaw sensor has also been investigated to improve positional accuracy for future work in this environment.

The project's access to sophisticated modelling software packages has improved throughout the project. Equally, the amount of data recorded has increased with the acquisition of a higher-specification LiDAR in 2004. The positioning accuracy has also improved by several upgrades of dGPS. The ability to accurately quantify recession and landslide movements has really only been achieved in the latter parts of the project. These factors have resulted in dramatic improvements in positional accuracy over the monitoring period. The Polyworks™ IMAlign package does allow for the possibility of rectifying GPS-related orientational errors in the early surveys, but only where multiple features common to scan epochs are identifiable (not possible at Happisburgh, for example).

The subject of surveying accuracy and errors has been addressed. However, there are many difficulties, particularly in assessing accuracy, due to the lack of fixed points on rapidly eroding coastlines, and to the wide variations of range within each scan (Buckley *et al.*, 2008). This sets terrestrial LiDAR somewhat apart from the aerial equivalent where range contrasts are usually smaller. The orientation of multiple scans to a common grid introduced its own errors, though baselines up to 100 m in length were generally re-surveyed, albeit using a reflective target, on numerous occasions to within +/- 1 mm using a laser with a nominal range accuracy of +/-15 mm. The use of a beach baseline running parallel to the cliff, first developed by 3DLaserMapping Ltd for the project, has proved effective. It has been demonstrated elsewhere by the Slope Dynamics project team that scanning from tripods mounted on solid rock, of subjects made of solid rock, creates more easily oriented and more accurate 3-D models than the equivalent survey on soft sediment.

As with all line-of-sight surveying methods the terrestrial LiDAR survey produces 'shadow' areas where the subject is obscured. If the obscuration is in the vertical plane, e.g. a promontory, the 'shadow' section of cliff can be scanned from the beach from a new aspect and the scans merged. However, if the obscuration is on a horizontal plane, e.g. a rotated slip mass, greater elevation is required to resolve this 'shadow'. At many project test sites this has been achieved by scanning from the cliff top. This was not possible at Sidestrand due to access restrictions, and at many coastal sites is ineffective due to a lack of vantage points. The

cliff at Happisburgh, due to its overall planar form, was notable for the absence of such shadows. In terms of the choice between terrestrial and aerial LiDAR methods the sites at Happisburgh and Weybourne best suit the former due to their steep slopes. The Sidestrand site probably falls between the two methods, though is sufficiently large and varied to benefit from both.

7.2   SITE SELECTION

The aim of initial site selection was to provide three test sites each with different geology, different cliff height, different landslide types and different recession rates. Of these, two were chosen as being active and the third inactive (i.e. a 'control' site). This aim has been successfully achieved with Weybourne as the control site featuring little or no recession during the monitoring period and with the strongly contrasting attributes of Happisburgh and Sidestrand. Happisburgh has produced over the period of study one of the largest recorded annual recession rates in Britain at about 9m per year. Of course, this has resulted from localised failure of coastal defences during the 1990's, and has thus been described here as 'accelerated', and as such is atypical of the North Norfolk coast. The selection of a terrestrial LiDAR monitoring site requires it to be locatable in space and of limited extent. It is always prone to being outdone by events beyond the site boundaries. This is the nature of landslide cyclicity, and happened in 2006 when a very large landslide occurred immediately to the east of the Sidestrand test site, and part of the active event was in fact observed (from a distance) by BGS staff. However, the Sidestrand site has been very active over the monitoring period with little respite from activity. Of course, much of the detail of such semi-continuous processes cannot be comprehensively captured by episodic mobile surveys.

Over the monitoring period 2000-2006 the three sites have vindicated their selection and the two 'active' sites at Happisburgh and Sidestrand have produced spectacular results. Over much of the monitoring period 2000 to 2006 large parts of the Sidestrand test site cliff have been inaccessible due to waterlogging. This has again reinforced the 'remote sensing' benefits of terrestrial laser scanning. It has become clear during the project that in order to validate cliff-top locations derived from the dGPS/laser scanning method, in particular height above Ordnance Datum, in sites with high recession rates and no ground control, it is important to have an accurate ground model of the hinterland. This can probably be best achieved by conventional surveying. Such surveys would have been beneficial at Happisburgh, and also at Sidestrand had access been available. To this end it is important in future to select sites where the cliff-top is accessible for surveying, or for which high resolution DEM data are available.

7.3   MONITORING INTERVALS

In some respects the intervals of a monitoring programme are limited by practical factors unrelated to geological processes. This includes both the duration of the overall project and the frequency of surveys. This has not been an issue at Happisburgh because of the speed and uniformity of the recession process although more frequent surveys would have resulted in a more detailed understanding of the recession.

At Sidestrand the overall time scale of the project has thus far been inadequate to capture the full cycle of landslide activity and hence coastal recession. This is suggested by activity in adjacent slopes and the measured change in overall cliff slope. The landslide cycle may extend over about 10 years or more. Comparisons may be drawn here with Warden Point (Isle of Sheppey) where the landslide regime is not dissimilar to Sidestrand, and where the cycle has been identified at between 30 and 40 years (Dixon, 1987; Dixon and Bromhead, 2002; Hutchinson, 1976); monitoring having taken place over a 30 year period from 1971 to 2001. It should be noted, however, that sea erosion at Warden Point is considerably less energetic than at Sidestrand due to the Isle of Sheppey's aspect and estuary location. This will tend to reduce

the landslide cycle time. Despite these reservations, major landslide events and trends at Sidestrand have been successfully 'captured' by the monitoring process.

At Weybourne, annual monitoring has been reduced because of landslide inactivity. Here, with the lack of defence structures, the anthropogenic effect on landslide activity is deemed to be minimal. That said, the gradient of gravel beach at Weybourne and Blakeney Spit to the west is believed to be maintained artificially to ensure its function as a barrier to storm waves.

The shoreline management plan for the stretch of coast between Winterton and Happisburgh contains various measurements and predictions on the rate of recession along this stretch of coast. The earliest results from 1883-1906 suggest that the cliff line was retreating at around 2.3 m/yr, which reduced to 0.3 m/yr in the period between 1906 and 1952. Predictions of cliff erosion vary over the timescales, Futurecoast predicts a loss of land between 50-100 m over the next 100 years whilst the Shoreline Management Plan suggests between 35-85 m between 1994 and 2068. The measurements recorded in this study suggest that at the scan site the average annual recession rate is between 6-8 m/yr. This is much higher than the published data but this may relate to the location of the scanning. This site appears to be particularly active and may not reflect average rates taken over a much wider stretch of coast.

7.4 VOLUME CHANGES

Volume changes between surveys for either a 100 m or 200 m cliff length within the test sites at Happisburgh and Sidestrand have been calculated using ER Mapper™ using data obtained from the 3-D models derived from the laser scans. The lower datum was taken at the 1.5m AOD contour and upper boundary to include the highest part of the scans. The survey results from Happisburgh show an average of 18,394 m^3 of sediment a year was removed from a 200 m section of cliff, which equates to approximately 36,000 t of sediment annually, with 2005-2006 showing a significant decrease in sediment loss.

At Sidestrand, an average of 24,260 m^3 of sediment a year was lost from a 200 m section of cliff. This equates to approximately 48,000 t of sediment annually. Comparison of each epoch between 2001 and 2006 shows that between 2002-2003 the least amount of sediment was lost, compared to a peak year of 2005-2006.

At Weybourne, between 2003 and 2004 there was a loss of material across the survey site of approximately 235 m^3 and a gain of material of 135 m^3 at the cliff toe due to sand runs and small earth falls.

Table 7-1 Volume changes calculated from 3D laser scan models

Monitoring epoch	Happisburgh Volume change (m^3) per 200m cliff	Sidestrand Volume change (m^3) per 200m cliff *	Sidestrand Volume change (m^3) per 100m cliff #
2000-2001			45,670
2001-2002		64,790	43,367
2002-2003	21,000	1,414	-11,124
2003-2004	12,600	4,132	2,357
2004-2005	36,785	12,084	1,896
2005-2006	-3193	38,880	9,600

 # embayments SD1 & SD2
 * embayments SD1, SD2 & SD3

The negative value obtained for Sidestrand in 2002 – 2003 appears to be due to errors in the registration of height, and to a lesser extent the inclusion of some beach material in the calculation. The negative value is confined to embayments SD1 and SD2, whilst embayment SD3 has a positive value. The small negative value for Happisburgh in 2005 – 2006 is again due to positional errors and the inclusion of some beach material. The relationship between rainfall and volume change has been investigated, but no correlations have been found.

7.5   CAUSES OF RECESSION HIATUS

Recession rates for the scanning period at Happisburgh and Sidestrand show a marked difference. At Happisburgh the rate of recession is on average between 6-8 m/yr whilst at Sidestrand the rate is between 1.6-5 m/yr, although the average is approximately 3 m/yr. As well as these differences in recession rate the two sites also experience accelerated recession as well as hiatuses over different time periods. At Happisburgh rapid erosion occurred between 2004 and 2005, before which erosion appeared to be relatively steady. This may be related to the addition of a rock bund built at Happisburgh in 2002 after a breach in the defences widened in 2001. However the rates of recession do not solely correspond to changes in the state of sea defences. The hiatus at Happisburgh could also be related to changes in rainfall and storm events as well as beach thickness. Levels of decreased recession in 2002 and 2003 were mirrored by decreases in the rainfall at Happisburgh. Similarly, increasing rainfall levels in 2005 were matched by increases in the rate of recession. Another factor in the rate of recession could be beach thickness, which was shown to vary annually. Between the 2004-2005 scans the cliff had suffered rapid recession rates, coincident with a low beach level observed during the 2005 scanning period. In the following epoch (2005-2006) the rate of recession slowed, this could be related to the greater thickness of beach which was observed in 2006.

At Sidestrand the rate of recession peaked between 2001-2002 with another high between 2005-2006. This increased rate of recession between 2005-2006 was markedly different to the hiatus in recession observed at Happisburgh during the same time period. The increase in recession observed from the 2005-2006 epoch corresponds to the highest rainfall peak observed for the whole scanning period (August 2006). It is possible that this high rainfall event may have led to increased landslide activity at the Sidestrand site. The peak rate of recession observed in 2001-2002 corresponds to the highest rainfall years recorded for the Sidestrand site, these being 2000 and 2001. Two wet years may have led to increases in the rate of erosion recorded during the 2001-2002 period. No data for beach thickness are held for Sidestrand so it is not known if this is a contributing factor in the rates of recession recorded.

7.6   LANDSLIDE TYPES

At Sidestrand there is a complex of deep-seated landslides, with multiple and large-scale shallow landslides and associated mudslides and mudflows. The overall slope inclination means that significant proportions of the landslipped masses remain on the slope and are subsequently involved in further landslides, or are overridden by them. Occasionally, large debris flows develop, which run-out across the beach and are sufficiently large to survive erosion by the sea for several weeks or even months. Large-scale multiple mudflow events are common. Early in the monitoring period deep-seated landsliding was observed, in one of the three embayments at Sidestrand, to extend beneath beach level and emerge with an upward component of movement, as indicated by Hutchinson (1976) at Cromer. The source area for most of the small and medium-sized landslides at Sidestrand appears to be the upper part of the cliff's embayments where the lithology is dominantly sandy and groundwater seepage is virtually ubiquitous. Most of these landslides have slip planes cropping out a few metres above beach level, the lowermost stratigraphic unit in the cliff acting as a bench over which the landslide moves. The largest landslides observed during the monitoring period, however,

did appear to have slip planes extending to a depth of several metres below beach level and cropped out from the beach (or platform) rather than the cliff. Some intermediate landslides were observed to emerge at beach level, in which case the uppermost half-metre or so of beach sediment was thrust forward by the movement. This type is more likely to be associated with flows rather than rotational movements.

At Happisburgh a significant mechanism of cliff recession appears to be the direct mechanical action of waves which has been observed to remove large quantities of sediment, particularly during storms. Landslides have also been observed to be of simple rock-fall (or soil-fall) type and to be small and very frequent. These usually do not involve the till at the base of the cliff, but deposit debris onto the till 'bench', if present. As such, the (mainly) annual monitoring programme has been unable to model such events individually. In addition, there are rotational slumps extending typically 5 m back from the cliff top and extending down to the till's upper surface. These produce small steep-sided embayments. The key modelling factor at Happisburgh has been the almost universal discretisation of the annual cliff positions. In other words, the consecutive models for the most part do not intersect at any point, as they do at Sidestrand. This is due to the low cliff height, high cliff angle and extreme erosion rate at Happisburgh. This tends to make change models easy to construct and interpret. The sole exception to this is the 2005-2006 interval where the two models are almost coincident.

At Weybourne the dominant mechanism of cliff erosion appears to be (dry) sand runs, and occasionally small rock (soil) falls in the sandy lithologies of the middle and upper cliff. In the lower cliff erosion is affected by mechanical abrasion, principally from beach pebbles, and dissolution of the chalk from groundwater, rainwater and seawater. Small embayments have resulted from these combined processes despite a lack of major landslides. Slope stability analyses have not been carried out at Weybourne as the instability mechanisms described above are unsuited.

The application of slope stability analysis to Happisburgh and Sidestrand has demonstrated that landslides on rapidly eroding cliffs may require variations to the normal method of analysis where significant suction is suspected (for example, see Dixon and Bromhead, 2002). The FLACslope finite element models appear to have produced reasonable values of factor of safety and reasonable 2-D deformation models from which slip planes or zones can be inferred, although overall the factors of safety tended to be below unity. The overall depth, scale and geometry of the modelled landslides do appear to match observation in most cases. However, the major point of dissimilarity between model and reality appears to be the amount of cliff-top recession indicated by the model being greater than observed. This amount is typically double that observed. This may be due to the development of vertical and sub-vertical fissures within the dominantly non-cohesive sandy lithologies of the upper cliffs at both sites. This may have led to a foreshortening of the actual slip surface profile in its upper part.

At Sidestrand, unlike at Happisburgh, the three model locations have produced different types of deformation which may be interpreted as different landslide types. At Sidestrand these include moderately deep-seated single rotational or double-rotational landslides, compound types and deep-seated compound types. The inclination of the rear part of the stability model's displacement zone tends to be steeper than the cliff profile, but nevertheless, as at Happisburgh, tends to produce a larger cliff-top recession than observed, in some cases up to 40 m. Despite the fact that a nearby failure at Overstrand resulted in 70 m recession in one landslide event in 1988, landsliding with this feature has not been observed at Sidestrand, at least during the period of monitoring, and this factor has thrown into doubt the suitability of the method. There are three primary reasons why this might be the case at Sidestrand. It should be noted that the FLACslope model assumes a first-time slide. Whilst at Happisburgh this matched the observed situation, it did not necessarily apply at Sidestrand where considerable thicknesses of pre-existing landslide deposit remained on the cliff, particularly

the lower part, and were available for re-activation. However, as one of the mechanisms at Sidestrand is deep-seated this factor becomes less-significant, although there remains the issue of pre-existing slip planes which are not capable of being satisfactorily modelled in the FLACslope program. Limit equilibrium slope stability methods require a known sliding surface. As this was an unknown at Sidestrand these methods could not be used.

With regard to the third factor, the ground water table within the cliff is unknown at Sidestrand. However, observations over the monitoring period suggest that ground water plays a key role in the instability at Sidestrand. The combination of a topographic low and a glaciotectonic syncline at Sidestrand results in a concentration of ground and surface water at the test site location. The FLACslope model is not capable of dealing, at least in a straightforward manner, with multiple (e.g. perched) water 'tables'. Such water 'tables' may be anticipated in complex glaciogenic sequences of alternating coarse and fine-grained sediments. When considering rapidly eroding cliffs which have significant clay content, the role of pore suction should be considered. Unfortunately, this is difficult and time consuming to measure, but could account for the low factors of safety produced by the FLACslope models; i.e. suctions had neither been measured nor modelled and would, if present, have tended to increase the factors of safety.

7.7   INFLUENCE OF GEOLOGY ON CLIFF STABILITY

The geology of two of the test sites, Happisburgh and Sidestrand, has an important influence on cliff stability. At Happisburgh the geology is very simple and the dominant influence is essentially that of the weakness of the geological materials present. The weakest of these (Ostend Clay Member) separates the overlying sand from the underlying till and its inability to resist erosion tends to undermine the sands. This juxtaposition in strengths was observed during the use of the PANDA penetrometer when the Ostend Clay was shown to be very soft and had the lowest shear strength parameters of the three materials. The Happisburgh Sand Member is very variable, ranging from very loose to dense and two weak horizons were observed from data collected using the PANDA. This material is prone to seepage erosion and is subject to surface runoff erosion at the cliff top which causes deep gullying and initiates instability in the upper cliff. The importance of this sequence of materials also relates to the flow of groundwater. Alternating permeable sands and impermeable clays can cause the seepage of water at the boundary of the two materials. Build up of water at this boundary may also lead to pore-water pressures increasing, leading to a reduction in shear strength and a greater susceptibility to failure. The tills forming the foot of the cliff are stronger than the overlying strata and as a result form a resistant 'bench' rising to one or two metres above platform level and extending seaward in places by up to 10 m. At some times of year this may be totally or partially covered by beach sand.

At Sidestrand the geology is extremely complex. Here the glaciogenic deposits and glaciotectonic structures have resulted in a complex suite of widely varying soil and rock types. In geotechnical terms these are difficult to model with any confidence. In consequence, the hydrogeology is itself complex, and difficult to model. The presence of thrust-related synclinal structures within the marls, in the lower and middle-cliff, and occasionally large relatively strong chalk talus 'rafts' in mid-cliff, has resulted in enhanced stability and resistant promontories or 'buttresses' at these locations. These features are sometimes difficult to locate due to a draping of landslide sediment or discolouration by seepage. The micro-folding due to glaciotectonism within the tills (Happisburgh Till Formation) in the lower cliff and platform is mainly of a pronounced 'chevron' or 'zig-zag' type and influences the formation of rock-falls and the development of pronounced notches at the base of the cliff. The geometry of the landslides is affected by the macro-glaciotectonism and rafting. For example, the presence of a steep-sided syncline limb at the eastern end of the Sidestrand site (embayment SD1) has provided a ready-made slip surface for medium- and deep-seated landslides to exploit.

7.8 RECOMMENDATIONS FOR FUTURE WORK

The Happisburgh site has been monitored through a significant and highly publicised cycle of accelerated coastal erosion, which was initiated by destruction of the defences during the late 1990's, has resulted in the loss of many houses, and which has attracted considerable media interest. It is recommended that monitoring continue using the same methodology, but that the test site is widened to include the cliff fronting the remainder of Beach Road, as this is likely to be the next location subject to accelerated erosion rates. The site is of interest to research because of the exceedingly high rates of erosion and the contrasting resistance to erosion of the till and sand lithologies. The installation of geotechnical instrumentation to measure pore pressures should be considered in an area of the site which can be guaranteed to continue receding rapidly, in order to investigate the role of suction on cliff stability. Prior to further recession monitoring, a detailed cliff top and hinterland topographic survey should be undertaken. This would provide control to the level of the cliff top following episodes of recession. During the present monitoring, it became clear that the cliff top surface was far for flat as had previously been assumed.

The Sidestrand site is of major research interest due to its high levels of activity, large scale and geological complexity, and also the wide variety of landslide types. It is currently one of the most significant active landslide sites in England. It is recommended that terrestrial LiDAR monitoring be continued, using the same methodology, but that efforts be made to obtain access to the cliff top so that large point cloud 'shadows' can be infilled in future. Terrestrial LiDAR is at present the only way of accurately monitoring the Sidestrand site; though there is the possibility of combining this to good effect with aerial LiDAR (the ability to do this has recently been demonstrated by the Slope Dynamics team at their 'inland' test site at Hollin Hill). The use of roving dGPS alone would not provide the geomorphological information which has been so valuable. It is unfortunate that the site appears to be unsuitable for visual monitoring using some form of CCTV installation and movement sensor to capture landslide events taking place. As for Happisburgh, the installation of geotechnical instrumentation to measure pore water pressures should also be considered for the Sidestrand site.

The site at Weybourne should probably not be pursued, at least in the foreseeable future, due to an overall lack of significant erosion over the monitoring period. The exception to this might be if a much longer monitoring interval, say five years, was considered, or if conditions at the site changed significantly, for example if the substantial shingle beach was lost or maintenance of it ceased. This would thus become a 'responsive' rather than 'regular' monitoring site.

An important application for the kind of 3-D models produced as part of this project is the measurement of geological, as well as geomorphological, features. Whilst not completed for this report, the ability to map 3-D variations in surfaces, such as the upper surface of the Happisburgh Till Member at Happisburgh, is already a reality. At Happisburgh the accelerated erosion effectively provides a series of annual cross-sections of the stratigraphy from which accurate measurements of the elevation of boundaries can be made and plotted to form 3-D surfaces which are correctly oriented in space and from which assessments on a sub-regional scale can be made. This capability is considerably enhanced by the incorporation of colour imagery to the scans, enabling lithologies and features to be clearly identified. Whilst colour imagery was unavailable prior to the 2004 survey, topographic variations may be used on black and white point clouds as an alternative but only where lithology-related erosion contrasts occur, as occurs at Happisburgh. Such data may be used to investigate the relationship between cliff morphology and strata thickness and inclination, for example.

The concept of a 'slope stability index', whereby individual engineering-type 2-D finite element slope stability analyses can be projected or extrapolated along the cliff to form a geohazard rating, shows promise and should be pursued. Current modelling, as reported here,

has proved inadequate for this purpose, but further refinement of software and a transition from 2-D to 3-D finite element slope stability analysis may provide solutions allowing geohazard models for extended sections of cliffed coastline to be made. A key problem at present is the lack of an accurate 3-D geology model at the coast. Whilst a 3-D geology model can be generated from a laser-scan monitoring model, it cannot be projected beyond the test site. Consideration of 3-D coastal geology mapping has been given by BGS, partly in connection with BGS's Geosure™ scheme (Wildman and Hobbs, 2005).

8 Conclusions

- The slope dynamics project has successfully monitored active cliff recession and landsliding at two of its three test sites, i.e. at Happisburgh and Sidestrand, over the period 2000 to 2006. During this period colour imaging has been introduced, and the accuracy and resolution of surveys has been steadily improved. Accelerated erosion at Happisburgh has reached record levels, averaging up to 9 m per year over the monitoring period. Monitoring at the Weybourne site ceased in 2004.

- Annual volume changes, derived from the laser scan models, have been calculated and are up to 65,000 m^3 at Sidestrand and 37,000m^3 at Happisburgh, per year, per 200 m run of cliff. These figures, whilst not necessarily indicating volumes of material displaced in individual landslide events, do indicate the net amount of sediment released to the sea from the cliff.

- Monitoring technology, specifically terrestrial LiDAR and dGPS, and BGS's ability to utilise it effectively, has made significant advances over this period. This has led to a steady and demonstrable improvement in the quality of output over the monitoring period. Point cloud densities have increased from less than ten thousand points in 2000 to over 3 million points in 2006. This has allowed both greater detail to be elicited from each survey and in some cases greater coverage.

- 3-D change models have been produced for Happisburgh and Sidestrand. These show annual or bi-annual changes in elevation; a key difference between the two sites being that the models for Happisburgh do not overlap, with the notable exception of 2005-2006, due to the simplistic nature of erosion, while those at Sidestrand are overlayed in the zone of accumulation due to the scale and complexity of processes and retention of landslipped material on the lower-cliff between epochs.

- Slope stability analysis of selected cliff sections has revealed certain discrepancies between modelled and observed results. These may, at least in part, be due to geotechnical factors unaccounted for in the algorithm, for example the contribution of suction to effective stress. Alternatively, they are due to errors in the geotechnical or hydrological data input to the model. Factors of safety against sliding have tended to lie between 0.7 and 1.0.

- The concept of a 'slope stability index', whereby individual engineering-type 2-D finite element slope stability analyses can be projected or extrapolated along the cliff to form a geohazard rating, has been explored but the input data and methodology have been considered inadequate in their present forms.

- The nature and cyclicity of landslide development has been characterised at Sidestrand, despite the relatively short monitoring period. The strong influence of lithology and structure in determining the scale and type of landslide has been confirmed. However, as the full cycle appears to be of the order of 10 years, work should continue at the site, possibly at a reduced frequency or in a 'responsive' monitoring mode.

- The monitoring periodicity of 12 months, and occasionally 6 months, has been adequate to record gross or long-lived features and events, but has not enabled all seasonal changes to be measured. Small mudflows, mudslides, debris flows and rock-falls could have occurred and been partly or completely removed between surveys. This has been an issue at Sidestrand, but not at Happisburgh. Changes in beach levels, though measurable by dGPS/laser scanning, cannot be inferred between surveys.

- It has been shown that to fulfil some of the objectives set by the project, a full understanding of the 3-D geology at the actively eroding sites was required. This was not available to the project. This is discussed in the recommendations section.

Appendix 1 Survey Schedule and Equipment

Monitoring, sampling, and testing programme for Happisburgh (2000-2006)

Test site	Oct 2000	Nov 2000	Apr 2001	Jun 2001	Sep 2001	Apr 2002	Sep 2002	Sep 2003	Aug/Sep 2004	Oct 2005	Oct 2006
Happisburgh		x	x S U P		x +			P			U P

Logging:	Psion Workabout				Sunscr.	Toughbook
Laser:	RieglLPM2K - 4shot				1shot	RieglLPM800HA
Panda:	Panda1				Panda2	

Key:
- LPM2K Laser scan + Garmin GPS control
- LPM2K Laser scan + Leica GS50 GPS control
- LPM2K Laser scan + Leica SR530 GPS control
- LPMi800HA Laser scan + Leica SR530 dGPS control
- Reconnaissance/geological survey
- x   Laser scan / GPS carried out for BGS by 3D Laser Mapping Ltd.
- +   Photogrammetry by Nottingham University
- **P**   Panda penetrometer tests
- **U**   Undisturbed U100 sample taken (+ disturbed)
- S   Disturbed samples only taken

Monitoring, sampling, and testing programme for Sidestrand (2000-2006)

Test site	Oct 2000	Nov 2000	Apr 2001	Jun 2001	Sep 2001	Apr 2002	Sep 2002	Sep 2003	Aug/Sep 2004	Oct 2005	Oct 2006
Sidestrand		x	x U P		x S +						

| Logging:	Psion Workabout				Sunscr.	Toughbook
Laser:	RieglLPM2K - 4shot				1shot	RieglLPM800HA
Panda:	Panda1				Panda2	

Key:
- LPM2K Laser scan + Garmin GPS control
- LPM2K Laser scan + Leica GS50 GPS control
- LPM2K Laser scan + Leica SR530 GPS control
- LPMi800HA Laser scan + Leica SR530 dGPS control
- Reconnaissance survey
- x   Laser scan / GPS carried out for BGS by 3D Laser Mapping Ltd.
- +   Photogrammetry by Nottingham University
- **P**   Panda penetrometer tests
- **U**   Undisturbed U100 sample taken (+ disturbed)
- S   Disturbed samples only taken

**Monitoring, sampling, and testing programme for Weybourne test site (2000-2004)**

Test site	Oct 2000	Nov 2000	Apr 2001	Jun 2001	Sep 2001	Apr 2002	Sep 2002	Sep 2003	Aug/Sep 2004	Oct 2005	Oct 2006
Weybourne		x	x S P		x +						

Logging:	Psion Workabout			Sunscr.	
Laser:	RieglLPM2K - 4shot			1shot	
Panda:	Panda1			Panda2	

Key:

- LPM2K Laser scan + Garmin GPS control
- LPM2K Laser scan + Leica GS50 GPS control
- LPM2K Laser scan + Leica SR530 GPS control
- Reconnaissance survey

x   Laser scan / GPS carried out for BGS by 3D Laser Mapping Ltd.

\+   Photogrammetry by Nottingham University

P   Panda penetrometer tests
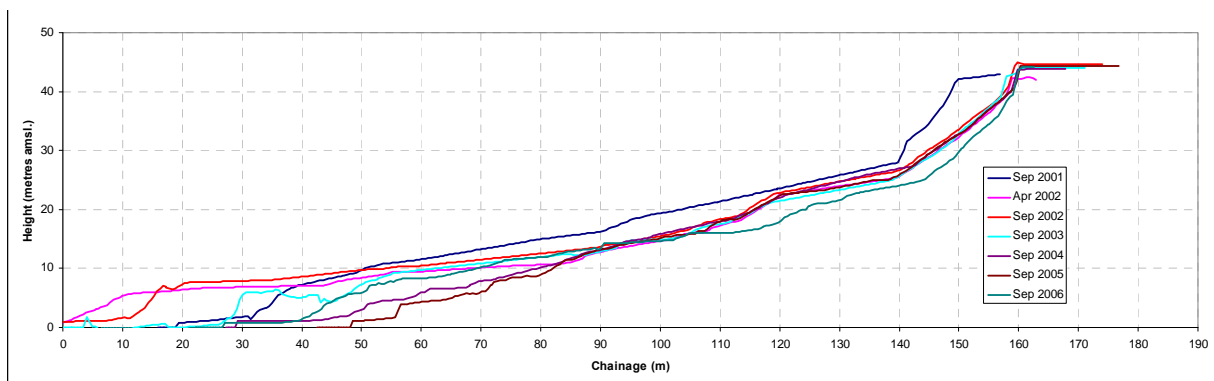
Disturbed samples only

S   taken

Appendix 2 Cross-sections used for slope stability analyses
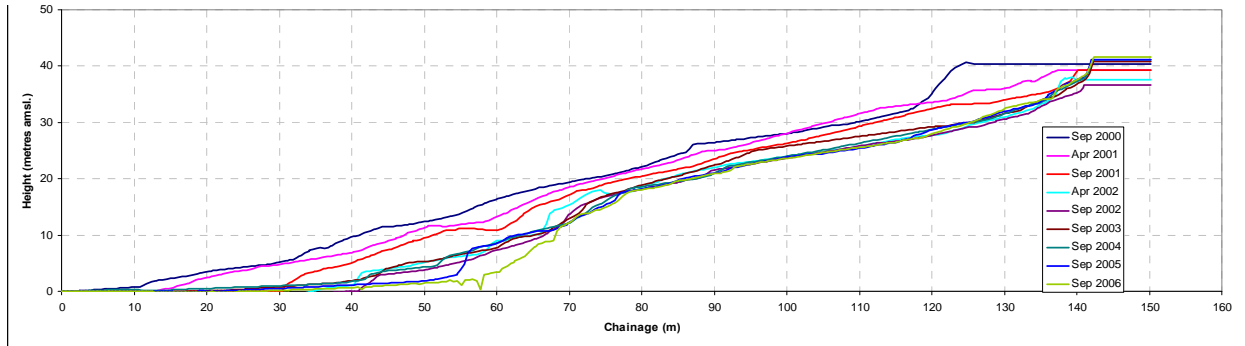
Cross-sections, Sidestrand (embayment SD1) Note: recession from left to right
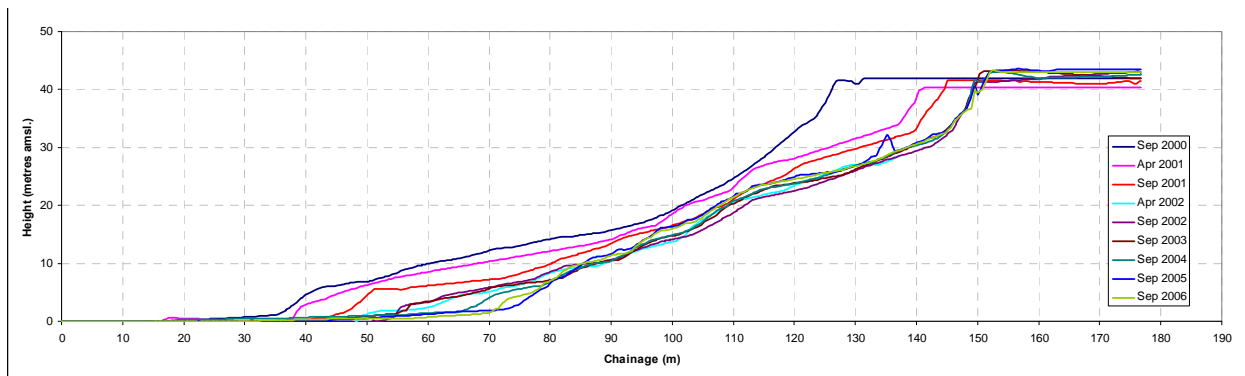
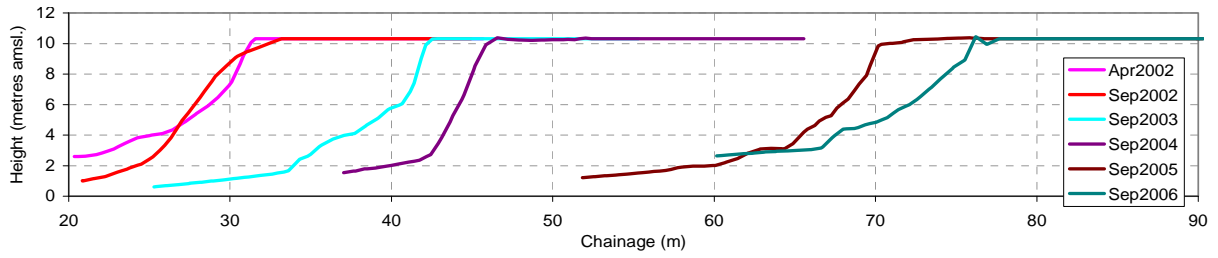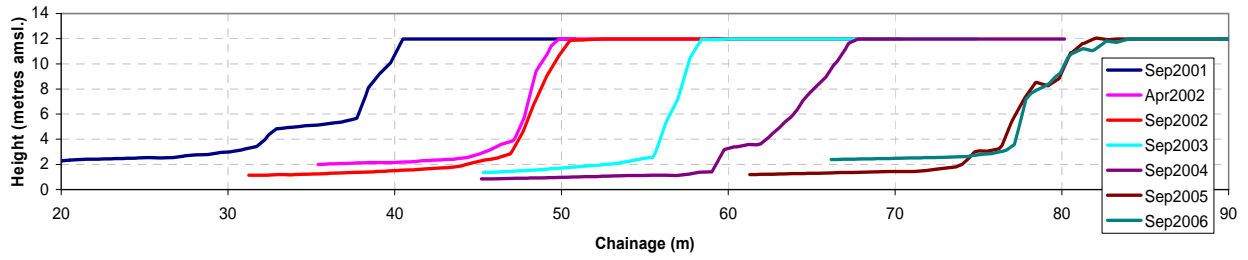**Cross-sections, Sidestrand (embayment SD2)** Note: recession from left to right

Cross-sections, Sidestrand (embayment SD3) Note: recession from left to right

Cross-sections Happisburgh (south)
Note: recession from left (NE) to right (SW)

Cross-sections Happisburgh (central)
Note: recession from left (NE) to right (SW)
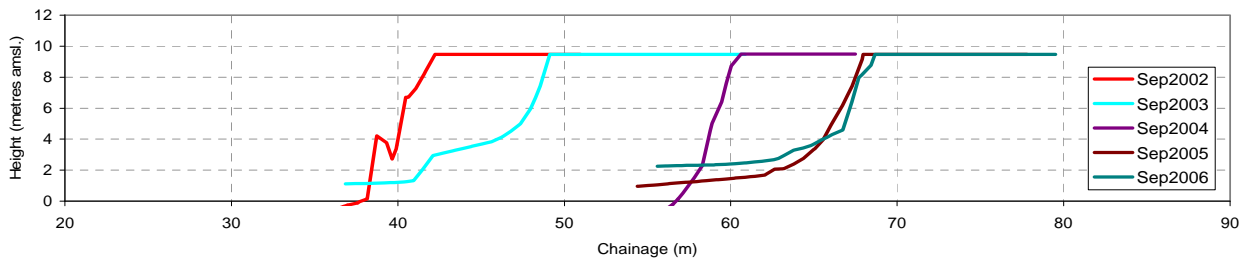
Cross-sections Happisburgh (north)
Note: recession from left (NE) to right (SW)

Appendix 3 Geological sections used for slope stability analyses
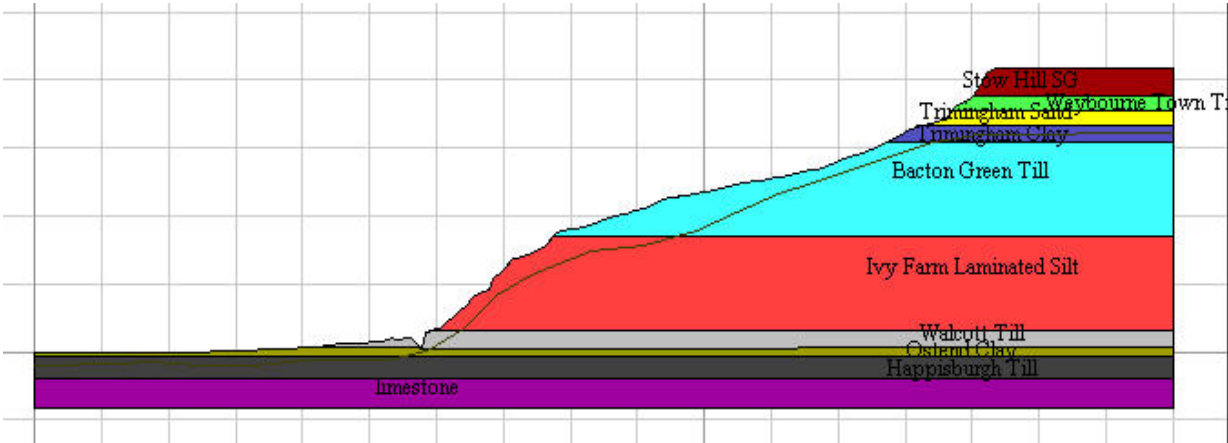
Geological layer model for embayment SD1 for slope stability analysis (Scale grid = 10m)
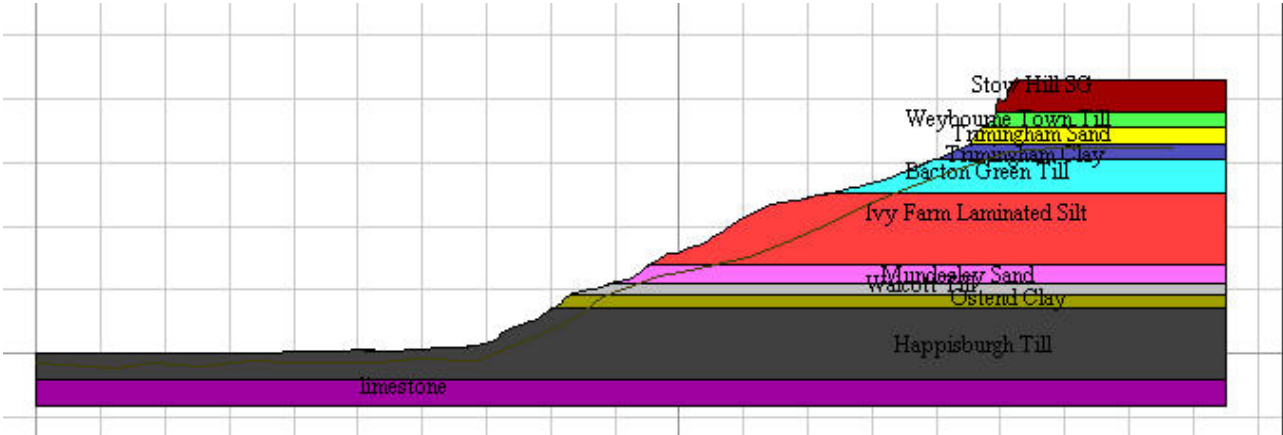
Geological model for embayment SD2 for slope stability analysis (Scale grid = 10m)
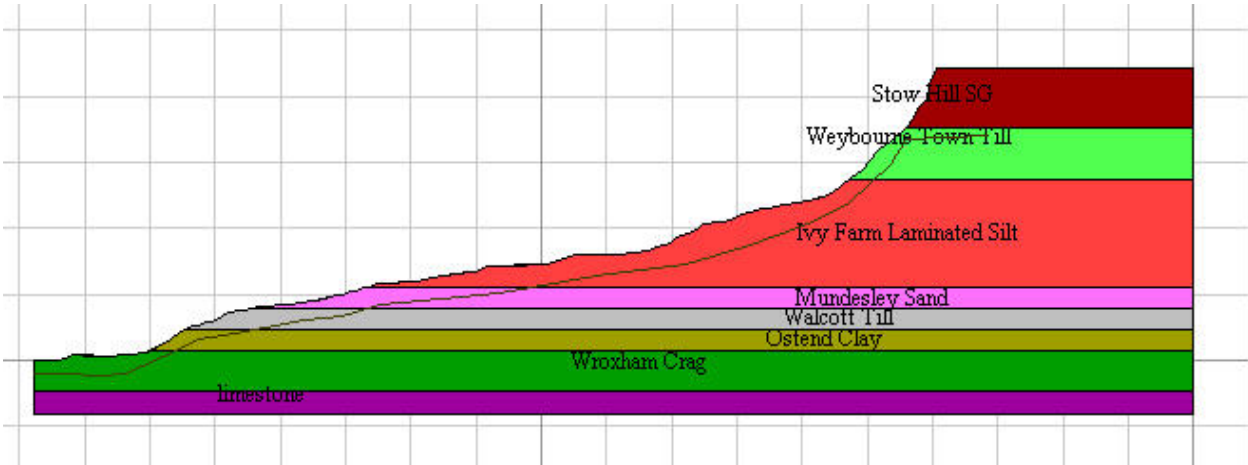
Geological model for embayment SD3 for slope stability analysis (Scale grid = 10m)

Appendix 4   Shear displacement contour/vector diagrams

Slope stability analysis
Finite Element (FLACslope, v.4)
Shear strain rate contours/vectors

Sidestrand
Embayment SD1

Sep 2000 - Sep 2006
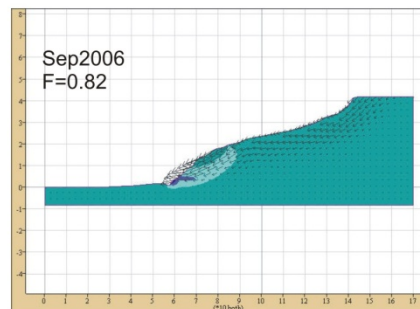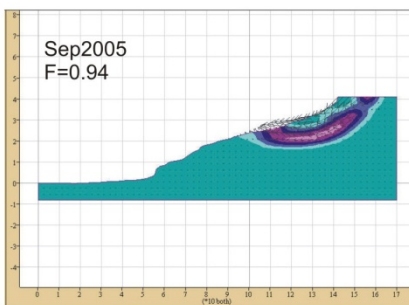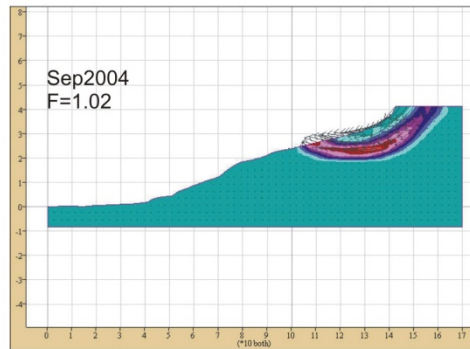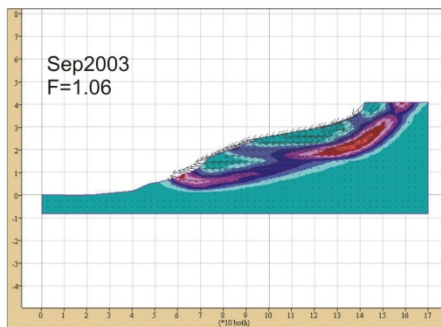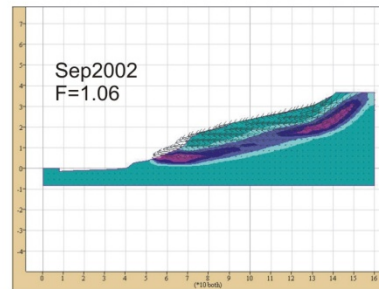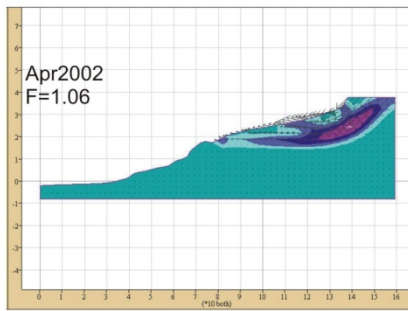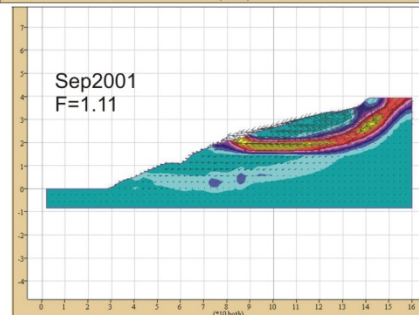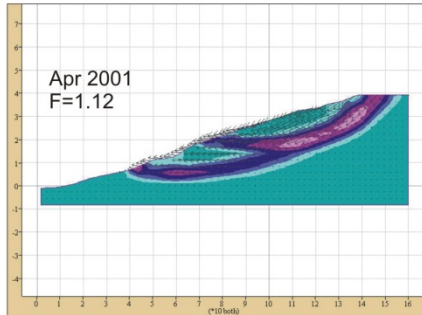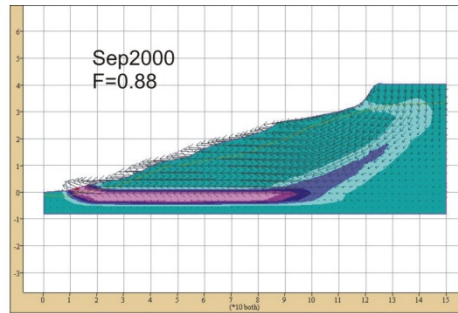
Plots of shear strain rate contours and vectors for Sidestrand embayment SD1 (FLACslope v.4) Note: Scale grid = 10 m

Slope stability analysis
Finite Element (FLACslope, v.4)
Shear strain rate contours/vectors

Sidestrand
Embayment SD 2

Sep 2000 - Sep 2006
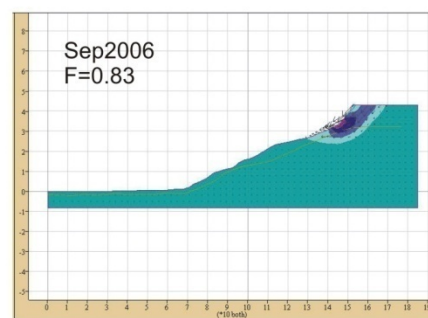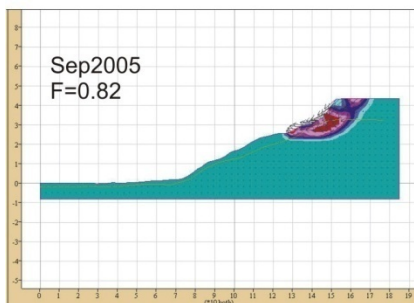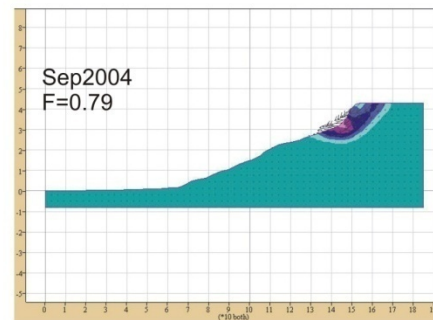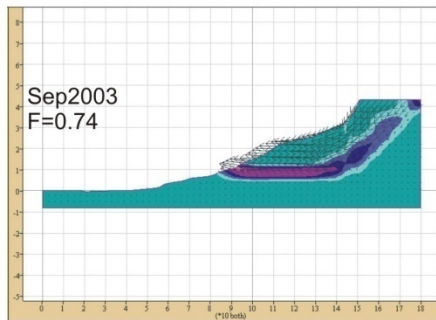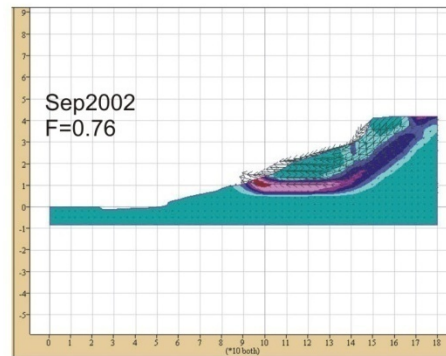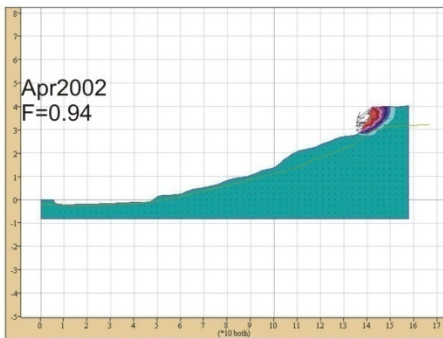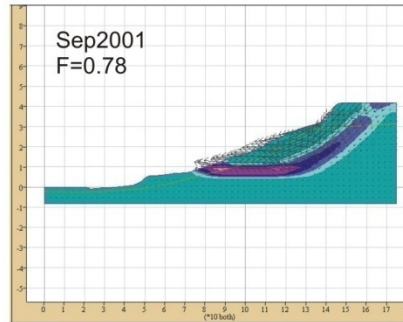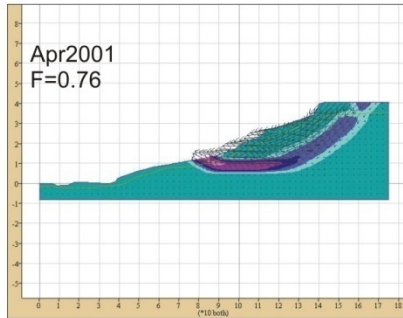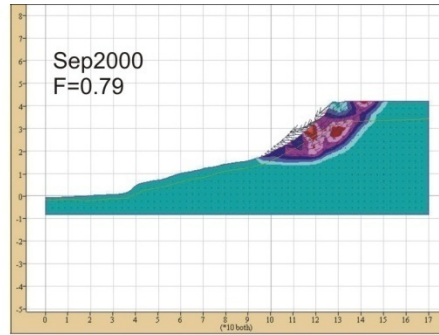
Plots of shear strain rate contours and vectors for Sidestrand embayment SD2 (FLACslope v.4) Note:
Scale grid = 10 m

133

Slope stability analysis
Finite Element (FLACslope, v.4)
Shear strain rate contours/vectors

Sidestrand
Embayment SD 3

Sep 2001 - Sep 2006

Sep2000

NO DATA

Apr2001

NO DATA

Sep2001
F=0.89

Apr2002
F=0.84

Sep2002
F=0.79

Sep2003
F=0.92

Sep2004
F=0.84

Sep2005
F=0.87
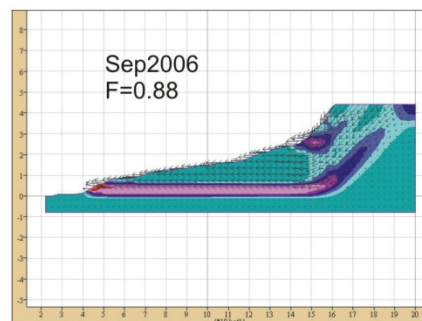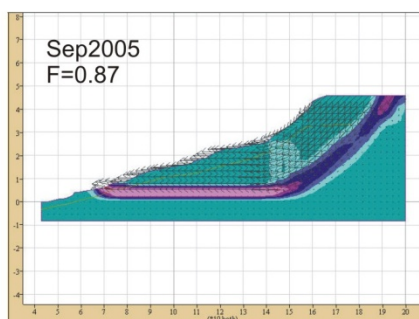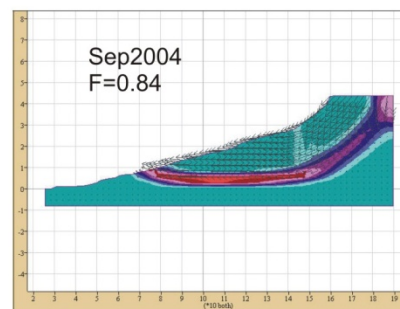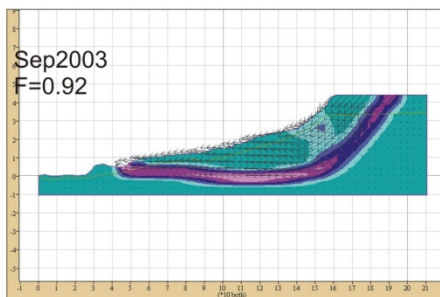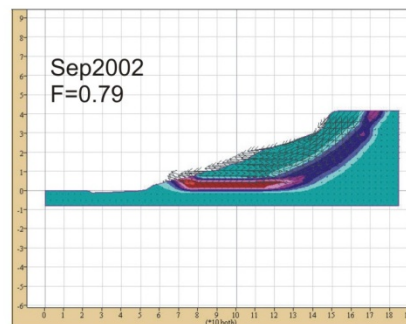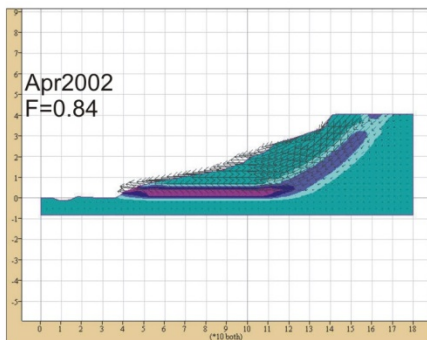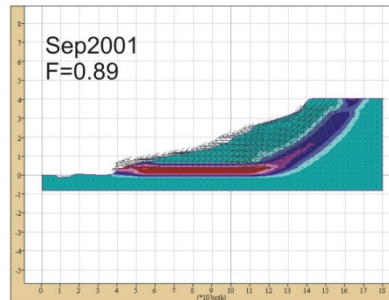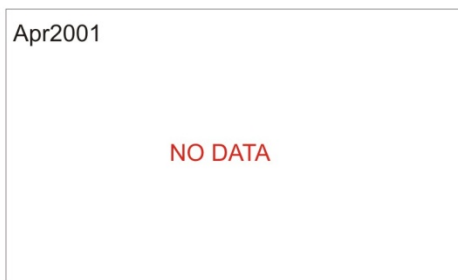
Sep2006
F=0.88

Plots of shear strain rate contours and vectors for Sidestrand embayment SD3 (FLACslope v.4) Note:
Scale grid = 10 m

Slope stability analysis
Finite Element (FLACslope, v.4)
Shear strain rate contours/vectors

Happisburgh
South

Sep 2001 - Sep 2006

NO DATA

NO DATA

NO DATA

Apr 2002
F=1.23

Sep2002
F=1.07

Sep2003
F=1.21

Sep2004
F=0.96

Sep2005
F=1.28
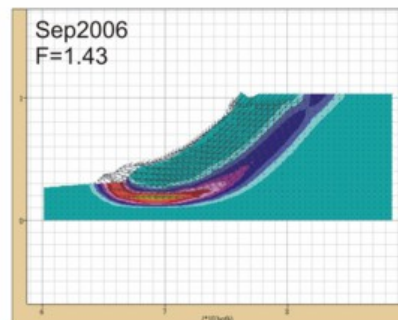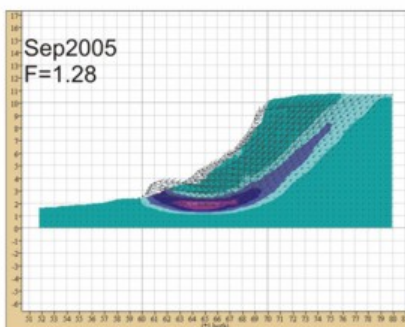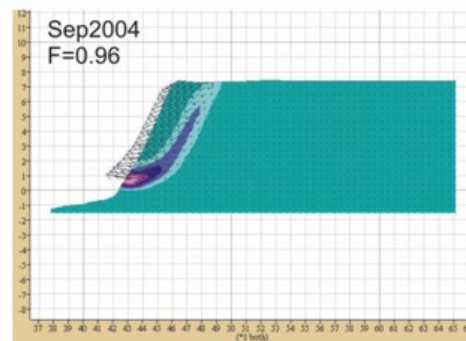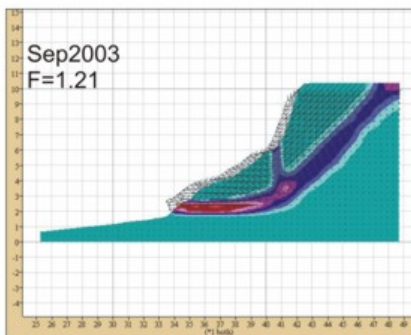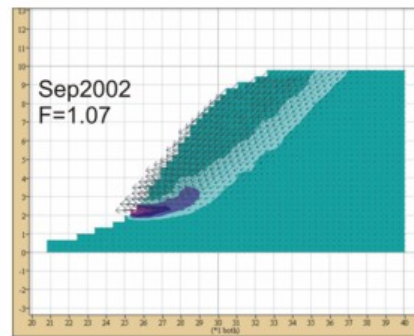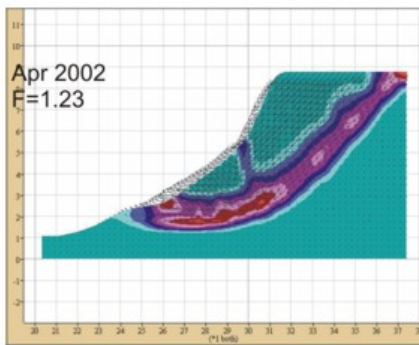
Sep2006
F=1.43

Plots of shear strain rate contours and vectors for Happisburgh (south)

Slope stability analysis
Finite Element (FLACslope, v.4)
Shear strain rate contours/vectors

Happisburgh
Central

Sep 2001 - Sep 2006

NO DATA

NO DATA

Sep2001
F=1.05

NO DATA

Sep2002
F=0.77

Sep2003
F=0.66

Sep2004
F=0.92

Sep2005
F=0.83
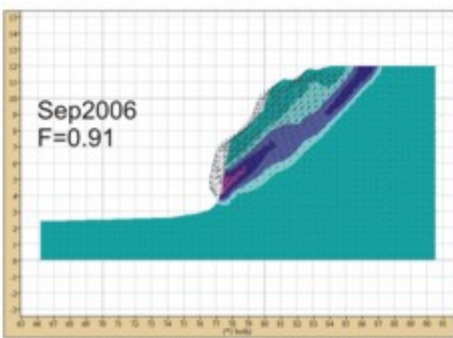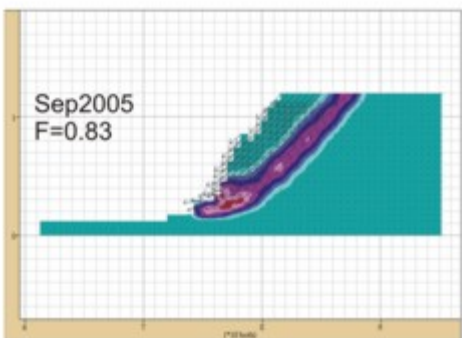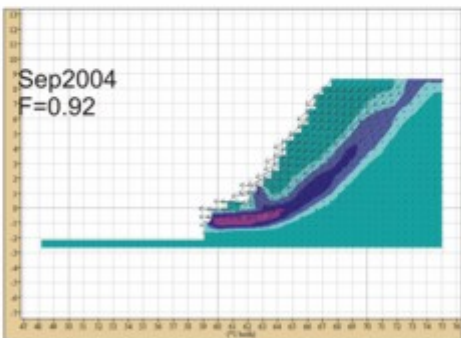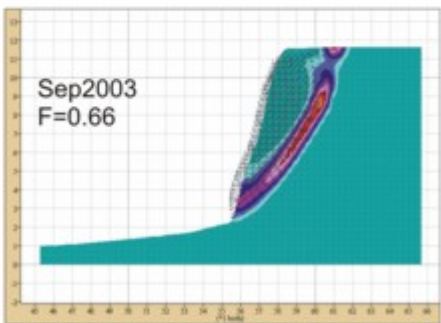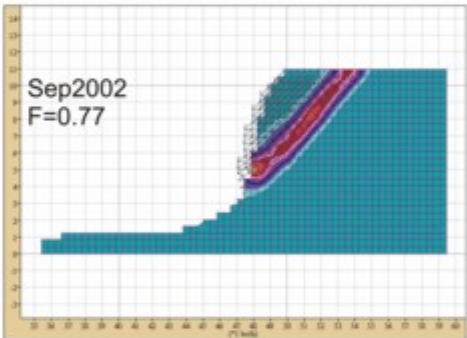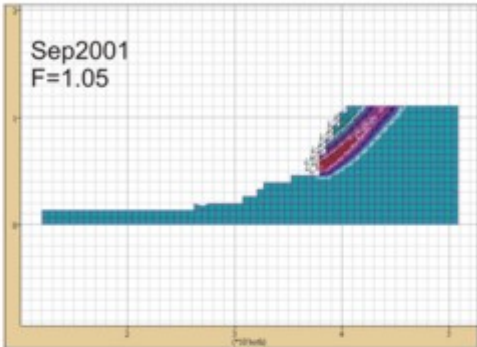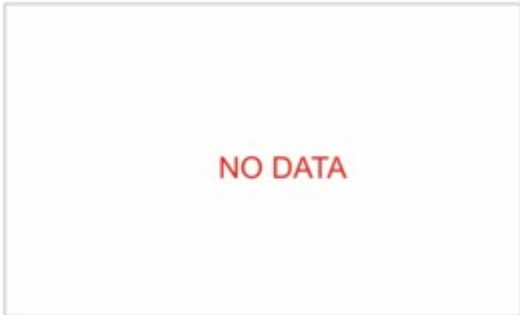
Sep2006
F=0.91

Plots of shear strain rate contours and vectors for Happisburgh (central)

Slope stability analysis
Finite Element (FLACslope, v.4)
Shear strain rate contours/vectors

Happisburgh
North

Sep 2000 - Sep 2006

NO DATA

NO DATA

NO DATA

NO DATA

Sep2002
F=0.73

Sep2003
F=1.22

Sep2004
F=0.69

Sep2005
F=1.03

Sep2006
F=1.10

Plots of shear strain rate contours and vectors for Happisburgh (north)

SHEAR STRAIN RATE

5.00E-07

1.00E-06

1.50E-06

2.00E-06

2.50E-06

3.00E-06

3.50E-06
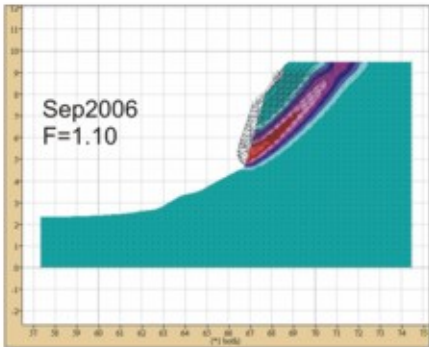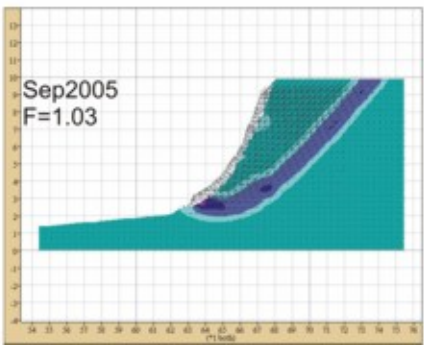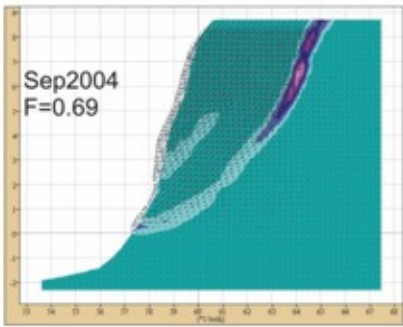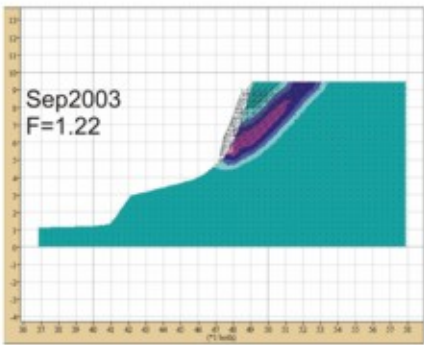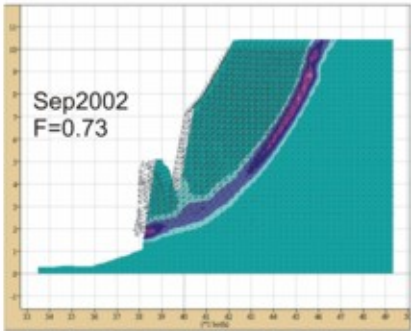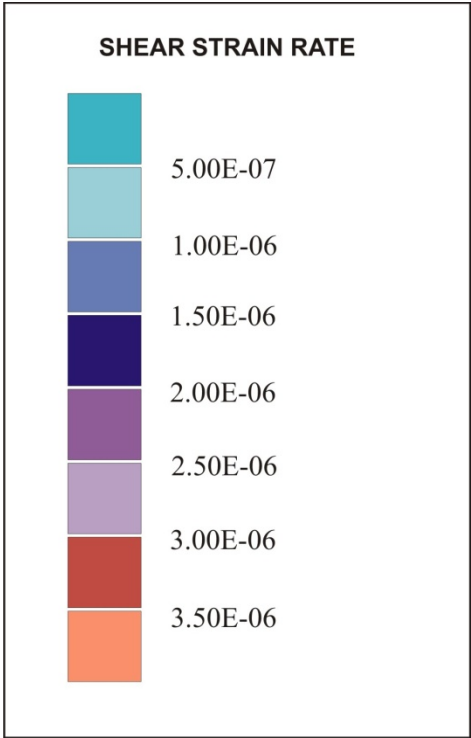
Key to figures Appendix 4

Appendix 5   Survey data

2001 (Apr)

Extract from survey report by 3DLaserMapping Ltd

Station	Easting	Northing	Height	
Sidestrand1	26976.43	39614.67	5.588	1.6
Sidestrand2	26973.35	39589.73	4.922	0.2
Happisburgh1	638696.5	330757.3	6.392	0
Happisburgh2	638376.4	331015.4	23.816	0
Weybourne1	611328.5	343672.1	5.127	1.4
Weybourrne2	611342.7	343656.7	20.301	0

GPS locations of survey points

2001 (Sep)

Survey Report by 3DLaserMapping Ltd (no GPS locations given)

The Coastal Survey for British Geological Survey during September 2001 included the following areas:-

Tues 4th Sept	Sidestrand, N. Norfolk		3.15pm	SD
Wed 5th Sept	Happisburgh, N. Norfolk		3.45pm	HB
Thurs 6th Sept	Weybourne, N. Norfolk	(return pm)	4.15pm	WB

Requirements

The required output was a Digital Terrain Model (DTM) of the coastal area which was obtained using the following hardware and software.

Hardware

(1)   Garmin handheld Single frequency receivers.
(2)   LPM 2K Long Range terrestrial LIDAR scanner.

Software

(1)   3DLM Scanner Software for data capture to a Psion.
(2)   3DLM orientation and conversion.
(3)   Microstation.
(4)   Gringo GPS

Method

The Garmin receivers were used to capture GPS rinex observation files for the base station and the rover beach stations generally setout as a base line.

The LPM 2K scanner was tripod mounted on the standard tribrach and set to scan a predetermined area at low tide in order to optimise the length of coastline coverage.

The Ordinance Survey internet data for the nearest O.S. Active stations were downloaded to obtain reference station 15second interval recordings.

In general, co-ordination of the DTM was obtained from post-processed GPS data rather than survey markers owing to the anticipated mass movement of beach material.

The local scan co-ordinates were transformed using the 3DLM software and loaded into Microstation Software for viewing, analysis and presentation.

The final scan data was output in the Eastings, Northings and Orthometric height format.

Results

In all of the areas mentioned above, complete observations obtained from the Garmin receivers and the LPM 2K. The results of the GPS post processed positioning and the scan data when compared with each other are within the tolerances accepted for the survey. Further scanning is included in the project for comparison.

Photos:

Miscellaneous (taken by BGS)

2002 (April)

Happisburgh

Tues. 9th April

Unable to scan from beach due to adverse tides/winds. Took photos from beach. No photogrammetry or targets used. Did one scan (S1) from cliff top adjacent to cottage garden wall. Considerable erosion noted at western end due to failure of corner of defence works since Sept 2001. (of the order of 5 m. at corner of plot). Probably also erosion progressing along scan area of cliff.

GPS data:

X	Y	Ellipsoid H	Incrementa	Object Cod	User-define	Object ID	Position Qt	Height Qua
638582.4	330892.7	55.21	1	station	s1	4	0.55	0.72
638582.5	330891.9	55.95	2	station	s1	5	0.4	0.51
638547.4	330902.9	55.81	3	target	gatepost	1	0.52	0.8
638792.7	330552	54.54	4	target	pillbox	2	0.57	0.81
638579.4	330850.5	55.15	5	target	gatepost 2	3	0.48	0.65

X,Y,Ellipsoid Height,Incremental ID,Object Code,User-defined Attributes,Object ID,Position Quality,Height Quality

Sidestrand

Wed. 10th April

Carried out 3 scans (S1, S2, S3) on beach. S1 & S2 covered former scan areas, S3 covered new debris flow on western edge of area. Location of S3 very close to S2 (moved due to incoming tide!). Time not available to scan opposite side of debris flow or source area of landslide. Photogrammetry (parallel overlapping images perpendicular to cliff line) carried out using D.T's own camera for eastern embayments with 12 large orange targets deployed on cliff. Panoramic sweeps using Rollei from S1 & S2. GPS used to locate scan locations (S) and photogrammetry camera (photo) & target locations (ta, tb etc).

Large debris flow noted at western edge of scan area. This extends over most of beach at low tide. It looks recent (last 2 months?) but locals say anything between 2 & 6 months old. Debris flow seems to involve mainly clays (including very light grey clay). Some evidence of uptilted beds at base of debris flow (further study of landslide required). Time was not available to investigate fully.

GPS data (Leica GS50):

X	Y	Ellipsoid Height	Incremental ID	Object Code	User-defined Attributes	Object ID	Position Quality	Height Quality
626924.58	339676.15	43.86	1 station		s1	1	0.6	0.91
626925.08	339675.98	44.17	2 station		s1	2	0.57	0.98
626995.11	339637.51	42.5	3 station		s1	33	0.56	0.79
626917.54	339668.37	45.99	4 station		s3	34	0.44	0.86
626925.93	339675.64	43.22	5 photo		photo 3\31	15	0.6	0.69
626931.72	339673.37	45.37	6 photo		photo 3\32	16	0.6	0.67
626940.11	339668.44	42.54	7 photo		photo 3\33	17	0.6	0.73
626945.86	339665.71	45.31	8 photo		photo 3\34	18	0.58	0.71
626954.1	339659.57	44.06	9 photo		photo 3\35	19	0.53	0.66
626960.83	339655.59	43.38	10 photo		photo 3\36	20	0.36	0.45
626968.55	339650.89	43.3	11 photo		photo 3\37	21	0.54	0.66
626975.67	339647.5	44.78	12 photo		photo 3\38	22	0.59	0.72
626982.89	339642.57	44.6	13 photo		photo 4\02	23	0.59	0.76
626990.26	339638.26	43.21	14 photo		photo 4\03	24	0.59	0.73
626996.3	339635.53	43.74	15 photo		photo 4\04	25	0.52	0.65
627003.21	339631.81	44	16 photo		photo 4\05	26	0.44	0.56
627010.47	339627.75	42.85	17 photo		photo 4\06	27	0.47	0.59
627017.39	339624.01	44.13	18 photo		photo 4\07	28	0.55	0.7
627024.72	339619.94	43.83	19 photo		photo 4\08	29	0.51	0.65
627031.81	339616.72	44.52	20 photo		photo 4\09	30	0.47	0.61
627039.04	339612.21	44.62	21 photo		photo 4\10	31	0.51	0.66
627045.95	339608.72	43.83	22 photo		photo 4\11	32	0.56	0.75
627011.98	339542.55	47.09	23 target		target ta	3	0.29	0.57
626998.2	339543.88	50.53	24 target		target tl	4	0.52	1.04
626989.75	339554.89	49.08	25 target		target tb	5	0.43	0.86
626956.32	339543.7	66.21	26 target		target tk	6	0.32	0.66
626946.27	339561.86	55.75	27 target		target tj	7	0.41	0.85
626924.78	339574.92	57.81	28 target		target th	8	0.35	0.75
626907.16	339533.08	74.26	29 target		target ti	9	0.24	0.52
626887.2	339564.23	73.47	30 target		target tg	10	0.4	0.81
626931.9	339611.65	50.49	31 target		target te	11	0.44	0.91
626888.64	339617.93	47.66	32 target		target tf	12	0.43	0.82
626953.34	339591.7	45.44	33 target		target td	13	0.47	0.87
626974.08	339570.73	46.6	34 target		target tc	14	0.44	0.86

X,Y,Ellipsoid Height,Incremental ID,Object Code,User-defined Attributes,Object ID,Position Quality,Height Quality

Travelled to Limekiln Farm, Gimingham to check OS passive GPS site no: B1TG2736. Discrepancy was typically 12 cm from published value with only 7 satellites available.

No survey was carried out at Weybourne

2002 (Sept)

Weybourne

The Weybourne site was visited on 26th September 2002. Two scans were taken from S1 and S2. The location for S2 is slightly further up the beach to the previous visit due to tides.

WeybSep02		X	Y
S1	-	611382	343678
S2	-	611349	343683
T1	Temporary ranging pole on cliff top	611366	343657

Minor sand runs. Not a lot of active slipping. Classic shingle storm beach.

BACKSIGHTS:

T1 taken from S1 and S2.

S1 taken from S2.

S2 taken from S1.

GPS SURVEY:

- Base of cliff – poor position quality for some sections so waited for it to recover before continuing.
- Top of cliff – offset 1m. Good position quality.

PHOTOS:

The Rollei stopped working so was not used on this site.

Using the Kodak camera the following photos were taken:

- DCP_1648 to DCP_1652: Panoramic from S1
- DCP_1663: laser from cliff
- View from top of cliff: DCP_1664 to DCP_1666
- Landslide taken from top of cliff: DCP_1668 to DCP_1670
- Cliff looking west towards landslide: DCP_1671
- Cliff looking south in front of landslide: DCP_1672
- Cliff looking southeast in front of landslide: DCP_1673
- Cliff looking east in front of landslide: DCP_1674 and DCP_1675
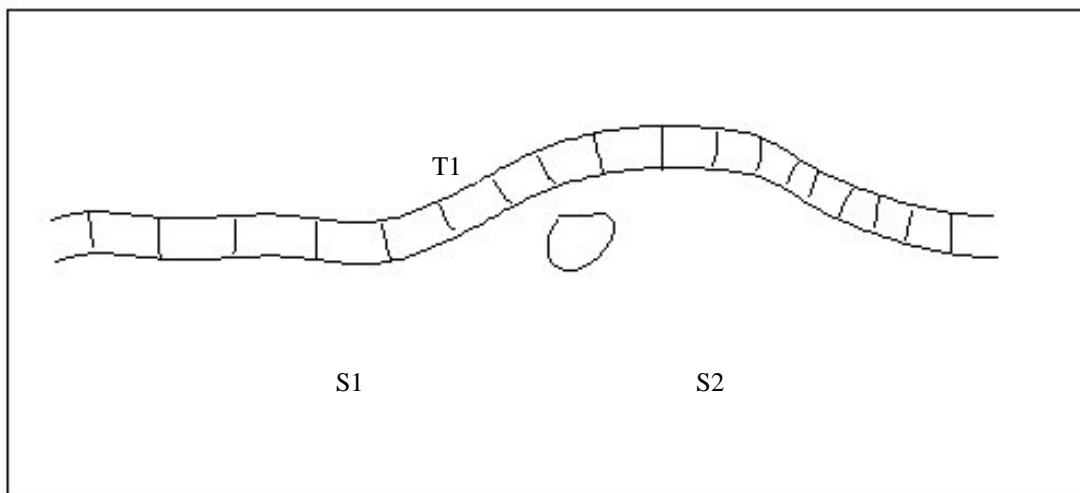
Sketch Map of Weybourne Site

Sidestrand

The Sidestrand site was visited on 25th September 2002. Three scans were taken from S1, S2 and S5.

SidesSep02			X	Y	Distance from S1	Distance from S5
S1		-	626996	339638	-	-
S2		-	626928	339673	76.834	166.842
S5		-	626785	339759	-	-
T1	Groyne to the west (inshore end post)		626153	340031	930.592	718.832
T2	Seaward end of groyne to the east of west bay		627883	339180	997.826	1241.858
B1	Old ball cock target (western)		-	-	154.214	203.100
B2	Old ball cock target (eastern)		-	-	111.788	312.068

PHOTOS:

Using the Kodak camera the following photos were taken:

- DCP_1677 to DCP_1682: Panoramic from S1
- DCP_1689 to DCP_1696: Panoramic from S5
- DCP_1683 to DCP_1687: Panoramic from S5
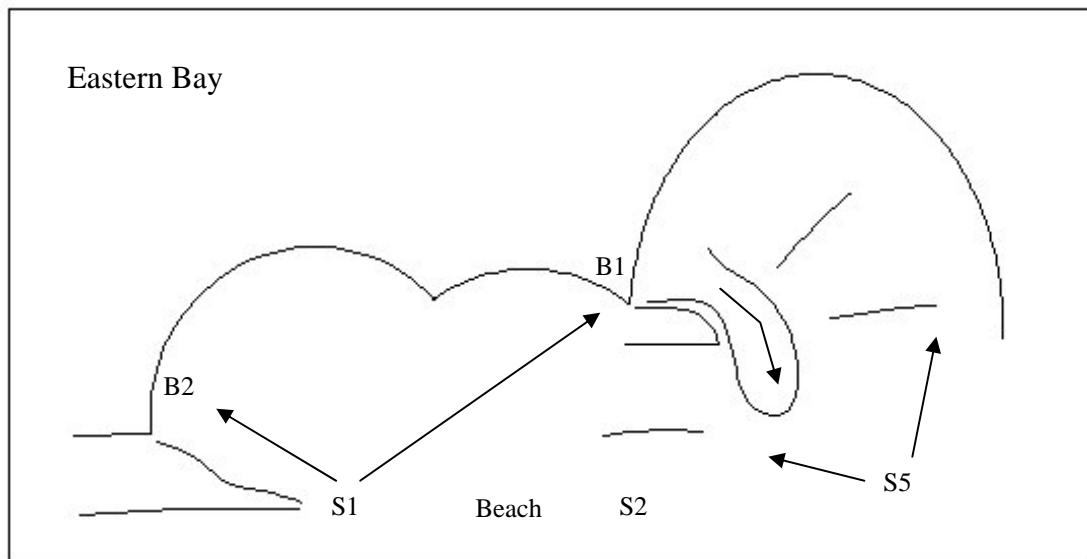
Sketch Map of Sidestrand Site

Happisburgh

The Happisburgh site was visited on 24th and 26th September 2002. Significant changes in the coastline were observed between these two dates (see photos) and active sliding was witnessed on 26th. Three scans were taken – S1, S2 and S3.

HappiSep02		X	Y
S1	-	638580	330894
S2	-	638671	330733
S3	-	638575	330899
T1	Fire Hydrant	638561	330897
T2	Lighthouse	-	-
T3	Corner of Pill Box	638793	330552
T4	House roof apex	-	-

Information from the public and other persons

The Coastal Protection Engineer for North Norfolk District Council, Brian Farrow, was out on site on the same day (24th) and he gave the following information:

- A 9.5m regression was recorded in one year.
- One hour prior to our visit, 2m of pathway had fallen as a small slip.
- If you draw a straight line from this area of unprotected coast in front of the pillar box to the area of unprotected coast in front of Happisburgh village, then the church will be lost if left undefended.
- North Norfolk District Council are trying to put forward a coastal protection scheme but it has received some objections so DEFRA are deciding what to do at the moment.

Lee Jones spoke to the people that run the teashop at the NE end of the series of houses. They said that the cliff regressed 4.5m in one event in August 2002.

Talking to walkers and residents:

- Four buildings and three caravans have been lost to the sea.
- The beach has dropped by several metres in living memory – the wooden sea defence originally stuck out of the beach by 1m, now ~6m.

Observations

There are some deteriorated sea defences (sheet pile and wooden wall) in front of the houses. The areas of more severe cliff erosion exactly matches the part of the sea defences that has been destroyed by the sea (see photos).

Several tension cracks were visible along the path near S1 and S3. These were slightly wider on 26th compared to 24th although these were not measured (see photos).

Steel rods are all over the beach. These rods are from cliff protection – backfill. Backfill is currently being carried out in the area in front of the houses (see photos).
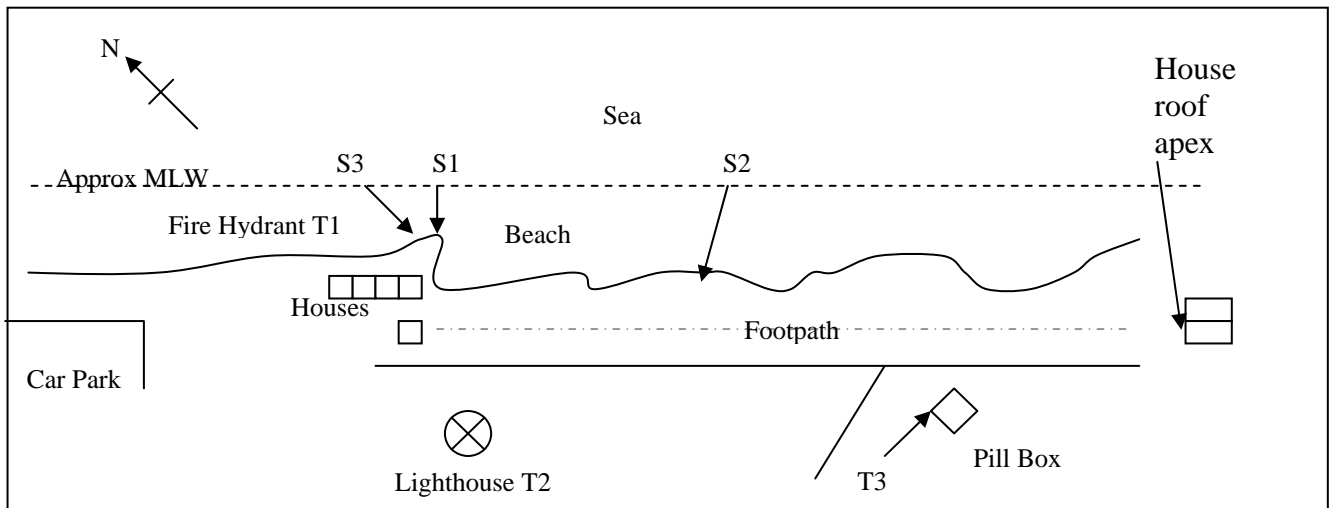
Sketch Map of Happisburgh Site

BACKSIGHTS:

Taken from S3:

T1, T2, T3, T4, S1 (ground, not target).

PHOTOS:

Rollei – photos taken at 15° increments from S2

Panorama – Nos 27, 28, 29 facing NW towards S1; No 30 facing SE towards T4.

Rollei – photos taken at 15° increments from S1

Panorama – Nos 31, 32, 33, 34, 35; Nos 36, 37 facing N.

2003

Weybourne

The Weybourne site was visited on 9th September 2003. Three scan locations were occupied: S1, S2, S3. Four scans were carried out. Low tide 13.38 hrs. Weather sunny, warm, light breeze. Targets corresponding to stratigraphic features in the cliff were backsighted (T1 – T4).

SCANS:

WB93		Inst.Ht.(m)	X	Y
S1	Cliff (E embayment)	1.134	611383.42	343679.14
S2a	Cliff (W embayment, W end)	1.324	611348.44	343681.05
S2b	Cliff (W embayment, E end)	1.324	611348.44	343681.05
S3	Cliff detail (W embayment)	1.235	611309.01	343686.93

From:	To:	Description:	Dist (m)
S1	S2	Scan location	35.154
S1	T1	Top of red sand (cliff)	24.466
S1	T2	Bottom of cobbles (cliff)	24.886
S1	T3	Top of cobbles (cliff)	33.278
S1	T4	Bottom of superficials (cliff)	39.414
S2	S1	Scan location	31.150
S3	S2	Scan location	40.000

GPS SURVEY:

The SR530 'base' station (X1) was set up on the beach near Weybourne (beach) car park on a tripod. The two SR530 units were used independently (without radio link) in this case. A total of > 4 hours base station logging was made. GS50 data were collected on the cliff top and cliff bottom. GS50 lock was difficult.

PHOTOS:

- Rollei panorama from S1 (pics 2 – 7)
- Rollei panorama from S3 (pics 9 – 11)
- Rollei detail of W embayment (pics15, 16, 17)
- Canon Film 1, photos1 – 11 (detail of chalk / cobble boundy.)

Note: Rollei pics not taken from tripod mount but adjacent & hand-held
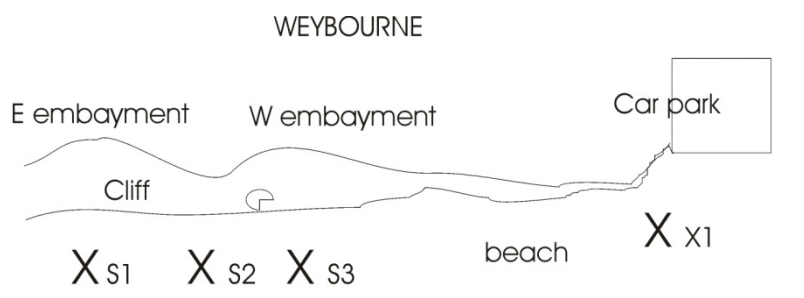
Happisburgh

The Happisburgh site was visited on 10th September 2003. Three scan locations were occupied. Four scans were carried out. Low tide: 14.24hrs. Weather: rain, wind. Stratigraphic cliff features were backsighted (T5 – T7). A joint frequency survey was done in the lower cliff (dark grey Till).

SCANS:

		Instr. Ht.	
HB93		**X**	**Y**
S4a	Cliff (NW section)	638692.57	330769.16
S4b	Cliff (Beach Road)	638692.07	330768.93
S5	Cliff (central section)	638729.27	330740.25
S6	Cliff (SE section)	638764.52	330711.51

From	To	Description	Dist (m)
S4	S5	Scan location	
S5	S4	Scan location	47.676
S4	T5	Stratigraphic feature (cliff)	
S4	T6	Stratigraphic feature (cliff)	
S4	T7	Stratigraphic feature (cliff)	
S6	S5	Scan location	
S6	T8	Post on cliff top	43.534
S6	T9	Top of Happisburgh church tower	908.870
S6	T10	Apex of roof (Green house, Cart Gap)	694.570

GPS SURVEY:

The SR530 'base' (X2) was set up on the vehicle roof (Ranger) using magnetic mount, in NW corner of Cart Gap car park.

The two SR530 units were used independently (without radio link) in this case. A total of >4 hours base station logging was made. GS50 data were collected on the cliff top and cliff bottom. GS50 lock was difficult. Due to fears of global GPS problems the GS50 was used to back up the SR530 for scan locations (S4, S5, S6).

PHOTOS:

- Rollei panorama from S4 (pics 17 – 24)
- Rollei panorama from S5 (pics 27 – 34)
- Rollei panorama from S6 (pics 35 - 38)

Canon Film 1, photos 15 – 18 (detail of typical failure mechanisms)

Note: Rollei pics not taken from tripod mount but adjacent & hand-held
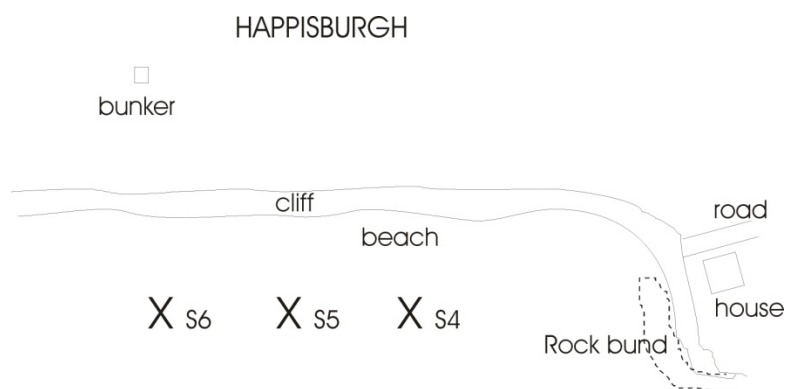
Sidestrand

The Sidestrand site was visited on 11th September 2003. Three scan locations were occupied (S7, S8, S9). Five scans were carried out. Low tide: 15.03 hrs. Weather: sunny, warm, light breeze.

SCANS:

		Instr Ht.	**X**	**Y**
S7	SE embayment		626988.24	339643.28
S8a	NW embayment (central)	1.290	626919.1921	339681.1501
S8b	Central promontory		626919.1921	339681.1501
S8c	NW embayment (NW)		626919.1921	339681.1501
S9	NW embayment (SE)		626845.54	339723.21

BACKSIGHTS:

From:	To:	Description	Dist (m)
S7	S8	Scan location	78.790
S7	T11	Small pinnacle, promontory	140.334
S8	S7	Scan location	78.776
S8	*TS1*	*Total station (instrument)*	47.276
S9	S8	Scan location	

GPS SURVEY:

- The SR530 'base' unit (X3) was located on roof of Ford Ranger using magnetic mount, parked on Clifton Way adjacent to bench for > 4 hours.
- The SR530 'rover' was positioned at scan locations S7, S8, but *not* S9 due to rapidly incoming tide (S9 was located with the GS50).

PHOTOS:

- Rollei panorama from S7 (pics 39– 42)
- Rollei detail of folded strata, dark grey Till, cliff toe (pics 43 - 50)
- Rollei panorama from S8 (pics 51 - 53)
- Rollei detail from S8 (pics 54 – 57)
- Rollei panorama from S9 (pics 58 - 61)
- Rollei details of foreshore (S. Pearson) (pics 62 – 69)
- Rollei cliff features off-site (pics 70 – 74)

Note: Rollei pics not taken from tripod mount but adjacent & hand-held
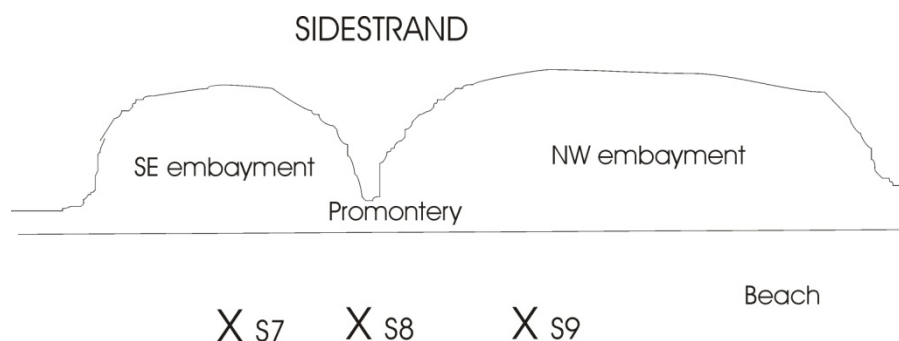
SIDESTRAND

2004

Sidestrand

The Sidestrand site was visited on 1st September, 2004. Three scan locations were occupied (S1, S2, S3) and three scans carried out.

Weather: Sunny, warm

Scanner: LPM2K.

Slope generally very wet and unpassable. Considerable seepage at lower clay/sand boundaries. Beach level is low revealing patches of chalk platform. NW Embayment has incipient rotational slump covering most of it (1-2 m backscarp). Stability of tripods at s1 and s2 were poor.

SCANS:

Norfolk08 04	Scan No.		Instr Ht. (m)	X	Y
S1	001	SE Embayment	1.100	626993.95	339616.06
S2	001	Central Embayment	1.119	626928.02	339651.19
S3	001	NW Embayment	1.127	626824.04	339692.22

BACKSIGHTS (TPLSOCS):

From:	To:	Description	Dist (m)
S1	S2	Scan location, target	
S2	S1	Scan location target	
S3	S2	Scan location target	

GPS SURVEY:

- The SR530 'base' unit was located on tripod adjacent to Ford Ranger on road (asphalt) at Clifton Way adjacent to bench for > 4 hours.
- The SR530 'rover' was positioned at scan locations s1, s2, & s3.
- The two SR530 units were used in RTK mode throughout using radio link between them.

PHOTOS:

- Olympus panorama from s1, s2, & s3 (hand-held)
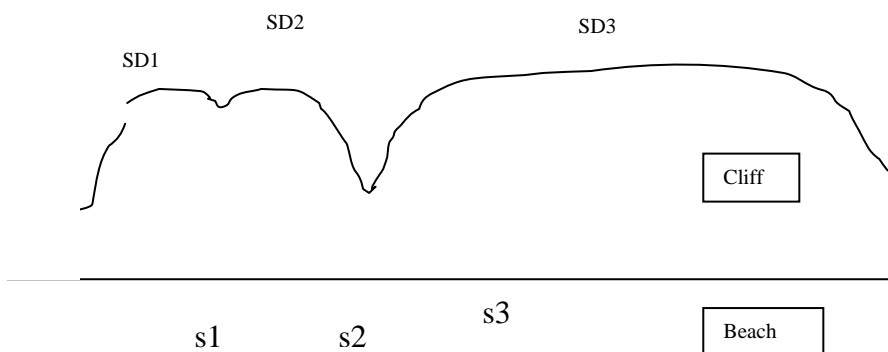
Plan of Sidestrand test site showing scan locations (s1, s2, s3) and major embayments (SD1, SD2, SD3).

Happisburgh

The Happisburgh site was visited on 2nd September 2004. Three scan locations were occupied: s1, s2, s3. Five scans were carried out (three at S1).

<u>Weather:</u> Sunny/cloudy, warm

<u>Scanner:</u> LPM2K.

A deep transverse gully was found in sands at the south end of the site. This may have been prepared by man (access to beach for defence works?). This provides a ramp for access, though it is suffering from surface runoff erosion. Run-off erosion runnels at cliff-top extending several meres below cliff-top. Extensive loss of sand from upper cliff resulting in a wide till platform in lower cliff. Minor sand run (central cliff).

SCANS:

	Scan No.			Instr Ht. (m)	X	Y
S1	001		North cliff (southern end)	1.105	638656.03	330773.08
	002		North cliff (centre)		-	-
	003		North cliff (northern end incl Beach Rd.)		-	-
S2	001		Central cliff	1.162	638696.37	330741.45
S3	001		South cliff	1.111	638738.73	330708.56

BACKSIGHTS (TPLSOCS):

From	To	Description	Dist (m)#
S1	S2	Scan location	
S2	S1	Scan location	
S2	S3	Scan location	
S3	S2	Scan location	53.618
S3	T1	Church (tower)	887.386
S3	T2	Green house (gable end)	712.636

GPS SURVEY:

The SR530 'base' (X1) was set up on the vehicle (Happisburgh car park).

The two SR530 units were used in RTK mode throughout using radio link between them. A total of >4 hours base station logging was made. A cliff-top traverse was carried out using the roving GS50.

PHOTOS:

Olympus panoramas (hand-held) from scan locations.
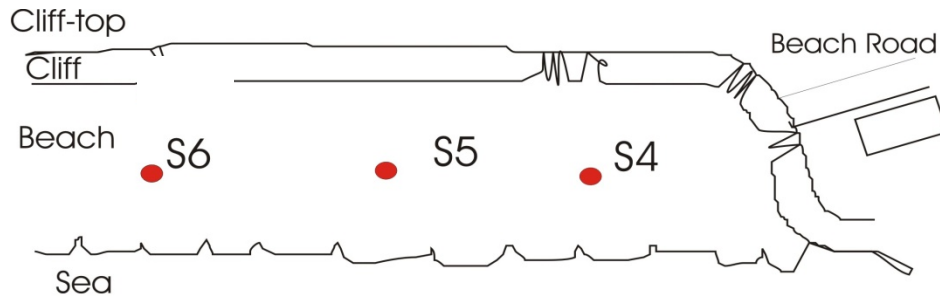
Laser scan locations at Happisburgh

Weybourne

The site was visited on 30th August 2004.

Weather: Cool, breezy

Scanner: LPM2K.

SCANS:

Scan No. *Norfolk 0904*			Instr Ht. (m)	X	Y
S1	001	East cliff (southern end)	1.077	611381.96	343678.78
S2	001	West cliff	1.041	611349.06	343683.98
S3	001	West cliff (detail)	0.997	611320.31	343684.65

BACKSIGHTS (TPLSOCS):

From	To	Description	Dist (m)
S1	S2	Scan location	33.294
S2	S1	Scan location	33.3
S3	S2	Scan location	28.716

GPS SURVEY:

The SR530 'base' (X1) was set up on the vehicle (Weybourne car park).

The two SR530 units were used in RTK mode throughout using radio link between them. A total of >4 hours base station logging was made. A cliff-top and a cliff toe traverse were carried out using the roving GS50.

2005

Sidestrand

The Sidestrand site was visited on 3rd October, 2005. Three scan locations were occupied (S1, S2, S3). Six scans were carried out of the test site slope from the beach using a 3-point baseline.

Low tide: 14.13 hrs (0.80 m).

Weather: sunny, warm, no wind.

The LPMi800HA scanner was used for the first time at Sidestrand.

Large-scale, deep-seated landsliding has occurred over a 300-400 m front to the west of the test site.

151

SCANS:

Norfolk10 05	Scan No.		Instr Ht. (m)	X	Y
S1	002	Embayments SD1 & SD2	??	626995.91	339640.54
	003	Embayments SD1 & SD2	-	-	-
	004	Embayment SD1	-	--	
S2	001	Embayments SD3 (west end)	2.060	626917.55	339682.77
	002	Embayments SD3 (east end) & SD2 (west end)	-	-	
S3	001	Embayment SD3 (centre)	1.198	626784.06	339723.76

BACKSIGHTS:

From:	To:	Description	Dist (m)
S1	S2	Scan location (not target)	88.991
S2	S1	Scan location (not target)	89.009
S3	S2	Scan location (target)	139.618

GPS SURVEY:

- The SR530 'base' unit was located on roof of Ford Ranger using magnetic mount, parked on Clifton Way adjacent to bench for > 4 hours.
- The SR530 'rover' was positioned at scan locations s1, s2, & s3.

PHOTOS:

- Olympus panorama from s1, s2, & s3 (hand-held)
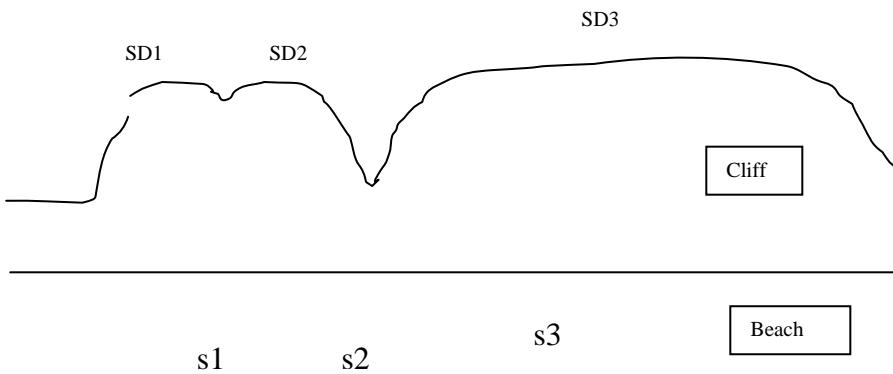
Plan of Sidestrand test site showing scan locations (s1, s2, s3) and major embayments (SD1, SD2, SD3)

Happisburgh

The Happisburgh site was visited on 4th October 2005. Four scan locations were occupied: s4, s5, s6, and s7. Eleven scans were carried out.

Low tide: 14.44hrs (0.72m).

<u>Weather:</u> Warm, sunny, little wind.

The LPMi800HA scanner was used for the first time at Happisburgh.

Deep gullies within the sand have further developed from 2004. These appear to be groundwater/surface runoff derived. The largest of these was scanned from s7. The lower till has further lagged behind the overlying sand in terms of recession, leaving low 'outliers' of till above beach level on the platform. Beach level appears to be high this year.

SCANS:

Norfolk 1005	Scan No.		Instr Ht. (m)	X	Y
S4	001	Cliff (northern end) incl. Beach Road	1.197	638615.72	330803.78
	002	Cliff (northern end) incl. Beach Road	-	-	
	003	Cliff (northern end) incl. Beach Road	-	-	
S5	001	Cliff (central)	1.25	638682.94	330742.94
	002	Cliff (central)	-	-	
	003	Cliff (central)	-	-	
	004	Cliff (central)	-	-	
S6	001	Cliff (southern end)	1.208	638780.66	330677.20
	002	Cliff (southern end)	-	-	
S7	001	Gully	1.108	638755.08	330636.23
	002	Rear of till platform	-	-	
			-	-	

BACKSIGHTS:

From	To	Description	Dist (m)
S4	S5	Scan location	303.782
S5	S4	Scan location	90.496
S5	S6	Scan location	117.663
S6	S5	Scan location	117.748
S6	T1	Lighthouse top	369.361
S6	T2	Church tower apex (top)	342.655
S7	S8*	Tripod-mounted target	48.295

* located close to s6

The SR530 'base' was set up on the vehicle roof (Ranger) using magnetic mount, in Happisburgh car park.

The two SR530 units were used independently (without radio link) in this case. A total of >4 hours base station logging was made. GS50 lock was found to be difficult and a cliff-top survey was not carried out.

PHOTOS:

Olympus panoramas (hand-held) from scan locations
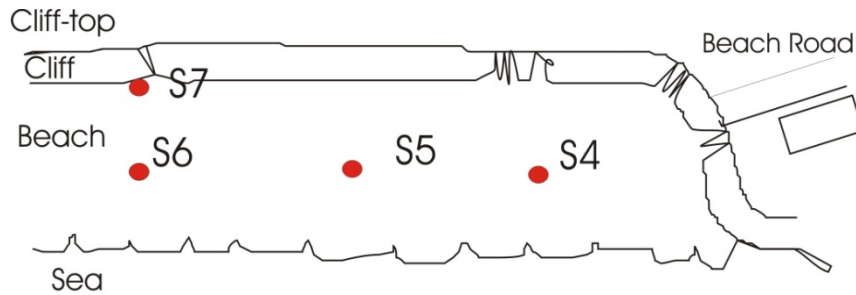
Laser scan locations at Happisburgh (Oct 2005)

2006

Sidestrand

The Sidestrand site was visited on 5th October, 2006. Three scan locations were occupied (S1, S2, S3). Six scans were carried out of the test site cliff from the beach using a 3-point baseline.

Low tide: 12.31 hrs (0.77 m).

Weather: dull, cool, light wind, rain.

The LPMi800HA scanner was used with Crain fibreglass tripod.

Extensive landsliding has taken place within the last 2 weeks, evidence of which was witnessed by Pete Hobbs, Dave Entwisle, & Tony Milodowski during a 'Tills' sampling trip at 09.30 on Thursday 28th Sept 2006. This had followed heavy & sustained rainfall on Mon 25th Sept 2006. Examples of topples, mudslides and rotational slumping had been observed through binoculars from the rock armour at Overstrand over a 15 minute period at a distance of approximately 1.5 km. Access was not possible due to high tide and no photos were taken.

A large, landslide was observed immediately to the SE of SD1 embayment (i.e. outside test site). The very large 'linear' rotational landslide initiated in 2005 at 200-400 m to the NW of the test site had developed further but without having broken up significantly. Embayment SD2 has been affected by a large landslide in the SE corner resulting in a dominantly grey earth flow(?) extending to the beach. Embayment SD1 remains largely unchanged since 2005 except for a recent fall/slide of the lower part of the promontory between SD1 & SD2. The promontory between SD2 & SD3 has been largely removed by a recent landslide.

The sand beach was particularly wet in front of the active landslides at embayment SD2 & SD3 due to ground water seepage. This adversely affected tripod stability at s3 which lost level during the scans.

Tiepointscans were used for the first time at Sidestrand. With this method, instead of the operator sighting the telescope cross-hairs manually on the yellow target board, a small scan is set up to include a special cylindrical reflective target. The laser then determines the centre point of the target automatically. This target is less susceptible to overturning by high winds. However, ***Note** that incorrect range is produced by tiepointscan due to the reflective surface of the target not coinciding with its axis, as is the case with the yellow target board. Radius of cylinder has been added to tiepointscan 'range' reading in the table.*

Scan *Norfolk10* No. 06			Instr Ht. (m)	X	Y
S1	001	aborted	1.155	626992.57	339628.31
	002	Embayments SD1 & SD2		-	-
	003	Recent landslide to SE of test site & beyond		-	-
S2	001	Embayments SD3 (east end) & part of SD2 (west end)	1.098	626917.92	339681.51
	002	Part of embayment SD2 (east end)		-	-
S3	001	Embayment SD3	1.045	626777.24	339720.97
	002	Embayment SD2		-	-

BACKSIGHTS (TPLSOCS):

From:	To:	Description	Dist (m)#
S1	S2	Scan location (tiepointscan)	91.677
S2	S1	Scan location (tiepointscan)	91.675
S3	S2	Scan location (tiepointscan)	146.093

50 MM ADDED TO ALLOW FOR TARGET (CYLINDER) RADIUS

GPS SURVEY:

- The SR530 'base' unit was located on tripod adjacent to Ford Ranger on road (asphalt) at Clifton Way adjacent to bench for > 4 hours.
- The SR530 'rover' was positioned at scan locations s1, s2, & s3.
- The two SR530 units were used in RTK mode throughout using radio link between them.

PHOTOS:

- Olympus panorama from s1, s2, & s3 (hand-held)
- Video of test site
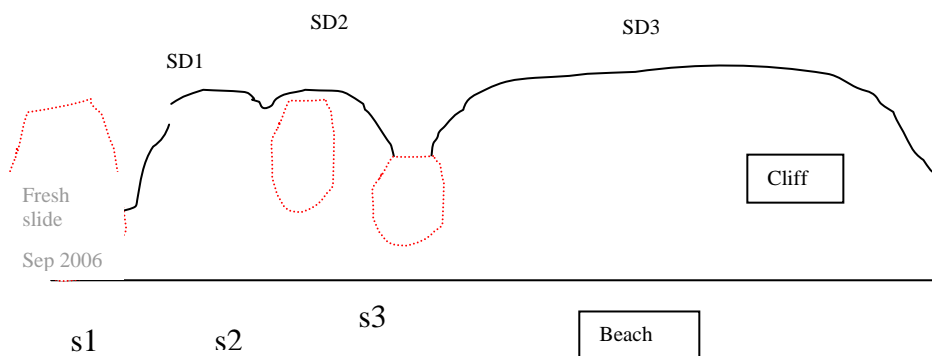
Plan of Sidestrand test site showing scan locations (s1, s2, s3) and major embayments (SD1, SD2, SD3). Recent landslides shown in red.

Happisburgh

The Happisburgh site was visited on 6th October 2006. Three scan locations were occupied: s1, s2, s3. Seven scans were carried out.

Low tide: 13.22hrs (0.46m).

Weather: Cool, dull, light wind, rain.

The LPMi800HA scanner was used mounted on the Crain fibreglass tripod.

Gullies within the sand have continued to develop. These appear to be groundwater/surface runoff derived. The lower till has further lagged behind the overlying sand in terms of recession, producing an unusual abutment shown in scan s2. Several small recent landslides have occurred with debris still in place on the beach. Beach level appears to be high this year with a slight crest at mid-beach. Cromer Forest Bed still exposed at low tide.

Note:

Site was also visited by UK Rocks & Soils project ('Tills' sub-project) on 27th Sept 2006 by P. Hobbs, D. Entwisle, & A. Milodowski. Geotechnical and mineralogical samples of Happisburgh Till Member and Ostend Clay Member were taken including block sample. Panda penetrometer and resistivity probe tests were also carried out.

SCANS:

Norfolk 1006	Scan No.		Instr Ht. (m)	X	Y
S1	001	North cliff (northern end) incl. Beach Road + promontory	1.138	638621.44	330778.02
	002	North cliff (northern end)		-	-
	003	North cliff (centre)		-	-
	004	North cliff (southern end)		-	-
S2	001	Central cliff	1.109	638659.62	330743.18
S3	001	South cliff (northern end)	1.058	638720.67	330692.37
	002	South cliff (southern end)		-	-

BACKSIGHTS (TPLSOCS):

From	To	Description	Dist (m)#
S1	S2	Scan location (tiepointscan)	51.689
S2	S1	Scan location (tiepointscan)	51.692
S3	S2	Scan location (tiepointscan)	79.418

 # 50 MM ADDED TO ALLOW FOR TARGET (CYLINDER) RADIUS

GPS SURVEY:

The SR530 'base' was set up on the cliff top (central cliff).

The two SR530 units were used in RTK mode throughout using radio link between them. A total of >4 hours base station logging was made. Two cliff-top traverses were carried out using the roving SR530.

Olympus panoramas (hand-held) from scan locations.
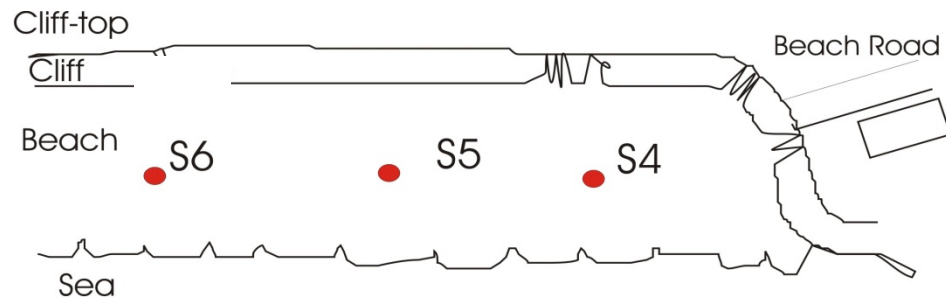
Laser scan locations at Happisburgh

9 Glossary

Argillaceous	Containing clay. Typically applied to fine-grained sedimentary rocks composed of clay and silt-sized particles.
Atterberg Limits	Consistency criteria for defining key water contents of a clay soil. They are: liquid limit, plastic limit and shrinkage limit.
Backshore	The upper part of the active beach above high water and extending to the toe of the beach head, affected by storm waves especially during high tides.
Beach Head	The cliff, dune or seawall forming the landward limit of the active beach.
Bedding	The arrangement of sedimentary rocks in beds or layers of varying thickness or character.
Bedrock.	Unweathered rock beneath a cover of soil or superficial deposits.
Berm	A horizontal ledge in an embankment or cutting to ensure the stability of a steep slope.
Bund	An embanked waterfront or quay
Calcareous	Carbonate-rich.
Calcite.	The crystalline form of calcium carbonate, $CaCO_3$.
Clay	A naturally occurring material which is a plastic material at natural water content and hardens when dried to form a brittle material. It is the only type of soil/rock susceptible to significant shrinkage and swelling. It is made up mainly, but not exclusively, of clay minerals. It is defined by its particle-size range (< 0.002 mm). Clay does not have to be the dominant component of a soil in order to impart clay-like properties to it.
Clay Minerals	A group of minerals with a layer lattice structure which occur as minute platy or fibrous crystals. These tend to have a very large surface area compared with other minerals, thus giving clays their plastic nature and the ability to support large suction forces. They have the ability to take up and retain water and to undergo base exchange.
Cohesion	Attractive force between soil particles (clay) involving a complex association of solid and water. Specifically, the shear strength of a soil at zero normal stress.
Cohesive Soil.	A soil in which particles adhere after wetting and subsequent drying and significant force is required to crumble the soil.
Consolidation.	The process in which pore water drains from a material under an applied load with a consequent reduction in volume of the material (see subsidence).
Density	The mass of a unit volume of a material. Often used (incorrectly) as synonym for Unit weight. Usually qualified by condition of sample (e.g. saturated, dry).
dGPS	Differential Geographical Positioning System
Diamict / Diamicton	Sediment (usually glacial) containing wide range of particle types and sizes.
Discontinuity	Any break in the continuum of a rock mass (e.g. faults, joints).
Drift	Archaic synonym for 'superficial' geological deposits; i.e. those overlying bedrock.

Effective Stress	The total stress minus pore pressure. The stress transferred across the solid matter within a rock or soil.
Exposure	A visible part of an outcrop that is unobscured by soil or other materials.
Faults	Planes in the rock mass on which adjacent blocks of rock have moved relative to each other. The relative vertical displacement is termed 'throw'. The faults may be discrete single planes but commonly consist of zones, perhaps up to several tens of metres wide, containing several fractures which have each accommodated some of the total movement. The portrayal of such faults as a single line on the geological map is therefore a generalization.
Ferruginous.	Iron-rich. Applied to rocks or soils having a detectable iron content.
Fissility	The ability of a rock (e.g. Mudstone) to be broken along closely spaced parallel planes (e.g. Shale).
FLAC	'Fast Lagrangian Analysis of Continua'. Brand name for finite element software suite produced by Itasca Corp.
Foreshore.	he intertidal area of the shore below highest tide level and above lowest tide level.
Fluvial/Fluviatile	Of, or pertaining to, rivers.
Formation	The basic unit of subdivision of geological strata, and comprises strata with common, distinctive, mappable geological characteristics.
Glacial	Of, or relating to, the presence of ice or glaciers; formed as a result of glaciation.
GPS	Global Positioning System. A system which uses satellite network to locate operator's xyz position on earth's surface. See also **dGPS**.
Grading	A synonym (engineering) for particle-size analysis (see also Sorting).
Groundwater	Water contained in saturated soil or rock below the water-table.
Group	A stratigraphical unit usually comprising one or more formations with similar or linking characteristics.
Gypsum	Mineral consisting of hydrous calcium sulphate ($CaSO_4.2H_2O$), common in weathered mudstone where it is formed by the breakdown of sulphide minerals in the presence of lime-rich groundwater.
Head	A deposit comprising material derived, transported and deposited by solifluction in periglacial regions. May include material derived also by hillwash, creep and other non-glacial slope processes. Composition is very variable and dependent on source material. Thickness is also very variable.
Holocene	The most recent subdivision of geologic time (RECENT) which represents the last 10,000 years.
Index Tests	Simple geotechnical laboratory tests which characterise the properties of soil (usually) in a remoulded, homogeneous form, as distinct from 'mechanical properties' which are specific to the conditions applied.
Ironpan	Hard layer formed by re-precipitation of iron compounds leached from overlying deposits.
Joint	A surface of fracture or parting in a rock, without displacement; commonly planar and part of a set.

Landslide	A down slope displacement of bedrock or superficial deposits subject to gravity, over one or more shear failure surfaces. Landslides have many types and scales. Landslides may be considered both as 'events' and as geological deposits. Synonym of 'landslip'.
Laser Scanner	A high-precision survey instrument, incorporating a laser rangefinder, for measuring distance and orientation of remote objects. The results are used to produce accurate 3-D terrain models. Varieties of laser-scanner are mounted in aircraft, road vehicles, or on conventional surveyor's tripods.
LiDAR	Light Detection And Ranging. A terrestrial or aerial based system using laser scanning to produce surface model of ground.
Lignite	Soft, brown-black earthy type of coal.
Lithology	The characteristics of a rock such as colour, grain size and mineralogy. The material constituting a rock.
Lithostratigraphic Unit	A rock unit defined in terms of lithology and not fossil content (Biostratigraphic unit).
Liquid Limit	The moisture content at the point between the liquid and the plastic state of a clay. An Atterberg limit.
Littoral	Of or pertaining to the shore, especially the sea.
Marl	A calcareous mudstone, sensu-strictu having >30% carbonate content.
Massive	Applied to a rock mass containing no visible internal structure.
Mean Low Water	The average height of all low waters measured over a time period.
Median	The 50th percentile of a distribution; that is, the value above and below which 50 % of the distribution lies.
Member	A distinctive, defined unit of strata within a formation characterised by relatively few and distinctive rock types and associations (for example, sandstones, marls, coal seams).
Micaceous	Containing mica, a sheet silica mineral.
Mineral	A naturally occurring chemical compound (or element) with a crystalline structure and a composition which may be defined as a single ratio of elements or a ratio which varies within defined end members.
Moisture Content	See **Water content**.
Morphology	River/estuary/lake/seabed form and its change with time.
mRAD	Milliradians. A measure of angle (one radian = 57.29 degrees)
Mudrock	A term used by engineers, synonymous with mudstone.
Mudstone	A fine-grained, non-fissile, sedimentary rock composed of predominately clay and silt-sized particles.
Natural Water Content	The water content of a geological or engineering material in its natural or 'as found' state.
Oriented	Referring to the process of transforming a point cloud (qv.) or surface model (qv.) to an established co-ordinate system.
Outcrop	The area over which a particular rock unit occurs at the surface.
Over-Consolidated (OC)	Deposit such as clay, which in previous geological times was loaded more heavily than now and consequently has a tendency to expand if it has access to water and is subject to progressive shear failure. The moisture content is less than that for an equivalent material which has been normally consolidated.
Panda	A brand of portable, hand-operated ultra-lightweight cone penetrometer manufactured by Sol Solutions.

Palisade	Coastal protective structure remote from the cliff (usually wood).
Particle-Size Analysis (PSA)	The measurement of the range of sizes of particles in a dis-aggregated soil sample. The tests follow standard procedures with sieves being used for coarser sizes and various sedimentation, laser or X-ray methods for the finer sizes usually contained within a suspension.
Particle-Size Distribution (PSD)	The result of a particle-size analysis. It is shown as a 'grading' curve, usually in terms of % by weight passing particular sizes. The terms 'clay', 'silt', 'sand' and 'gravel' are defined by their particle sizes.
Perched Ground Water	Unconfined groundwater separated from an underlying main body of groundwater by an unsaturated zone.
Periglacial	An environment beyond the periphery of an ice sheet influenced by severe cold, where permafrost and freeze-thaw conditions are widespread. Fossil periglacial features may persist to the present day or may have been removed by subsequent glaciation or erosion.
Permeability	The property or capacity of a rock, sediment or soil for transmitting a fluid; frequently used as a synonym for 'hydraulic conductivity' (engineering). The property may be measured in the field or in the laboratory using various direct or indirect methods.
Permafrost	Permanently frozen ground, may be continuous (never thaws), discontinuous (with unfrozen patches, especially in summer) or sporadic (unfrozen areas exceed frozen areas). The surface layer subject to seasonal thaw is the 'active layer'.
pH	Measure of acidity/alkalinity on a scale of 1 to 14 (<7 is acid, >7 is alkaline).
Plasticity Index	The difference between the liquid and plastic limits. It shows the range of water contents for which the clay can be said to behave plastically. It is often used as a guide to swell/shrink behaviour, compressibility, strength and other geotechnical properties.
Plastic Limit	The water content at the lower limit of the plastic state of a clay. It is the minimum water content at which a soil can be rolled into a thread 3mm in diameter without crumbling. The plastic limit is an Atterberg limit.
Pleistocene	The first epoch of the Quaternary Period prior to the Holocene from about 2 million years to 10.000 years ago.
Point Cloud	The raw data produced by laser scanning. Each point has a discrete xyz location which is initially related to the co-ordinate system of the scanner.
Pyrite	The most widespread sulphide mineral, FeS_2 (iron pyrites).
Shear Box	A laboratory apparatus for measuring the shear strength (qv.) of a rectangular shaped soil sample
Quartz	The most common silica mineral (SiO_2) on Earth.
Quaternary	A sub-era that covers the time from the end of the Tertiary to the present, approximately the last 2.0 Ma, and includes the Pleistocene and Holocene.
Residual Shear Strength	The strength along a shear surface which has previously failed or has undergone significant displacement. Generally the minimum shear strength. Tends to be constant for a given soil.

Revetement	Coastal protective structure covering the cliff base (usually stone or concrete).
Rockhead	The upper surface of bedrock at surface (or its position) or below a cover of superficial deposits.
Running Sand	Fluidisation of sand and flow into an excavation below the water table or into a perched water table, under the influence of water flow into an excavation.
Sand	A soil with a particle-size range 0.06 to 2.0 mm. Commonly consists of quartz particles in a loose state.
Sandstone	Sandstones are clastic rocks of mainly sand-sized particles (0.06 - 2.0mm diameter), generally with quartz being the dominant component. Sandstones exhibit some form of cementation.
Saturation	The extent to which the pores within a soil or rock are filled with water (or other liquid).
Sedimentary Rocks	Rocks which formed from sediments deposited under the action of gravity through a fluid medium and were subsequently lithified. Commonly: mudstone, siltstone, sandstone and conglomerate.
Sediment Budget	The balance between sediment added to and removed from the coastal system. To calculate the sediment budget for a coastal segment, one must identify all the sediment sources and sinks, and estimate how much sediment is being added to or taken from the system.
Shale	A fissile mudstone.
Shear Planes/Surfaces	A series of closely spaced, parallel surfaces along which differential movement has taken place. Usually associated with landslides or stress-relief. May be polished/striated (slickensides).
Shear Strength	The maximum stress that a soil or rock can withstand before failing catastrophically or being subject to large unrecoverable deformations.
Shore Platform	A surface of erosion that slopes gently seaward from the beach head.
Siderite	Carbonate mineral of iron ($FeCO_3$).
Silt	A soil with a particle-size range 0.002 to 0.06 mm (between clay and sand).
Siltstone	A sedimentary rock intermediate in grain size between sandstone and mudstone.
Slickensides	See shear planes.
Solid	A term used in geology to indicate mappable bedrock (see also Superficial).
Solifluction	The slow, viscous, down slope flow of waterlogged surface material, especially over frozen ground.
Sorting	A descriptive term to express the range and distribution of particle sizes in a sediment or sedimentary rock, which has implications regarding the environment of deposition. Well-sorted (=poorly graded of engineering geology terminology) indicates a small range of particle sizes, poorly sorted (=well-graded) indicates a larger range.
Standard Penetration Test (SPT)	A long-established in-situ test for soil where the number of blows (N) with a standard weight falling through a standard distance to drive a standard cone or sample tube a set distance is

	counted. Used as an indication of lithology and bearing capacity of a soil.
Stiffness	The ability of a material to resist deformation.
Strain	A measure of deformation resulting from application of stress.
Stratigraphy	The study of the sequence of deposition of rock units through time and space.
Stress	The force per unit area to which it is applied. Frequently used as synonym for pressure.
Subcrop	The area over which a particular rock unit or deposit occurs immediately beneath another deposit, e.g. the Solid unit lying below Superficial Deposits (i.e. at rockhead).
Superficial Deposits	A general term for usually unlithified deposits of Quaternary age overlying bedrock; formerly called 'drift'.
Till	An unsorted mixture which may contain any combination of clay, sand, silt, gravel, cobbles and boulders (diamict) deposited by glacial action without subsequent reworking by meltwater.
Triaxial Test	A laboratory test designed to measure the stress required to deform a sample until it fails, or until a constant rate of deformation is obtained.
Undrained	Condition applied to strength tests where pore fluid is prevented from escaping under an applied load. This does not enable an effective stress condition to develop.
Uniaxial Compressive Strength (UCS)	The strength of a rock sample (usually a cylinder) subjected to an axial stress causing failure (usually in an undrained condition) in the laboratory.
Unit Weight	The weight of a unit volume of a material. Often used (incorrectly) as synonym for Density. Usually qualified by condition of sample (e.g. saturated, dry)
Water Content	In a geotechnical context: the mass of water in a soil/rock as a % of the dry mass (usually dried at 105°C). Synonymous with moisture content.
Water Table	The level in the rocks at which the pore water pressure is at atmospheric, and below which all voids are water filled; it generally follows the surface topography, but with less relief, and meets the ground surface at lakes and most rivers. Water can occur above a water table.
Weathering	The physical and chemical processes leading to the breakdown of rock materials (e.g. due to water, wind, temperature).

10 References

Most of the references listed below are held in the Library of the British Geological Survey at Keyworth, Nottingham. Copies of the references may be purchased from the Library subject to the current copyright legislation.

Amor, S.J., Burtwell, M.H., and Turner, A.S., 1999, Panda dynamic cone penetrometer assessment, Transport Research Laboratory,

Anglian Water, 1988, Anglian Coastal Management Atlas, 42 figures, Anglian Water and Sir William Halcrow & Partners,

Arthurton RS, Booth SJ, Morigi AN, Abbott MAW, Wood CJ. 1994. Geology of the Country around Great Yarmouth, Sheet Memoir 162. British Geological Survey. HMSO: London

Babtie & Birkbeck College, 1996, Spits and nesses: basic processes and effects on long-term coastal morphodynamics, University of London, Report CSA 3052.

Banham, P.H., 1968, A preliminary note on the Pleistocene stratigraphy of northeast Norfolk: Proceedings of the Geological Association, v. 79 507-512.

—, 1988, Polyphase glaciotectonic deformation in the contorted drift of Norfolk, *in* Croot, D.G., ed., Glaciotectonics; Forms and Processes: Rotterdam, Balkema, p. 27-32.

Banham, P.H., and Ranson, C.E., 1965, Structural study of the Contorted Drift and disturbed Chalk at Weybourne, North Norfolk: Geological Magazine, v. 102 (2), p. 165-174.

Bell, F.G., 2002, The geotechnical properties of some till deposits occurring along the coastal areas of eastern England: Engineering Geology, v. 63 49-68.

Bell, F.G., and Forster, A., 1991, The geotechnical characteristics of the Till deposits of Holderness. In:. (eds.). pp . . *in* Forster, A., Culshaw, M.G., Cripps, J.C., Little, J.A., and Moon, C.F., eds., Quaternary Engineering Geology, Engineering Geology Special Publications, Volume 7: London, Geological Society, p. 111-118.

Bowen, D.Q., 1999, A revised correlation of Quaternary deposits in the British Isles. Special Report of the Geological Society. , The Geological Society of London.

British Oceanographic Data Centre, 2008, Cromer Wave Data Series, http://www.bodc.ac.uk/data/online_request/waves/ [Accessed 1st February 2008], Updated monthly.

Brown, S., and Barton, M.E., 2007, Downdrift erosion and the frequency of coastal landsliding, *in* McInnes, R.G., Jakeways, J., Fairbank, H., and Mathie, E., eds., Landslides and Climate Change - Challenges and Solutions: Ventnor, Isle of Wight, UK, Taylor & Francis Group, p. 429-433.

Brown, S., Barton, M.E., and Nicholls, R.J., 2007, Down-drift erosion and management of our future coastline - lessons from the past: Poster.

Buckley, S.J., Howell, J.A., Enge, H.D., and Kurz, T.H., 2008, Terrestrial Laser scanning in geology: data acquisition, processing and accuracy considerations: Journal of the Geological Society of London, v. 165 625-638.

Butcher, A.P., McElmeel, K., and Powell, J.J.M., 1997, Dynamic probing and its use in clay soils, *in* C, C., ed., Advances in site investigation practice., Thomas Telford.

Cambers, G., 1976, Temporal scales in coastal erosion systems: Transcripts of the Institute of British Geographers, v. 1 246 - 256.

Cameron, T.D.J., Crosby, A., Balson, P.S., Jeffery, D.H., Lott, G.K., Bulat, J., and Harrison, D.J., 1992, UK offshore regional report: The geology of the southern North Sea: Keyworth, British Geological Survey.

Clark, C.D., Gibbard, P.L., and Rose, J., 2003, Pleistocene glacial limits in England, Scotland, and Wales, *in* Ehlers, J., and Gibbard, P.L., eds., Quaternary Glaciations - Extent and chronology, Part 1: Europe: Amsterdam, Elsevier, p. 47-82.

Clayton, K.M., 1989, Sediment input from the Norfolk cliffs, Eastern England - a century of coast protection and its effects: Journal of Coastal Research, v. 5 (3), p. 433-442.

Clayton, K.M., McCave, I.N., and Vincent, C.E., 1983, The establishment of a sand budget for the East Anglian coast and its implications for coastal stability, Shoreline Protection: University of Southampton, Thomas Telford Ltd, p. 91-96.

Craig, R.F., 2004, Craigs Soil Mechanics: London, Spon Press, 447 p.

Dawson, E.M., Roth, W.H., and Drescher, A., 1999, Slope Stability analysis by strength reduction: Geotechnique, v. 49 (6), p. 835-840.

Dixon, N., 1987, The mechanics of coastal landslides in London Clay at Warden Point, Isle of Sheppey [PhD thesis], Kingston Polytechnic.

Dixon, N., and Bromhead, E.N., 2002, Landsliding in London Clay coastal cliffs: Quarterly Journal of Engineering Geology & Hydrology, v. 35 327-343.

Domesday Book, 1086, National Archives Reference E31. Exchequer: Treasury of the Receipt: Domesday Book.

Fresco, A., 2004, The old man and the sea – and the council, The Times Newspaper, London, 25th February 2004.

Frew, P., and Guest, S., 2001, Geotechnical and other aspects of the Overstrand coast protection scheme.,

Griffiths, D.V., and Lane, P.A., 1999, Slope stability analysis by Finite Elements: Geotechnique, v. 49 (3), p. 387-403.

Halcrow, 2002, Futurecoast [CD-ROM], produced for Department for Environment, Food & Rural Affairs.

Hamblin, R.J.O., 2000, A new glacial stratigraphy for East Anglia: Mercian Geologist, v. 15 (1), p. 59-62.

Hamblin RJO, Moorlock BSP, Rose J. 2000. A new glacial stratigraphy for Eastern England. *Quaternary Newsletter* **92**: 35-43.

Hart, J.K., 1987, The genesis of the north east Norfolk Drift [Unpublished PhD thesis], University of East Anglia.

—, 1999, Glacial sedimentology: a case study from Happisburgh, Norfolk, *in* Jones, A., Tucker, M., and Hart, J.K., eds., The Description and Analysis of Quaternary Stratigraphic Field Sections, Volume Technical Guide 7: London, Quaternary Research Association, p. 209-234.

—, 2007, An investigation of subglacial shear zone processes from Weybourne, Norfolk, UK: Quaternary Science Reviews, v. 26 (19-21), p. 2354-2374.

Hart, J.K., and Boulton, G.S., 1991, The glacial drifts of Norfolk, *in* Ehlers, J., Gibbard, P.L., and Rose, J., eds., Glacial Deposits in Great Britain and Northern Ireland: Rotterdam, Balkema,, p. 233-243.

Head, K.H., 1996, Manual of Soil Laboratory Testing, Whittles Publishing.

Hiatt, M.E., 2002, Sensor Integration Aids Mapping at Ground Zero: Photogrammetric Engineering and Remote Sensing, v. 68 (9), p. 877-879.

Hobbs, P., Humphreys, B., Rees, J., Tragheim, D., Jones, L., Gibson, A., Rowlands, K., Hunter, G., and Airey, R., 2002, Monitoring the role of landslides in 'soft cliff' coastal recession, *in* McInnes, R.G., and Jakeways, J., eds., Instability Planning and Management: Isle of Wight, Thomas Telford, p. 589-600.

HR Wallingford, 2001, Ostend to Cart Gap Coastal Strategy Study,

—, 2002, Southern North Sea Sediment Transport Study Phase 2: Sediment Transport Report, Report produced for Great Yarmouth Borough Council by HR Wallingford, CEFAS/UEA, Posford Haskoning and Dr Brian D'Olier, Report EX 4526.,

Hulme, M., Jenkins, G.J., Lu, X., Turnpenny, J.R., Mitchell, T.D., Jones, R.G., Lowe, J., Murphy, J.M., Hassell, D., Boorman, P., McDonald, R., and Hill, S., 2002, Climate Change Scenarios for the United Kingdom: The UKCIP02 Scientific Report, Tyndall Centre for Climate Change Research, School of Environmental Sciences, University of East Anglia,

Hunter, G., Pinkerton, H., Airey, R., and Calvari, S., 2003, The application of a long-range laser scanner for monitoring volcanic activity on Mount Etna: Journal of Volcanology and Geothermal Research, v. 123 203-210.

Hutchinson, J.N., 1976, Coastal landslides in cliffs of Pleistocene deposits between Cromer and Overstrand, Norfolk, England, *in* Janbu, N., Jorstad, F., and Kjaernsli, B., eds., Laurits Bjerrum Memorial Volume, Contributions to Soil Mechanics: Oslo, Norwegian Geotechnical Institute, p. 155-182.

Jones, L.D., 2006, Monitoring landslides in hazardous terrain using terrestrial LiDAR: an example from Montserrat: Quarterly Journal of Engineering Geology and Hydrogeology, v. 39 371-373.

Kazi, A., and Knill, J.L., 1969, The sedimentation and geotechnical properties of the Cromer Till between Happisburgh and Cromer, Norfolk: Quarterly Journal of Engineering Geology, v. 2 63-86.

Klein, A.H.d.F., Filho, L.B., and Schumacher, D.H., 2002, Short-term beach rotation processes in distinct headland bay beach systems: Journal of Coastal Research, v. 18 (3), p. 442-458.

Klein, A.H.F., and Menezes, J.T., 2001, Beach morphodynamics and profile sequence for a headland bay coast: Journal of Coastal Research, v. 17 (4), p. 812-835.

Knight, J., 2005, Formation of thrust structures in front of coastal landslides: The Journal of Geology University of Chicago, v. 113 107-114.

Langton, D.D., 1999, The PANDA lightweight penetrometer for soil investigation and monitoring material compaction: Ground Engineering 33-37.

Lavalle, P.D., and Lakhan, C., 1997, A spatial-temporal analysis of the development of a log-spiral shaped embayment: Earth Surface Processes and Landforms, v. 22 (7), p. 657-667.

LeBlond, P.H., 1979, An explanation of the logarithmic spiral plan shape of headland-bay beaches: Journal of Sedimentary Research, v. 49 (4), p. 1093-1100.

Lee, E.M., and Clark, A.R., 2002, Investigation and management of soft rock cliffs, DEFRA, Thomas Telford,

Lee, J.R., 2001, Genesis and palaeogeographic significance of the Corton Diamicton (basal member of the North Sea Drift Formation), East Anglia, UK: Proceedings of the Geologists' Association, v. 112 43-67.

—, 2003, Early and Middle Pleistocene lithostratigraphy and palaeoenvironments in northern East Anglia, UK. (Unpublished) [Ph.D. thesis], University of London.

Lee, J.R., and Booth, S.J., 2006, Quaternary Field Mapping: lowland Britain, British Geological Survey, IR/06/99.

Lee, J.R., Booth, S.J., Hamblin, R.J.O., Jarrow, A.M., Kessler, H.K.E., Moorlock, B.S.P., Morigi, A.M., Palmer, A., Pawley, S.J., Riding, J.B., and Rose, J., 2004a, A new stratigraphy for the glacial deposits around Lowestoft, Great Yarmouth and Cromer, East Anglia, UK: Bulletin of the Geological Society of Norfolk, v. 53 3-60.

Lee, J.R., Rose, J., Hamblin, R.J.O., and Moorlock, B.S.P., 2004b, Dating the earliest lowland glaciation of eastern England: a pre-M1512 early Middle Pleistocene Happisburgh Glaciation: Quaternary Science Reviews.

Lee, J.R., Rose, J., Riding, J.B., Hamblin, R.J.O., and Moorlock, B.S.P., 2002, Testing the case for a Middle Pleistocene Scandinavian glaciation in Eastern England: evidence for a Scottish ice source for tills within the Corton Formation of East Anglia, UK: Boreas, v. 31 345-355.

Leggett, D., 1993, Happisburgh to Winterton: Changes in beach levels July 1992 to March 1993, Environment Agency Internal Report,

Lord, J.A., Clayton, C.R.I., and Mortimore, R.N., 2002, Engineering in chalk, CIRIA, 2002.,

Lunkka, J.P., 1988, Sedimentation and deformation of the North Sea Drift Formation in the Happisburgh area, North Norfolk, *in* Croot, D., ed., Glaciotectonics: Forms and Processes: Balkema, Rotterdam, p. 109-122.

—, 1994, Sedimentation and lithostratigraphy of the North Sea Drift and Lowestoft Till Formations in the coastal cliffs of northeast Norfolk, England: Journal of Quaternary Science, v. 9 (3), p. 209-233.

Marques, F.M.S.F., 1997, Sea cliff retreat and related hazards: a quantitative approach, IV Symposium nacional sobre taludes y laderas inestables: Granada.

McCave, I.N., 1978, Grain-size trends and transport along beaches: examples from Eastern England: Marine Geology, v. 28 M43-M51.

—, 1987, Fine sediment sources and sinks around the East Anglian coast (UK): Journal of the Geological Society of London, v. 144 (1), p. 149-152.

Miller, L., and Douglas, B.C., 2004, Mass and volume contributions to twentieth-century global sea level rise: Nature, v. 428 406-409.

Mills, J.P., Buckley, S.J., Mitchell, H.L., Clarke, P.J., and Edwards, S.J., 2005, A geomatics data integration technique for coastal change monitoring: *Earth Surface Processes & Landforms*, v. 30 (6), p. 651-664.

Moorlock, B.S.P., Booth, S., Fish, P., Hamblin, R.J.O., Kessler, H., Riding, J., Rose, J. & Whiteman**, C.A.**, 2000. A revised glacial stratigraphy of Norfolk. *In:* Lewis, S.G., Whiteman, C.A. & Preece, R.C. (eds): The Quaternary of Norfolk and Suffolk: Field Guide. Quaternary Research Association (London): 53-54.

Moorlock, B., Hamblin, R., SJ, B., Woods, M., Kessler, H., and Hobbs, P., 2002, Geology of the Cromer District: a brief explanation of the geological map sheet 131 Cromer, British Geological Survey.

Ohl, C., Frew, P., Sayers, P., Watson, G., Lawton, P., Farrow, B., Walkden, M., and Hall, J., 2003, North Norfolk - a regional approach to coastal erosion management and sustainability practice, *in* McInnes, R.G., ed., International Conference on Coastal Management 2003: Brighton, Thomas Telford, p. 226-240.

Paul, F., and Iwan, P., 2001, Data Collection at Major Incident Scenes using Three Dimensional Laser Scanning Techniques, The Institute of Traffic Accident Investigators: 5th International Conference held at York: New York.

Pawley, S.M., Rose, J., Lee, J.R., Moorlock, B.S.P., and Hamblin, R.J.O., 2004, Middle Pleistocene sedimentology and lithostratigraphy of Weybourne, northeast Norfolk, England: Proceedings of the Geologists' Association, v. 115 25-42.

Poulton, C.V.L., Lee, J.R., Jones, L.D., Hobbs, P.R.N., and Hall, M., 2006, Preliminary investigation into monitoring coastal erosion using terrestrial laser scanning: case study at Happisburgh, Norfolk, UK: Bulletin of the Geological Society of Norfolk, v. 56 45-65.

Reid, C., 1882, The geology of the country around Cromer, Sheet 68., British Geological Survey, 137 p.

Rowlands, K., Jones, L., and Whitworth, M., 2003, Photographic Feature: Landslide Laser scanning: a new look at an old problem: Quarterly Journal of Engineering Geology, v. 36 (2), p. 155-158.

Shennan, I., Coulthard, T., Flather, R., Horton, B., Macklin, M., Rees, J., and Wright, M., 2003, Integration of shelf evolution and river basin models to simulate Holocene sediment dynamics of the Humber Estuary during periods of sea-level change and variation in catchment sediment supply: The Science of the Total Environment, v. 314-316 (Special Issue), p. 737-754.

Short, A.D., and Masselink, G., 1999, Embayed and structurally controlled beaches, *in* Short, A.D., ed., Handbook of beach and shoreface morphodynamics: Chichester, Wiley, p. 142-161.

Terzaghi, K., 1955, The Influence of geological factors in the engineering properties of sediments.: Economic Geology, v. 50th Anniversary Volume 557-618.

Thomalla, F., and Vincent, C.E., 2003, Beach Response to Shore-Parallel Breakwaters at Sea Palling, Norfolk, UK: Estuarine, Coastal and Shelf Science, v. 56 203-212.

Trenter, N.A., and Warren, C.D., 1996, Further investigations at the Folkestone Warren landslide: Géotechnique, v. 46 (4), p. 589-620.

White, W., 1845, History, Gazeteer, and Directory of Norfolk 1845.

Wildman, G., and Hobbs, P.R.N., 2005, Scoping study for coastal instability hazard susceptibility - Filey Bay, Beachy Head and Lyme Bay, Internal Report, British Geological Survey, IR/05/018.